



# North Raccoon River Watershed Hydrologic Assessment Report

IIHR Report  
No. 532  
October 2019



Photo by: Barb Farrow

Prepared by:  
Iowa Flood Center / IIHR — Hydrosience & Engineering

Sponsored by:  
North Raccoon River Watershed Management Coalition



Iowa Watershed Approach  
Phase I Report



IIHR — Hydrosience & Engineering  
The University of Iowa  
C. Maxwell Stanley Hydraulics Laboratory  
Iowa City, Iowa 52242



# Hydrologic Assessment of the North Raccoon River Watershed

October 2019

IIHR Technical Report No. 532

*Prepared by:*  
Iowa Flood Center | IIHR—Hydroscience & Engineering  
The University of Iowa  
C. Maxwell Stanley Hydraulics Laboratory  
Iowa City, Iowa 52242



## **Acknowledgements**

The Iowa Flood Center and IIHR—Hydrosience & Engineering would like to thank the following agencies and organizations for providing data and engaging in discussions that contributed to this assessment:

Iowa Department of Natural Resources

Natural Resources Conservation Service

Members of the North Raccoon River Watershed Management Coalition

Buena Vista County

United States Geological Survey

Iowa State University



# Table of Contents

<b>Acknowledgements</b> .....	<b>iii</b>
<b>List of Tables</b> .....	<b>xiv</b>
<b>Introduction</b> .....	<b>1</b>
<b>1. Iowa’s Hydrology and Water Quality</b> .....	<b>5</b>
a. Land Surface and Use.....	5
b. Climate and Water Cycle.....	10
i. Statewide Precipitation .....	10
ii. The Water Cycle in Iowa.....	12
iii. Shallow Groundwater and Soil Moisture Trends.....	13
iv. Floods.....	14
v. Droughts .....	17
c. Hydrological Alterations in Iowa and the Iowa Watershed Approach Study Areas .....	18
i. Hydrological Alterations from Agricultural-Related Land Use Changes.....	18
ii. Hydrological Alterations Induced by Climate Change .....	20
iii. Hydrological Alterations Induced by Urban Development.....	21
d. Assessment of Iowa’s Water Quality .....	22
i. Iowa Water-Quality History .....	22
ii. Water Quality in the Post-Clean Water Act Era .....	22
e. Web-Based Information Systems of Flood and Water-Quality Data.....	24
i. The Iowa Flood Information System (IFIS) .....	25
ii. The Iowa Water-Quality Information System.....	28
iii. The Iowa Watershed Approach Information System (IWAIS) .....	29
<b>2. Conditions in the North Raccoon River Watershed</b> .....	<b>31</b>
a. Hydrology .....	31
b. Geology and Soils.....	32
c. Topography.....	37
d. Land Use and BMP Mapping Project .....	40
e. Potential BMPs – Agricultural Conservation Planning Framework .....	42
f. Instrumentation/Data Records .....	42
g. Baseflow and Runoff Historic Trends.....	45
h. Monthly Water Cycle .....	52
i. Floods of Record .....	53

j. Flood Frequency Estimates .....	57
<b>3. North Raccoon River Watershed Hydrologic Model Development.....</b>	<b>60</b>
a. Model Development.....	61
i. Incorporated Structures.....	62
ii. Development of Model Inputs and Parameters.....	63
b. Calibration .....	69
c. Validation.....	69
<b>4. Analysis of Watershed Scenarios .....</b>	<b>70</b>
a. High Runoff Potential Areas.....	70
b. Mitigating the Effects of High Runoff with Increased Infiltration.....	72
i. Conversion of Row Crop Agriculture to Tall-Grass Prairie .....	73
ii. Improved Agricultural Conditions from Planting Cover Crops .....	74
c. Mitigating the Effects of High Runoff with Distributed Storage.....	76
i. Siting of Ponds in the North Raccoon River Watershed .....	77
d. Mitigating the Effects of High Runoff with Distributed Storage and Increased Infiltration.....	86
e. Comparison of Watershed Scenarios for Historic Storm Events .....	88
<b>5. Summary and Conclusions .....</b>	<b>127</b>
a. North Raccoon River Water Cycle and Watershed Conditions.....	127
b. North Raccoon River Hydrologic Model .....	127
c. Watershed Scenarios for the North Raccoon River.....	128
i. Increased Infiltration in the Watershed.....	129
ii. Increased Storage on the Landscape.....	130
iii. Increased Infiltration and Increased Storage: A Blend of Cover Crops and Flood Storage Ponds .....	130
d. Concluding Remarks.....	131
<b>Appendix A – Maps .....</b>	<b>A-1</b>
<b>Appendix B – Calibration and Validation.....</b>	<b>B-1</b>
Calibration.....	B-1
i. Calibration Measures .....	B-1
ii. Summary of Calibrated HMS Model Parameters .....	B-2
iii. Validation Storm Events .....	B-5
iv. Calibration/Validation Summary .....	B-6
<b>Appendix C – Incorporated Structures .....</b>	<b>C-1</b>

**Appendix D – References..... D-1**

## List of Figures

Figure 1. Bank failure along the Raccoon River near Booneville, Iowa, September 2017. ....	1
Figure 2. Tour of a flood mitigation project in the Soap Creek Watershed, which was one of the basins that participated in the Iowa Watersheds Project (2010–16). ....	2
Figure 3. Flood mitigation structure in the Soap Creek Watershed. ....	3
Figure 4. Current IWA watersheds in blue and completed IWP watersheds in red. ....	4
Figure 1.1. Iowa Watershed Approach study areas. ....	5
Figure 1.2. Landform regions of Iowa. ....	7
Figure 1.3. Historic vegetation of Iowa 1832–59. Raw data downloaded from the Iowa Geographic Map Server ( <a href="https://ortho.gis.iastate.edu/">https://ortho.gis.iastate.edu/</a> ). ....	8
Figure 1.4. Land use composition in the state of Iowa 2016. Cropland Data Layer. ....	9
Figure 1.5. Percent of Iowa’s total area planted with row crops between 2001 and 2016. Cropland Data Layer. ....	9
Figure 1.6. Soils requiring tile drainage for full productivity and drainage districts. ....	10
Figure 1.7. Average precipitation (inches): (a) annual; and (b) growing season (April–October). Precipitation estimates are based on the 30-year annual average (1981–2010). (Raw data downloaded from: <a href="http://www.prism.oregonstate.edu/">http://www.prism.oregonstate.edu/</a> ). ....	11
Figure 1.8. Statewide average monthly precipitation. Precipitation estimates are based on the 30-year annual average (1981–2010). (Raw data downloaded from: <a href="http://www.prism.oregonstate.edu/">http://www.prism.oregonstate.edu/</a> ). ....	12
Figure 1.9. Iowa water cycle for the IWA watersheds. This shows the partitioning of average precipitation into evapotranspiration, surface flow, and baseflow components. ....	13
Figure 1.10. Shallow groundwater data (USGS wells). ....	14
Figure 1.11. The extent of the flooding during the 1993 and 2008 floods (Bradley, 2010). ....	14
Figure 1.12. Number of flood-related federally declared disasters in Iowa counties (1988–2016). Data source: <a href="https://www.fema.gov/">https://www.fema.gov/</a> . ....	16
Figure 1.13. The number of flood-related federally declared disasters in Iowa (1988–2016). Data source: <a href="https://www.fema.gov/">https://www.fema.gov/</a> . ....	16
Figure 1.14. Drought conditions, October 09, 2012. (Source: <a href="http://droughtmonitor.unl.edu/">http://droughtmonitor.unl.edu/</a> ). ....	17
Figure 1.15. Observed change in heavy precipitation (the heaviest 1%) between 1958 and 2016. Figure taken from The Climate Science Special Report (Easterling et al. 2017) ( <a href="https://science2017.globalchange.gov/">https://science2017.globalchange.gov/</a> ). ....	20
Figure 1.16. Projected change in heavy precipitation. Twenty-year return period amount for daily precipitation for mid- (left maps) and late-21 <sup>st</sup> century (right maps). Results are shown for a lower emissions scenario (top maps; RCP4.5) and for a higher emissions scenario (bottom maps, RCP8.5). Figure taken from The Climate Science Special Report (Easterling et al. 2017) ( <a href="https://science2017.globalchange.gov/">https://science2017.globalchange.gov/</a> ). ....	21
Figure 1.17. Causes of impairments in Iowa’s impaired waters. (Iowa Department of Natural Resources, 2018). ....	24
Figure 1.18. Number of impaired Iowa waters, 1998–2016. (Iowa Department of Natural Resources, 2018). ....	24
Figure 1.19. Statewide floodplain map data showing different levels of annual flood risk. ....	26
Figure 1.20. Flood inundation map library for the Des Moines and Raccoon rivers in the city of Des Moines. ....	27

Figure 1.21. USGS (green) and Iowa Flood Center (blue) stream-stage monitoring locations displayed in the Iowa Flood Information System (IFIS).....	28
Figure 1.22. IIHR—Hydroscience & Engineering and USGS surface water-quality monitoring locations as displayed in the Iowa Water Quality Information System (IWQIS). ....	29
Figure 1.23. Example IWAS interface view showing the number of existing ponds within each HUC 12 in the Middle Cedar River Watershed.....	30
Figure 2.1. The North Raccoon River Watershed (HUC 8 07100006), drains 2471 mi <sup>2</sup> . The North Raccoon River joins the South Raccoon River near Van Meter, Iowa. ....	31
Figure 2.2. Defined Landform Regions of the North Raccoon River Watershed.....	32
Figure 2.3. Typical Des Moines Lobe cross-section (Prior 1991). ....	33
Figure 2.4. Typical Southern Iowa Drift Plain cross-section (Prior 1991). ....	34
Figure 2.5. Depth to bedrock in the North Raccoon River Watershed.....	35
Figure 2.6. Distribution of Hydrologic Soil Groups in the North Raccoon River Watershed. Hydrologic Soil Groups reflect the degree of runoff potential a particular soil has, with Type A representing the lowest runoff potential and Type D representing the highest runoff potential. ....	37
Figure 2.7. Topography of the North Raccoon River Watershed. ....	38
Figure 2.8. Terrain slopes derived from LiDAR data. ....	39
Figure 2.9. Delineated potholes and the land area that drains to them within the Des Moines Lobe in the North Raccoon River Watershed.....	40
Figure 2.10. Land use composition in the North Raccoon River Watershed, according to the 2009 HRLC dataset provided by Iowa DNR.....	41
Figure 2.11. Annual totals for: (a) precipitation; (b) streamflow; (c) baseflow; and (d) runoff at Jefferson, IA.....	46
Figure 2.12. Annual totals for: (a) precipitation; (b) streamflow; (c) baseflow; and (d) runoff at Van Meter, IA.....	47
Figure 2.13. Cumulative annual totals for: (a) precipitation; (b) streamflow; (c) baseflow; and (d) runoff at Jefferson, Iowa.....	48
Figure 2.14. Cumulative annual totals for: (a) precipitation; (b) streamflow; (c) baseflow; and (d) runoff at Van Meter, Iowa.....	49
Figure 2.15. Double-mass curves using cumulative annual precipitation with cumulative annual (a) streamflow, (b) baseflow, and (c) runoff at Jefferson, Iowa. Fitted lines show segments have different slopes beginning around 1980. ....	50
Figure 2.16. Double-mass curves using cumulative annual precipitation with cumulative annual (a) streamflow, (b) baseflow, and (c) runoff at Van Meter, Iowa. Fitted lines show segments have different slopes beginning around 1980. ....	51
Figure 2.17. Monthly water cycle for the North Raccoon River Watershed at Jefferson, Iowa. The plots show the average monthly precipitation (inches) and the average monthly streamflow (inches). The average monthly estimates for precipitation and streamflow are based on the period 1950–2017. ....	52
Figure 2.18. Monthly water cycle for the North Raccoon River Watershed at Van Meter, Iowa. The plots show the average monthly precipitation (inches) and the average monthly streamflow (inches). The average monthly estimates for precipitation and streamflow are based.....	53
Figure 2.19. Annual maximum peak discharges observed at the Jefferson (left) and Van Meter (right) USGS stream gauge stations. ....	54

Figure 2.20. Annual maximum peak discharge and the calendar day of occurrence at the Jefferson (left) and Van Meter (right) USGS stream gauge stations.....	54
Figure 2.21. Flood occurrence frequency by month at both the Jefferson and Van Meter USGS stream gauge stations. ....	55
Figure 2.22. Upstream drainage area throughout the stream network in the North and South Raccoon River Watersheds. ....	59
Figure 3.1. Hydrologic processes that occur in a watershed. Phase I modeling only considered the precipitation, infiltration, and overland components of the water cycle. ....	60
Figure 3.2. HMS model development of the North Raccoon River Watershed. The watershed was divided into 1156 subbasins for modeling. ....	62
Figure 3.3. Example of the Stage IV rainfall product used as the precipitation input in the North Raccoon River Watershed HMS model. The Stage IV product provides hourly cumulative rainfall estimates for each 4 km x 4 km grid cell. The scale shown indicates estimates of the depth of rainfall (in inches) for a one-hour period.....	64
Figure 3.4. Subbasin runoff hydrograph conceptual model. Rainfall is partitioned into a runoff depth using the NRCS curve number methodology, which is then converted to discharge using either the ModClark or Clark unit hydrograph method. ....	67
Figure 4.1. SCS design storm hyetograph, showing the timing of the rainfall and example infiltration for a given subbasin area.....	71
Figure 4.2. Runoff potential coefficients computed for each subbasin (left) and HUC 12 watershed (right) for a 6-inch, 24-hour design storm are shown. Higher runoff coefficients appear in red. Many areas with lower runoff potential are the result of prairie pothole areas that are isolated from the subbasin outlet. ....	72
Figure 4.3. Peak discharge reductions for subbasins (left) and junctions (right) for conversion of row crop agriculture to native prairie for a 6-inch, 24-hour design storm. Simulation results at junctions with large drainage area are not realistic for this design storm event, therefore, results are not shown at junctions with drainage area greater than 100 mi <sup>2</sup> .....	74
Figure 4.4. Peak discharge reductions for subbasins (left) and junctions (right) for the 6-inch, 24-hour design storm with improved soil infiltration after many years of using cover crops during the dormant season for all row crop agriculture. Simulation results at junctions with large drainage area are not realistic for this design storm event, therefore, results are not shown at junctions with drainage area greater than 100 mi <sup>2</sup> . ....	76
Figure 4.5. Schematic of a pond constructed to provide flood storage. ....	77
Figure 4.6. Areas draining to nutrient reduction wetlands (NRWs), identified by the Agricultural Conservation Planning Framework (ACPF) toolbox. NRW ponds were used to develop storage-discharge relationships for corresponding subbasins.....	79
Figure 4.7. Aggregation of pond storage-discharge curves and drainage areas within a subbasin. Overlapping drainage areas of ponds in a series configuration were dissolved.....	80
Figure 4.8. Flood storage (acre-feet) provided by ponds in each subbasin. Aggregated ACPF pond characteristics were used to develop hypothetical ponds in subbasins where ACPF data were not available.....	82
Figure 4.9. Model index locations selected for comparisons of hypothetical flood mitigation scenarios to current conditions. ....	83
Figure 4.10. Junction peak discharge reductions with ACPF ponds in place for a 6-inch, 24-hour SCS Design Storm. . Simulation results at junctions with large drainage area are not realistic	

for this design storm event, therefore, results are not shown at junctions with drainage area greater than 100 mi <sup>2</sup> . .....	85
Figure 4.11. Peak discharge reductions for subbasins (left) and junctions (right) with ACPF ponds in place and improved soil infiltration following many years of 50% utilization of cover crops for a 6-inch, 24-hour SCS Design Storm. Simulation results at junctions with large drainage area are not realistic for this design storm event, therefore, results are not shown at junctions with drainage area greater than 100 mi <sup>2</sup> . .....	87
Figure 4.12. Rainfall totals for the period June 24 – July 5, 2005. ....	89
Figure 4.13 Junction peak discharge reductions with 100% conversion of agricultural lands to prairie for the June 2005 event. Junction points along the main stream are denoted by triangles. ....	90
Figure 4.14. Junction peak discharge reductions with 100% utilization of cover crops on agricultural lands for the June 2005 event. Junction points along the main stream are denoted by triangles. ....	91
Figure 4.15. Junction peak discharge reductions with all ponds in place for the June 2005 event. Junction points along the main stream are denoted by triangles. ....	92
Figure 4.16. Junction peak discharge reductions with 50% utilization of cover crops on agricultural lands and all ponds in place for the June 2005 event. Junction points along the main stream are denoted by triangles. ....	93
Figure 4.17. Hydrograph comparisons – with all agricultural lands converted to prairie, ACPF ponds, with 100% utilization of cover crops, and a combination of ACPF ponds and 50% utilization of cover crops for the June 2005 event. ....	94
Figure 4.18. Percent reduction in peak discharge at model index locations with implementation of each watershed scenario for the June 2005 event. ....	95
Figure 4.19. Reduction in stage at model index locations with implementation of each watershed scenario for the June 2005 event. ....	95
Figure 4.20. Rainfall totals for the period April 22 – May 3, 2007. ....	97
Figure 4.21. Junction peak discharge reductions with 100% conversion of agricultural lands to prairie for the April 2007 event. Junction points along the main stream are denoted by triangles. ....	98
Figure 4.22. Junction peak discharge reductions with 100% utilization of cover crops on agricultural lands for the April 2007 event. Junction points along the main stream are denoted by triangles. ....	99
Figure 4.23. Junction peak discharge reductions with all ponds in place for the April 2007 event. Junction points along the main stream are denoted by triangles. ....	100
Figure 4.24. Junction peak discharge reductions with 50% utilization of cover crops on agricultural lands and all ponds in place for the April 2007 event. Junction points along the main stream are denoted by triangles. ....	101
Figure 4.25. Hydrograph comparisons – with all agricultural lands converted to prairie, ACPF ponds, with 100% utilization of cover crops, and a combination of ACPF ponds and 50% utilization of cover crops for the April 2007 event. ....	102
Figure 4.26. Percent reduction in peak discharge at model index locations with implementation of each watershed scenario for the April 2007 event. ....	103
Figure 4.27. Reduction in stage at model index locations with implementation of each watershed scenario for the April 2007 event. ....	103

Figure 4.28. Rainfall totals for the period May 25 – June 4, 2013.....	105
Figure 4.29. Junction peak discharge reductions with 100% conversion of agricultural lands to prairie for the May 2013 event. Junction points along the main stream are denoted by triangles. ....	106
Figure 4.30. Junction peak discharge reductions with 100% utilization of cover crops on agricultural lands for the May 2013 event. Junction points along the main stream are denoted by triangles.....	107
Figure 4.31. Junction peak discharge reductions with all ponds in place for the May 2013 event. Junction points along the main stream are denoted by triangles. ....	108
Figure 4.32. Junction peak discharge reductions with 50% utilization of cover crops on agricultural lands and all ponds in place for the May 2013 event. Junction points along the main stream are denoted by triangles. ....	109
Figure 4.33. Hydrograph comparisons – with all agricultural lands converted to prairie, ACPF ponds, with 100% utilization of cover crops, and a combination of ACPF ponds and 50% utilization of cover crops for the May 2013 event.....	110
Figure 4.34. Percent reduction in peak discharge at model index locations with implementation of each watershed scenario for the May 2013 event. ....	111
Figure 4.35. Reduction in stage at model index locations with implementation of each watershed scenario for the May 2013 event. ....	111
Figure 4.36. Rainfall totals for the period July 21 – 22, 2010, transposed from a location in northwest Iowa to the center of the North Raccoon River Watershed.....	113
Figure 4.37. Junction peak discharge reductions with 100% conversion of agricultural lands to prairie for the July 2010 transposed event. Junction points along the main stream are denoted by triangles.....	114
Figure 4.38. Junction peak discharge reductions with 100% utilization of cover crops on agricultural lands for the July 2010 transposed event. Junction points along the main stream are denoted by triangles.....	115
Figure 4.39. Junction peak discharge reductions with all ponds in place for the July 2010 transposed event. Junction points along the main stream are denoted by triangles.....	116
Figure 4.40. Junction peak discharge reductions with 50% utilization of cover crops on agricultural lands and all ponds in place for the July 2010 transposed event. Junction points along the main stream are denoted by triangles. ....	117
Figure 4.41. Hydrograph comparisons – with all agricultural lands converted to prairie, ACPF ponds, with 100% utilization of cover crops, and a combination of ACPF ponds and 50% utilization of cover crops, and distributed Saylorville Reservoir ponds for the July 2010 transposed event.....	118
Figure 4.42. Percent reduction in peak discharge at model index locations with implementation of each watershed scenario for the July 2010 transposed event. ....	119
Figure 4.43. Reduction in stage at model index locations with implementation of each watershed scenario for the July 2010 transposed event. ....	119
Figure 4.44. Relationship developed relating storage multiplier and percent of headwater drainage area intercepted by ponds.....	121
Figure 4.45. Rainfall totals for the period July 21 – 22, 2017, transposed from a location in northeast Iowa to the center of the North Raccoon River Watershed. ....	122

Figure 4.46. Junction peak discharge reductions with all ACPF ponds in place for the July 2017 transposed event. Junction points along the main stream are denoted by triangles.....123

Figure 4.47. Junction peak discharge reductions with different pond storage scenarios for the July 2017 transposed event. Junction points along the main stream are denoted by triangles. ...124

Figure 4.48. Hydrograph comparisons –with ACPF ponds, and multiples of typical pond storage for the July 2017 transposed event. ....125

Figure 4.49. Percent reduction in peak discharge at model index locations with implementation of each pond storage scenario for the July 2017 transposed event. ....126

Figure 4.50. Reduction in stage at model index locations with implementation of each pond scenario for the July 2017 transposed event.....126

## List of Tables

Table 1.1. FEMA disaster declarations in Iowa (1988–2016).....	15
Table 1.2. Agricultural-Related Alterations and Hydrologic Impacts. ....	19
Table 2.1. Soil properties and characteristics generally true for hydrologic soil groups A-D. ....	36
Table 2.2. Approximate Hydrologic Soil Group percentages by area of the North Raccoon River Watershed within the Des Moines Lobe. ....	36
Table 2.3. Stage/Discharge Gauges and Precipitation Gauges in the North Raccoon River Watershed. ....	43
Table 2.4. Discharges from the Six Largest Flooding Events at USGS Gaging Stations in the North Raccoon River Watershed, the South Raccoon River at Redfield, IA, the Gaging Stations on the Raccoon River Downstream of the Confluence of the North and South Raccoon Rivers, and Walnut Creek at Des Moines. ....	56
Table 2.5. The dates of the 10 largest peak annual discharges observed at Van Meter, IA, compared to the dates of peak annual discharges on South Raccoon River at Redfield, IA, and the North Raccoon River at Jefferson, IA. ....	57
Table 2.6. Flood frequency estimates generated using a Bulletin 17C Analysis of observed annual peak discharges at Jefferson and Van Meter, IA. ....	57
Table 3.1. Curve number assignment in the North Raccoon River Watershed based on land use and soil type. All dual hydrologic soil groups were treated as type D. ....	65
Table 4.1. Curve numbers used to define the tall-grass prairie and cover crop land use conditions. ....	74
Table 4.2. The flood storage available upstream of the model index locations. In general, the smaller the upland drainage area, the larger the percentage of drainage area is controlled by ponds, and the more flood storage is available. ....	84
Table 4.3. Pond scenarios multiplying the total pond storage distributed across headwater subbasins. ....	120

## Introduction

From 2011–13, Iowa suffered eight Presidential Disaster Declarations encompassing 73 counties and more than 70% of the state. As devastating as these events were, this period is but a small portion of Iowa’s long history of enduring and recovering from major floods. Figure 1 shows just one form of damage as a consequence of repeated flooding events. Long-term data shows that heavy precipitation and flood events are increasing in frequency across the Midwest, and Iowans need to be prepared for the economic, social, and environmental impacts of these changing trends.

In January 2016, the state of Iowa received a \$97 million award for the Iowa Watershed Approach (IWA). The grant was part of the U.S. Department of Housing and Urban Development’s (HUD) National Disaster Resilience Competition, which funds cutting-edge projects to address unmet needs from past natural disasters and reduce Americans’ vulnerability to future disasters. The project will end in September 2021.



Figure 1. Bank failure along the Raccoon River near Booneville, Iowa, September 2017.

The Iowa Watershed Approach (IWA) program takes a holistic approach to address flooding at the watershed scale, recognizing that upstream and downstream communities need to voluntarily work together to increase community flood resilience.

The IWA will accomplish six specific goals:

- 1) Reduce flood risk;
- 2) Improve water quality;
- 3) Increase community flood resilience;
- 4) Engage stakeholders through collaboration, outreach, and education;
- 5) Improve quality of life and health for Iowans, especially for vulnerable populations; and
- 6) Develop a program that is scalable and replicable throughout the Midwest and United States.

The IWA brings Iowans together to address factors that contribute to floods. Nine distinct watersheds are involved in the project, including the Upper Iowa River, Upper Wapsipinicon River, Middle Cedar River, Clear Creek, English River, North Raccoon River, East Nishnabotna River, West Nishnabotna River, and Bee Branch Creek. In addition, urban projects in the cities of

Dubuque, Coralville, and Storm Lake will focus on infrastructure improvements to mitigate flood risk.



Figure 2. Tour of a flood mitigation project in the Soap Creek Watershed, which was one of the basins that participated in the Iowa Watersheds Project (2010–16).

Each watershed has formed a Watershed Management Authority (WMA) that brings local stakeholders together to prioritize their watershed improvement needs, share resources, and foster new partnerships and collaborations. IIHR—Hydroscience & Engineering (IIHR) and the Iowa Flood Center (IFC) are developing a hydrologic assessment of each watershed that will provide WMAs, local leaders, landowners, and residents with an understanding of the hydrology – the movement of water – within their watershed. This assessment will deliver valuable information to stakeholders to help guide strategic decision-making to efficiently address flooding and water-quality concerns.

IIHR and IFC have developed this report for the North Raccoon River Watershed. Information in this report will be integrated into a comprehensive watershed resiliency plan. The watershed resiliency plan will guide long-term watershed management initiatives and planning efforts, as well as identify goals and objectives to meet the current and future needs of local stakeholders and community members.

WMAs in the IWA watersheds have identified eligible sub-watersheds (e.g., HUC 12s) for practice implementation efforts. This report will help guide the implementation of small-scale flood mitigation projects. Through the IWA, volunteer landowners will be eligible to receive 90% cost-

share assistance to implement best management practices (BMPs) such as ponds, wetlands, and water and sediment control basins (WASCOBS) to reduce the magnitude of downstream flooding and improve water quality during and after flood events. The implementation of BMPs is an essential step toward the long-term recovery to improve Iowa's future flood resiliency.



Figure 3. Flood mitigation structure in the Soap Creek Watershed.

The success of the IWA depends on collaborative partnerships among many statewide organizations and local stakeholders who together will carry out the work necessary to achieve the goals of the IWA. Partnerships include, but are not limited to:

- U.S. Department of Housing and Urban Development (HUD)
- U.S. Army Corps of Engineers
- Iowa Silver Jackets Flood Risk Management Team
- Iowa Economic Development Authority
- Iowa Homeland Security and Emergency Management
- University of Iowa (IIHR—Hydroscience & Engineering, Iowa Flood Center, Center for Evaluation and Assessment)
- Iowa State University (Iowa Nutrient Research Center, Iowa Water Center, Daily Erosion Project, ISU Extension & Outreach)
- University of Northern Iowa (Tallgrass Prairie Center)
- Iowa Department of Natural Resources
- Iowa Department of Transportation
- Iowa Association of Counties
- Iowa Department of Agriculture and Land Stewardship
- Iowa Soybean Association

- Iowa Natural Heritage Foundation
- Iowa Corn Growers Association
- Iowa Farm Bureau
- Iowa Agricultural Water Alliance
- Cities of Dubuque, Coralville, and Storm Lake
- Local Resource Conservation and Development Offices
- Benton, Buena Vista, Fremont, Iowa, Johnson, Mills, Winneshiek, and Howard counties

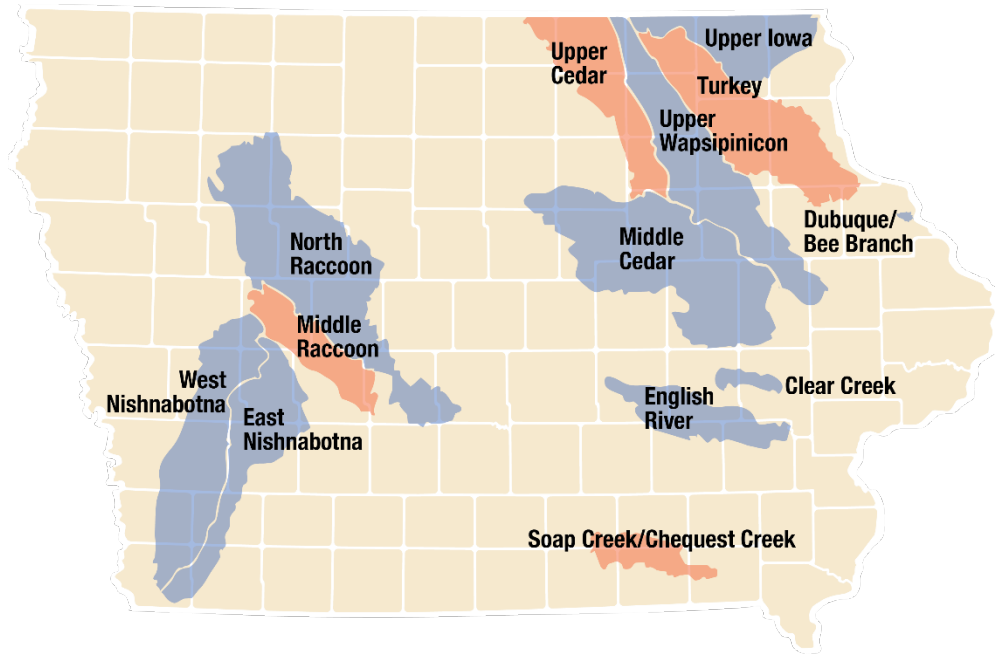


Figure 4. Current IWA watersheds in blue and completed IWP watersheds in red.

The IWA is an expansion of the Iowa Watersheds Project (IWP) (Weber et al. 2018), a similar effort in the five Iowa watersheds (Upper Cedar River, Turkey River, Soap Creek, Middle Raccoon, and Chequest Creek) shown in Figure 4. HUD funded the IWP in the aftermath of the devastating 2008 floods; and the project was active from 2010–16. The success of the IWP served as a significant source of leverage for the state of Iowa to receive funding for the IWA, providing a framework to build upon, continuing Iowa’s leadership and commitment to working together and improving flood resiliency. For more information on the Iowa Watersheds Project, visit <http://iowafloodcenter.org/projects/watershed-projects/>. For more information about the Iowa Watershed Approach, visit [www.iowawatershedapproach.org](http://www.iowawatershedapproach.org).

# 1. Iowa's Hydrology and Water Quality

This chapter summarizes Iowa's water cycle, geology, land use, hydrology, and water quality across the state. The authors examined precipitation, streamflow, and shallow groundwater records to describe how much precipitation falls, how that water moves through the landscape, when storms typically produce river flooding, and how Iowa's hydrology, land use, and water quality have changed over the past decades and century. In addition, this chapter includes an overview of two novel web-based platforms that allow access to Iowa's flood and water-quality data. The information presented in this chapter is valid for the entire state, but some sub-sections place emphasis on the eight IWA watersheds shown in Figure 1.1.



Figure 1.1. Iowa Watershed Approach study areas.

## a. Land Surface and Use

Iowa has a unique and diverse landscape that is the culmination of geologic processes occurring over millennia. Iowa has been subdivided into seven distinct landform regions, shown in Figure 1.2. The Iowa Watershed Approach projects are primarily contained within four of these regions: the Paleozoic Plateau, the Iowan Surface, the Southern Iowa Drift Plain, and the Des Moines Lobe landform regions. Surficial materials are underlain by a host of sedimentary bedrock formations including carbonate (limestone and dolomite), sandstone, and shale. Most of these rocks were deposited during the Paleozoic Era (541–299 million years ago), with others being deposited during the earlier Mesozoic Era (201–66 million years ago).

Following an extensive period of non-deposition and erosion, Iowa was glaciated numerous times during the Quaternary Period. At least seven episodes of glaciation occurred between 2.6 and 0.5 million years ago. These are collectively known as the Pre-Illinoian glacial advances. More recently, the Des Moines Lobe glacier advanced into north-central Iowa, reaching its maximum extent approximately 14,000 years ago. Subsequent loess (wind-blown silt) deposition occurred during and after this time, mantling much of the state. These glacial processes and erosional periods shaped the landform regions of Iowa.

The Southern Iowa Drift Plain encompasses the southern portion of the state and consists of several layers of Pre-Illinoian till deposits mantled by loess. Landscape development following the ice retreat eroded most of the features typically associated with glaciers and created the well-developed drainage network we see today. The Loess Hills landform region in the western part of the state has the same stratigraphic units as the Southern Iowa Drift Plain, but with thicker loess deposits because of its proximity to the source – the Missouri River alluvial plains.

In contrast, northeastern Iowa experienced a period of extreme cold (21,000 to 16,500 years ago) during the last glacial maximum, resulting in extensive erosion of the landscape and the formation of the Iowan Surface landform region. Characteristic features include gently rolling topography, common glacial “erratics” (rocks and boulders not native to Iowa transported here by glaciers), and loess-mantled paha (northwest to southeast trending uneroded upland remnants of the former landscape). The depth to bedrock is often shallow on this landform region. Surficial materials consist of poorly consolidated glacial deposits with the potential for extensive local sand bodies. In areas where the depth to bedrock is shallow, these materials provide limited protection from surface water infiltrating into bedrock.

The Paleozoic Plateau borders the Iowan Surface and experienced many of the same processes. The primary difference is that shallow bedrock dominates the Paleozoic Plateau. Characteristic features include steep sided, deeply entrenched valleys; abundant rock exposures; and common karst features. The unconsolidated materials consist of relatively thin glacial deposits with a loess mantle. Carbonate bedrock is susceptible to the formation of karst features, and numerous caves, springs, and sinkholes are identified throughout this landform region.

The younger Des Moines Lobe landform region is in north-central Iowa. This region was glaciated between approximately 15,000 and 12,000 years ago, with several advances and retreats before the glacier finally receded. Because of the relative youth of this region, erosional processes have not erased the surficial features typical of glacial landscapes. Characteristic features include glacial moraines (arcuate ridges associated with stationary periods), ice contact features (knobs, kettles, and hummocky terrain), fine-grained lake and pond deposits, and outwash (coarse sand and gravel carried by rivers draining glaciers). Natural drainage on the Des Moines Lobe is typically very poor.



Figure 1.2. Landform regions of Iowa.

Prairies covered Iowa before the arrival of European settlers, as depicted in historical vegetation shown in Figure 1.3. Forests and wetlands created a diverse set of habitats for animals, and prairies contained up to 300 species of grasses and flowers. As settlers tilled the prairie and planted crops such as corn, oats, and alfalfa, the land cover of Iowa shifted to a majority agricultural state (Schilling et al., 2008).

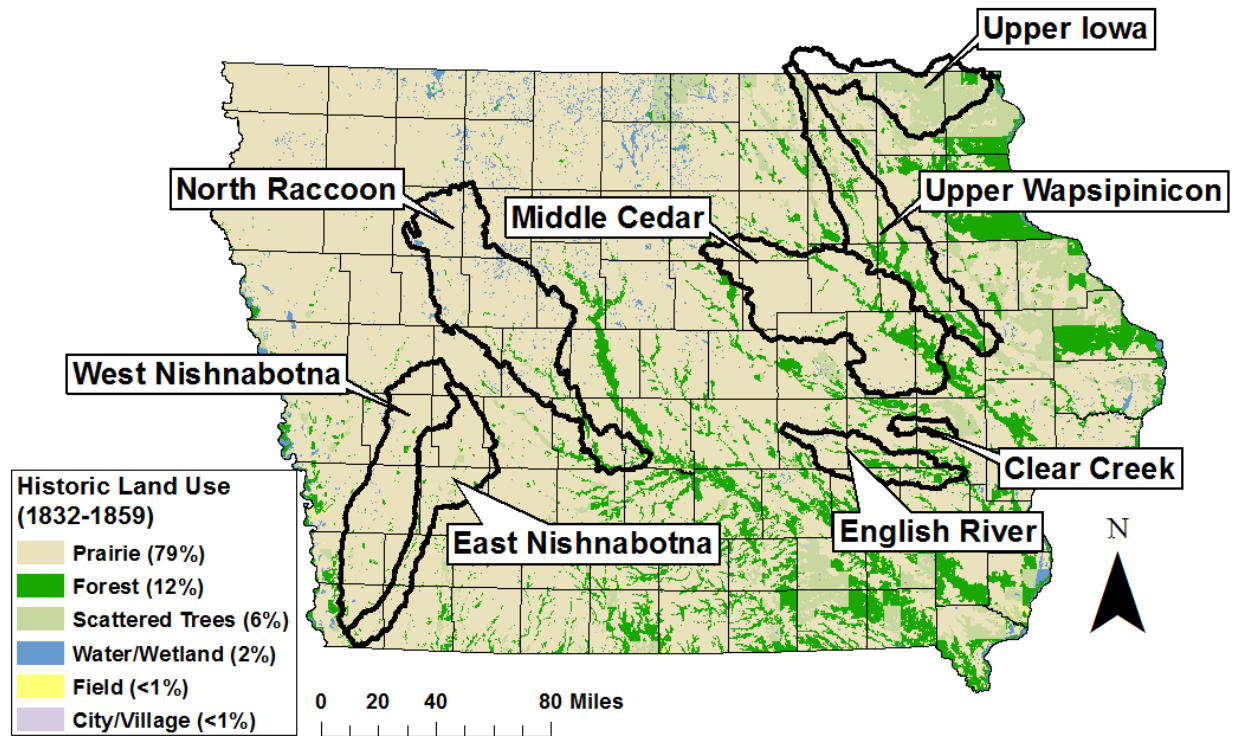


Figure 1.3. Historic vegetation of Iowa 1832–59. Raw data downloaded from the Iowa Geographic Map Server (<https://ortho.gis.iastate.edu/>).

Today, corn and soybeans cover 64% of Iowa, with only small prairie remnants remaining, which are shown in Figure 1.4. Several factors make Iowa an excellent place to sustain agricultural activities, including the rich topsoil left behind by the prairies; advances in farming technology including fertilizers, pesticides, and herbicides; and rainfall patterns, among others. Over the past 15 years, the percentage of Iowa’s land used for growing corn and soybeans has stayed relatively stable at near 60%. The percentage of Iowa land area devoted to growing corn or soybeans is shown in Figure 1.5.

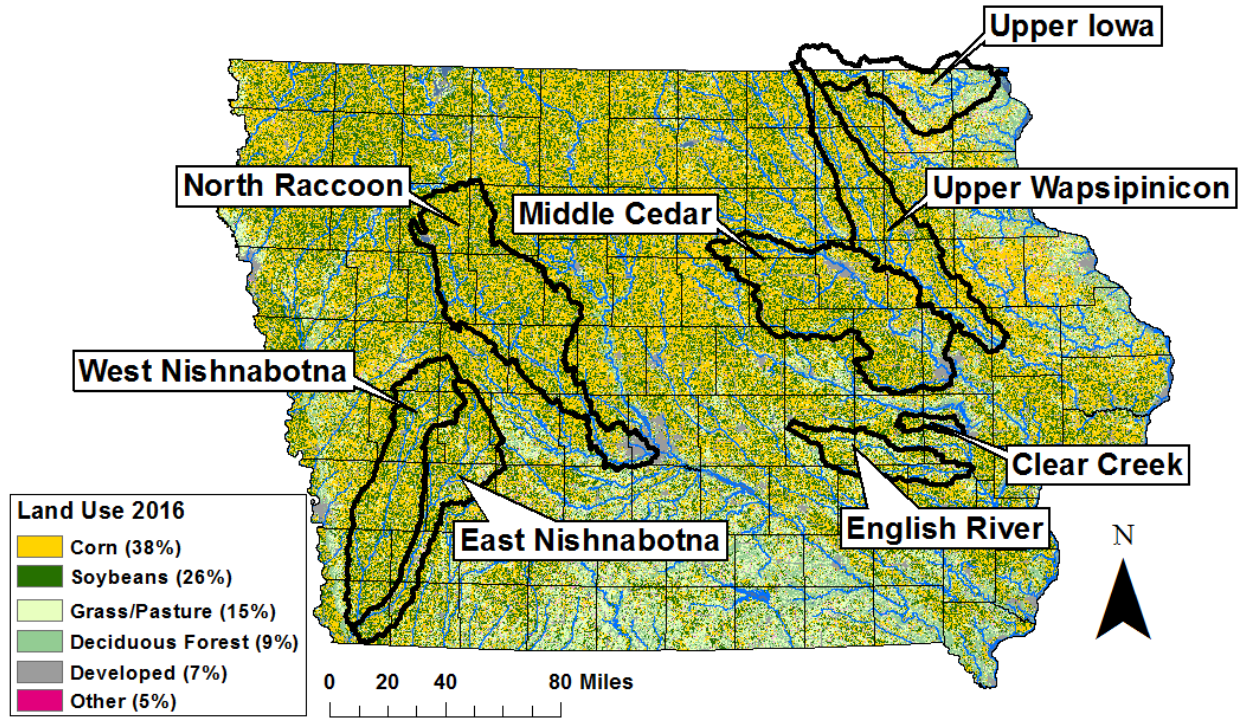


Figure 1.4. Land use composition in the state of Iowa 2016. Cropland Data Layer.

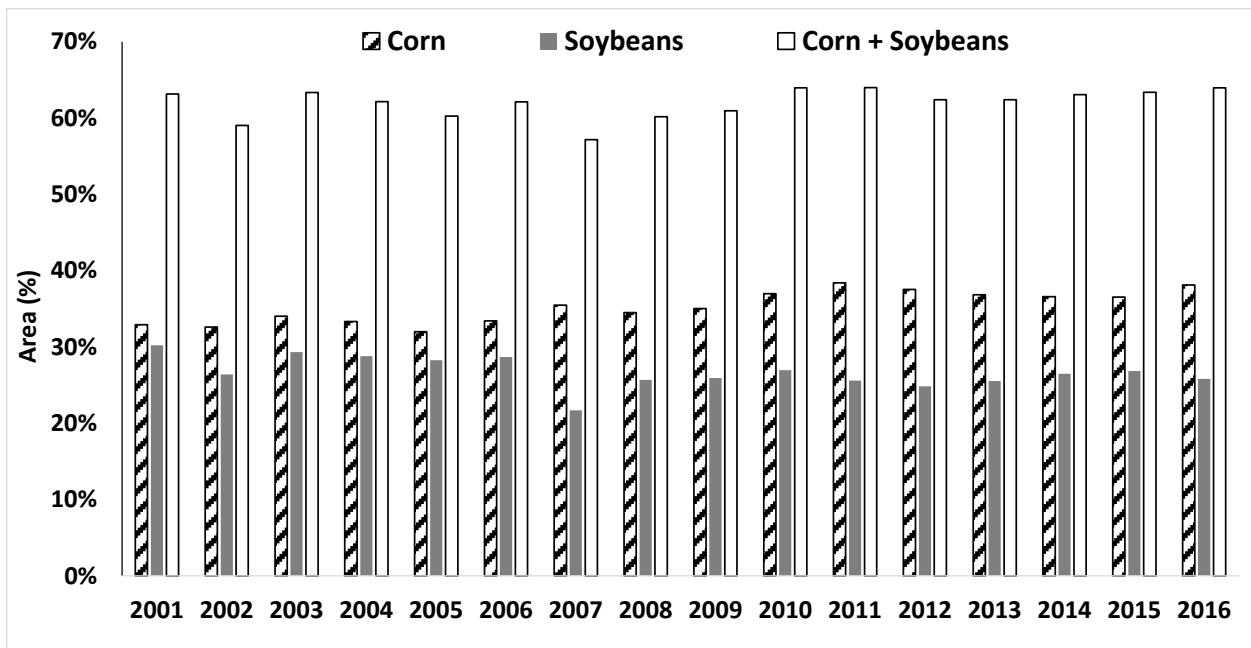


Figure 1.5. Percent of Iowa's total area planted with row crops between 2001 and 2016. Cropland Data Layer.

A significant portion of Iowa soils require sub-surface drainage to achieve optimal yields for row crops. Areas that likely require tile drainage are shown in Figure 1.6. It is estimated that installation of tile drainage peaked between the late 1800s and the mid-1900s, but today landowners continue to expand and upgrade drainage systems. In some areas (mostly in the Des Moines Lobe), public drainage districts were created to facilitate drainage over large areas. Drainage districts, also shown in Figure 1.6, have the power to tax and bond and are governed by trustees.

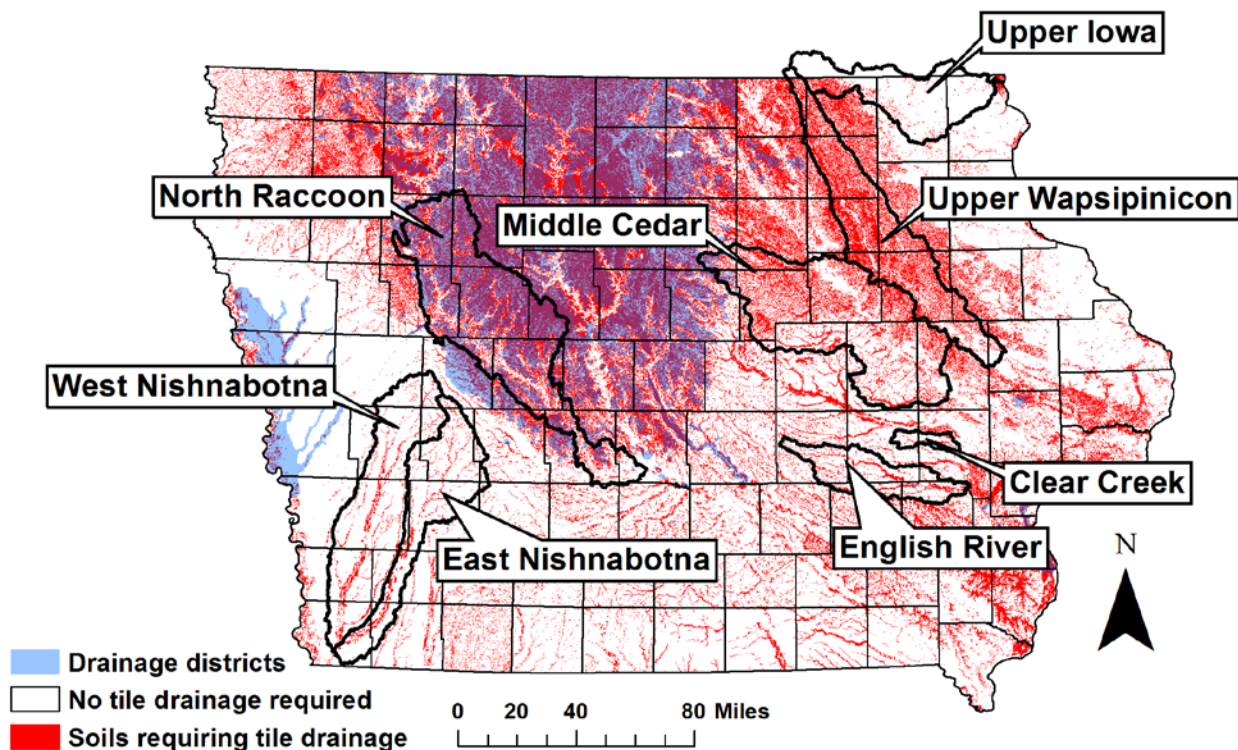


Figure 1.6. Soils requiring tile drainage for full productivity and drainage districts.

## b. Climate and Water Cycle

Iowa is characterized by a humid continental climate with marked seasonal temperature variations, typically experiencing hot summers and cold winters. Annual average temperatures range between approximately 40°F and 60°F. Severe weather can impact regions of the state between the spring and fall; heavy rains and tornados are the most common of these events. Precipitation records show that Iowa typically receives the bulk of its annual precipitation in the spring and the summer.

### i. Statewide Precipitation

Iowa's precipitation spatial patterns are marked by a smooth transition of annual precipitation across its landscape from the southeast to the northwest, as shown in Figure 1.7. The average annual precipitation reaches 40 inches in the southeast corner and decreases to 26 inches in the northwest corner.

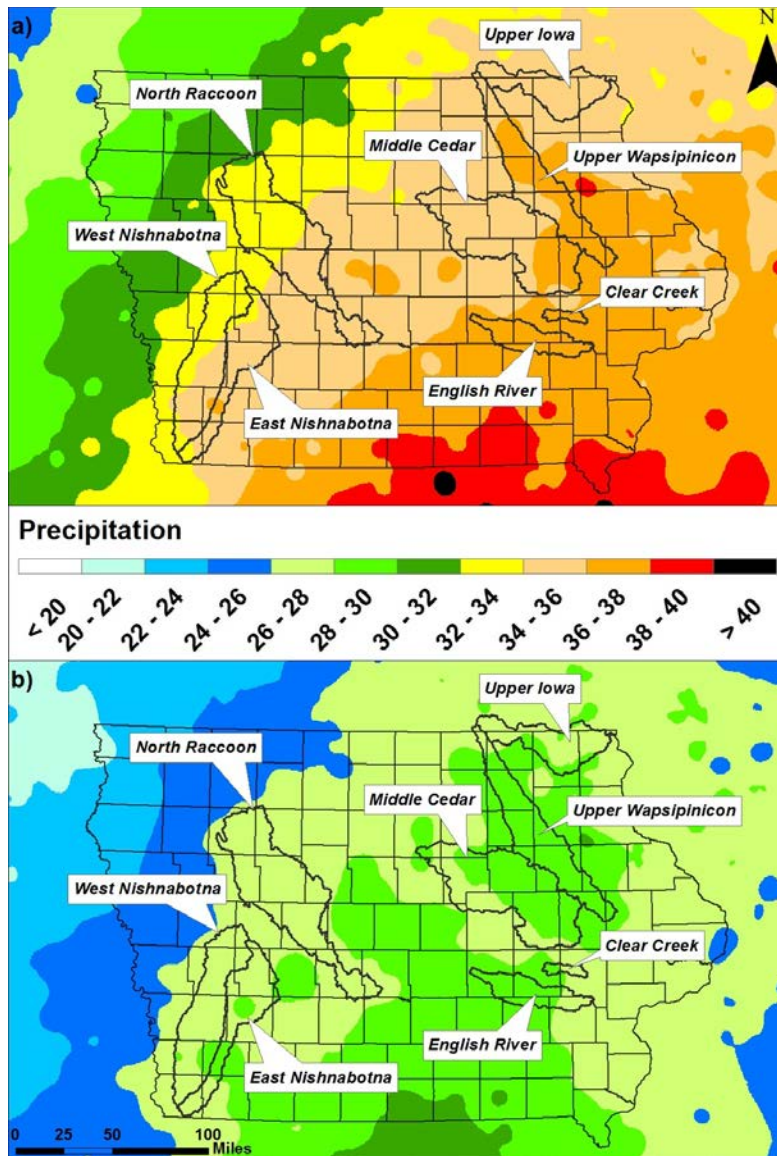


Figure 1.7. Average precipitation (inches): (a) annual; and (b) growing season (April–October). Precipitation estimates are based on the 30-year annual average (1981–2010). (Raw data downloaded from: <http://www.prism.oregonstate.edu/>).

Records show small variations in average annual precipitation among the eight IWA watersheds; the North Raccoon receives the least (33.8 inches), and the English River the most (36.6 inches). Historically, the quantity of annual precipitation presented in Figure 1.7b has been ideal for agricultural needs, such that Iowa has not required irrigation systems like other parts of the country. The state average precipitation between April and October is approximately 27 inches, and the months with highest precipitation accumulation (May, June, and July) occur during the peak of the growing season. These climatological characteristics make Iowa an ideal place for agriculture.

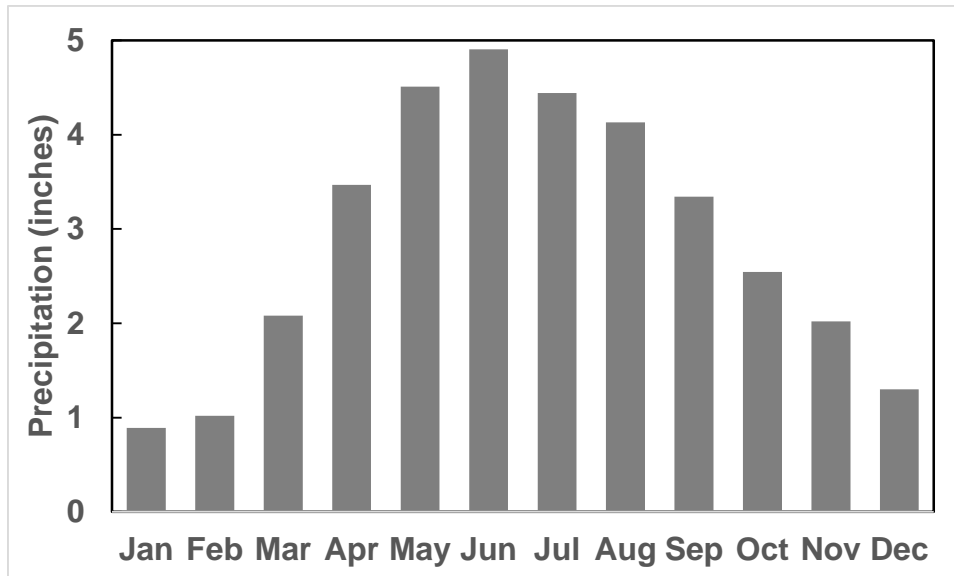


Figure 1.8. Statewide average monthly precipitation. Precipitation estimates are based on the 30-year annual average (1981–2010). (Raw data downloaded from: <http://www.prism.oregonstate.edu/>).

## ii. The Water Cycle in Iowa

A large portion of Iowa’s precipitation evaporates into the atmosphere — either directly from lakes and streams, or by transpiration from crops and vegetation. What doesn’t evaporate drains into streams and rivers. The average annual partitioning of precipitation into evapotranspiration, surface flow, or base flow in each IWA watershed is shown in Figure 1.9.

### *Evapotranspiration*

In Iowa, most precipitation leaves by evapotranspiration; for the IWA watersheds, evapotranspiration accounts for between 66% and 79% of precipitation. Moving westward in the state, a larger fraction of the precipitation evaporates, as can be seen in Table 1.1.

### *Surface Flow*

The precipitation that drains into streams and rivers can take two different paths. During rainy periods, some water quickly drains across the land surface, causing streams and rivers to rise in the hours and days following the storm. This portion of the flow is often called “surface flow,” even though some of the water may soak into the ground and discharge later (e.g., through a tile drainage system).

### *Baseflow*

The rest of the water that drains into streams and rivers takes a longer, slower path; first it infiltrates into the ground, percolates down to the groundwater, and then slowly moves toward a stream. The groundwater eventually reaches the stream, maintaining flows in a river even during extended dry periods. This portion of the flow is often called “baseflow.” In hydrologic analyses, sub-surface drainage flows are typically lumped with groundwater flows.

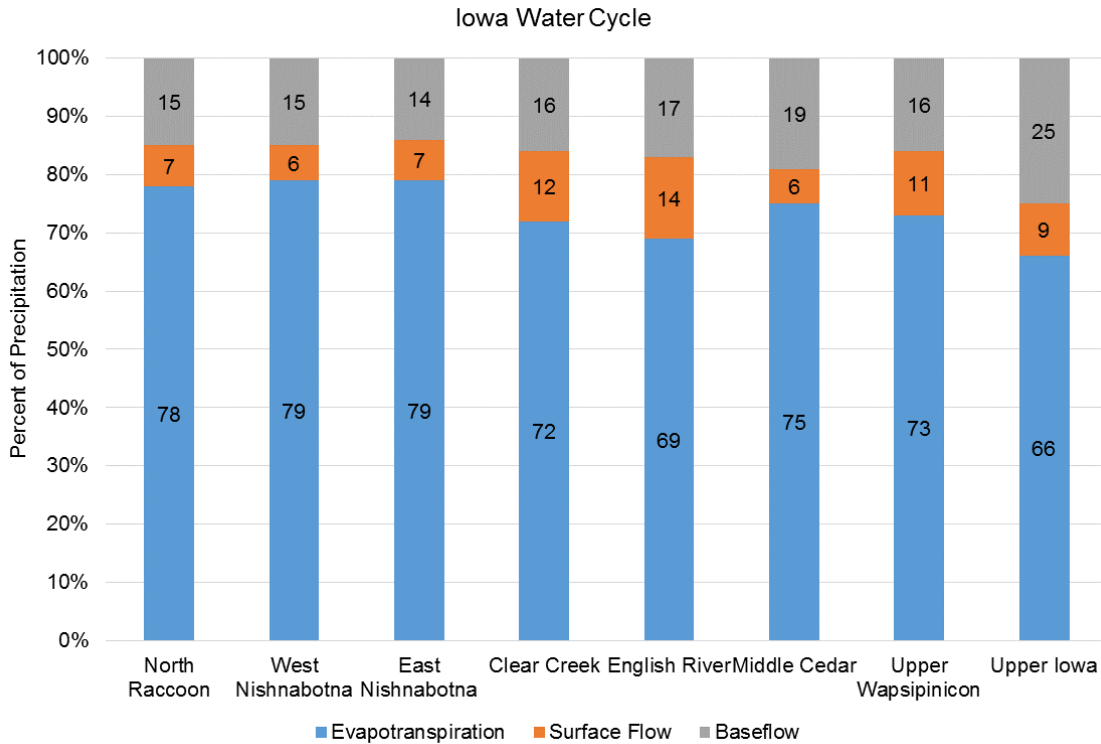


Figure 1.9. Iowa water cycle for the IWA watersheds. This shows the partitioning of average precipitation into evapotranspiration, surface flow, and baseflow components.

### iii. Shallow Groundwater and Soil Moisture Trends

Shallow groundwater and soil moisture conditions can play an important role in the transformation of rainfall into runoff. For example, several studies have identified the occurrence of very wet winters and springs (and the subsequent high soil moisture and groundwater levels) as contributing factors to the major floods in 1993 and 2008 (Linhart and Eash, 2010; Mutel, 2010; Bradley, 2010; Smith et al., 2013). Across the state, almost 400 sensors continuously monitor the condition (e.g., streamflow and stage) of the Iowa rivers. In contrast, long-term continuous data on groundwater levels or soil moisture are sparse. Figure 1.10 displays shallow groundwater information from two United States Geological Survey (USGS) wells located in two different Iowa counties. The location of the water table is influenced by several factors, such as location on the landscape, land cover, soil type, etc. In Iowa, it is very common to find the location of the water table within the first 25 feet of the soil column, except in the deep loess hills in western Iowa and incised bedrock valleys of northeast Iowa.

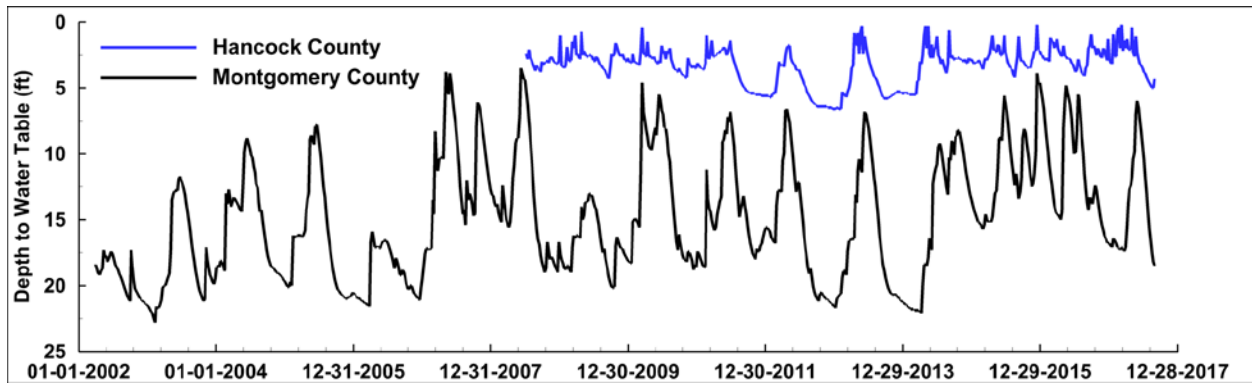


Figure 1.10. Shallow groundwater data (USGS wells).

#### iv. Floods

Rivers and streams have a finite capacity to convey water within their banks. When the amount of water surpasses that capacity, flooding occurs. Floods are typically related to large amounts of precipitation or snow melt and saturated or frozen soil. In Iowa, historic records show that the great majority (>90%) of floods occur in the spring and summer; the month of June shows the highest number of flood events. Precipitation records show that heavy rains occurred in the fall as well; however, Iowa soils have a larger capacity to infiltrate water late in the year, and therefore fall floods are less common. In Iowa’s flood history, the events of 1993 and 2008 are on an entirely different scale than the others. These two events stand out from the rest when looking at the extent of the area impacted, recovery costs, precipitation amounts, and streamflows recorded (Bradley 2010; Smith et al., 2013). Figure 1.11 shows the extent of the flooding during the flood events of 1993 and 2008. In both years, flooding impacted the eight IWA watersheds.

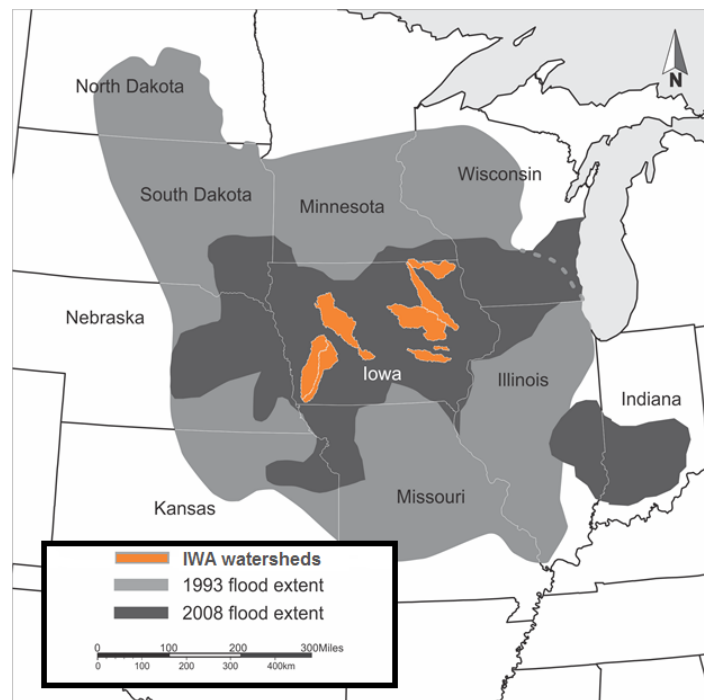


Figure 1.11. The extent of the flooding during the 1993 and 2008 floods (Bradley, 2010).

Federal disaster declarations give impacted regions access to federal recovery assistance. Current regulation permits two kinds of disaster declarations: emergency declarations and major disaster declarations (Stafford Act). Both are granted at the discretion of the president of the United States after the governor of the impacted state makes the request. FEMA records on disaster declarations are open to the public and were used to write the text and create the figures below.

- FEMA records show 952 flood-related disaster declarations (FRDD) in Iowa between 1988 and 2016. Of these, 951 were reported for Iowa counties (see Figure 1.12) and one for the Sac and Fox Tribe of the Mississippi in Iowa. All the FRDD in Iowa have been major disaster declarations except the 99 related to Hurricane Katrina evacuation (see Table 1.1), which were classified as emergency disaster declarations.

Table 1.1. FEMA disaster declarations in Iowa (1988–2016).

DISASTER TITLE	COUNT 1988-2016
SEVERE STORMS, TORNADOES, AND <i>FLOODING</i>	223
SEVERE STORMS & <i>FLOODING</i>	195
SEVERE STORMS, TORNADOES AND <i>FLOODING</i>	106
<i>HURRICANE</i> KATRINA EVACUATION	99
SEVERE STORMS AND <i>FLOODING</i>	98
SEVERE STORMS, <i>FLOODING</i> , AND TORNADOES	97
SEVERE STORMS, TORNADOES, STRAIGHT-LINE WINDS, AND <i>FLOODING</i>	79
SEVERE WINTER STORM	62
SEVERE WINTER STORMS	48
ICE STORM	44
SEVERE STORMS, STRAIGHT-LINE WINDS, AND <i>FLOODING</i>	34
SNOW	30
SEVERE WINTER STORMS AND SNOWSTORM	27
SEVERE STORMS, AND <i>FLOODING</i>	15
SEVERE SNOWSTORMS	13
<i>FLOODING</i>	6
SEVERE STORMS, TORNADOES, AND STRAIGHT-LINE WINDS	6
RAIN, WINDS, & TORNADOES	1
SEVERE STORM	1

1184

- In the last 30 years, every county in Iowa has experienced sufficiently large and severe flood events to warrant a presidential disaster declaration. The number of FRDDs for each Iowa county from 1988–2016 is shown in Figure 1.12.
- The eastern half of the state has received more FRDDs than the western part. In addition, most counties in Northeast Iowa have received at least 10 FRDDs in the last three decades. The two counties with the lowest and highest number of FRDDs are O'Brien (4) and Clayton (17), respectively.
- Since 1988, the longest period with no FRDDs in Iowa was two years, which can be seen in Figure 1.13. The years with the highest number of FRDDs were 1993, 2005, and 2008. Remarkably, the number of FRDDs in 1993 is higher than the number of counties in Iowa. In that year, 15 counties received two FRDDs, one in late April and the second in early July (Buchanan, Butler, Des Moines, Linn, Black Hawk, Muscatine, Benton, Cedar, Louisa, Tama, Webster, Floyd, Mitchell, Kossuth, and Scott counties).

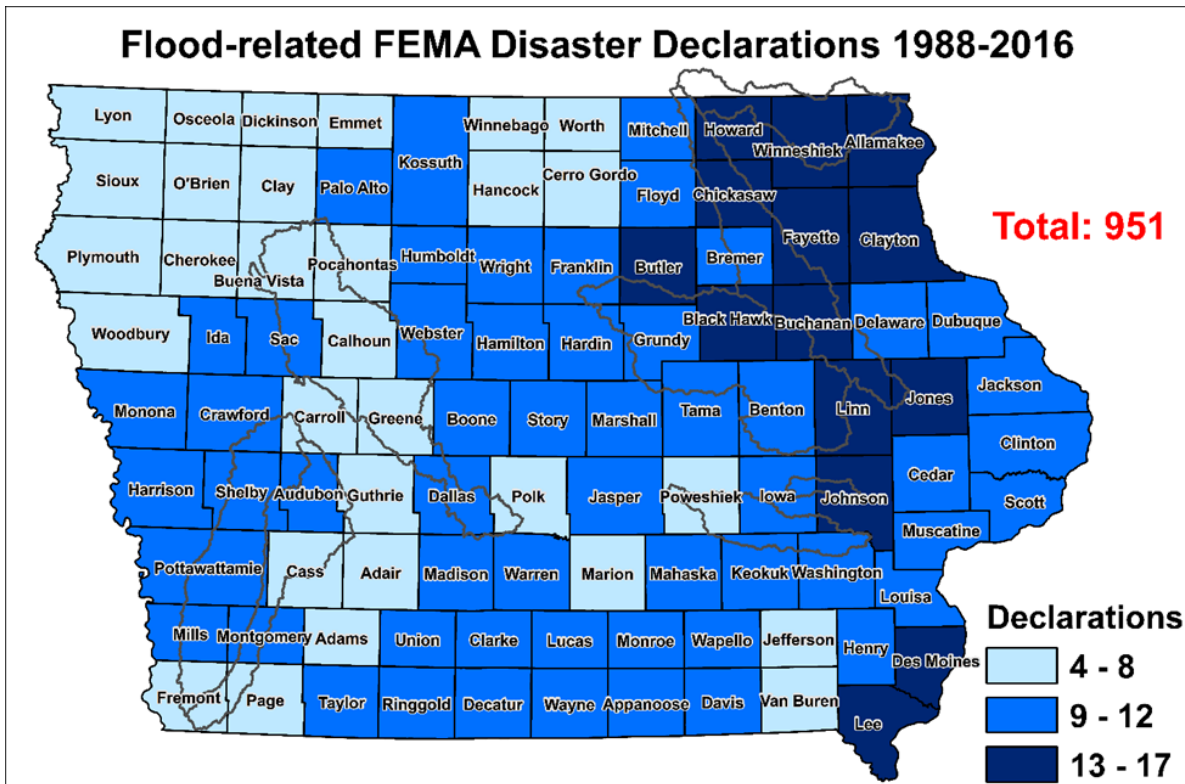


Figure 1.12. Number of flood-related federally declared disasters in Iowa counties (1988–2016). Data source: <https://www.fema.gov/>.

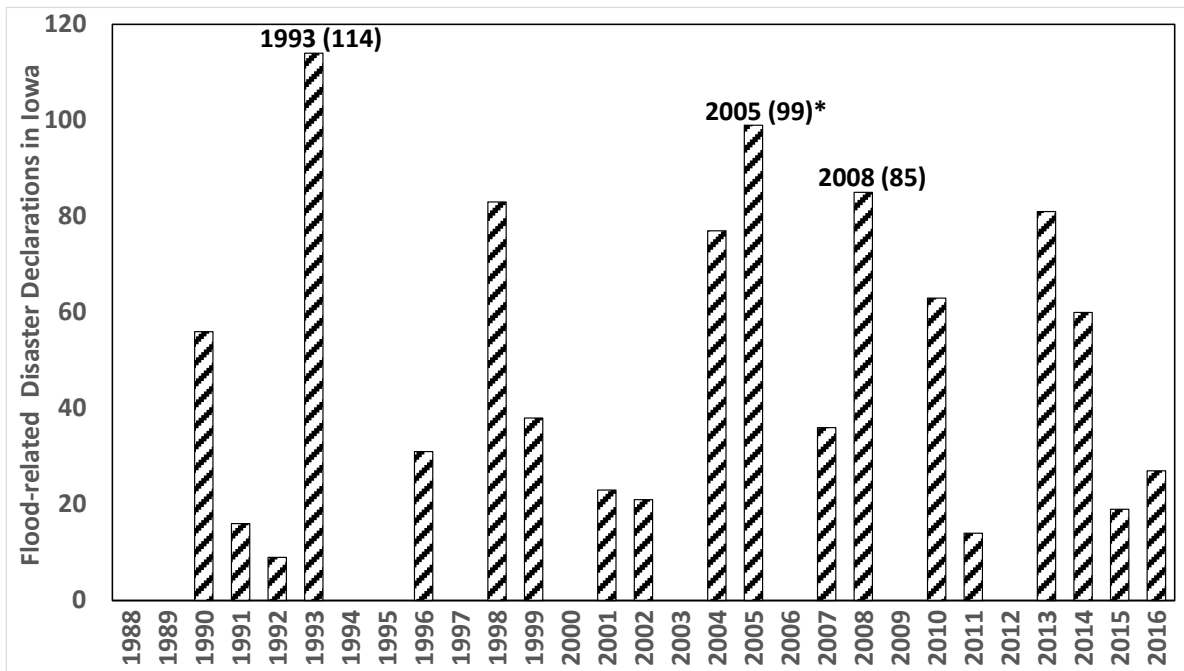


Figure 1.13. The number of flood-related federally declared disasters in Iowa (1988–2016). Data source: <https://www.fema.gov/>.

## v. Droughts

Like floods, droughts are a recurrent phenomenon and part of the Earth's climate. Droughts are characterized by periods with precipitation deficits; depending on their severity, these can also include very low streamflows as well as reduced soil moisture and groundwater levels.

Unlike floods, droughts tend to progress slowly, and their onset is not easily identifiable. The extremely dry period of the 1930s (known as the "Dust Bowl") is still considered the unsurpassable benchmark against which all other droughts will be measured. In Iowa's recent history, both 1988 and 2012 stand out as drought years. Overall, comparisons of these two droughts reveal some similarities. In 1988, Iowa had its 4<sup>th</sup> hottest and 14<sup>th</sup> driest summer; whereas the 2012 summer was the 14<sup>th</sup> hottest and 5<sup>th</sup> driest in the observational record (Harry Hillaker, state climatologist).

Since 1999, several federal agencies and academic institutions partnered to create the U.S. Drought Monitor (USDM, <http://droughtmonitor.unl.edu/>), which releases a weekly map of drought conditions for the United States. Drought conditions are classified in five categories: Abnormally Dry (D0), Moderate Drought (D1), Severe Drought (D2), Extreme Drought (D3), and Exceptional Drought (D4). The map presented in Figure 1.14, shows the extent of 2012 drought in Iowa using data generated by the USDM.

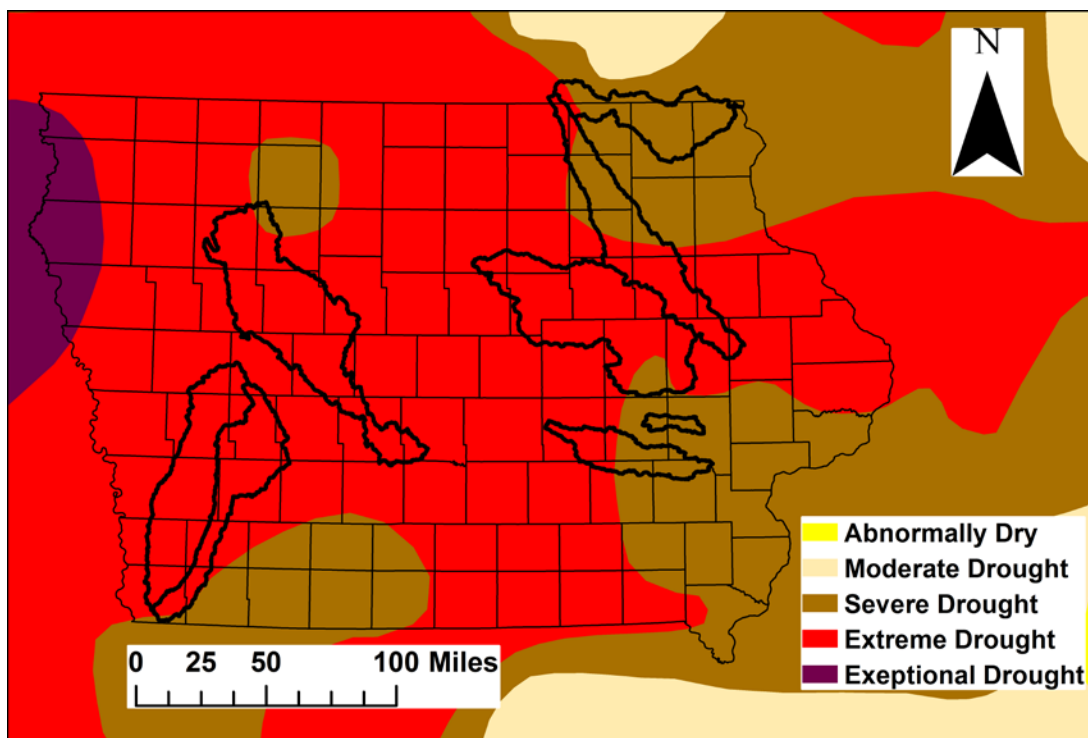


Figure 1.14. Drought conditions, October 09, 2012. (Source: <http://droughtmonitor.unl.edu/>).

## c. Hydrological Alterations in Iowa and the Iowa Watershed Approach Study Areas

Although the hydrologic conditions presented for the Iowa Watershed Approach study areas illustrate the historical water cycle, the watersheds themselves are not static; historical changes have occurred that have altered the water cycle. In this section, we discuss the hydrological alterations of Iowa's watersheds.

### i. Hydrological Alterations from Agricultural-Related Land Use Changes

The Midwest, with its low-relief poorly-drained landscape, is one of the most intensively managed areas in the world (Schilling et al., 2008). With European-descendent settlement, most of the land was transformed from low-runoff prairie and forest to higher-runoff farmland (see Figure 1.3 and 1.4). Within Iowa, the land cover changes in the first decades of settlement occurred at an astonishing rate (Wehmeyer et al., 2011). Using land cover information obtained from well-documented studies in 1859, 1875, and 2001, Wehmeyer et al. (2011) estimated that the increase in runoff potential in the first 30 years of settlement represents the majority of predicted change in the 1832 to 2001 study period.

Still, other transformations associated with an agricultural landscape have also impacted runoff potential (see Table 1.2). For example, the introduction of conservation practices in the second half of the 20<sup>th</sup> century tend to reduce runoff, as suggested by a recent study of an Iowa watershed (Papanicolaou et al., 2015). The Conservation Reserve Program (CRP) originally began in 1950s. The federal government established many programs in the 1970s to remove lands from agricultural production and establish native or alternative permanent vegetative cover; in an effort to reduce erosion and gully formation, government agencies also encouraged practices such as terraces, conservation tillage, and contour cropping. The Farm Bill of 1985 was the first act that officially established the CRP as we know it today; the Farm Bills of 1990, 1996, 2002, and 2008 expanded these activities. The 2014 Farm Bill gradually reduced the CRP cap from 32 million acres to 24 million acres, although the 2018 Farm Bill is expected to increase the CRP cap to 29 million acres. Table 1.2 summarizes the timeline of agriculture-driven land use changes and their impacts on local hydrology.

Table 1.2. Agricultural-Related Alterations and Hydrologic Impacts.

<i>Timeline</i>	<i>Land use status, change, &amp; interventions</i>	<i>Hydrologic effect(s)</i>	<i>Source</i>
1830s–Prior	Native vegetation (tall-grass prairies and broad-leaved flowering plants) dominate the landscape	Baseflow dominated flows; slow response to precipitation events	Petersen (2010)
1830–1980	Continuous increase in agricultural production by replacement of perennial native vegetation with row crops 1940: <40% row crop (Raccoon) 1980: 75% row crop (statewide)	Elimination of water storage on the land; acceleration of the upland flow; expanded number of streams; increased stream velocity	Jones & Schilling (2011); Knox (2001)
1820–1930	Wetland drainage, stream channelization (straightening, deepening, relocation) leading to acceleration of the rate of change in channel positioning	Reduction of upland and in-stream water storage, acceleration of stream velocity	Winsor (1975); Thompson (2003); Urban & Rhoads (2003)
1890–1960 2000–present	Reduction of natural ponds, potholes, wetlands; development of large-scale artificial drainage system (tile drains)	Decrease of water storage capacity, groundwater level fluctuations, river widening	Burkart (2010); Schottler et al. (2013)
1940–1980	Construction of impoundments and levees in Upper Mississippi Valley	Increased storage upland	Sayre (2010);
1950–present	Modernization/intensification of the cropping systems	Increased streamflow, wider streams	Zhang & Schilling (2006); Schottler et al. (2013)
1970–present	Conservation practices implementation: Conservation Reserve Program (CRP); Conservation Reserve Enhancement Program (CREP); Wetland Reserve Program (WRP)	Reduction of runoff and flooding; increase of upland water storage	Castle (2010); Schilling (2000); Schilling et al. (2008);
2001–present	62% of Iowa’s land surface is intensively managed to grow crops (dominated by corn and soybeans up to 63% of total)	About 25% to 50% of precipitation converted to runoff (when tiling is present)	Burkart (2010)

## ii. Hydrological Alterations Induced by Climate Change

The U.S. government recently released The Climate Science Special Report (Wuebbles et al., 2017) summarizing the state-of-the-art science on climate change and its physical effects. The CSSR writing team is comprised of three coordinating lead authors from the National Science Foundation and U.S. Global Change Research Program, NOAA Earth System Research Laboratory, and NASA Headquarters. In addition, more than 50 experts from federal agencies, departments, and universities are listed as lead authors, review editors, and contributing authors. CSSR is “designed to be an authoritative assessment of the science of climate change, with a focus on the United States, to serve as the foundation for efforts to assess climate-related risks and inform decision-making about responses.” The information below presents text and figures taken from the CSSR that are relevant to the IWA watersheds, Iowa, and the Midwest.

*“Heavy rainfall is increasing in intensity and frequency across the United States (see Figure 1.15) and globally and is expected to continue to increase over the next few decades (2021–2050, see Figure 1.16), annual average temperatures are expected to rise by about 2.5°F for the United States, relative to the recent past (average from 1976–2005), under all plausible future climate scenarios.”*

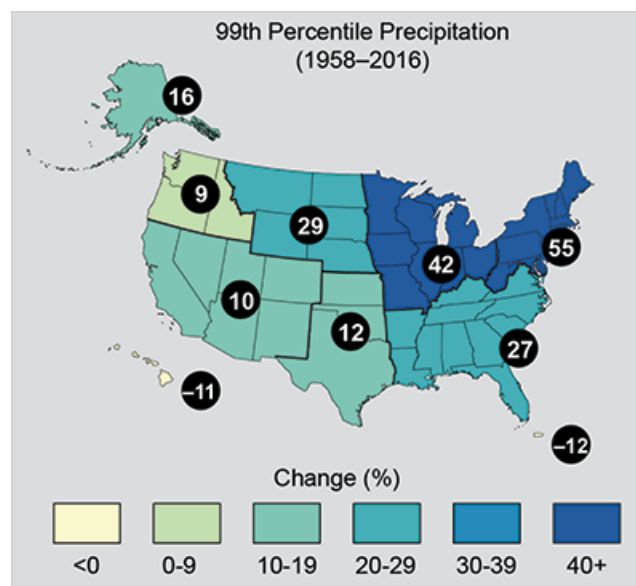


Figure 1.15. Observed change in heavy precipitation (the heaviest 1%) between 1958 and 2016. Figure taken from The Climate Science Special Report (Easterling et al. 2017) (<https://science2017.globalchange.gov/>).

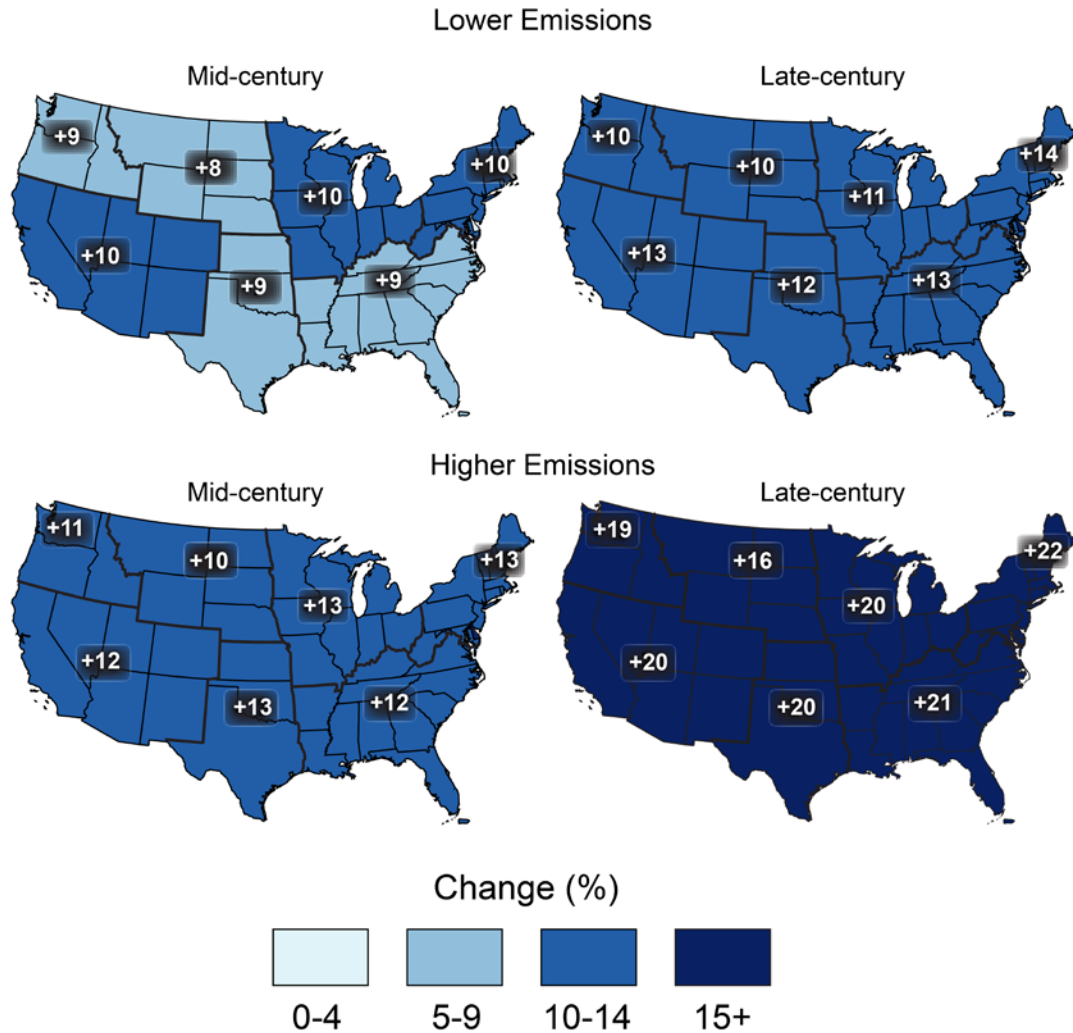


Figure 1.16. Projected change in heavy precipitation. Twenty-year return period amount for daily precipitation for mid- (left maps) and late-21<sup>st</sup> century (right maps). Results are shown for a lower emissions scenario (top maps; RCP4.5) and for a higher emissions scenario (bottom maps, RCP8.5). Figure taken from The Climate Science Special Report (Easterling et al. 2017) (<https://science2017.globalchange.gov/>).

### iii. Hydrological Alterations Induced by Urban Development

Although Iowa remains an agricultural state, a significant majority of its population resides in urban areas. The transition from agricultural to urban land uses has a profound impact on local hydrology, increasing the amount of runoff, the speed at which water moves through the landscape, and the magnitude of flood peaks. The factors that contribute to these increases (Meierdiercks et al., 2010) are the increase in the percentage of impervious areas within the drainage catchment and its location (Mejia et al., 2010), and the more efficient drainage of the landscape associated with the constructed drainage system – the surface, pipe, and roadway channels that add to the natural stream drainage system. Although traditional stormwater

management practices aim to reduce increased flood peaks, urban areas have long periods of high flows that can erode stream channels and degrade aquatic habitat.

## d. Assessment of Iowa's Water Quality

### i. Iowa Water-Quality History

Prior to European settlement in the 19<sup>th</sup> century, Iowa was covered with prairies, oak savannahs, wetlands, and forests (see Figure 1.3). Much of the landscape was internally drained, meaning that rainfall and snowmelt drained to small depressional areas, rather than streams. Groundwater-fed streams meandered across the landscape and likely ran shallow and clear, carrying low levels of sediment and nutrients. Rivers easily spilled out into the flood plain after heavy rains, and river banks re-vegetated during drought, reducing streambank erosion.

Over several decades, the native prairie was broken and cultivated for corn, oats, and alfalfa, as well as a few other minor crops. Soil erosion was intense in the first years following a field's cultivation. From the period of 1880 to 1920, pervious clay pipes drained many of Iowa's wettest areas. This was most common in the recently-glaciated area of north-central Iowa known as the Des Moines Lobe, shown in Figure 1.2. Many new streams were constructed in ditches to drain water externally to the river network. Many existing streams were straightened to facilitate crop production.

The post-World War II era brought new developments to agriculture. The emergence of chemical fertilizers, soybeans, and continued drainage of the landscape with plastic drainage tiles helped Iowa become a world leader in crop and livestock production.

The loss of the native ecosystems, stream straightening and incision, artificial drainage, and discharges from industries and municipalities degraded water quality. Although the decline in water quality probably subsided in the early 1980s, Iowa's streams still carry more nutrients and sediment than most people find acceptable.

### ii. Water Quality in the Post-Clean Water Act Era

The Federal Water Pollution Control Act of 1948 was the first major U.S. law to address water pollution. Growing public awareness and concern for controlling water pollution led to sweeping amendments in 1972. The amended law became commonly known as the Clean Water Act (CWA). The 1972 Amendments achieved the following: (1) established the basic structure for regulating pollutant discharges into the waters of the United States; (2) gave EPA the authority to implement pollution control programs, such as setting wastewater standards for industry; (3) maintained existing requirements to set water-quality standards for all contaminants in surface waters; (4) made it unlawful for any person to discharge any pollutant from a point source into navigable waters, unless a permit was obtained under its provisions; (5) funded the construction of sewage treatment plants under the construction grants program; and (6) recognized the need for planning to address the critical problems posed by nonpoint source pollution.

After passage of the CWA, construction began on many new wastewater treatment facilities in Iowa, and upgrades were implemented on many existing treatment works. Undoubtedly these efforts improved water quality in several of Iowa's major interior rivers, in addition to the Missouri and Mississippi rivers on its borders. Improvements in the levels of ammonia, oxygen demand, Kjeldahl (organic) nitrogen, and dissolved oxygen were particularly important. These improvements made river water quality much more suitable for recreation and aquatic life, especially near Iowa's larger cities. However, the CWA provisions to address non-point source pollution (i.e., pollution from diffuse areas) proved relatively ineffective in reducing levels of nutrients and sediment in Iowa streams. The main CWA program designed to address non-point source pollution was the 319 Grant Program, which was amended to the CWA in 1987.

The Food Security Act of 1985 (Farm Bill) required farmers participating in most programs administered by the Farm Service Agency (FSA) and the Natural Resources Conservation Service (NRCS) to abide by certain conditions on any highly erodible land owned or farmed, or land considered a wetland. To comply with the highly erodible land conservation and wetland conservation provisions, farmers were required to certify that they would not: (1) produce an agricultural commodity on highly erodible land without a conservation system; (2) plant an agricultural commodity on a converted wetland; and (3) convert a wetland to produce an agricultural commodity. As result of these requirements, sediment levels in Iowa streams declined and water clarity improved (Jones and Schilling, 2011). Phosphorus levels also declined in unison with the improvements in sediment transport and water quality (Wang et al., 2016). However, conservation compliance, as these requirements are known, has not had a similar beneficial effect on stream nitrate levels (Sprague et al., 2011; Jones et al., 2017).

Iowa policy-makers and watershed stakeholders look to the Impaired Waters list, Section 303(d), as a common reference point to gauge statewide water quality. According to Section 303(d) of the CWA, from "time to time," states must submit a list of lakes, wetlands, streams, rivers and portion of rivers for which effluent limits will not be sufficient to meet all state water-quality standards. The EPA has defined "time to time" to mean April 1 of even numbered years. The failure to meet water-quality standards might be due to an individual pollutant, multiple pollutants, "pollution," or an unknown cause of impairment. The 303(d) listing process includes waters impaired by point sources and non-point sources of pollution. States must also establish a priority ranking for the listed waters, considering the severity of pollution and uses. In 2016, there were 608 category 5 Iowa waterbodies with 818 impairments. In 2014, there were 571 impaired waterbodies with 754 impairments. Category 5 waterbodies are those where a Total Maximum Daily Load assessment is required. Category 4 includes waterbodies that are impaired but at either impaired by something other than a pollutant or where a TMDL has already been completed. Combined, categories 4 and 5 constitute all the impaired waters in the state. About 58% of Iowa's assessed streams (not all streams have been assessed), are considered "impaired"; 23% are considered "potentially impaired"; and 19% are considered to have "good" water quality. Indicator bacteria (i.e., *E. coli*) are the most common cause of impairment, causing about half of all such designations. Biological impairments are next, followed by fish kills. Figure 1.17 lists the main causes. Figure 1.18 shows historical numbers of impaired Iowa waters.

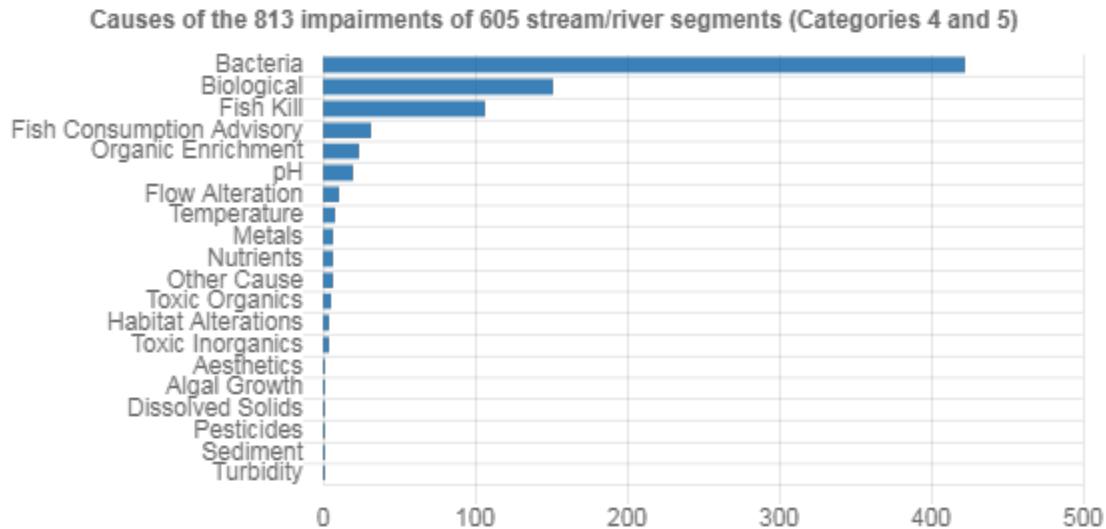


Figure 1.17. Causes of impairments in Iowa’s impaired waters. (Iowa Department of Natural Resources, 2018).

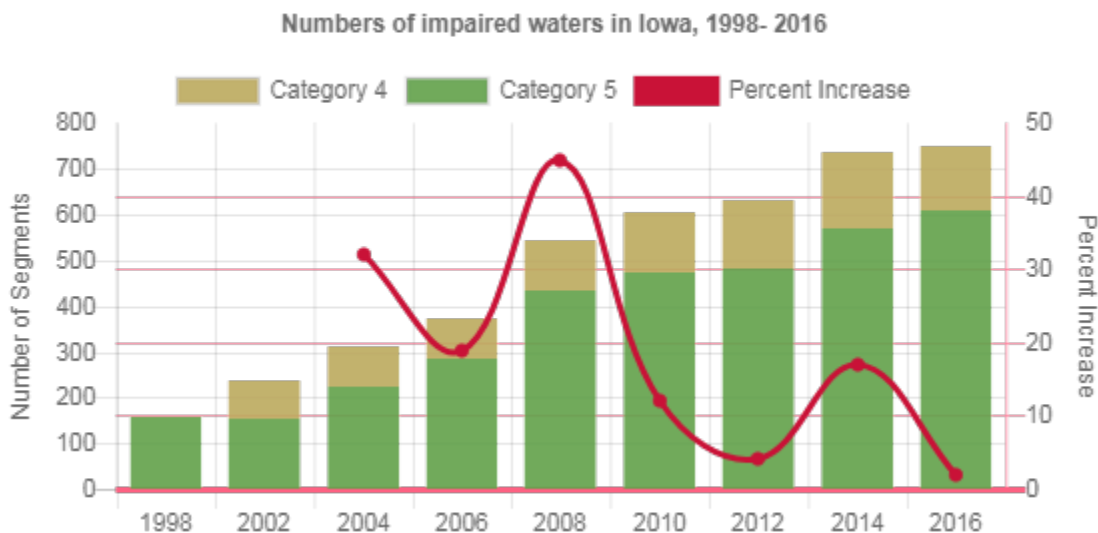


Figure 1.18. Number of impaired Iowa waters, 1998–2016. (Iowa Department of Natural Resources, 2018).

### e. Web-Based Information Systems of Flood and Water-Quality Data

IIHR—Hydroscience & Engineering and the IFC at the University of Iowa have pioneered the creation of user-friendly, interactive, web-based information systems (WBIS) to communicate environmental information in Iowa and the United States. These two institutions also have expertise in the installation of real-time environmental monitoring systems and currently administer and maintain extensive networks that record flood and water-quality data in Iowa. WBIS displays this information, along with data collected by other federal institutions.

## **i. The Iowa Flood Information System (IFIS)**

The Iowa Flood Information System (IFIS) is a one-stop web-platform to access community-based flood conditions, forecasts, visualizations, inundation maps, and flood-related information, visualizations, and applications. IFIS can be accessed using this URL: <http://ifis.iowafloodcenter.org/ifis/>. Below is an overview on some of the information available on IFIS.

### ***Floodplain inundation maps***

In partnership with the IDNR, the IFC has created statewide floodplain maps that estimate flood hazard extents and depths for every stream in the state of Iowa draining greater than one square mile. The maps depict flood boundaries and depths for eight different annual probabilities of occurrence: 50-, 20-, 10-, 4-, 2-, 1-, 0.5-, and 0.2-%, allowing Iowans to better understand their flood risks and make informed land management decisions. The statewide floodplain maps can be accessed through IFIS or at <http://www.iowafloodmaps.org/>. Figure 1.19 shows an example of statewide floodplain map data.

### ***Community-based inundation maps***

The IFC has also developed online inundation map libraries for more than 20 Iowa communities that relate forecasted or observed flow conditions to flood extents and depths. These inundation map libraries use detailed computer models that consider small-scale floodplain and channel features, bridges, and dams to better simulate the physics of flowing water. The maps allow a user to “translate” a forecasted river stage at a USGS gauge to flood extents and depths in the community, to better anticipate and respond to immediate flood hazards, and to consider “what-if” scenarios for long-term planning. Community inundation map libraries can be accessed on IFIS. Figure 1.20 shows the inundation map library interface for the city of Des Moines.

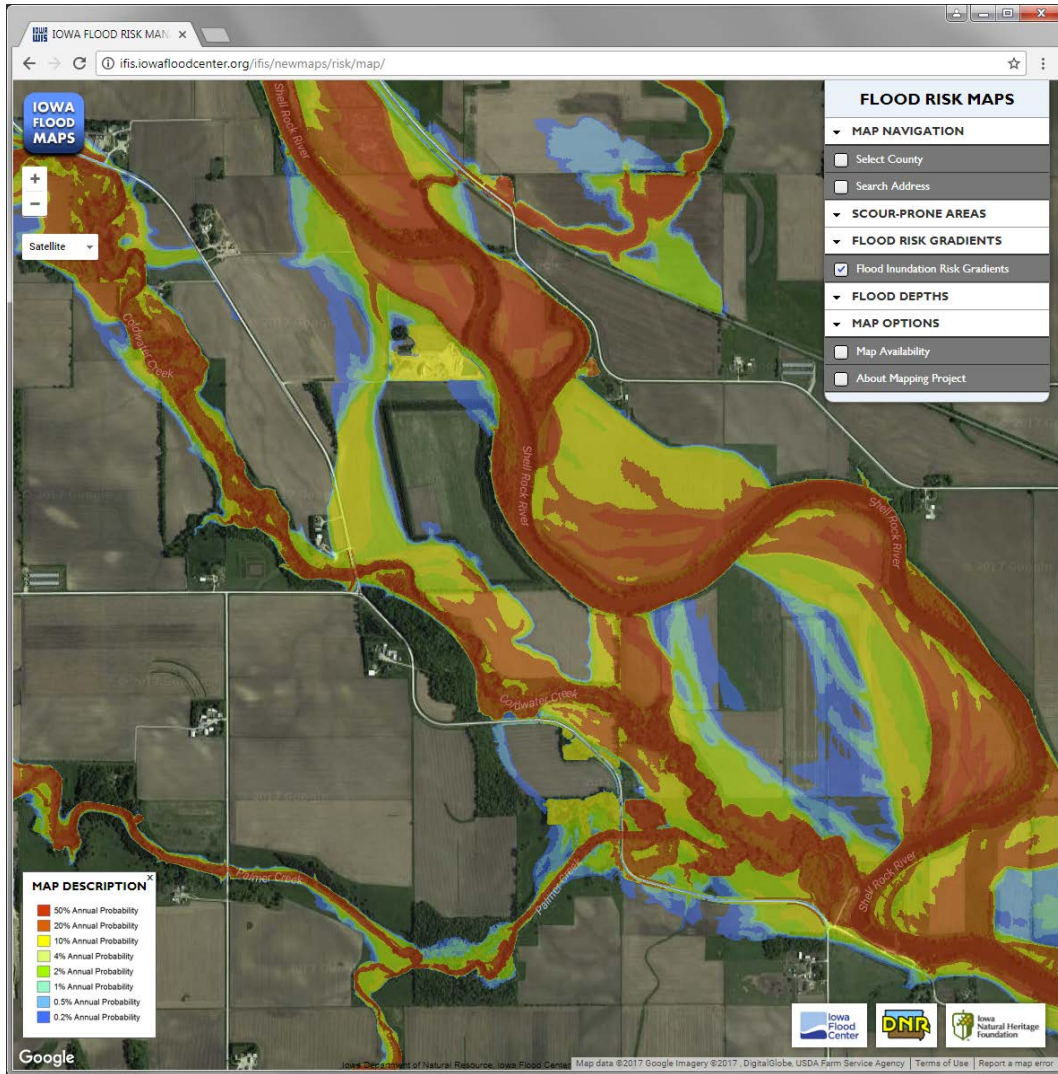


Figure 1.19. Statewide floodplain map data showing different levels of annual flood risk.

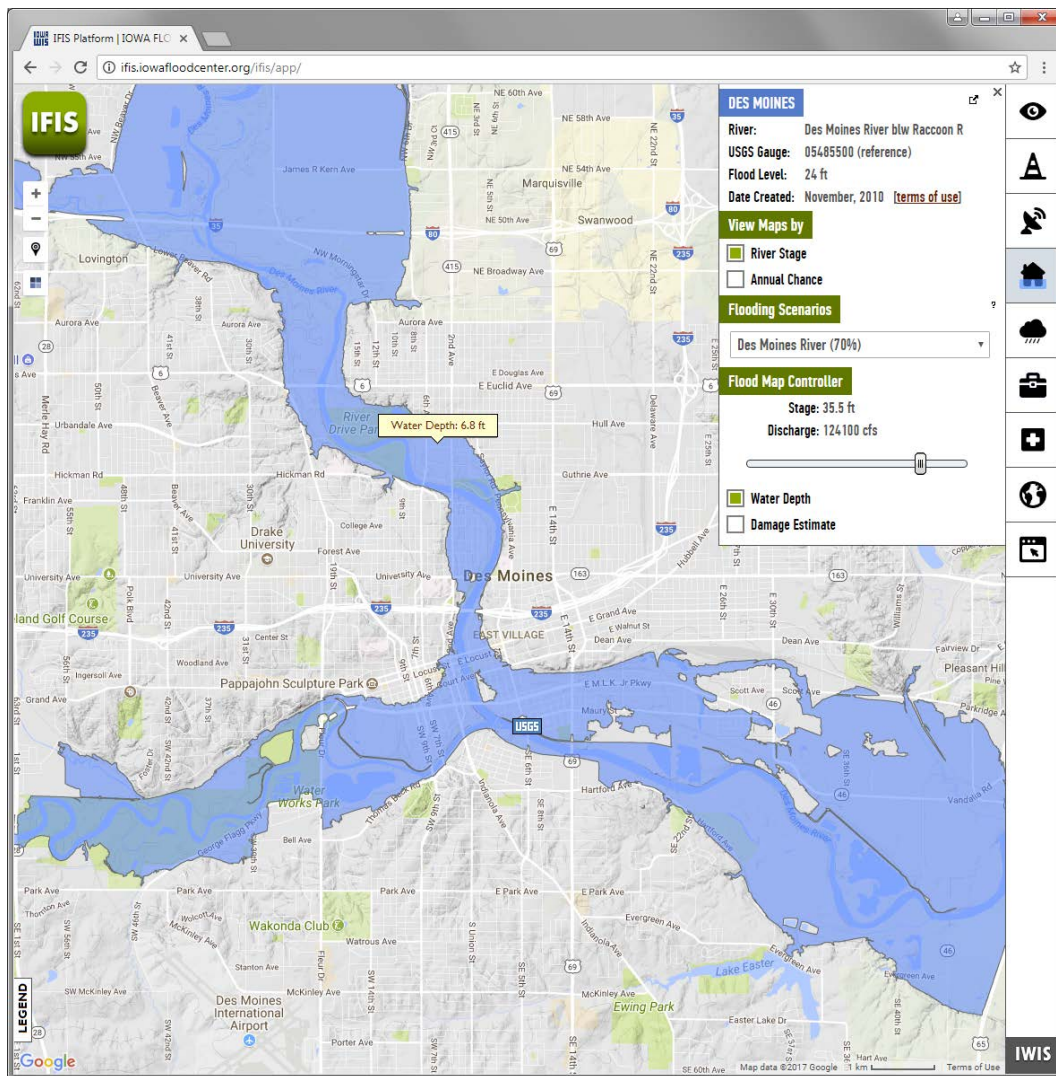


Figure 1.20. Flood inundation map library for the Des Moines and Raccoon rivers in the city of Des Moines.

### ***Observed stream conditions***

IFIS displays data from more than 400 sensors continuously monitoring Iowa stream conditions in real-time, which is shown in Figure 1.21. Currently, the USGS collects streamflow data at approximately 200 locations, and the IFC administers and maintains a growing network of more than 250 stream-stage sensors that record stage conditions.

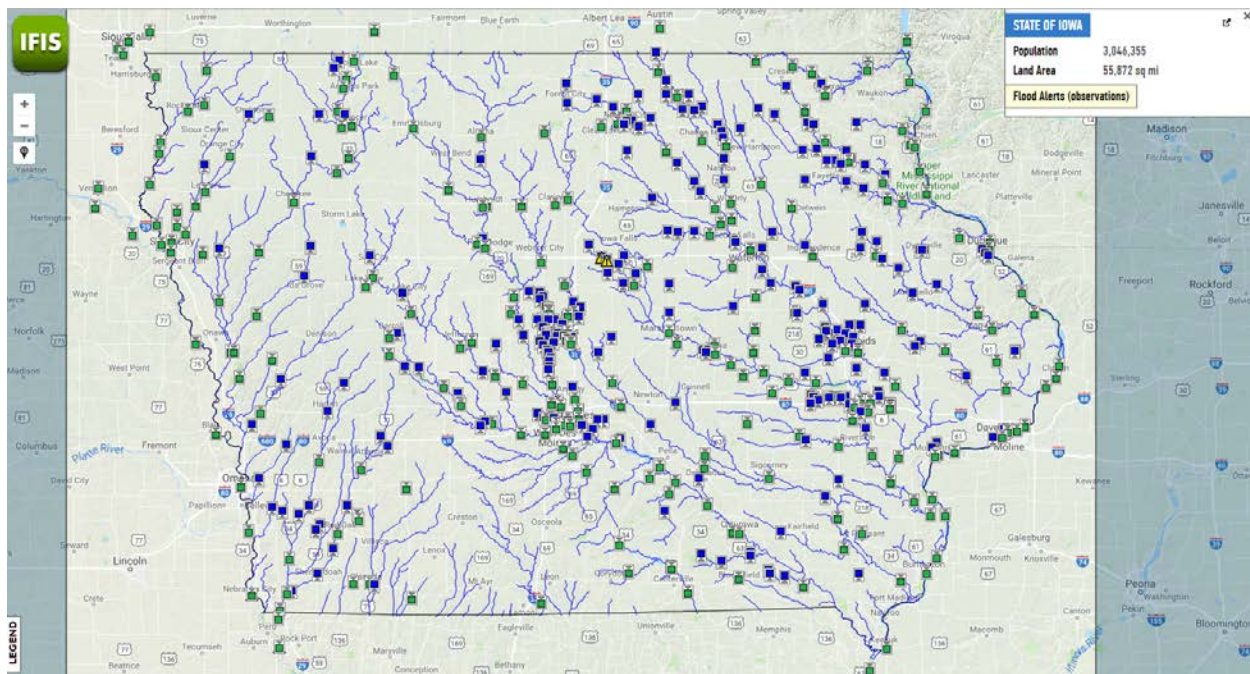


Figure 1.21. USGS (green) and Iowa Flood Center (blue) stream-stage monitoring locations displayed in the Iowa Flood Information System (IFIS).

### ***Flood alerts, warnings, and forecasts***

IFIS provides flood alerts for stream sensors with stage values higher than the threshold values for the four flood levels defined by National Weather Service (NWS) and the IFC. Different colors represent the four flood stage levels (action, flood, moderate flood, and major flood). The flood forecast products included in IFIS are the NWS six-hourly forecast for 48 hours and the NWS seasonal forecast for 90 days. IFIS integrates short-term NWS forecasts into real-time data series and more-info views. The NWS shares a seasonal forecast probability for minor, moderate, and major flooding for a three-month period. The Iowa Flood Center has developed a real-time, high-performance computing based flood forecasting model that provides quantitative stage and discharge forecasts and a five-day flood risk outlook in IFIS for more than 1,500 locations (e.g., communities and stream gauges) in Iowa.

The IFC system complements the operational forecasts issued by the NWS and is based on sound scientific principles of flood genesis and spatial organization. At its core is a continuous rainfall-runoff model based on landscape decomposition into hillslopes and channel links. The input to the system comes from a radar-rainfall algorithm, developed in-house, that maps rainfall every 5 min with high spatial resolution.

### **ii. The Iowa Water-Quality Information System**

The Iowa Water-Quality Information System (IWQIS) integrates real-time water-quality data collected by IIHR and the USGS, along with a variety of watershed-related information such as precipitation, stream flow and stage, soil moisture, and land use. IWQIS (<https://iwqis.iowawis.org/>) provides useful information for researchers, agencies, landowners,

and other watershed stakeholders as they study, analyze, and work to better understand the fate and transport of nutrients in Iowa’s waterways. Iowa WQIS also helps Iowa monitor progress toward achieving the goals of the Iowa Nutrient Reduction Strategy. Iowa has the largest concentration of continuous nutrient and water-quality sensors in the United States; as of 2018, the state has a water-quality network comprised of:

- 74 nitrate sensors (14 operated by USGS)
- 27 hydrolabs (pH, SC, DO, temp)
- 26 turbidimeters
- 4 ortho-P sensors
- 4 ISCOs

This network generates data for science and policy-making, facilitates individual BMP performance assessments, and allows Iowa to quantify the nutrient loads leaving the state. Figure 1.22 is a screenshot of IWQIS displaying the WQ network (2018).

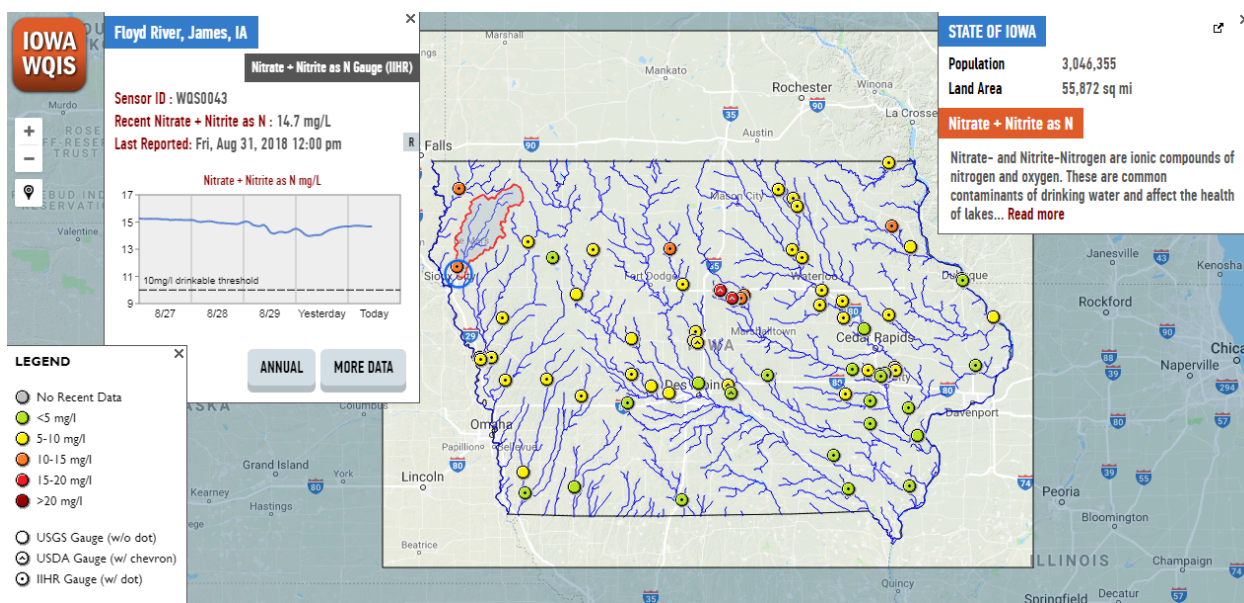


Figure 1.22. IIHR—Hydroscience & Engineering and USGS surface water-quality monitoring locations as displayed in the Iowa Water Quality Information System (IWQIS).

### iii. The Iowa Watershed Approach Information System (IWAIS)

IIHR and IFC are developing a web-based information system to provide public access to general information and updates on the IWA project, existing and potential BMPs in IWA watersheds, hydrologic and water-quality data collected in the IWA watersheds, and resources to improve flood resiliency. The website can be accessed at: <http://iowawatershedapproach.org>. Figure 1.23 shows an example view of the IWAIS interface showing the number of existing ponds within each HUC 12 in the Middle Cedar River Watershed.

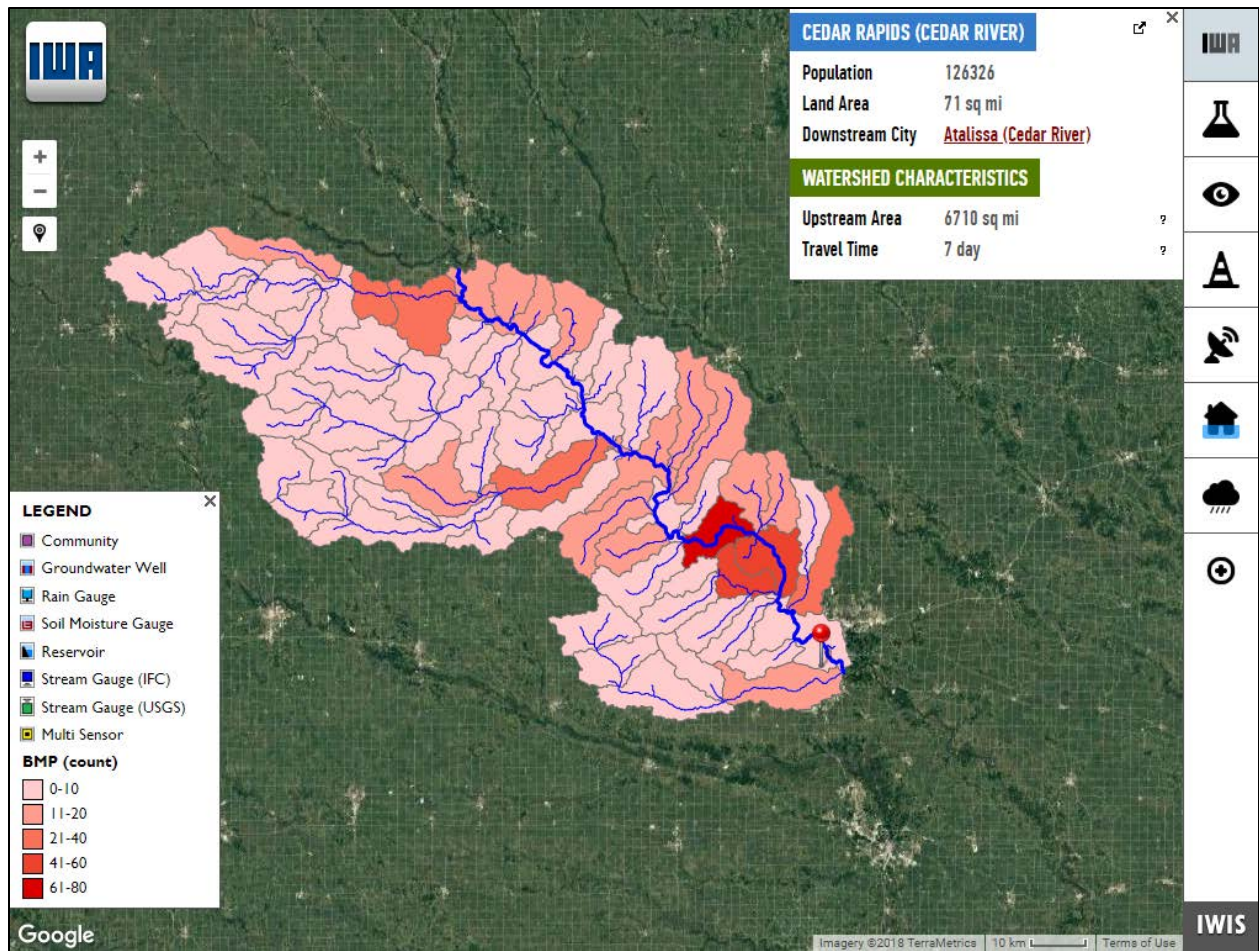


Figure 1.23. Example IWAIS interface view showing the number of existing ponds within each HUC 12 in the Middle Cedar River Watershed.

## 2. Conditions in the North Raccoon River Watershed

This chapter provides an overview of current North Raccoon River Watershed conditions, including hydrology, geology, topography, land use, and hydrologic/meteorologic instrumentation, and historic water cycle, as well as a summary of previous floods of record.

### a. Hydrology

The North Raccoon River Watershed as defined by the boundary of eight-digit Hydrologic Unit Code (HUC 8) 07100006 is in west-central Iowa and encompasses approximately 2471 square miles (mi<sup>2</sup>). The North Raccoon River is joined by South Raccoon River (HUC 8) 07100007 near Van Meter, Iowa, forming the Raccoon River, flowing west to east into the Des Moines River at Des Moines, Iowa. The total drainage area of the Raccoon River at Des Moines is approximately 3608 mi<sup>2</sup>. The North Raccoon River Watershed boundary falls within 15 counties in total, as shown in Figure 2.1; however, most of the watershed area lies within Buena Vista, Pocahontas, Sac, Calhoun, Webster, Carroll, Greene, Dallas, and Polk Counties.

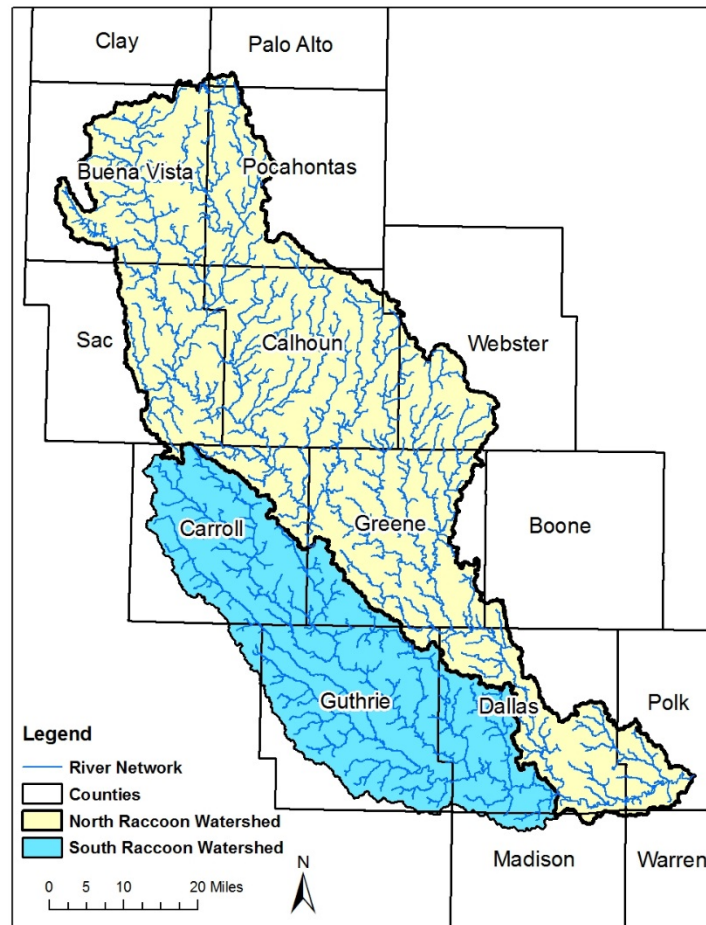


Figure 2.1. The North Raccoon River Watershed (HUC 8 07100006), drains 2471 mi<sup>2</sup>. The North Raccoon River joins the South Raccoon River near Van Meter, Iowa.

Average annual precipitation in Iowa ranges from 26–40 inches, with the lowest precipitation in the northwest corner of the state and the highest in the southeast corner. The average annual precipitation ranges from roughly 33–36 inches in the North Raccoon River Watershed (PRISM, 1981–2010). About 75% of the annual precipitation falls as rain during the months of April–September. During this period, thunderstorms capable of producing torrential rains are possible, with the peak frequency of such storms occurring in June. Central Iowa has experienced increased variability in annual precipitation since 1975, along with a general increase in the amount of spring rainfall (U.S. Department of Agriculture — Iowa State University, 2011).

## b. Geology and Soils

A landscape is a collection of terrain features or landforms (Iowa Geological & Water Survey, 2013). These combinations of surface features and underlying soils influence how water moves through the landscape.

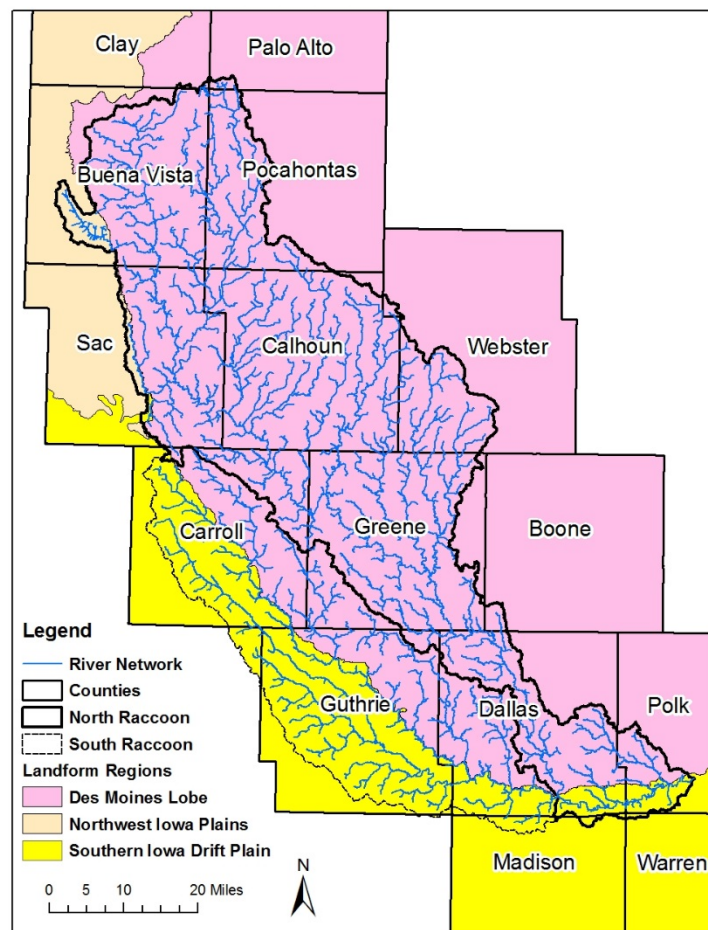


Figure 2.2. Defined Landform Regions of the North Raccoon River Watershed.

The North Raccoon River Watershed is located within three identified landform regions, the Des Moines Lobe, Northwest Iowa Plains, and Paleozoic Southern Iowa Drift Plain. While each

landform region has a unique influence on the rainfall-runoff characterization, the North Raccoon River watershed is dominated by the Des Moines Lobe.

The Des Moines Lobe was shaped by the last glacier to enter Iowa. The glacier entered Iowa in a series of surges beginning 15,000 years ago. By 12,000 years ago, the slowly decaying ice sheet was gone, leaving behind a poorly drained landscape underlain by pebbly clay and areas of sands and gravels from swift meltwater streams. Today, broadly curved bands of ridges and knobby hills called moraines, mark the position of stationary ice fronts (Iowa Geological & Water Survey, 2017). Natural lakes have formed in large, scoured depressions. Abundant smaller depressions dot the landscape and are characterized as wetlands known as potholes. These depressions may hold water year-round, however many do not and only intermittently fill during heavy rainfall events or with snowmelt in the spring of the year. Many have been drained through the use of intakes and piping networks. Figure 2.3 shows a typical Des Moines Lobe cross-section.

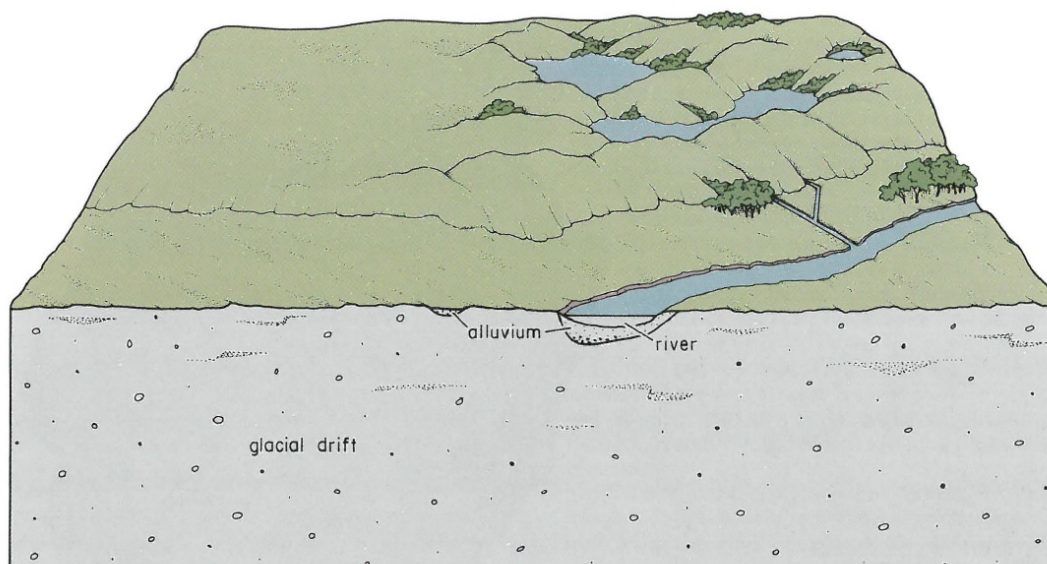


Figure 2.3. Typical Des Moines Lobe cross-section (Prior 1991).

The southern portion of the watershed, primarily the Raccoon River downstream of the confluence of the North and South Raccoon Rivers, lies in the Southern Iowa Drift Plain. This region is dominated by glacial deposits left by ice sheets that extended south into Missouri over 500,000 years ago. The deposits were carved by deepening episodes of stream erosion so that only a horizon line of hill summits marks the once-continuous glacial plain. Numerous rills, creeks, and rivers branch out across the landscape shaping the old glacial deposits into steeply rolling hills and valleys. A mantle of loess drapes the uplands and upper hill slopes (Iowa Geological & Water Survey, 2017). Figure 2.4 shows a typical Southern Iowa Drift Plain cross-section.

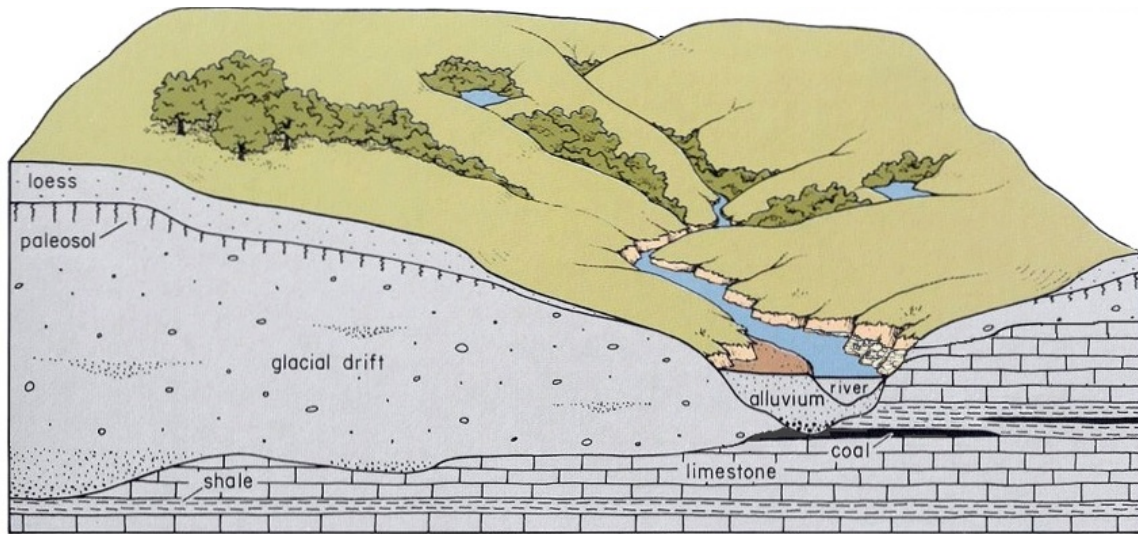


Figure 2.4. Typical Southern Iowa Drift Plain cross-section (Prior 1991).

Depth to bedrock varies from 0–500 feet throughout the watershed, as shown in Figure 2.5. Isolated areas of shallow depth to bedrock are found in southern Dallas and Polk counties. A shapefile developed by IGS showing likely locations of bedrock exposed or within 30 inches of the surface shows isolated exposures through Dallas and Polk counties, and is shown in the inset of Figure 2.5.

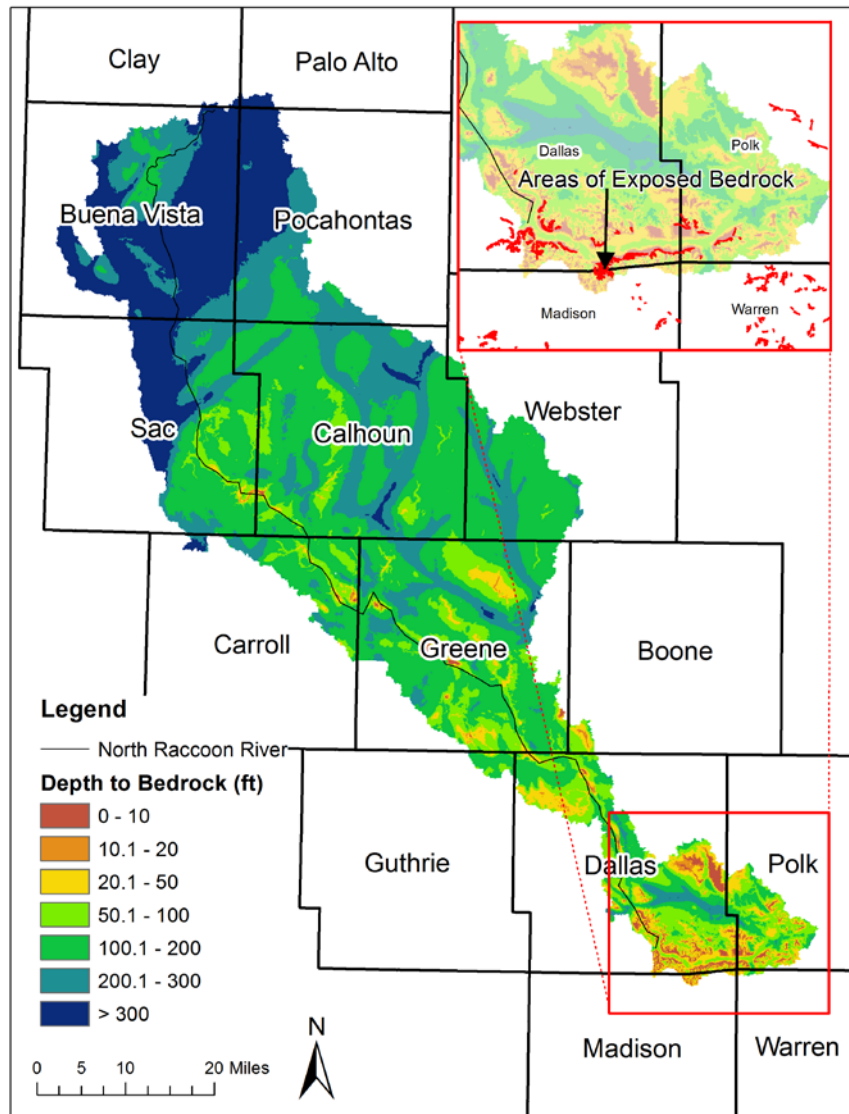


Figure 2.5. Depth to bedrock in the North Raccoon River Watershed.

The Natural Resources Conservation Service (NRCS) classifies soils into four hydrologic soil groups (HSG) based on the soil’s runoff potential. The four HSGs are A, B, C, and D, where A-type soils have the lowest runoff potential and D-type have the highest. In addition, there are dual code soil classes A/D, B/D, and C/D that are assigned to certain wet soils. For these soil groups, even though the soil properties may be favorable to allow infiltration (water passing from the surface into the ground), a shallow groundwater table (within 24 inches of the surface) typically prevents much from doing so. For example, a B/D soil will have the runoff potential of a B-type soil if the shallow water table were to be drained away, but the higher runoff potential of a D-type soil if it is not. Table 2.1 summarizes some of the properties generally true for each HSG (A-D). This table is meant to provide a general description of each HSG and is not all-inclusive. Complete descriptions of the HSGs can be found in USDA-NRCS National Engineering Handbook, Part 630 – Hydrology, Chapter 7.

Table 2.1. Soil properties and characteristics generally true for hydrologic soil groups A-D.

Hydrologic Soil Group	Runoff Potential	Soil Texture	Composition	Minimum Infiltration Rate <sup>1</sup> (in/hr)
A	Low	Sand, gravel	< 10% clay > 90% sand/gravel	>5.67
B	Moderately low	Loamy sand, sandy loam	10–20% clay 50–90% sand	1.42-5.67
C	Moderately high	Loam containing silt and/or clay	20–40% clay <50% sand	0.14–1.42
D	High	Clay	>40% clay <50% sand	<0.14

<sup>1</sup> For HSG A-C, infiltration rates based on a minimum depth to any water impermeable layer and the ground water table of 20 and 24 inches, respectively.

The Des Moines Lobe consists of a mix of HSG B and B/D type soils. The area closer to the North Raccoon River is generally B type soils, resulting in moderate runoff potential. The soil in the area north and east of the main river channel as one moves further into the Des Moines Lobe is primarily classified as B/D. Dual code HSGs, such as B/D, indicate a shallow groundwater table would inhibit infiltration, creating type D soil behavior; however, if drained, the soil would behave as type B. Much of this area has had tiling placed to drain away this shallow groundwater. The soil distribution of the North Raccoon River Watershed per digital soils data (SSURGO) available from the USDA-NRCS Web Soil Survey (WSS) is shown in Figure 2.6. Viewing the soil distribution at this map scale is difficult, but the map does illustrate how much soils vary in space and the noticeable difference in soil types of the main river channel area versus moving further inward toward the center of the Des Moines Lobe. Table 2.2 shows the approximate percentages by area of each soil type for the North Raccoon River Watershed within the Des Moines Lobe.

Table 2.2. Approximate Hydrologic Soil Group percentages by area of the North Raccoon River Watershed within the Des Moines Lobe.

<i>Hydrologic Soil Group</i>	<i>Des Moines Lobe Approximate %</i>
A	0.3
A/D	0.1
B	48.8
B/D	44.9
C	1.0
C/D	4.1
D	0.8

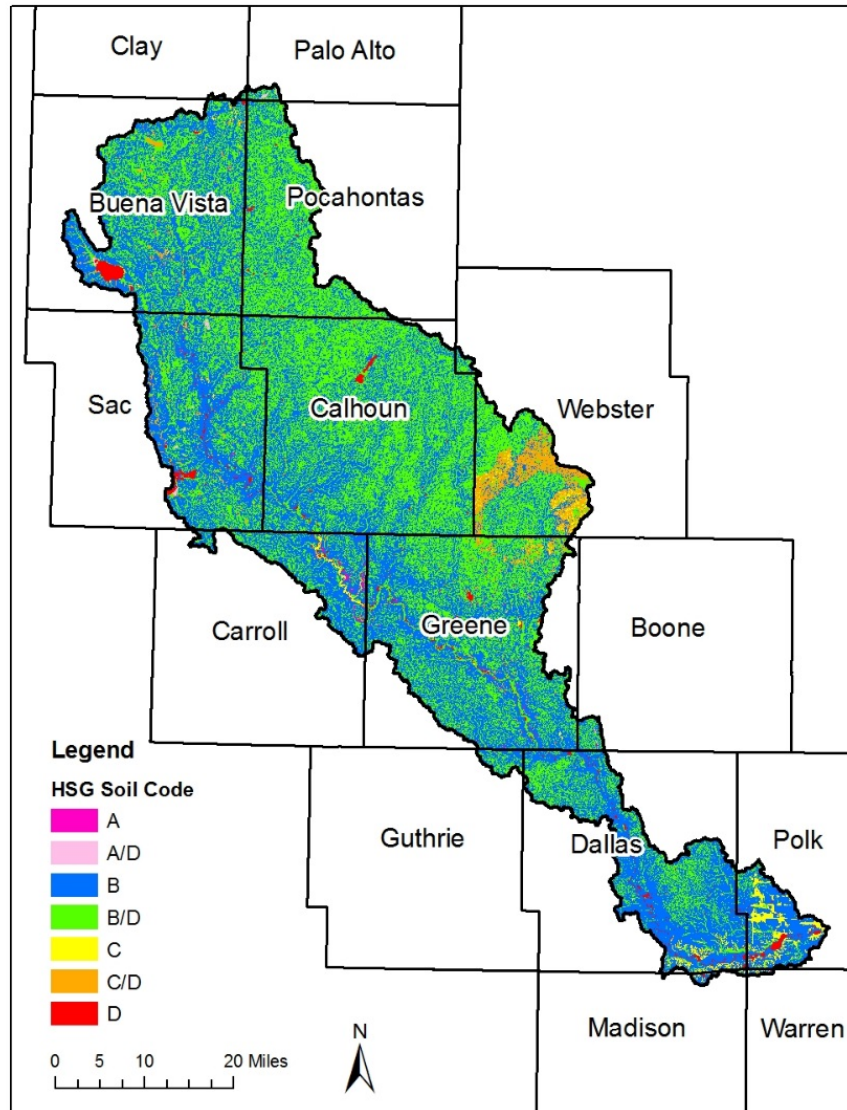


Figure 2.6. Distribution of Hydrologic Soil Groups in the North Raccoon River Watershed. Hydrologic Soil Groups reflect the degree of runoff potential a particular soil has, with Type A representing the lowest runoff potential and Type D representing the highest runoff potential.

### c. Topography

The topography of the North Raccoon River Watershed reflects its geologic past. As previously mentioned, much of the watershed lies within the Des Moines Lobe, which characterized as minimally sloping ground, interrupted by many isolated potholes. To facilitate drainage of the region, much of the drainage network is comprised of constructed channels. Figure 2.7 shows topography provided by Iowa DNR in the form of bare-earth light detection and ranging (LiDAR) data. Elevations range from approximately 1510 feet above sea level in the uppermost part of the watershed upstream of Storm Lake to 785 feet at the Des Moines River outlet at Des Moines. Typical land slopes are between 0.3 and 1.4% (25th and 75th percentiles), with the steepest areas occurring in along the major stream valleys throughout watershed, as shown in Figure 2.8.

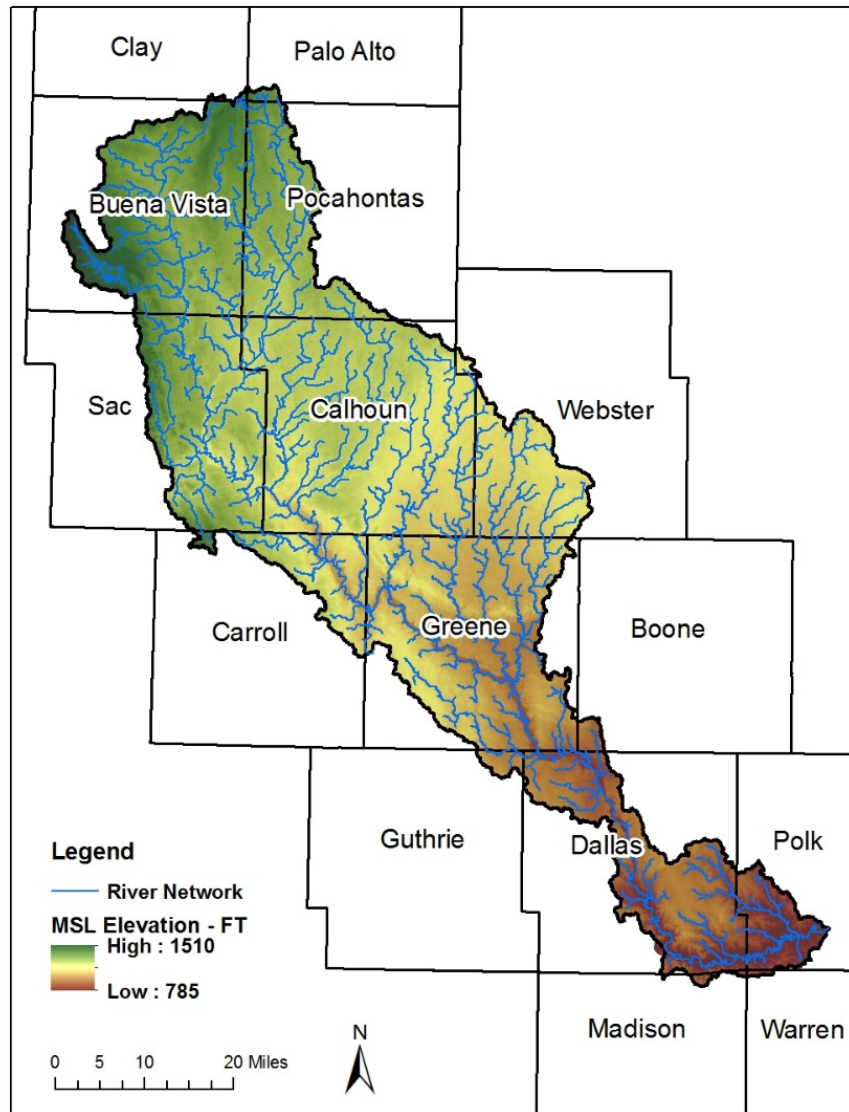


Figure 2.7. Topography of the North Raccoon River Watershed.

Potholes were identified using Geographic Information System (GIS) tools. Identifying the location of these isolated depressions is an important consideration in replicating the rainfall-runoff process of the region. These isolated pockets do not lead directly to runoff, rather they will store water until it either fills completely and spills over onto the adjacent draining land surface, evaporates, infiltrates naturally into the ground, or infiltration is aided by drainage inlets and pipe networks. In addition to identifying these isolated potholes, the area draining to each depression was also identified. These drainage areas were incorporated into the hydrologic modeling conducted for this hydrologic assessment as areas that do not contribute directly to surface runoff. Figure 2.9 shows an example of delineated potholes and their respective drainage area. A constructed/maintained channel can also be observed to the east of the potholes.

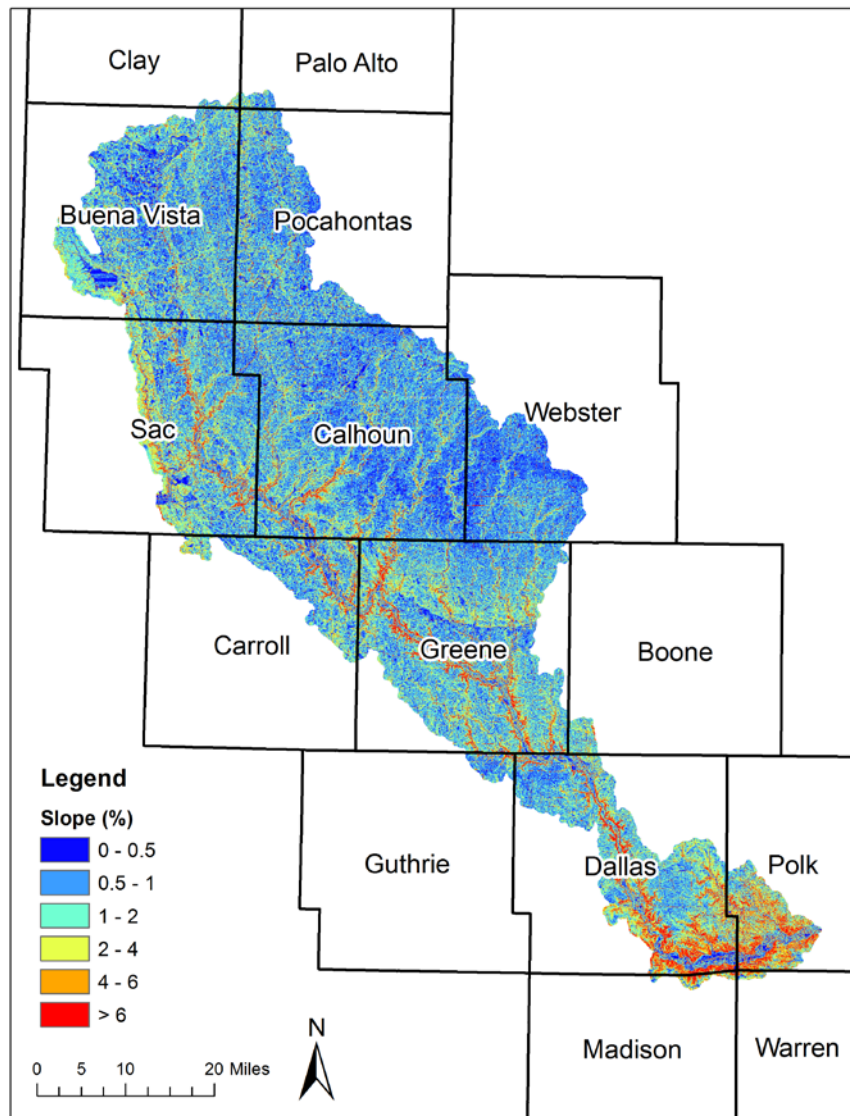


Figure 2.8. Terrain slopes derived from LiDAR data.

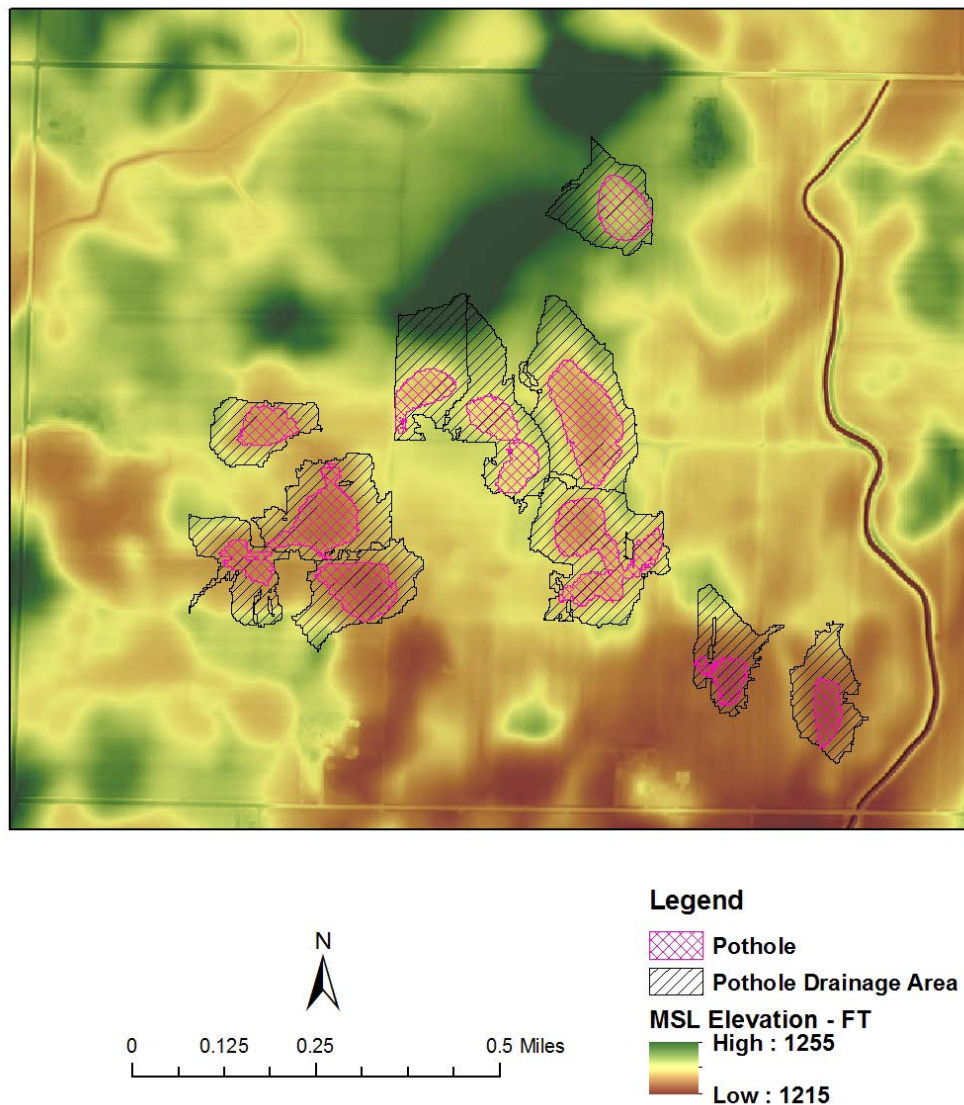


Figure 2.9. Delineated potholes and the land area that drains to them within the Des Moines Lobe in the North Raccoon River Watershed.

#### d. Land Use and BMP Mapping Project

Land use in the North Raccoon River Watershed is predominantly agricultural, dominated by cultivated crops (corn/soy beans) on approximately 77.7% of the acreage (approximately 1,228,250 acres), followed by grass/hay/pasture at approximately 11.9%. The remaining acreage in the watershed is about 4.6% forest (primarily deciduous forest), 3.2% developed land, and 2.6% open water and/or wetlands, per the 2009 High Resolution Land Cover (HRLC) dataset provided by Iowa DNR. Figure 2.10 shows the spatial distribution of land cover in the watershed.

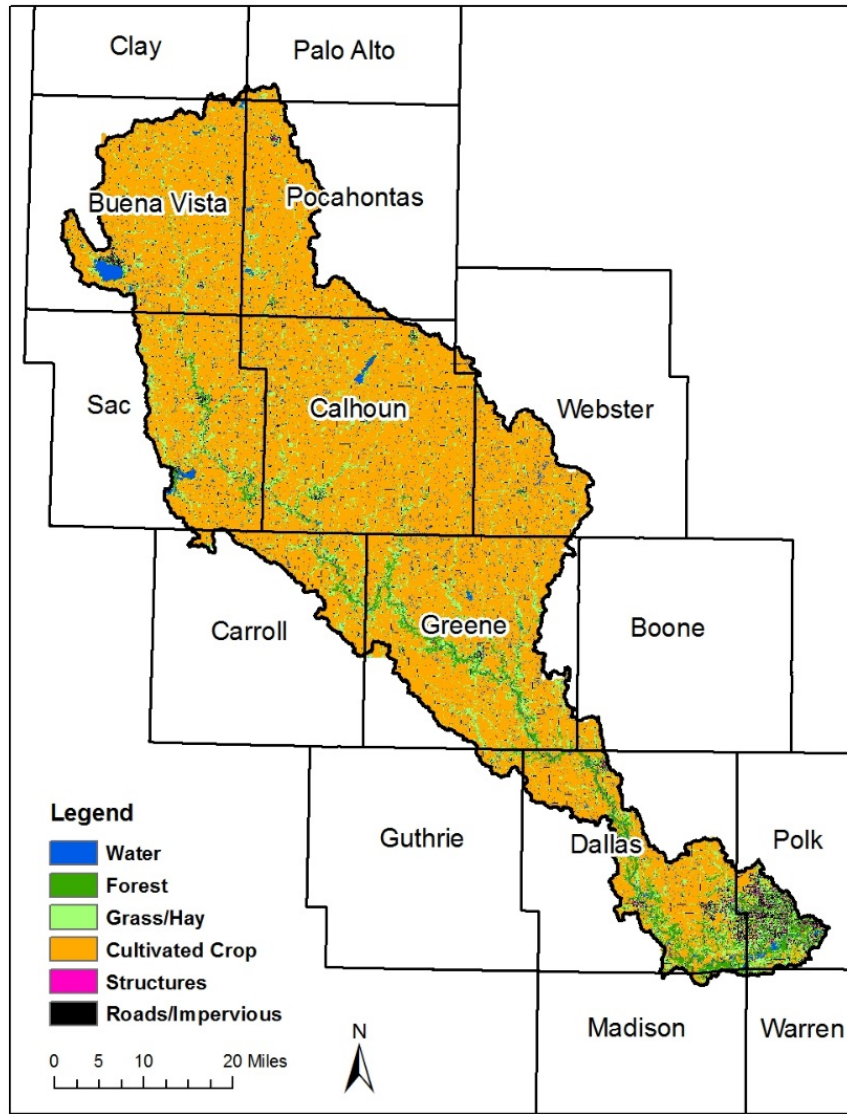


Figure 2.10. Land use composition in the North Raccoon River Watershed, according to the 2009 HRLC dataset provided by Iowa DNR.

The Iowa Best Management Practices (BMP) Mapping Project is a collaborative effort led by the Iowa State University Geographic Information Systems (GIS) Facility, in association with the Iowa DNR, Iowa Flood Center, Iowa Department of Agriculture and Land Stewardship, Iowa Nutrient Research Center, National Laboratory for Agriculture and the Environment, and the Iowa Nutrient Research and Education Council. The goal of the project is to provide a complete baseline set of BMPs during the 2007–10 timeframe for use in watershed modeling, historic documentation, and future practice tracking. These practices include terraces, water and sediment control basins (WASCOBs), grassed waterways, pond dams, contour strip cropping, and contour buffer strips. The data has been manually digitized for each HUC 12 using LiDAR products, color-infrared (CIR) imagery, National Agriculture Imagery Program imagery, and historic aerial photography.

Appendix A shows individual BMPs and practices aggregated based on HUC 12 area.

#### **e. Potential BMPs – Agricultural Conservation Planning Framework**

Development of an effective watershed planning document will require identification of potential conservation practices and viable locations to implement them. One cutting-edge tool available for practical conservation planning is the Agricultural Conservation Planning Framework (ACPF) watershed planning toolbox, developed by Mark Tomer and his research team at the USDA-ARS in Ames, Iowa (Tomer et al., 2013). ACPF is a watershed approach to conservation planning facilitated with a set of semi-automated tools within ArcGIS software. Freely available and pre-packaged GIS data can be used for terrain analyses to determine which fields within the watershed are most prone to runoff into streams. Users can apply the ACPF toolbox to identify locations where field-scale and edge-of-field practices could be installed based on general design criteria. These practices include controlled drainage, surface intake filters or restored wetlands, grassed waterways, contour buffer strips, WASCObS, nutrient removal wetlands (NRWs), or edge-of-field bioreactors (North Central Region Water Network 2018).

Using the ACPF toolbox, IFC has generated potential BMPs for 20 of the most northern HUC 12s in the North Raccoon River Watershed. Appendix A shows the locations of these BMPs and aggregations based on HUC 12 area.

#### **f. Instrumentation/Data Records**

The North Raccoon River Watershed has instrumentation installed to collect and record stream stage, discharge, and precipitation measurements. Nine USGS-operated stage and discharge gauges and nine IFC stream-stage sensors are located within the watershed. There are seven National Oceanic and Atmospheric Administration (NOAA) 15-minute/hourly precipitation gages within or near the watershed and an additional thirty-one NOAA-partnered daily-measuring precipitation gages within or near the watershed. The operational period of record varies for each of these gages. The following figure and tables detail the instrumentation and its period of record. Only the NOAA-partnered daily-measuring precipitation gauges that fall within the watershed boundary are listed in Table 2.3.

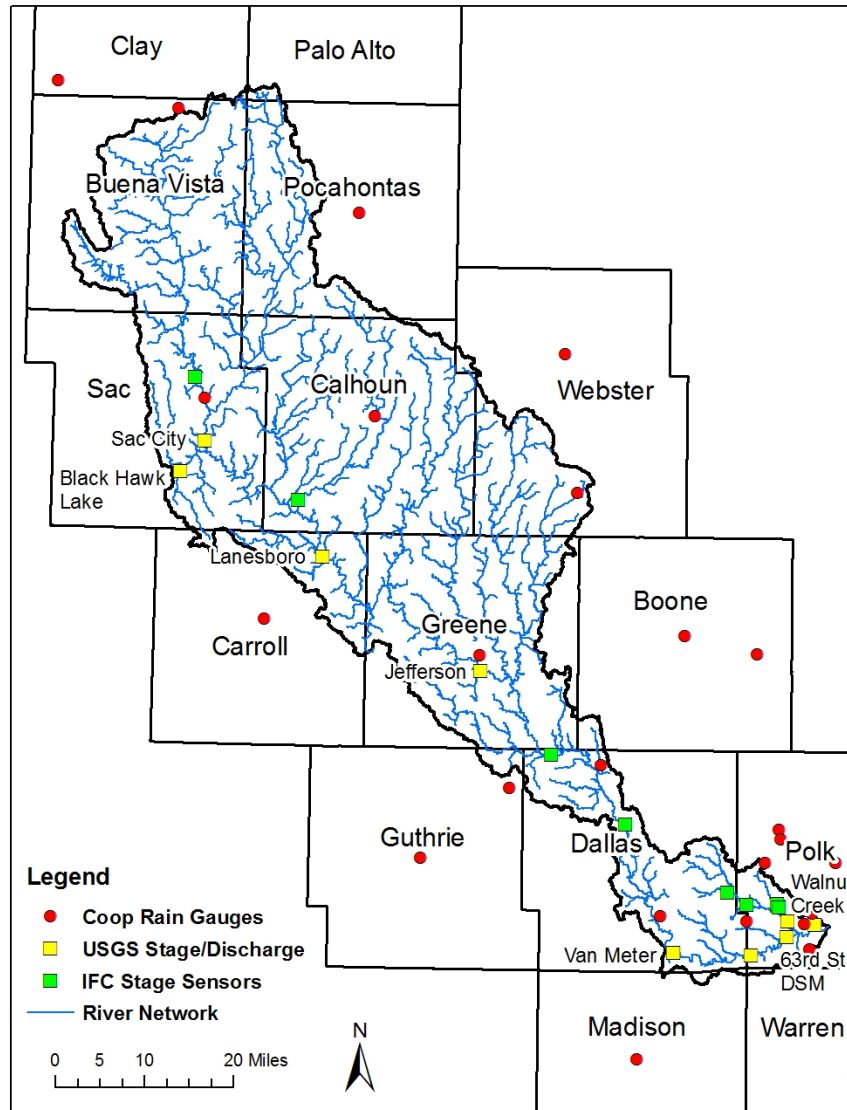


Figure 2.8. Hydrologic and meteorologic instrumentation in the North Raccoon River Watershed. Stage/discharge gages (18) are shown in yellow or green while NOAA-partnered daily-measuring precipitation gages (31) are shown in red.

Table 2.3. Stage/Discharge Gauges and Precipitation Gauges in the North Raccoon River Watershed.

<i>Gage Type</i>	<i>Location</i>	<i>Period of Record</i>
USGS Stage/Discharge	N. Raccoon River near Sac City, IA 05482300	1958 – present
USGS Stage Only	Black Hawk Lake at Lake View, IA 05482315	1970 – 1975 1978 – 1992 1994 – present
USGS Stage Only	N. Raccoon River near Lanesboro, IA 05482430	2009 – present
USGS Stage/Discharge	N. Raccoon River near Jefferson, IA 05482500	1940 – present

USGS Stage/Discharge	Raccoon River at Van Meter, IA 05484500	1915 – present
USGS Stage Only	Raccoon River near West Des Moines, IA 05484600	2000 – present
USGS Stage/Discharge	Raccoon River at 63 <sup>rd</sup> St. Des Moines, IA 05484650	1991 – present
USGS Stage/Discharge	Raccoon River at Fleur Dr. Des Moines, IA 05484900	1995 – present
USGS Stage/Discharge	Walnut Creek at Des Moines, IA 05484800	1971 – present
IFC Stream Sensor (stage)	N. Raccoon River, 230 <sup>th</sup> St., North of Sac City, IA NRCCNRV03	2011 – present
IFC Stream Sensor (stage)	Lake Creek, 365 <sup>th</sup> St./HWY 165, North of Lanesboro, IA LAKECR01	2010 – present
IFC Stream Sensor (stage)	N. Raccoon River, P46/D Ave., Near Dallas/Greene County Line NRCCNRV02	2014 – present
IFC Stream Sensor (stage)	N. Raccoon River, Milburn Road., Dallas County, IA NRCCNRV01	2014 – present
IFC Stream Sensor (stage)	Raccoon River, R16/R Ave., Near Van Meter, IA RCCNRV01	2014 – present
IFC Stream Sensor (stage)	Little Walnut Creek, NW 156 <sup>th</sup> St., Dallas County, IA LTLWLNT01	2010 – present
IFC Stream Sensor (stage)	Walnut Creek, South of Hickman Rd./HWY 6, Polk County, IA WLNTCR01	2016 – present
IFC Stream Sensor (stage)	North Walnut Creek, Hickman Rd./HWY 6, Polk County, IA NWLNTCR02	2010 – present
IFC Stream Sensor (stage)	North Walnut Creek, West of 75 <sup>th</sup> St., Polk County, IA NWLNTCR01	2011 – present
NOAA 15min/1hr Precip	Rockwell City #1	1948 – 1968
NOAA 15min/1hr Precip	Rockwell City #2	1968 – 2012
NOAA 15min/1hr Precip	Beaver, IA	1948 – 1953
NOAA 15min/1hr Precip	Ogden, IA	1953 – 2012
NOAA 15min/1hr Precip	Johnston, IA	1998 – 2006
NOAA 15min/1hr Precip	Des Moines, SE 6 <sup>th</sup> St.	1948 – 1975
NOAA 15min/1hr Precip	Des Moines Airport	1948 – 2013
NOAA-partnered Daily Precip	Sac City, IA	2008 – present
NOAA-partnered Daily Precip	Rockwell City, IA	2008 – present
NOAA-partnered Daily Precip	Hartcourt 2 N	2008 – present
NOAA-partnered Daily Precip	Jefferson 2 NW	2008 – present
NOAA-partnered Daily Precip	Perry, IA	2008 – present

NOAA-partnered Daily Precip	Adel, IA	2009 – present
NOAA-partnered Daily Precip	West Des Moines, IA	2008 – present
NOAA-partnered Daily Precip	Des Moines Waveland	2008 – present
NOAA-partnered Daily Precip	Des Moines NWS (Snow)	2012 – present

### g. Baseflow and Runoff Historic Trends

Annual precipitation volumes were estimated for each water year (October 1–September 30) from 1950 to 2017 using daily precipitation records near the watershed areas upstream of Jefferson and Van Meter. Total annual discharge for each water year was also calculated at Jefferson and Van Meter, using daily discharge observations from USGS gauging stations 05482500 and 05484500. Using these historical precipitation and discharge records, it is possible to estimate partitioning of precipitation into baseflow and direct runoff on an annual basis. Using the local minimum method, daily discharges were separated into baseflow and runoff. Figure 2.9 shows plots of annual precipitation, streamflow, baseflow, and runoff at Jefferson, Iowa. All datasets have a slight positive trend, with low correlation values. Similar datasets are shown in Figure 2.12 for Van Meter, Iowa.

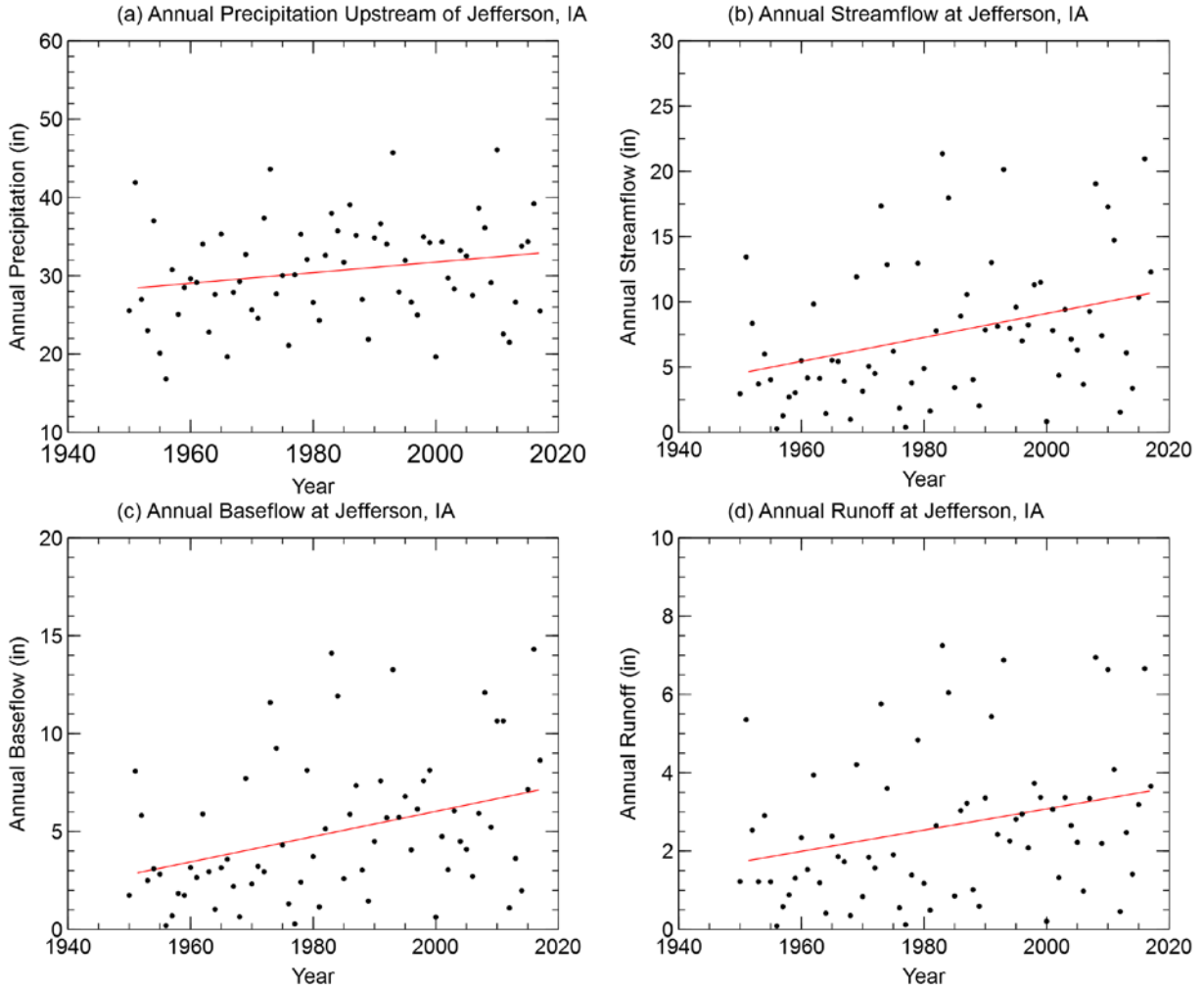


Figure 2.11. Annual totals for: (a) precipitation; (b) streamflow; (c) baseflow; and (d) runoff at Jefferson, IA.

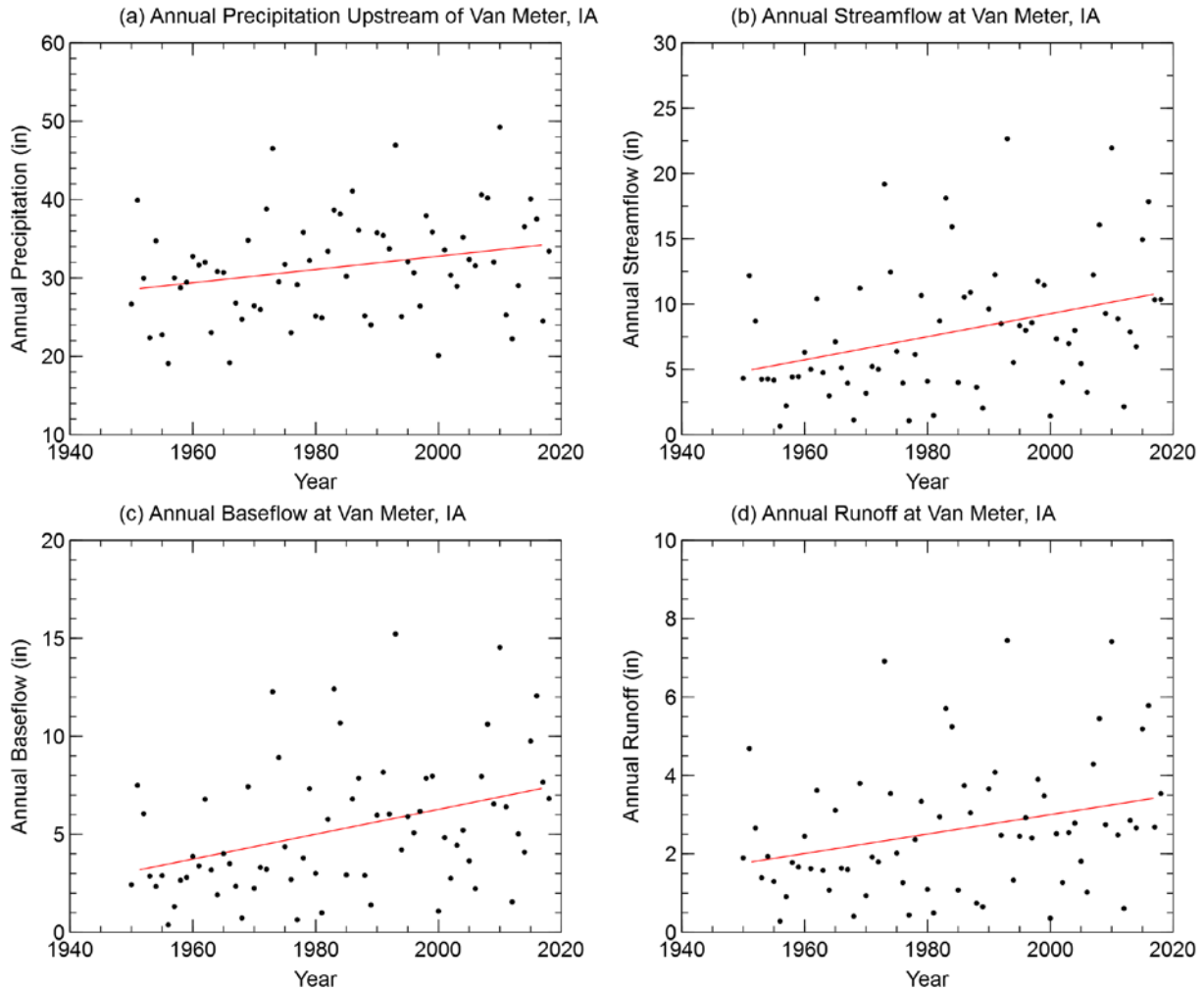


Figure 2.12. Annual totals for: (a) precipitation; (b) streamflow; (c) baseflow; and (d) runoff at Van Meter, IA.

Cumulative mass curves were developed to further visualize and investigate any historic trends associated with these data. Cumulative mass curves allow visualization of long-term discharge or precipitation trends, with changes in slope indicating possible historical change points. Cumulative mass curves at Jefferson and Van Meter were created for precipitation, streamflow, baseflow, and runoff by summing each consecutive annual total volume (inches), and are shown in Figure 2.13 and Figure 2.14. Cumulative annual precipitation closely follows a linear trend, with little deviation from the fitted trend line. This indicates no significant change in long-term total precipitation upstream of both Jefferson and Van Meter. Beginning in the 1980s, cumulative annual streamflow totals at both locations indicate a departure from the historical trend, with the largest departures beginning in the mid-1990s and continuing to the present. This change appears to be a result of increased baseflow, which shows more noticeable departures from the historic trend than does cumulative annual runoff. It is worth noting that the 1993 water year appears to contribute to an abrupt departure from the historic trend.

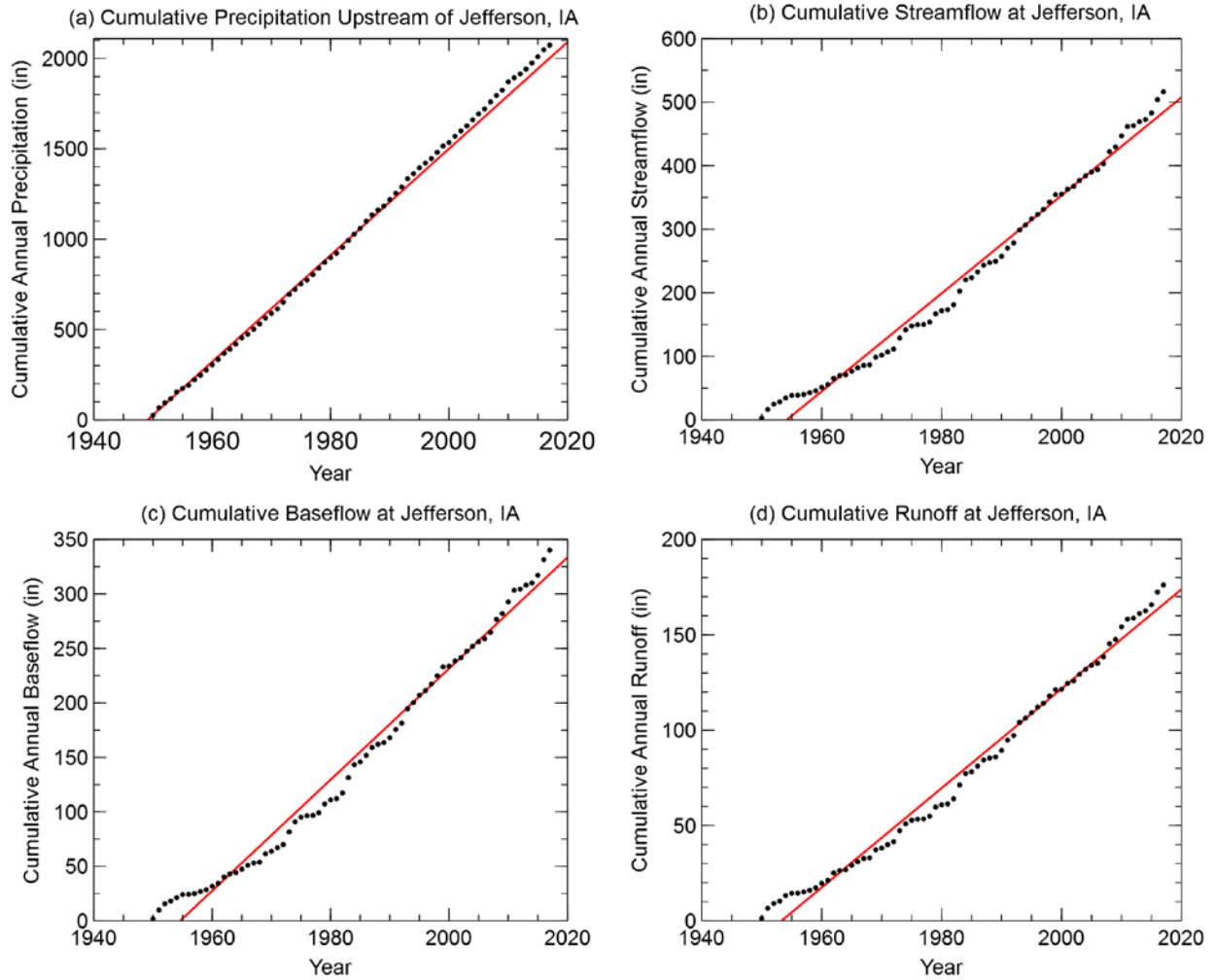


Figure 2.13. Cumulative annual totals for: (a) precipitation; (b) streamflow; (c) baseflow; and (d) runoff at Jefferson, Iowa.

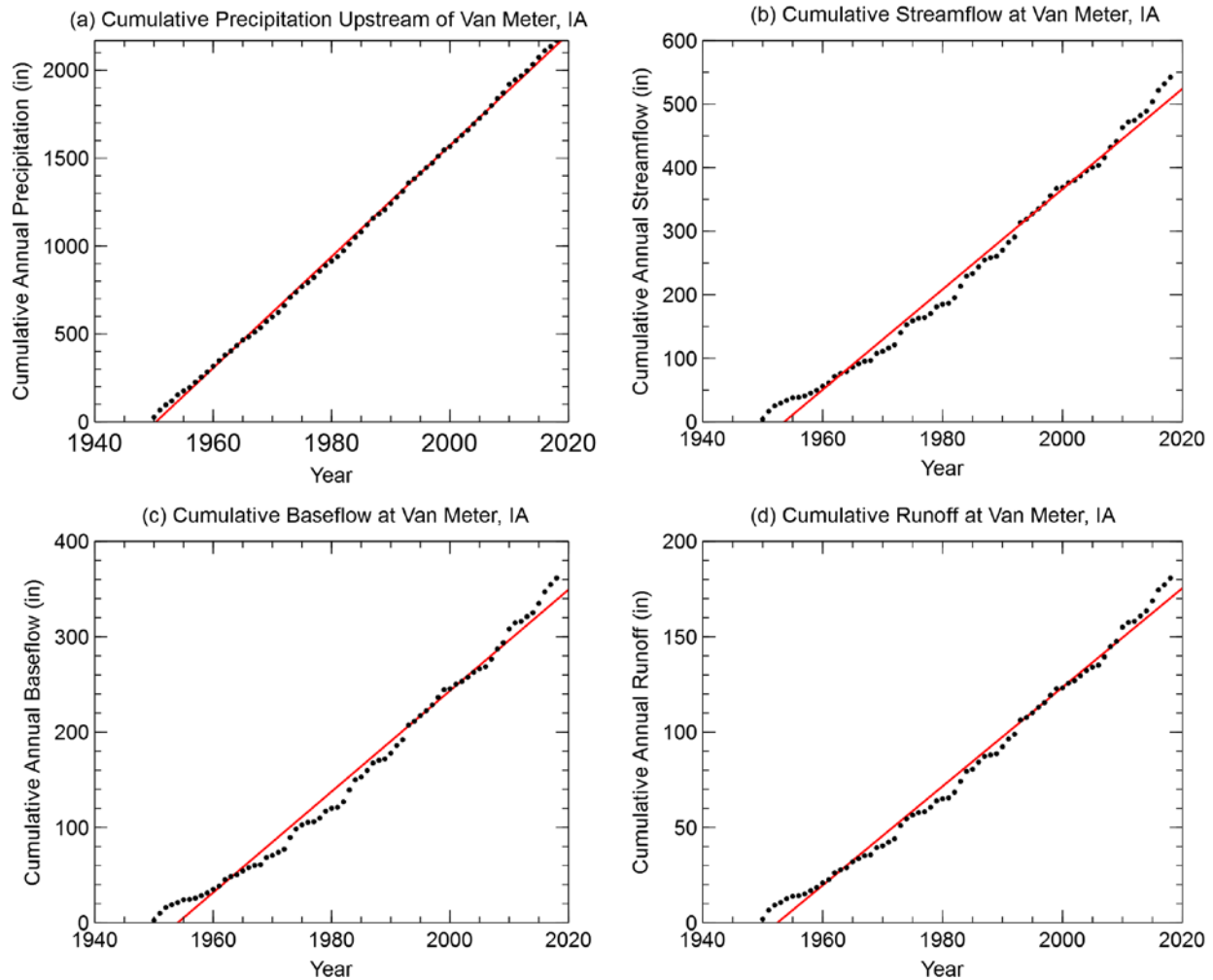


Figure 2.14. Cumulative annual totals for: (a) precipitation; (b) streamflow; (c) baseflow; and (d) runoff at Van Meter, Iowa.

The influence of extremely wet years, such as 1993, on the linear trend can be accounted for using a double-mass curve. A double-mass curve based on a plot of two cumulative quantities during the same period will follow a straight line if the proportionality between the quantities remains unchanged (Gao et al. 2010). Figure 2.15 and Figure 2.16 show double mass curves of cumulative precipitation with cumulative streamflow, baseflow, and runoff at Jefferson and Van Meter, respectively. These plots indicate that changes in historic streamflow totals are likely a result of historic increases in baseflow beginning in the 1980s, with the largest changes occurring in the last two decades. The reason for changes in streamflow continues to be intensely investigated (Mora et al. 2013, Frans et al. 2013, Yiping et al. 2013); likely drivers include improved conservation practices promoting infiltration, greater artificial drainage, increasing row crop production, and channel incision (Schilling and Libra, 2003).

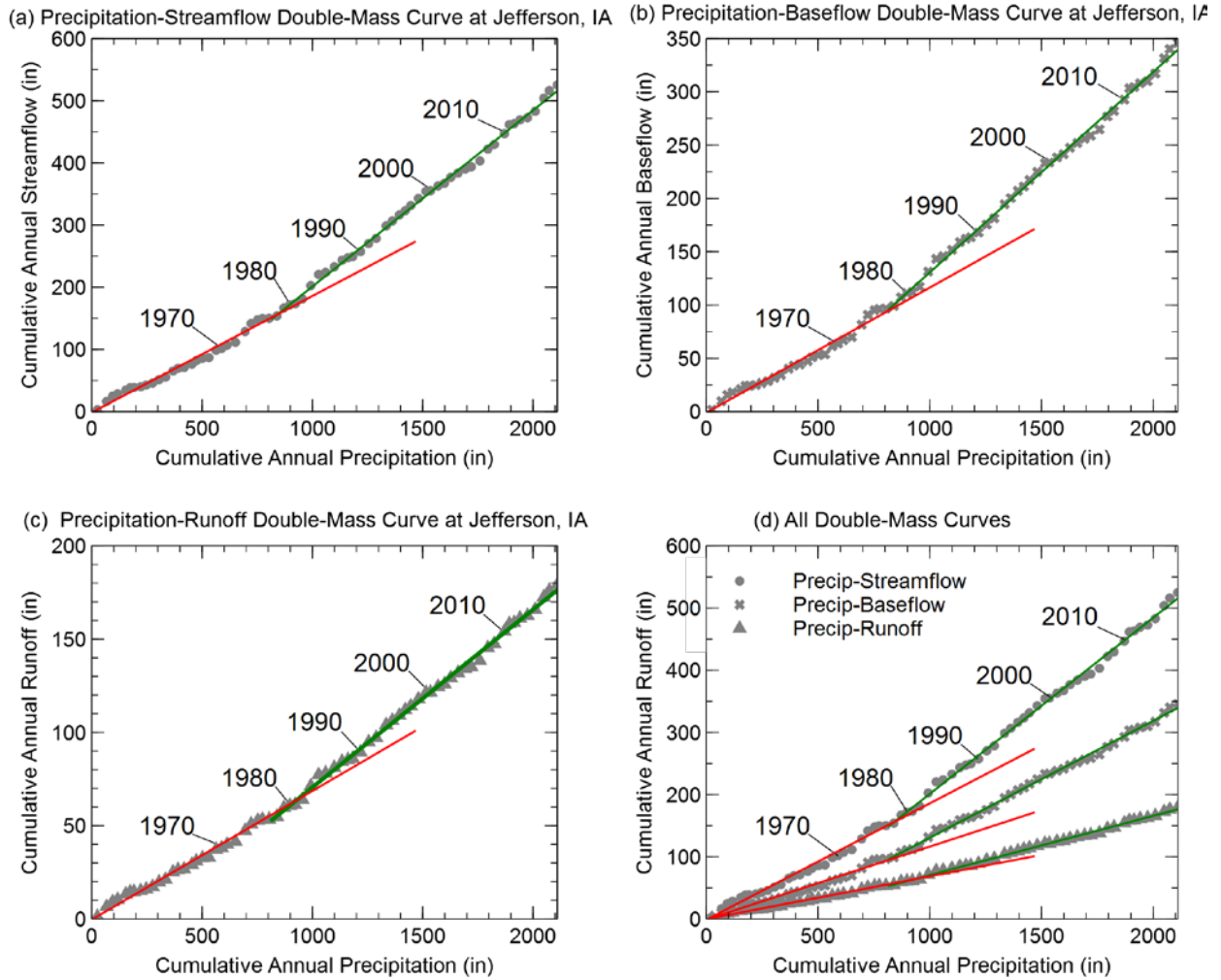


Figure 2.15. Double-mass curves using cumulative annual precipitation with cumulative annual (a) streamflow, (b) baseflow, and (c) runoff at Jefferson, Iowa. Fitted lines show segments have different slopes beginning around 1980.

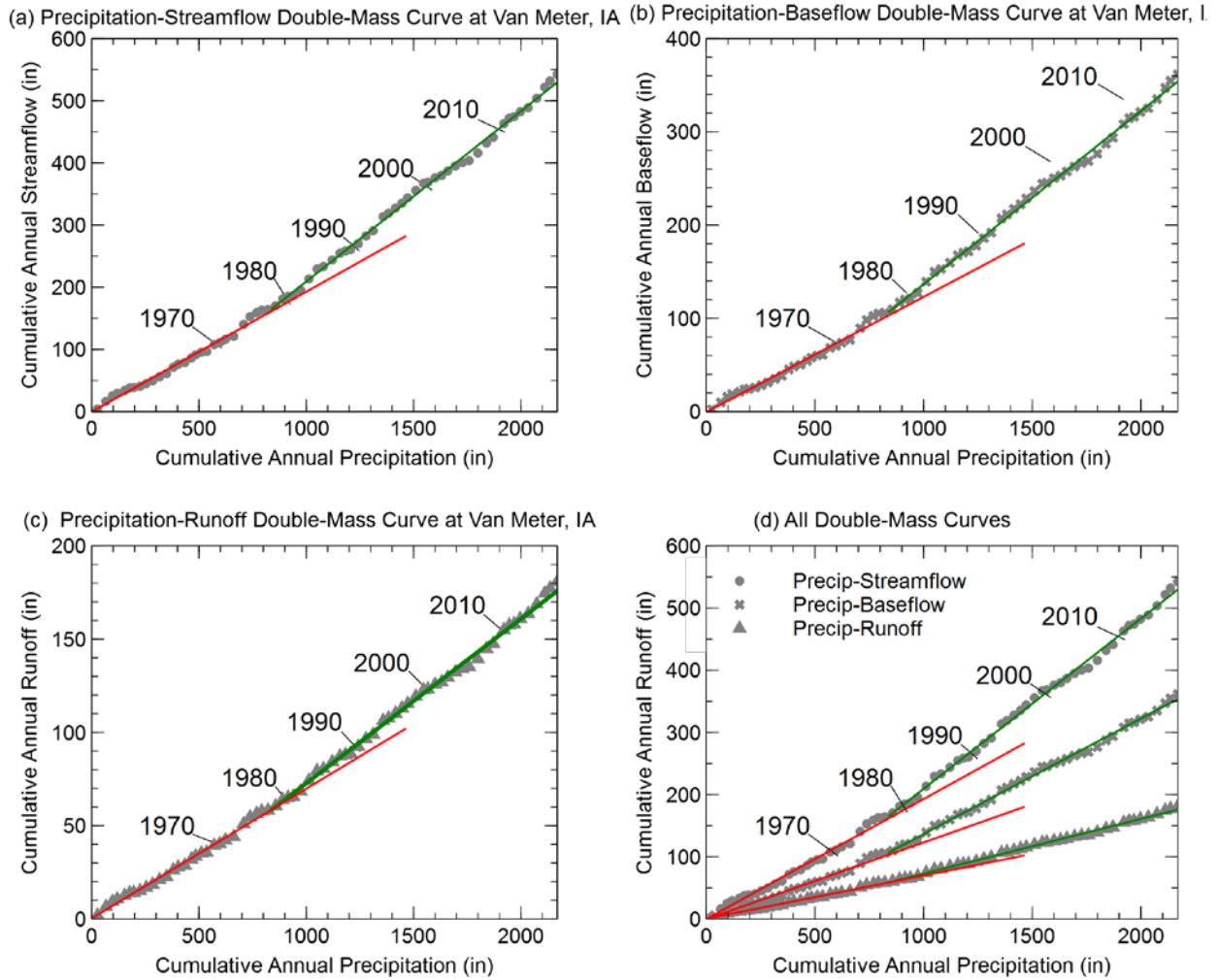


Figure 2.16. Double-mass curves using cumulative annual precipitation with cumulative annual (a) streamflow, (b) baseflow, and (c) runoff at Van Meter, Iowa. Fitted lines show segments have different slopes beginning around 1980.

## h. Monthly Water Cycle

Using historic USGS streamflow and precipitation records, the average monthly stream flow and upstream precipitation at Jefferson and Van Meter were calculated for the period 1950-2017. Monthly averages for Van Meter and Jefferson are shown in Figure 2.17 and Figure 2.18, respectively. The monthly trends are very similar at both locations. Precipitation amounts are lowest during the winter months. However, this precipitation is likely snowfall, which accumulates before melting in the warmer spring temperatures. A large increase in the average precipitation occurs in the spring months, before peaking in the months of May and June. Streamflow follows a similar trend; the largest monthly average streamflow occurs in May and June. Precipitation slowly decreases through late summer and early fall, while streamflow drops significantly after the summer months.

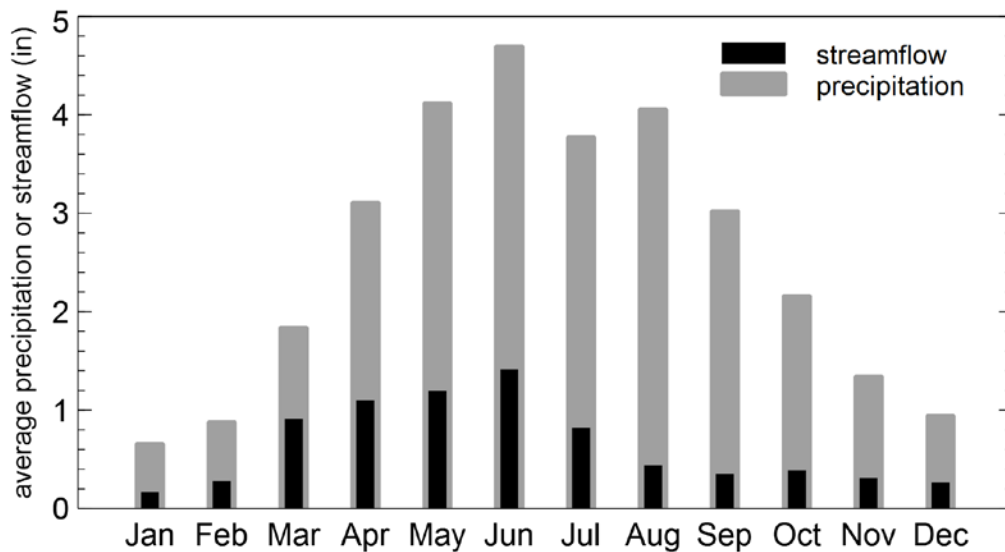


Figure 2.17. Monthly water cycle for the North Raccoon River Watershed at Jefferson, Iowa. The plots show the average monthly precipitation (inches) and the average monthly streamflow (inches). The average monthly estimates for precipitation and streamflow are based on the period 1950–2017.

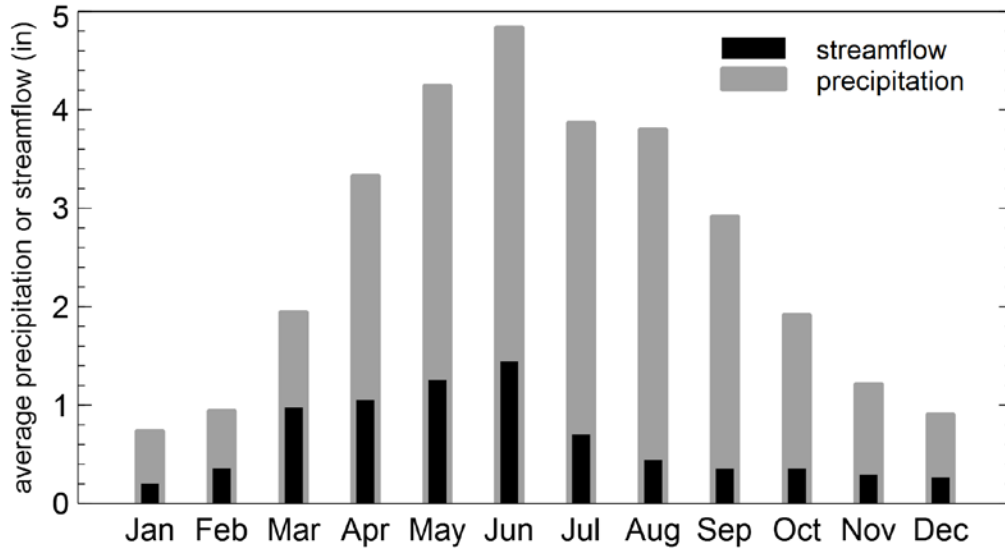


Figure 2.18. Monthly water cycle for the North Raccoon River Watershed at Van Meter, Iowa. The plots show the average monthly precipitation (inches) and the average monthly streamflow (inches). The average monthly estimates for precipitation and streamflow are based

### i. Floods of Record

Figure 2.19 shows the annual maximum peak discharges observed at the Jefferson and Van Meter USGS gauging stations. While these are annual maximum, many were not flood events. Calculating the mean annual peak discharge by averaging all annual peak observations can serve as a reasonable threshold for flooding occurrences. Of the 103 annual maximum peak discharges at Jefferson, Iowa, 42 peaks were greater than the mean annual peak discharge. Of the 78 annual maximum peak discharges at Van Meter, Iowa, 35 peak were greater than the mean annual peak discharge. It is important to note the Van Meter gauging station is downstream of the confluence with the South Raccoon River.

Further analyses of these annual maximum peak discharges reveal the seasonal flood pattern for the North Raccoon Watershed. Figure 2.20 shows the calendar day of occurrence for each of the annual maximum peak discharges at Jefferson and Van Meter. There is an abrupt drop in annual maximum around in the month of July for both locations. This is further visualized in Figure 2.21 with the number of flood occurrences for each calendar month. Most flooding events occur during the months of May and June. A secondary peak occurs in March, likely caused by snowmelt and spring rains. Late summer and early fall see a small increase in the occurrence of flood events.

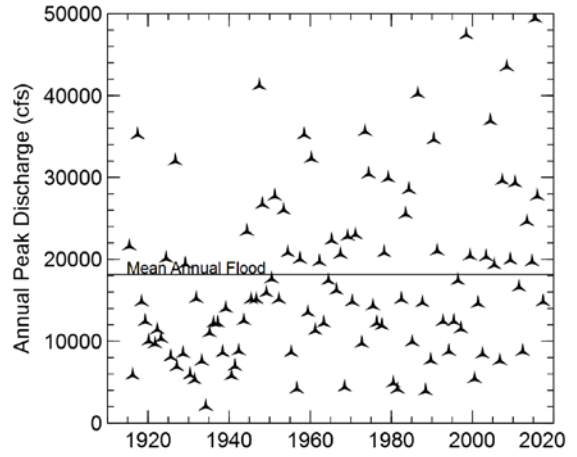
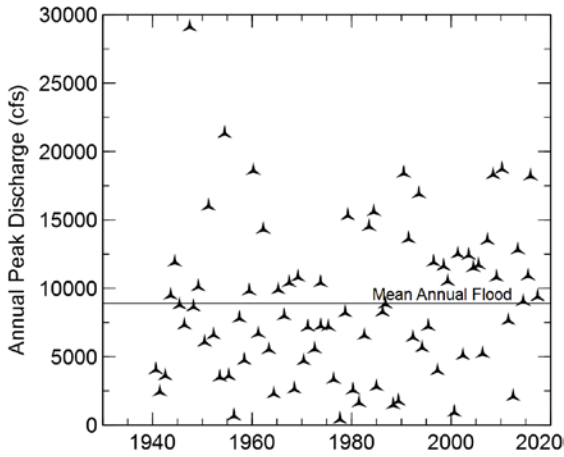


Figure 2.19. Annual maximum peak discharges observed at the Jefferson (left) and Van Meter (right) USGS stream gauge stations.

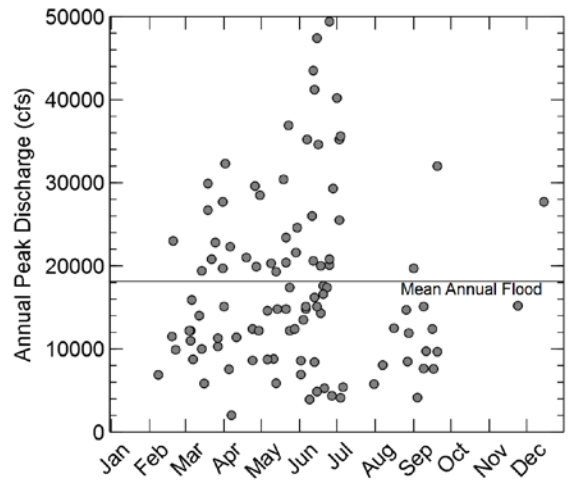
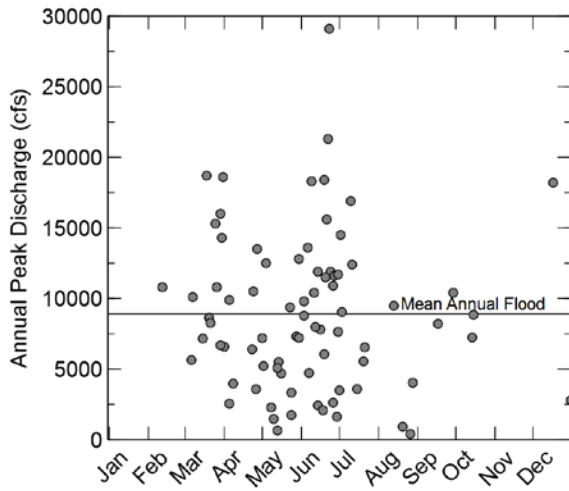


Figure 2.20. Annual maximum peak discharge and the calendar day of occurrence at the Jefferson (left) and Van Meter (right) USGS stream gauge stations.

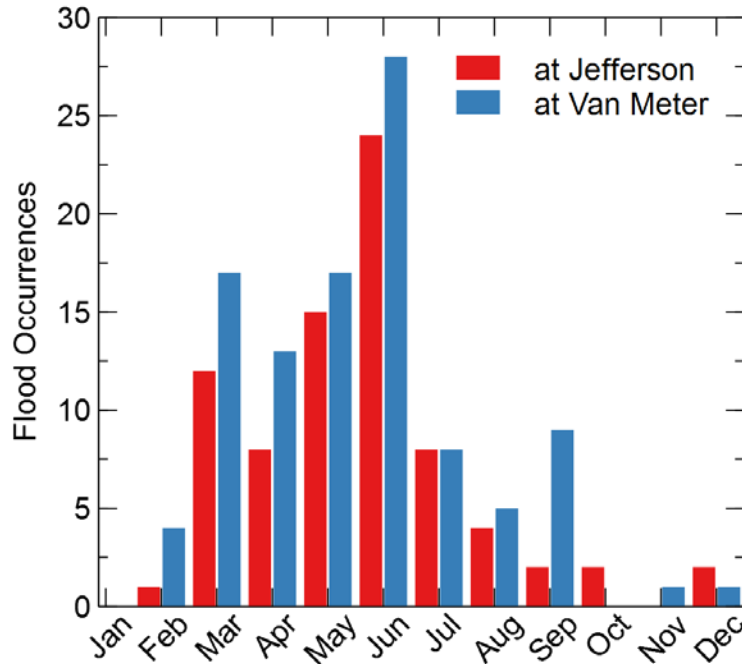


Figure 2.21. Flood occurrence frequency by month at both the Jefferson and Van Meter USGS stream gauge stations.

Six large flood events (discharge greater than 40,000 cfs) have been recorded at the USGS Raccoon River gaging station at Van Meter, Iowa since 1947. The four largest of these flood peaks have occurred since 1993: July 10, 1993 – 70,100 cubic feet per second (cfs); June 25, 2015 - 49,400 cfs; June 15, 1998 – 47,400 cfs; June 12, 2008 – 43,500 cfs. The fifth and sixth largest peak discharges since 1915 at this gage were 41,200 cfs on June 13, 1947 and 40,200 cfs on July 1, 1986. Large discharges at this location may develop in the North Raccoon River Watershed upstream of the confluence with the South Raccoon River near Van Meter, may develop in the South Raccoon River Watershed, or may develop as a combination of discharges from both rivers from widespread rain events. Ultimately, the discharge that is observed here continues downstream on the Raccoon River and into Des Moines.

Table 2.4 shows the six largest discharges at two USGS gaging stations on the North Raccoon River, the USGS gaging station on the South Raccoon River near Redfield, the USGS gaging station on the Raccoon River near Van Meter (downstream of the confluence of the North and South Raccoon Rivers) and at 63<sup>rd</sup> Street in Des Moines. Table 2.4 also shows the USGS gaging station on Walnut Creek at Des Moines.

**Table 2.4. Discharges from the Six Largest Flooding Events at USGS Gaging Stations in the North Raccoon River Watershed, the South Raccoon River at Redfield, IA, the Gaging Stations on the Raccoon River Downstream of the Confluence of the North and South Raccoon Rivers, and Walnut Creek at Des Moines.**

N. Raccoon Sac City (1958 - Present)	3/23/1979 13,100 cfs	9/01/1962 10,800 cfs	6/17/1990 9,930 cfs	3/16/2010 9,820 cfs	6/21/1983 9,390 cfs	3/30/1960 9,020 cfs
N. Raccoon Jefferson (1940 - Present)	6/23/1974 29,100 cfs	6/22/1954 21,300 cfs	3/18/2010 18,700 cfs	3/31/1960 18,600 cfs	6/19/1990 18,400 cfs	6/09/2008 18,300 cfs
S. Raccoon Redfield (1940 - Present)	7/10/1993 44,000 cfs	6/25/2015 38,000 cfs	7/28/2008 37,100 cfs	6/15/1998 35,100 cfs	7/02/1958 35,000 cfs	5/23/2004 28,300 cfs
Raccoon Van Meter (1915 - Present)	7/10/1993 70,100 cfs	6/25/2015 49,400 cfs	6/15/1998 47,400 cfs	6/12/2008 43,500 cfs	6/13/1947 41,200 cfs	7/01/1986 40,200 cfs
Raccoon DSM 63rd (1991 - Present) *estimated by USGS	7/11/1993 66,000 cfs*	6/13/2008 52,000 cfs	6/26/2015 46,600 cfs	6/16/1998 40,300 cfs	4/26/2007 33,500 cfs	5/24/2004 30,800 cfs
Walnut Creek DSM (1971 - Present)	5/10/1986 12,500 cfs	8/09/2010 11,700 cfs	6/25/2015 9,720 cfs	7/01/1973 9,000 cfs	6/09/1974 8,160 cfs	6/16/1990 7,780 cfs

At the Raccoon River USGS gaging station near Van Meter, the largest discharge was experienced on July 10, 1993 (70,100 cfs), roughly 70 percent of the discharge was observed passing the USGS gaging station on the South Raccoon River near Redfield. The peak discharge observed at the North Raccoon USGS gaging station near Jefferson was 16,900 cfs on July 10, 1993 as well. With travel time factored in, the peak observed on the North Raccoon River would have passed the Raccoon River gaging station at Van Meter on July 12th. For the 2008 event at Van Meter on June 12, 2008 (43,500 cfs), both the North and South Raccoon Watersheds contributed equally to the development of the peak discharge, with the observed peak discharge of 18,300 cfs for the North Raccoon near Jefferson on June 9<sup>th</sup> and an observed discharge of 26,300 cfs for the South Raccoon on June 12th. It is worth noting the South Raccoon's largest peak discharge in 2008 was actually from another storm event (July 28, 2008).

Further analysis of annual peak discharges reveals a strong correlation between dates of peak annual discharges on the South Raccoon River near Redfield and the Raccoon River at Van Meter, as shown in Table 2.5. Of the largest 10 annual peak discharges observed at Van Meter, nine of the annual peaks observed on the South Raccoon River at Redfield occurred during the same event. The correlation between the dates of annual peak events at Van Meter and Jefferson are much lower – only 4 of the largest 10 annual peaks at Van Meter coincided with the annual peaks at Jefferson.

Table 2.5. The dates of the 10 largest peak annual discharges observed at Van Meter, IA, compared to the dates of peak annual discharges on South Raccoon River at Redfield, IA, and the North Raccoon River at Jefferson, IA.

Water Year	Rank	Date of Annual Peak at Van Meter (Confluence of N. and S. Raccoon)	Date of Annual Peak at Redfield (S. Raccoon)	Coincident Peak at Redfield (S. Raccoon)	Date of Annual Peak at Jefferson (N. Raccoon)	Coincident Peak at Jefferson (N. Raccoon)
1993	1	7/10/1993	7/10/1993	Yes	7/10/1993	Yes
2015	2	6/25/2015	6/25/2015	Yes	6/26/2015	Yes
1998	3	6/15/1998	6/15/1998	Yes	6/27/1998	no
2008	4	6/12/2008	7/28/2008	no	6/9/2008	Yes
1947	5	6/13/1947	6/12/1947	Yes	6/23/1947	no
1986	6	7/1/1986	7/1/1986	Yes	3/21/1986	no
2004	7	5/23/2004	5/23/2004	Yes	6/20/2004	no
1973	8	7/4/1973	7/4/1973	Yes	9/29/1973	no
1958	9	7/3/1958	7/2/1958	Yes	6/7/1958	Yes
1990	10	6/16/1990	6/16/1990	Yes	6/19/1990	no

## j. Flood Frequency Estimates

Flood frequency estimates for Jefferson and Van Meter were generated using a Bulletin 17C Analysis of observed annual peak discharges at Jefferson and Van Meter, IA, and are shown in Table 2.6. These estimates represent the percent annual chance exceedance probability of the discharge occurring in any given year. For example, the 1-percent annual chance exceedance event has a probability of 1 out of 100 chance of occurring in any given year, hence it has been frequently referred to as the “100 Year Flood”. However, when you consider longer periods, like a typical 30 year home mortgage, the 1-percent annual chance exceedance event has a 26% chance of occurring at least once over that 30 year period.

Table 2.6. Flood frequency estimates generated using a Bulletin 17C Analysis of observed annual peak discharges at Jefferson and Van Meter, IA.

Percent Annual Chance Exceedance	Return Period	Estimated Flowrate at Jefferson, IA, cfs	Estimated Flowrate at Van Meter, IA, cfs
0.2	500	32670	79948
0.5	200	28969	68335
1	100	26125	59863
2	50	23235	51648
5	20	19320	41148
10	10	16253	33423

20	5	13032	25786
50	2	8239	15332

The magnitude of peak annual exceedance estimates are highly correlated with upstream drainage area. Logically, more area draining to a point would result in higher flood flowrates. Drainage areas throughout the stream networks of the North and South Raccoon River Watersheds are shown in Figure 2.22.

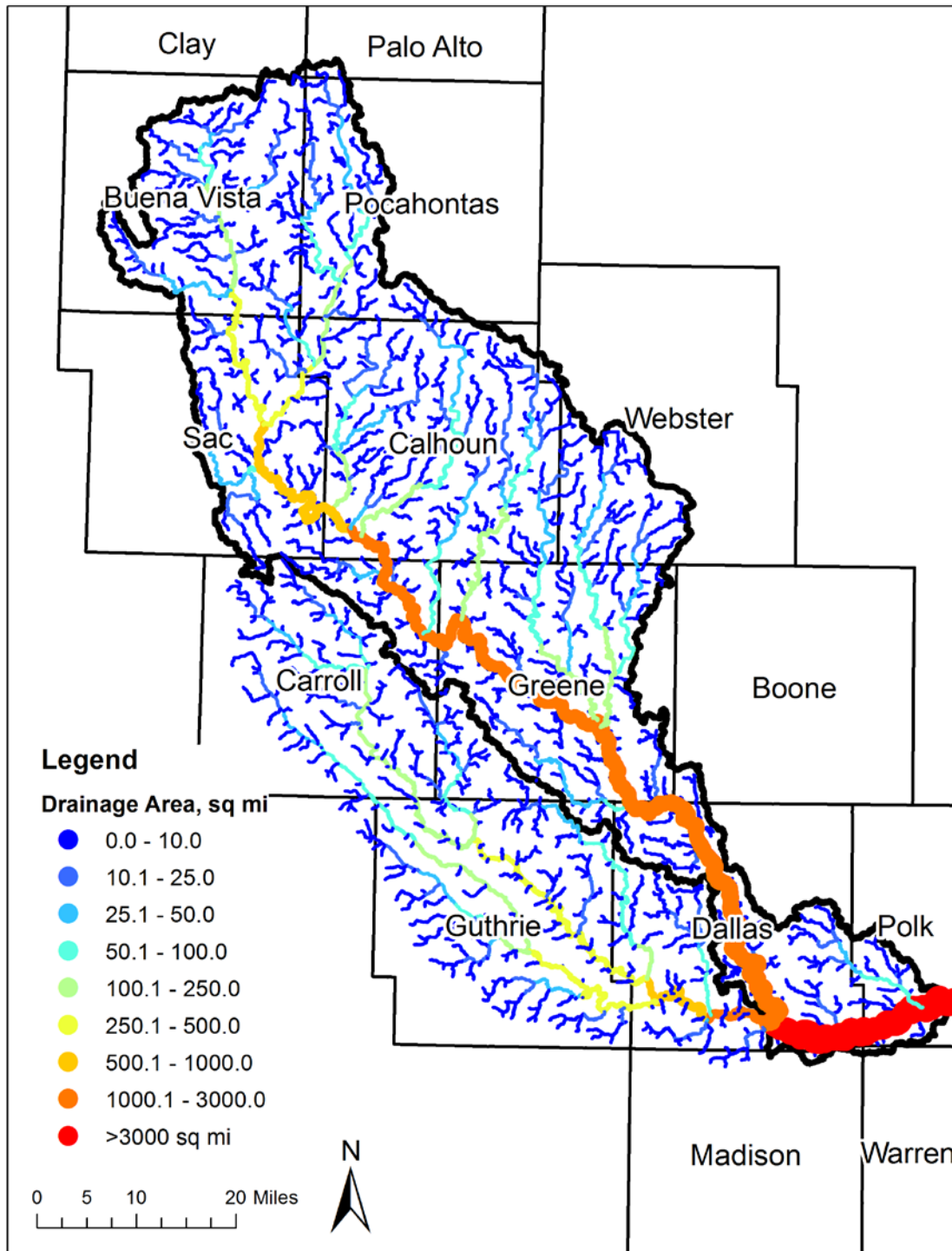


Figure 2.22. Upstream drainage area throughout the stream network in the North and South Raccoon River Watersheds.

### 3. North Raccoon River Watershed Hydrologic Model Development

This chapter summarizes the development of the model used in the Phase I Hydrologic Assessment for the North Raccoon River Watershed. Researchers used the U.S. Army Corps of Engineers' (USACE) Hydrologic Engineering Center's Hydrologic Modeling System (HEC-HMS), Version 4.0.

HEC-HMS is designed to simulate rainfall-runoff processes of a watershed. It is applicable in a wide range of geographic areas and for watersheds ranging in size from very small (a few acres) to very large (the size of the North Raccoon River Watershed or larger). Figure 3.1 reviews the water cycle and major hydrologic processes that occur in a watershed. The physical processes of the North Raccoon River Watershed explicitly modeled with HEC-HMS include the partitioning of precipitation into infiltrated and overland flow volumes, transformation of excess runoff to subbasin outflow, and flood wave routing. The model accounts for the cumulative effects of all other physical processes through antecedent conditions or general approximation.

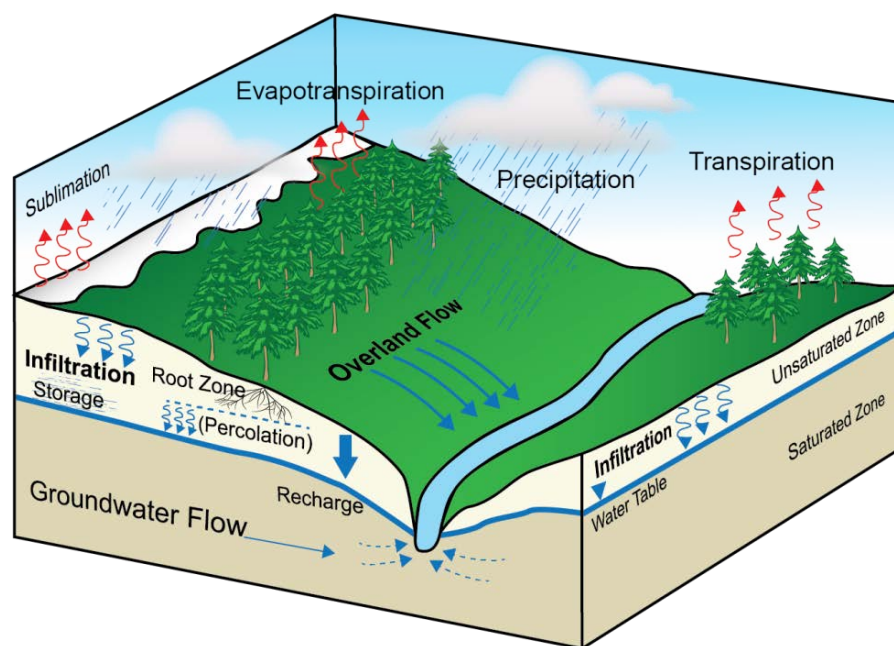


Figure 3.1. Hydrologic processes that occur in a watershed. Phase I modeling only considered the precipitation, infiltration, and overland components of the water cycle.

HMS is a mathematical, lumped parameter, uncoupled, surface water model. The authors of this report will briefly discuss each of these characteristics. HMS is a mathematical model, which implies that it represents the different hydrologic processes with mathematical expressions that are often empirically developed to best describe observations or controlled experiments. HMS is also a lumped parameter model, meaning physical characteristics of the watershed, such as land use and soil type, are “lumped” together into a single representative value for a given land area,

often referred to as a “subbasin”. Once HMS establishes these averaged values, they remain constant throughout the simulation, rather than varying over time. HMS is an uncoupled model, meaning that it solves the different hydrologic processes independent of one another rather than jointly. In reality, surface and subsurface processes are dependent on one another and their governing equations should be solved simultaneously (Scharffenberg, 2013). Finally, HMS is a surface water model, meaning that it works best to simulate large storm events or when the ground is nearly saturated because overland flow is expected to dominate the partitioning of rainfall in both cases. Due to the model structure and prevalence of subsurface drainage infrastructure in this watershed, storm events that do not result in overland flow dominating rainfall partitioning are not ideal.

The two major components of the HMS hydrologic model are the basin model and the meteorologic model. The basin model defines the hydrologic connectivity of the watershed and how rainfall is converted to runoff, as well as how water is routed from one location to another. The meteorologic model stores the precipitation data that define when, where, and how much it rains over the watershed. Simulated hydrographs from HMS can be compared to discharge observations.

## a. Model Development

The North Raccoon River Watershed modeled and described herein comprises approximately 2471 square miles. However, the North Raccoon River is joined by the South Raccoon River (HUC8 07100007) near Van Meter, Iowa. Downstream of the confluence is then called the Raccoon River, flowing west to east, and flows into the Des Moines River at Des Moines, Iowa. The total drainage area of the Raccoon River at Des Moines is approximately 3608 mi<sup>2</sup>. For modeling, the North Raccoon Watershed was divided into 1156 smaller units, called subbasins in HMS. These have an average area of approximately 2.1 square miles but can be as large as 7.6 square miles. Smaller subbasins were delineated, averaging 0.5 square miles, in HUC 12s selected for implementation of demonstration projects. Figure 3.2 illustrates subbasin delineation of the North Raccoon River Watershed as implemented in HMS.

ESRI ArcGIS and Arc Hydro tools were used for terrain preprocessing, creating flow direction and flow accumulation grids, defining the stream network, and delineating the subbasins. The stream network was defined by channels draining at least 1.5 square miles; subbasins were created such that a subbasin was defined upstream of all stream confluences. GIS-defined subbasins were further split manually to create an outlet point at each USGS gauge location, as well as the discharge point of incorporated structures. Potholes within the watershed were identified using Geographic Information System (GIS) tools as well. Identifying the location of these isolated depressions is important in replicating the rainfall-runoff process of the region. These isolated pockets do not lead directly to runoff, rather they will store water until it either fills completely and spills over onto the adjacent draining land surface, evaporates, infiltrates naturally into the ground, or infiltration is aided by drainage inlets and pipe networks. In addition to identifying the actual isolated pothole, the area draining to that low pocket was also identified. These drainage areas were incorporated into the hydrologic modeling as areas that do not contribute directly to surface runoff.

In HMS, the model performs the averaging previously described for lumped parameter models within the boundary of each subbasin. Each subbasin was assigned a single value for the parameter being developed.

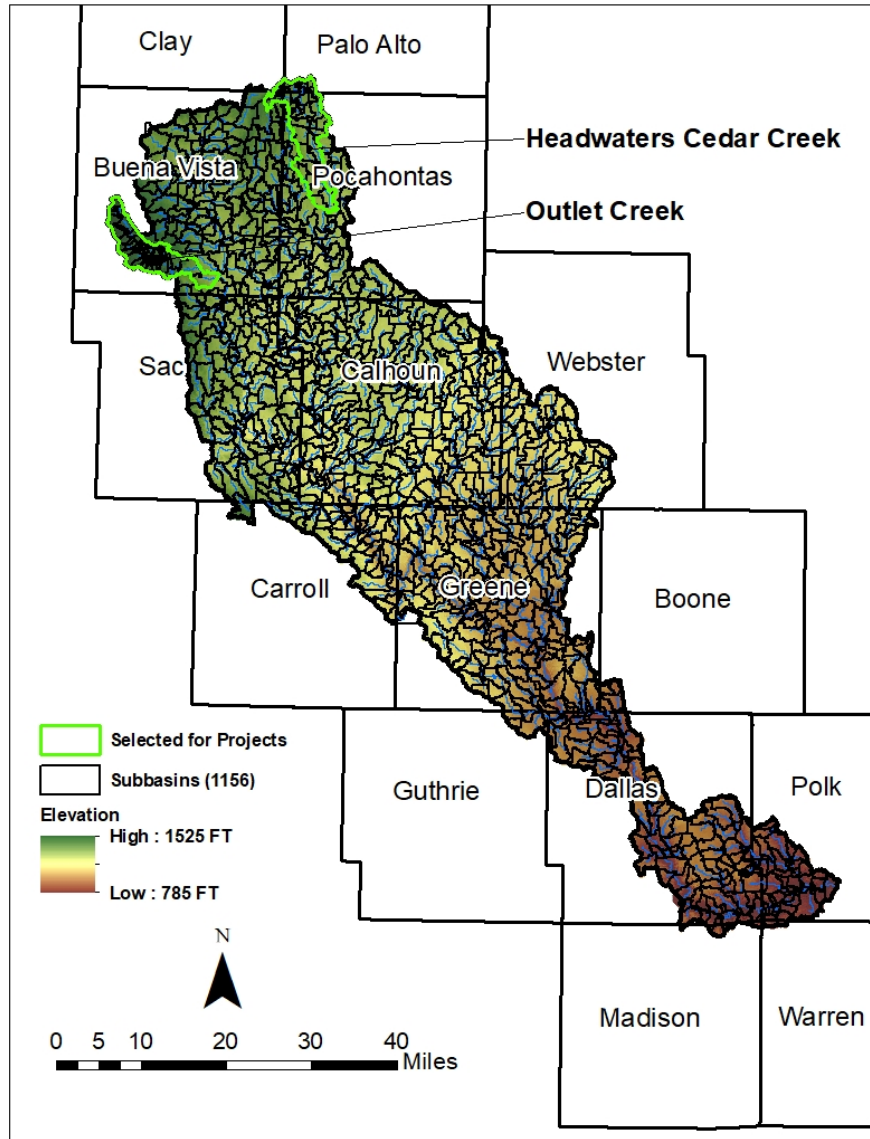


Figure 3.2. HMS model development of the North Raccoon River Watershed. The watershed was divided into 1156 subbasins for modeling.

### **i. Incorporated Structures**

Little Storm Lake, the Storm Lake Bridge Inlet, Storm Lake, Black Hawk Lake, and Twin Lakes were incorporated into the HMS model. Design and/or stage-storage-discharge relationship information were obtained from Iowa Department of Natural Resources' Office of Dam Safety in Des Moines, Iowa for each of these structures. The stage-storage-discharge rating curves used in

the North Raccoon River Watershed HMS model are available in Appendix C. Existing farm ponds or any other possible water storage structures were not included in the HMS model.

## **ii. Development of Model Inputs and Parameters**

This section provides a brief overview of data inputs used and assumptions made to develop the HMS model. Appendix B of this report provides more detailed information on the hydrologic model development.

### ***Rainfall (meteorological model)***

Stage IV radar rainfall estimates (NCEP/EMC 4KM Gridded Data [GRIB] Stage IV Data) were used as the precipitation input to simulate actual rainfall events known to have occurred within the watershed. The National Center for Environmental Prediction (NCEP) produced the Stage IV data set by taking radar rainfall estimates produced by the 12 National Weather Service (NWS) River Forecast Centers across the continental United States and combining them into a nationwide 4 km x 4 km (2.5 mile x 2.5 mile) gridded hourly precipitation estimate data set. These data are available from Jan. 1, 2002–present.

Figure 3.3, developed using HEC-GridUtil 2.0, shows an example of the Stage IV radar rainfall estimates of cumulative rainfall during a one-hour period (May 05, 2007, 9–10 p.m.) in the North Raccoon River Watershed. This figure demonstrates the gridded nature of the radar rainfall estimate data, as well as the distribution of rainfall in time and space during large storm events.

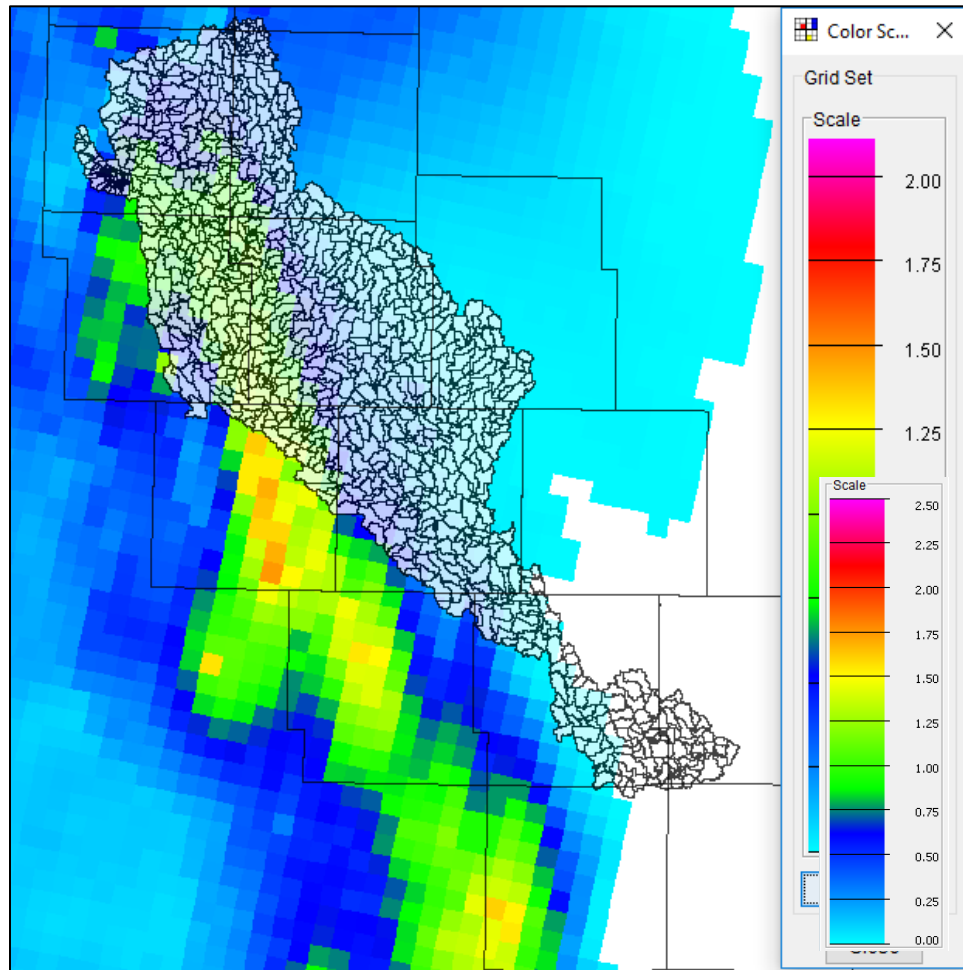


Figure 3.3. Example of the Stage IV rainfall product used as the precipitation input in the North Raccoon River Watershed HMS model. The Stage IV product provides hourly cumulative rainfall estimates for each 4 km x 4 km grid cell. The scale shown indicates estimates of the depth of rainfall (in inches) for a one-hour period.

Radar rainfall provides increased accuracy in spatial and temporal distribution of precipitation over the watershed. In addition, Stage IV estimates provide a level of manual quality control (QC), performed by the NWS, which incorporates available rain gauge measurements into the rainfall estimates. Actual storms using Stage IV data provided the basis for model calibration and validation.

A hypothetical storm was developed for comparative analyses, such as potential runoff generation, increased infiltration capacity, and increased distributed storage within the watershed. The hypothetical storm applies a uniform depth of six inches of rainfall across the entire watershed with the same timing everywhere. A Soil Conservation Service (SCS) Type-II distribution, 24-hour storm was used for the hypothetical storm. In reality, rainfall does not occur uniformly across the entire watershed. However, the hydrologic response of subbasin can be compared and analyzed more easily if all the subbasins are subject to the same rainfall depth and timing.

**Watershed (basin model)**

Iowa’s statewide LiDAR dataset provided elevation data. The USGS has performed quality assurance testing on these LiDAR data, which have reported vertical positional accuracy of +/- 18 cm. The LiDAR product used had a resolution of 3-meters and was processed as a bare earth product, with structures and vegetation removed. Using ESRI ArcGIS, LiDAR data was clipped to the watershed boundary and mosaicked into a seamless digital elevation model. The Universal Transverse Mercator (UTM) Zone 15 North geographic coordinate system was used, referencing the North American Datum of 1983 (NAD 83). All elevation values are in feet and are referenced to the North American Vertical Datum of 1988 (NAVD 88).

The Soil Conservation Service (SCS) Curve Number (CN) methodology was used to determine the rainfall-runoff partitioning for the North Raccoon River Watershed HMS modeling. Curve number values range from 30–100, and as the CN becomes larger, less water infiltrates the ground and a higher percentage of runoff occurs. CN values are an estimated parameter based primarily on the intersection of a specific land use and the underlying soil type. General guidelines for developing curve numbers based on land use and soil type are available in technical references from the U.S. Department of Agriculture–Natural Resource Conservation Service (USDA-NRCS), previously known as the SCS. Table 3.1 shows the CNs assigned to each land use and soil type combination for the North Raccoon River HMS model. Dual hydrologic soil groups (e.g., A/D, B/D, C/D) are typically located in areas with water tables at a depth of 24 inches or less. For example, type A/D would behave like soil type A when drained and like soil type D when undrained. To be conservative, all dual hydrologic soil groups were treated like soil type D.

Table 3.1. Curve number assignment in the North Raccoon River Watershed based on land use and soil type. All dual hydrologic soil groups were treated as type D.

<i>Land Cover Description</i>	<i>Hydrologic Soil Group</i>			
	<i>A</i>	<i>B</i>	<i>C</i>	<i>D</i>
Water	100	100	100	100
Wetland	100	100	100	100
Shadow	100	100	100	100
Roads / Impervious	100	100	100	100
Structures	100	100	100	100
Barren / Fallow	98	98	98	98
Soybeans	67	78	85	89
Corn	67	78	85	89
Cut Hay	49	69	79	84
Grass 2	49	69	79	84
Grass 1	49	69	79	84
Deciduous Tall	32	58	72	79
Deciduous Medium	32	58	72	79
Deciduous Short	32	58	72	79
Coniferous Forest	32	58	72	79

### ***Antecedent moisture conditions***

Rainfall-runoff partitioning for an area is also dependent on the antecedent soil moisture conditions (how wet the soil is) (AMC) at the time rain falls on the land surface. The wetter the soil is, less water is able to infiltrate and more water is then converted to runoff. Therefore, when using SCS Curve Number methods to determine runoff volumes, determination of antecedent soil moisture content and classification into the antecedent moisture classes AMC I, AMC II, and AMC III, representing dry, average, and wet conditions, is an essential matter for the application of the SCS Curve Number (Silveira et al., 2000) and Curve Numbers may need adjustment to accurately simulate runoff for dryer or wetter than normal conditions.

### ***Runoff hydrographs***

The Clark and ModClark Unit Hydrograph methods were used to convert excess precipitation into a direct runoff hydrograph for each subbasin. The ModClark method requires the same grid used for radar rainfall, so this method was used to simulate historical storms in calibration and validation steps, while the traditional Clark method was used for hypothetical design storm analysis. Both methods account for translation (delay) and attenuation (reduction) of the peak subbasin hydrograph discharge due to travel time of the excess precipitation to the subbasin outlet and temporary surface storage effects. The primary difference between the two methods is that the traditional Clark Unit Hydrograph method uses a pre-developed time-area histogram, while the ModClark method uses a grid-based travel time model to account for translation (lag) of the subbasin hydrograph. Both methods route the hydrograph through a linear reservoir to account for temporary storage effects.

Both the ModClark and Clark unit hydrograph methods require two inputs — time of concentration and a time storage coefficient. The time of concentration is the time required for water to travel from the hydraulically most remote point in the subbasin to the subbasin outlet. This was estimated to be 5/3 times the lag time, where lag time is the time difference between the center of mass of the excess precipitation and the peak of the runoff hydrograph. This is a reasonable approximation, according to NRCS methodology (Woodward, 2010). Lag time is a function of land slope, longest flow path, and soil retention (represented through CN); these parameters were estimated for each subbasin using ArcGIS tools.

Figure 3.4 illustrates the NRCS methodologies for runoff depth estimation and how this runoff depth is converted to discharge (using one of the Clark unit hydrograph methods).

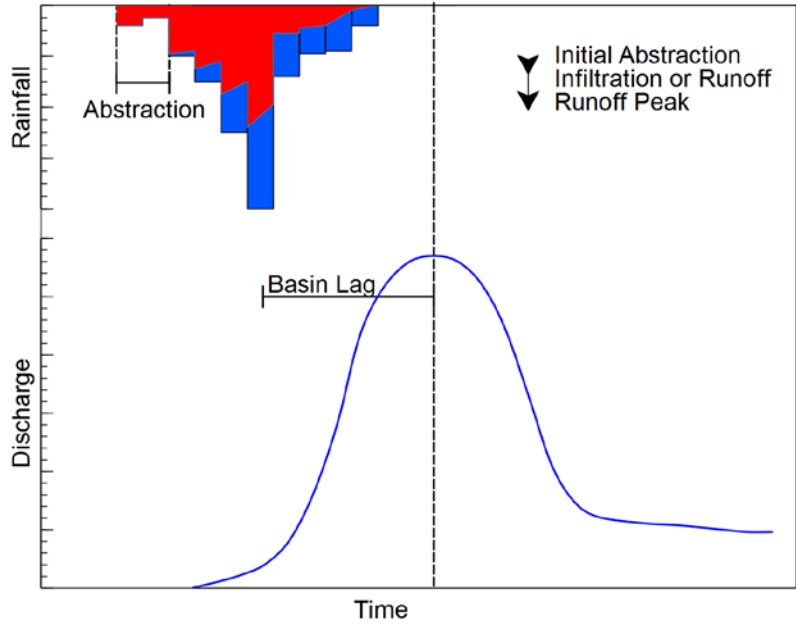


Figure 3.4. Subbasin runoff hydrograph conceptual model. Rainfall is partitioned into a runoff depth using the NRCS curve number methodology, which is then converted to discharge using either the ModClark or Clark unit hydrograph method.

### ***ArcGIS to HEC-HMS***

Upon completion of GIS processing to prepare the basin topography data, establish the stream network, delineate the subbasins, and develop and assign the necessary parameters to describe the rainfall-runoff partitioning for each subbasin, HEC-GeoHMS tools were used to intersect the subbasins with the appropriate grid system (HRAP) to allow use of the Stage IV radar rainfall estimates. Lastly, from ArcGIS, HEC-GeoHMS tools were used to create a new HMS project and export all the data developed in ArcGIS to the appropriate format such that the model setup was mostly complete upon opening HMS for the first time. Once in the HEC-HMS user's interface, quality checks were performed to ensure the connectivity of the subbasins and stream network of the watershed.

### **Parameters Assigned in HEC-HMS**

#### ***Baseflow***

Baseflow was approximated using a first order exponential decay relationship for all historical storms. The USGS stage/discharge gauges for the North Raccoon River near Sac City and Jefferson as well as the Raccoon River near Van Meter and West Des Moines were used to develop discharge-drainage area (cfs/mi<sup>2</sup>) relationships to set initial conditions for streamflow prior to each historical storm event simulation. Initial baseflow conditions were applied to the appropriate subbasins in HMS for each historical storm event simulation. A baseflow recession constant describing the rate of decay of baseflow per day was specified and a threshold indicating when baseflow should be reactivated. No baseflow was modeled for the hypothetical design storms, as these analyses are more concerned with the effects of how much direct runoff is produced. The contribution of baseflow during these analyses was assumed to be relatively small compared to the amount of runoff produced.

#### ***Flood Wave Routing***

Conveyance of runoff through the river network, or flood wave routing, was accomplished using Muskingum-Cunge routing methods for major streams and Muskingum routing methods for smaller tributaries. The Muskingum-Cunge routing model uses an eight-point cross-section configuration and quasi-physical parameters to route channel and floodplain flow. Each routing reach requires specification of a reach length, roughness coefficients (channel, left and right overbanks), and energy grade. Roughness coefficients were adjusted as part of the calibration process to best reproduce observations.

Two inputs are required to use the Muskingum routing model in HMS — the flood wave travel time in a reach (K) and a weighting factor that describes storage within the reach as the flood wave passes through (X). The allowable range for the X parameter is 0–0.5; values of 0.1–0.3 are generally applicable to natural streams. A value of 0.2 is frequently used in engineering practice and was used in this modeling analysis. Great accuracy in determining X may not be necessary because the results are relatively insensitive to the value of this parameter (Chow et al., 1988). The flood wave travel time, K, is much more important and can be estimated by dividing the reach length by a reasonable travel velocity (1–6 feet per second, in general) as a starting point, but is generally best obtained by adjustment in the model calibration process using measured discharge records, if available. For this modeling analysis, a flood wave travel velocity of 1-3- feet per second

was used for all Muskingum routing reaches. All reservoirs or ponds incorporated into the model were assumed to be filled to the normal pool level at the beginning of each simulation.

## **b. Calibration**

To calibrate a model, an initial set of parameters are developed for a hydrologic model through GIS and other means and adjust so the model's simulated results match an observed time series as closely as possible. Typically, this is stream discharge at a gauging station. However, modelers should not make extreme adjustments to parameters just to manipulate the end results to match the observed time series. If this is necessary, the model does not reasonably represent the watershed, and it is requisite upon the modeler to change methods used within the model or find out which parameter(s) might be needed to better represent the watershed's hydrologic response. The North Raccoon River Watershed HMS model was calibrated to two storm events that occurred in May 2013 and April 2007. Storms were selected based on their range of antecedent conditions, magnitude, time of year they took place, and availability of Stage IV radar rainfall estimates and USGS discharge estimates. Large, high runoff storms were selected that occurred between late April and September so the impacts of snow, rain on frozen grounds, and freeze-thaw effects were minimized. Global adjustments to the runoff (CN) and timing (river routing and unit hydrograph) parameters were made to best match the simulated response to the observed discharge time series at each USGS discharge gauge location. Appendix B provides more details on calibration and validation.

## **c. Validation**

For model validation, the intent is to use the model parameters developed during calibration to simulate other events and evaluate how well the model is able to replicate observed stream flows. With several of the largest storms already having been selected for calibration or having occurred before the availability of Stage IV radar rainfall estimates (January 2002), the next best available storms were selected. A June 2005 event was considered for model validation.

As with calibration, the HMS model validation results are not perfect. Plots of validation simulation are shown in Appendix B. However, the general runoff volume, hydrograph shape, and peak flow timing are very similar to the observed streamflow hydrographs. Because HMS is a surface water model, it struggles to simulate conditions where overland flow does not dominate the partitioning of rainfall, as well as the complexity added by artificially drained agricultural landscapes.

## **4. Analysis of Watershed Scenarios**

The HEC-HMS model of the North Raccoon River Watershed was used to identify areas in the watershed with high runoff potential and run simulations to help understand the potential impact of alternative flood mitigation strategies in the watershed. Scenarios were developed to help understand the impacts of: (1) increasing infiltration in the watershed; and (2) implementing a system of distributed storage projects (ponds) across the landscape. There are many BMP practices not investigated in this report that could potentially increase infiltration or runoff storage at the watershed scale. However, the analysis was limited by the resolution and capability of the HEC-HMS model to simulate effects of BMP practices aggregated across subbasin areas of several square miles. Therefore, the investigations were limited to distributed storage provided by ponds, which are relatively large BMP structures, and broad-scale land cover changes. Simulation of other much smaller BMP structures or field management practices would require considering many more individual structures to make any impact at the watershed scale, and a much higher degree of model resolution to reliably quantify impacts.

### **a. High Runoff Potential Areas**

Identifying areas of the watershed with higher runoff potential is the first step in selecting mitigation project sites. High runoff areas offer the greatest opportunity to retain more water from large rainstorms on the landscape and to reduce downstream flood peaks.

In the HMS model of the North Raccoon River Watershed, the runoff potential for each subbasin is defined by the SCS Curve Number (CN). The runoff CN assigned to a subbasin depends on its land use and the underlying soils. The fraction of rainfall converted to runoff — also known as the runoff coefficient — is a convenient way to illustrate runoff potential. Areas with higher runoff coefficients have higher runoff potential. To evaluate the runoff coefficient, the HMS model simulates runoff from each subbasin area for the same rainstorm; a rainstorm was selected with a total accumulation of 6.0 inches in 24 hours (approximately 25-year average recurrence interval) (National Oceanic and Atmospheric Administration, 2013). The timing of the rainfall and example infiltration is shown in Figure 4.1. This design storm corresponds to approximately the 25-year return interval at small scales, similar to the size of model subbasins. Applying this design storm across the entire North Raccoon Watershed results in unrealistic peak discharge values at many locations with moderate drainage area. However, subjecting each model subbasin to the same storm allows for direct comparison among them.

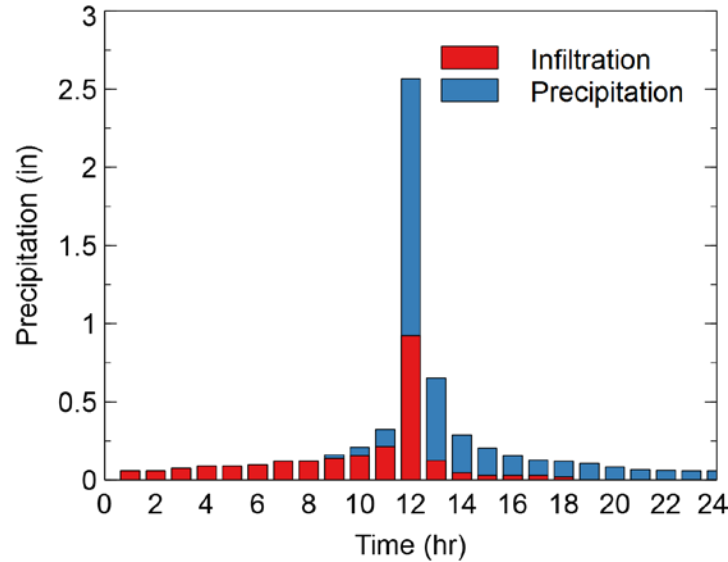


Figure 4.1. SCS design storm hyetograph, showing the timing of the rainfall and example infiltration for a given subbasin area.

Figure 4.2 shows the runoff coefficient as a percentage (from 0% for no runoff to 100% when all rainfall is converted to runoff). Since the subbasin areas shown were defined for numerical modeling purposes, the results were also aggregated to more commonly used subbasin areas — namely, hydrologic units defined by the USGS. The smallest hydrologic units, known as HUC 12 watersheds, are also shown in Figure 4.2. Area-weighted average runoff coefficients were developed for each of the 75 HUC 12 watersheds in the North Raccoon River Watershed. Areas with the lowest runoff potential are located on the Des Moines Lobe landform region, an area with numerous isolated depressions that are not hydraulically connected to a natural water course. These areas appear to generate less runoff, but it likely some of the precipitation that is ponded eventually infiltrates and enters the drainage system through field drainage tile. Areas with relatively higher runoff potential occur along the main stem of the North Raccoon River, or the southern edge of the watershed. From a hydrologic perspective, flood mitigation projects that can reduce runoff from these higher runoff areas should be a higher priority.

Higher runoff potential is only one factor in selecting locations for potential projects. Taken alone, it has limitations. The watershed’s low degree of subbasin slope and lack of topographic relief will make identifying sites favorable for traditional flood mitigation ponds difficult. However, prairie pothole features throughout regions of this watershed could provide alternative opportunities for flood mitigation and conservation efforts. Other practices besides flood mitigation ponds can be employed to encourage infiltration and detention of runoff. Landowner willingness to participate is essential. Also, existing conservation practices may be in place, and areas such as timber should not be disturbed. Stakeholder knowledge of places with repetitive loss of crops or roads/road structures is also valuable in selecting locations.

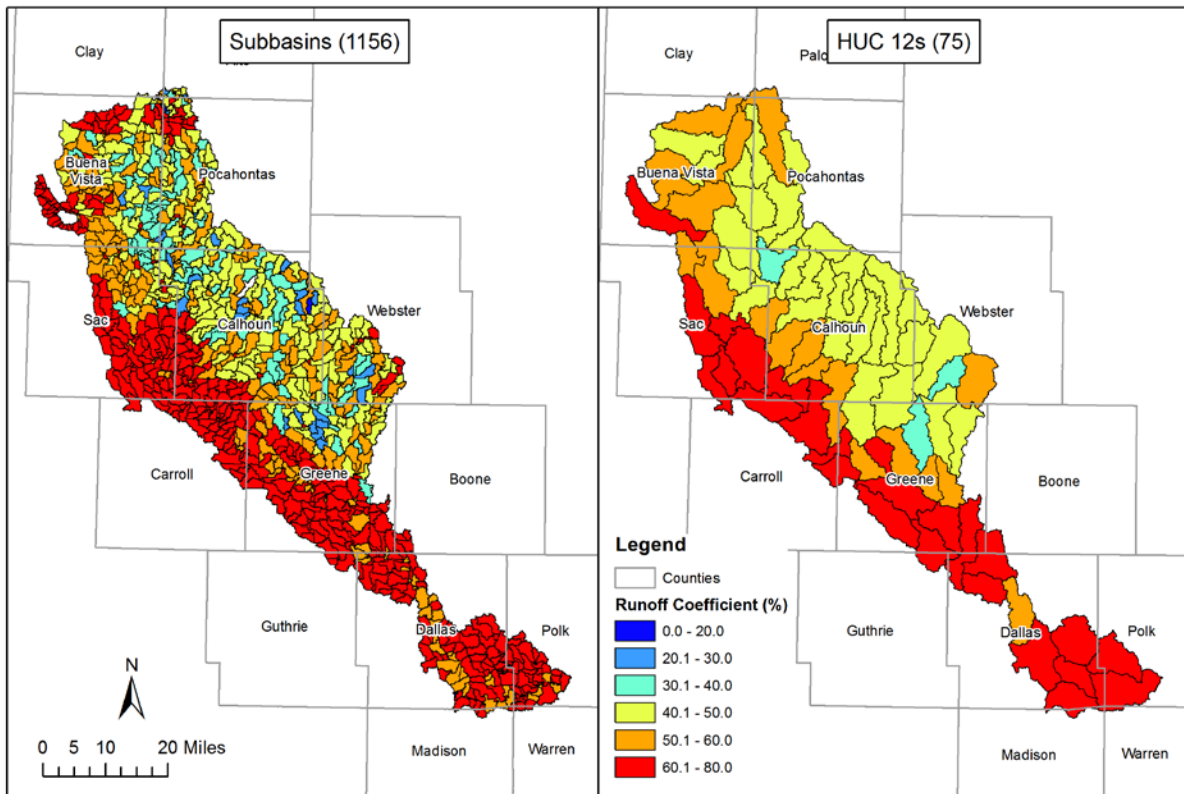


Figure 4.2. Runoff potential coefficients computed for each subbasin (left) and HUC 12 watershed (right) for a 6-inch, 24-hour design storm are shown. Higher runoff coefficients appear in red. Many areas with lower runoff potential are the result of prairie pothole areas that are isolated from the subbasin outlet.

## b. Mitigating the Effects of High Runoff with Increased Infiltration

Runoff can be reduced from areas with high runoff potential by increasing how much rainfall infiltrates into the ground. Changes that result in higher infiltration reduce the volume of water that drains off the landscape during and immediately after the storm. The extra water that soaks into the ground may later evaporate or transpire. Or it may slowly travel through the soil, either seeping deeper into the groundwater storage or traveling beneath the surface to a stream. Increasing infiltration has several benefits. Even if the infiltrated water reaches a stream, it arrives much later (long after the event has ended, and flooding has subsided). Also, its late arrival keeps rivers running during long periods without rain.

In this section, several different alternatives to reduce runoff through either land use changes or soil quality improvements were examined. One hypothetical land use change would be the conversion of row crop agriculture back to native tall-grass prairie. Another possible land use change would be improvements to agricultural conditions that would result from planting cover crops during the dormant season. These are hypothetical examples; they are meant to illustrate the potential effects on flood reduction. Hypothetical examples provide valuable benchmarks on the limits of flood reduction that are physically possible with broad-scale land cover changes.

## **i. Conversion of Row Crop Agriculture to Tall-Grass Prairie**

Much has been documented about the historical water cycle of the native tall-grass prairie of the Midwest. Prior to the transformation to agricultural landscape, tall-grass prairies dominated the landscape. This ecosystem infiltrated, transpired, and stored extremely large volumes of water throughout the entire year (Mutel, 2010; Hernandez-Santana et al., 2013). The deep, loosely packed organic soils and the deep root systems of the prairie plants (Jackson et al., 1996), allowed a high volume of the rainfall to infiltrate into the ground (Bharati et al., 2002). The soils retained the water instead of allowing it to travel rapidly to a nearby stream as surface flow. Once in the soils, much of the water was actually taken up by the root systems of the prairie grasses (Brye et al., 2000).

An analysis to quantify the impact of human-induced land use changes on the flood hydrology of the North Raccoon River Watershed was completed. In this example, all current agricultural land use is converted to native tall-grass prairie with its much higher infiltration characteristics. Obviously, returning to this pre-settlement condition is unlikely to occur. Still, this scenario is an important benchmark to compare with any watershed improvement project considered.

To simulate the conversion to native tall-grass prairie with the HMS model, the model parameters affecting runoff potential across the landscape were adjusted to reflect the tall-grass prairie condition. Specifically, existing agricultural land use, which accounts for 78% of the watershed area, was redefined as tall-grass prairie. New CNs, reflecting the lower runoff potential of prairie, were assigned to each subbasin as shown in Table 4.1. It is important to note that other parameters estimated from CNs — such as the water flow travel time through the subbasin — were not adjusted. Thus, this scenario only considers the runoff reduction resulting from the much-improved infiltration characteristics of the native prairie and not the additional attenuation and delay in the timing of the peak discharge that would be expected due to a higher surface roughness. Following new assignment of subbasin CNs, the model was run using the design storm with total accumulation of 6.0 inches in 24 hours.

### **Six-Inch, 24-Hour SCS Design Storm**

As expected, improving the infiltration of 78% of the watershed area by converting row crop agriculture to native tall-grass prairie has a significant effect on the flood hydrology. For the 6-inch design storm, the simulated tall-grass prairie infiltrates 0.7 inches more rainfall into the ground than does the current agricultural landscape. Figure 4.3 shows reductions in subbasin and junction peak discharges. Most of the watershed experienced greater than a 20% reduction in subbasin peak discharge. Application of this design storm across the entire watershed produces unrealistic peak discharges at junction locations with relatively large drainage area, therefore, results are not shown at junctions with drainage area greater than 100 mi<sup>2</sup>.

Table 4.1. Curve numbers used to define the tall-grass prairie and cover crop land use conditions.

Land Use	Hydrologic Soil Group			
	A	B	C	D
Row Crops	67	78	85	89
Tall-Grass Prairie	30	58	71	78
Row Crops after Planting Cover Crops	64	74	81	85

Note: Curve number combinations derived from the *Urban Hydrology for Small Watersheds (TR-55)*, Table 2-2, June 1986.

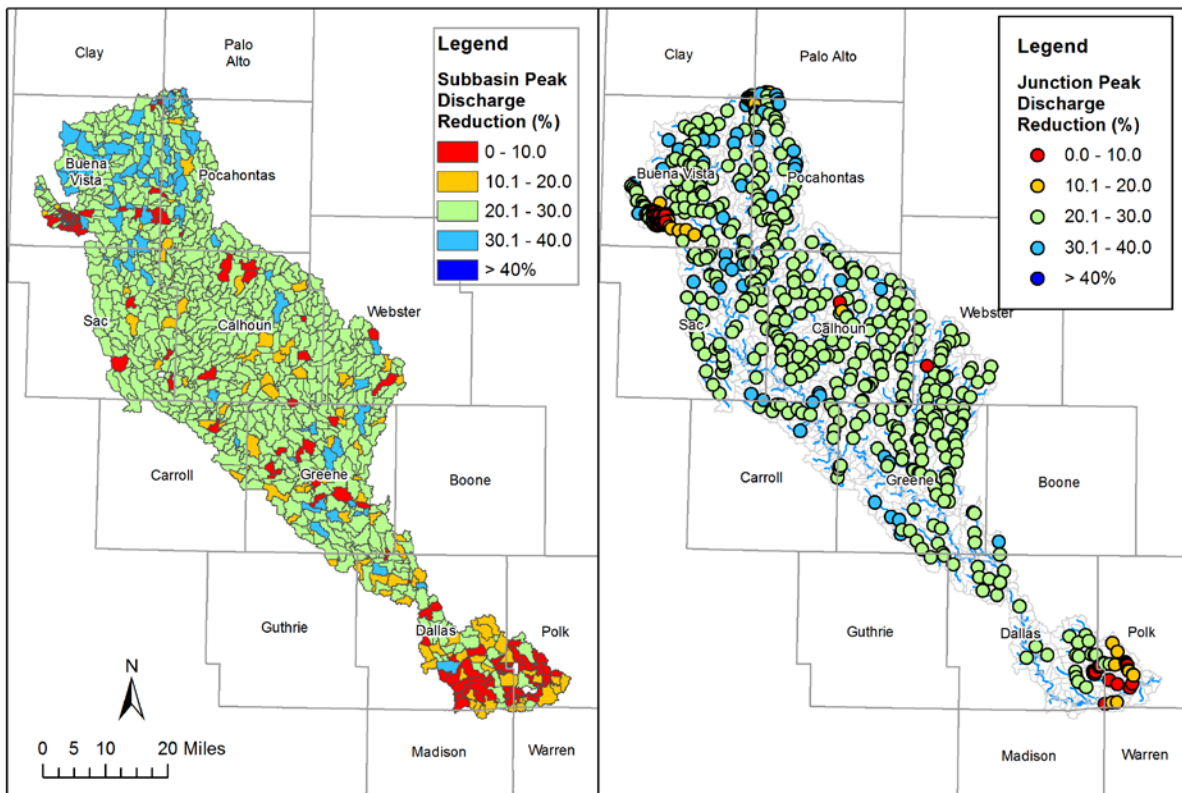


Figure 4.3. Peak discharge reductions for subbasins (left) and junctions (right) for conversion of row crop agriculture to native prairie for a 6-inch, 24-hour design storm. Simulation results at junctions with large drainage area are not realistic for this design storm event, therefore, results are not shown at junctions with drainage area greater than 100 mi<sup>2</sup>.

## ii. Improved Agricultural Conditions from Planting Cover Crops

Cover crops can be an effective farming conservation practice that also enhances infiltration. Farmers typically plant cover crops after the harvest of either corn or soybeans and “cover” the ground through the winter until the next growing season begins. The cover crop can be killed off in the spring by rolling it or herbicide application; afterwards, row crops can be planted directly into the remaining cover crop residue. Cover crops provide a variety of benefits, including

improved soil quality and fertility, increased organic matter content, increased infiltration and percolation, reduced soil compaction, and reduced erosion and soil loss. Cover crops also retain soil moisture and enhance biodiversity (Mutch, 2010). One source suggests that for every one percent increase in soil organic matter (e.g., from 2% to 3%), the soil can retain an additional 17,000–25,000 gallons of water per acre (Archuleta, 2014). Examples of cover crops include clovers, annual and cereal ryegrasses, winter wheat, and oilseed radish (Mutch, 2010).

The purpose of this hypothetical example is to investigate the impact improved agricultural management practices could have on reducing flood peak discharges throughout the watershed. It was hypothesized that planting cover crops across all agricultural areas in the watershed during the dormant (winter) season would lower the runoff potential of these same areas during the growing season (spring and summer) because of increased soil health and fertility. To be clear, this scenario does not represent the conversion of the existing agricultural landscape (primarily row crops) to cover crops. Rather, the existing agricultural landscape is still mostly intact, but its runoff potential during the growing season has been slightly reduced by planting cover crops during the dormant season. Similar to the tall-grass prairie scenario, Table 4.1 shows the new runoff CNs assigned to each subbasin, reflecting the landscape's lower runoff potential from improved agricultural management practices. Comparisons were made between current and cover crop simulations for the 6-inch, 24-hour SCS design storm.

#### **Six-Inch, 24-Hour SCS Design Storm**

Improved agricultural management practices, represented by planting cover crops during the dormant season, reduces runoff and peak discharges less than the native tall-grass prairie simulation does. On average for the basin, planting cover crops increases infiltration by 0.15 inches for the 6-inch, 24-hour SCS Design Storm. Figure 4.4 shows the peak discharge reductions for each subbasin resulting from improved agricultural conditions due to cover crops for the 6-inch, 24-hour design storm. Peak discharge reductions of approximately 5% are common at the subbasin scale. Application of this design storm across the entire watershed produces unrealistic peak discharges at junction locations with relatively large drainage area, therefore, results are not shown at junctions with drainage area greater than 100 mi<sup>2</sup>.

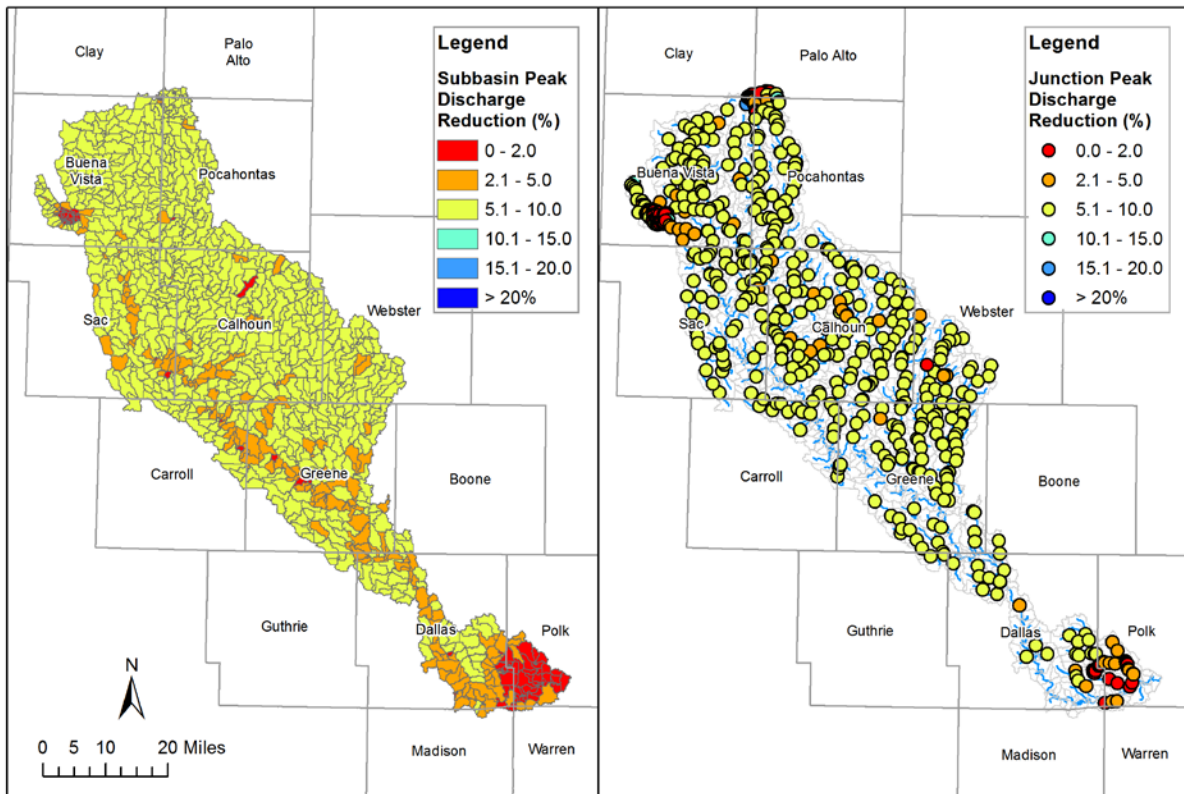


Figure 4.4. Peak discharge reductions for subbasins (left) and junctions (right) for the 6-inch, 24-hour design storm with improved soil infiltration after many years of using cover crops during the dormant season for all row crop agriculture. Simulation results at junctions with large drainage area are not realistic for this design storm event, therefore, results are not shown at junctions with drainage area greater than 100 mi<sup>2</sup>.

### c. Mitigating the Effects of High Runoff with Distributed Storage

In general, a system providing distributed storage, does not change the volume of water that runs off the landscape. Instead, storage ponds (Figure 4.5) hold floodwater temporarily and release it at a slower rate. Therefore, the peak flood discharge downstream of the storage pond is lowered. The effectiveness of any one storage pond depends on its size (storage volume) and how quickly water is released. By adjusting the size and the pond outlets, storage ponds can be engineered to efficiently use available storage for large floods.

Generally, these ponds have a permanent storage area, that holds water all the time. This is achieved by constructing an earthen embankment across a stream and setting an outlet (usually a pipe called the principal spillway) at some elevation above the floor of the pond. When a storm event occurs, runoff enters the pond. Once the elevation of the water surface is higher than the pipe inlet, water will pass through the pipe, leaving the pond at a controlled rate. Additionally, the earthen dam is built higher than the pipe, allowing for more storage capacity within the pond. An auxiliary or emergency spillway that can discharge water at a much faster rate than the pipe does is set at an elevation higher than the pipe. This auxiliary spillway is designed to release rapidly

rising waters in the pond, so they do not damage the earthen embankment. The volume of water stored between the principal spillway and the emergency spillway is called flood storage.

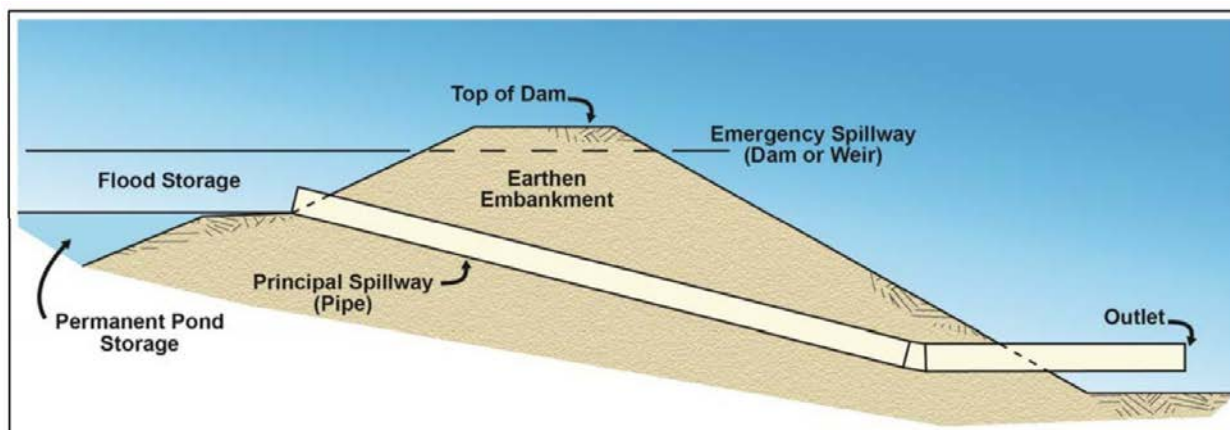


Figure 4.5. Schematic of a pond constructed to provide flood storage.

The hypothetical distributed storage analysis performed using the North Raccoon River HMS model was based on the flood control concept developed by the Soap Creek Watershed. The Soap Creek Watershed Board formed in the 1980s when landowners banded together to reduce flood damage and erosion within their watershed. They adopted a plan to identify potential locations for 154 distributed storage structures (mainly ponds) that could be built within the watershed. As of 2018, 135 of these structures have been built (Stolze, 2018).

The Soap Creek Watershed drains approximately 250 square miles, equaling an average density of 1 built pond for every 1.9 square miles of drainage area. Further analysis of the Soap Creek structures shows that most are constructed in the headwater areas of the watershed, which allows for smaller structures, rather than large, high-hazard class structures on the main rivers. The average pond density in the headwater areas where most of the ponds are sited is approximately 1 pond per 1.4 square miles of drainage area.

### **i. Siting of Ponds in the North Raccoon River Watershed**

Figure 4.6 shows the 87 locations in the North Raccoon Watershed identified as potential locations for nutrient reduction wetlands using the ACPF toolbox. With these ACPF data, we can design a pond for each specific nutrient reduction wetland location. With detailed information about the pond site and drainage area, the NRCS Water Resources Site Analysis Computer program (SITES) was ran to design the principal and auxiliary (emergency) spillway of each pond.

SITES requires a time-of-concentration (TOC) estimate at each NRW location. TOCs were estimated using the Watershed Lag method from the National Engineering Handbook (NEH) Part 630, Chapter 15 (National Resources Conservation Service, 2010). The flow length (l) is found using Equation 4.1,

$$l = 209A^{0.6} \quad 4.1$$

where A is the drainage area in acres and l is in feet.

the flow length was used to compute the TOC using Equation 4.2,

$$TOC = \frac{l^{0.8}(S+1)^{0.7}}{1140Y^{0.5}} \quad 4.2$$

where Y is the average watershed land slope in percentage, and S is the maximum potential retention inches calculated by  $\frac{1000}{CN} - 10$ .

The SITES analysis makes the following assumptions for each ACPF NRW location:

- The principal spillway is an open-top drop inlet riser with a 10-inch minimum pipe diameter;
- The principal spillway elevation is the NRW permanent pool elevation reported by ACPF;
- The auxiliary spillway has a 12-foot width;
- The auxiliary spillway elevation is the NRW buffer elevation reported by ACPF, 4.9 feet above the principal spillway elevation; and
- The principal spillway is sized such that a 25-year NRCS Type II design rainfall event does not activate the auxiliary spillway.

The SITES program was ran iteratively for each pond until the designed principal spillway pipe diameter was large enough so that the auxiliary spillway was not activated for the 25-year design storm. Storage-discharge relationships were developed for each of the 87 pond locations.

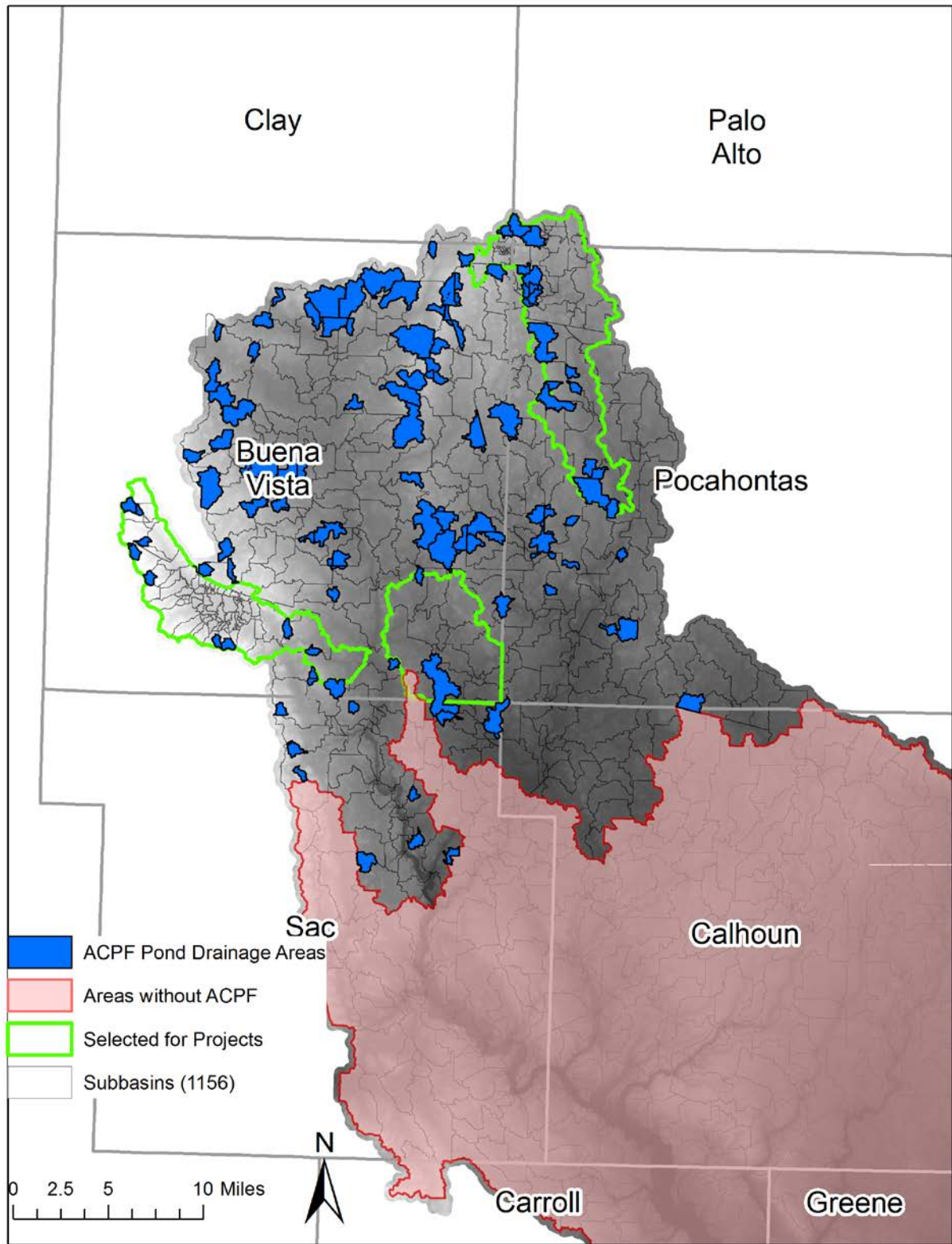


Figure 4.6. Areas draining to nutrient reduction wetlands (NRWs), identified by the Agricultural Conservation Planning Framework (ACPF) toolbox. NRW ponds were used to develop storage-discharge relationships for corresponding subbasins.

Numerous HEC-HMS model subbasins contained more than one pond within the subbasin area. This required aggregation of the ponds to simulate their cumulative impact. All the ponds were treated as if they were in a parallel configuration. The abscissae and ordinates of the storage-discharge curves were summed for a given group of ponds within a subbasin. A single pond HMS model element was inserted within each HMS model subbasin containing ponds and applied the aggregated storage-discharge relationship. The cumulative subbasin drainage area intercepted by the ACPF ponds was used to divert the appropriate percentage of subbasin runoff to the aggregated pond or allowed to bypass to the downstream subbasin outlet. For example, if a single subbasin contained three ponds, the storage and outflow curves were summed and diverted the corresponding drainage area to the ponds, with the remaining drainage area allowed to bypass to the downstream junction. Overlapping pond drainage areas for those in a series configuration were dissolved to prevent over-estimating intercepted drainage area. Figure 4.7 depicts the treatment of multiple ponds within a subbasin and the aggregation process. The variable storage available for runoff provided by aggregated ACPF ponds for each subbasin is shown in Figure 4.8.

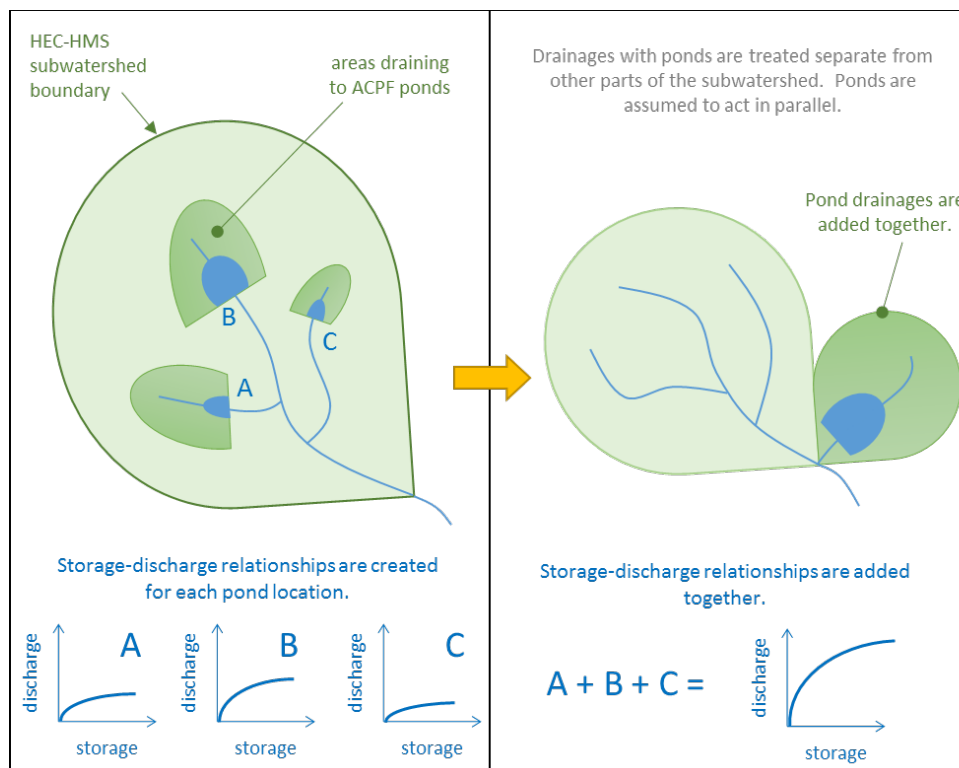


Figure 4.7. Aggregation of pond storage-discharge curves and drainage areas within a subbasin. Overlapping drainage areas of ponds in a series configuration were dissolved.

Some HUC 12s, shown in the previous figures, did not have ACPF data available prior to the completion of the report. For completeness, the relationships between subbasin drainage area, cumulative drainage area intercepted by ponds, and aggregated storage-discharge curves were used to develop hypothetical ponds in selected headwater subbasins lacking ACPF data. Headwater subbasins were selected based on subbasin slopes similar to those ACPF areas that pond structures were sited. This method allows us to consider a similar distributed system of ponds in areas where ACPF data are not available. Specific siting considerations for these

hypothetical ponds in the non-ACPF area would need to be completed prior to any implementation. The variable storage available for runoff provided by these hypothetical ponds for each subbasin is also shown in Figure 4.8.

There are relatively fewer potential ACPF pond locations in this area compared to ACPF data developed for other parts of Iowa, likely due to differences in topographic relief and other suitability factors. Development of hypothetical ponds in a selected set of headwater subbasins likely overestimates the number of suitable pond locations for this low topographic relief watershed. It is important to note that these ACPF ponds were initially sited using nutrient reduction criteria, rather than flood reduction criteria. Simulation results discussed later in this report provide some context for the expected benefit of structural flood mitigation practices versus broad spatial adoption of in-field practices.

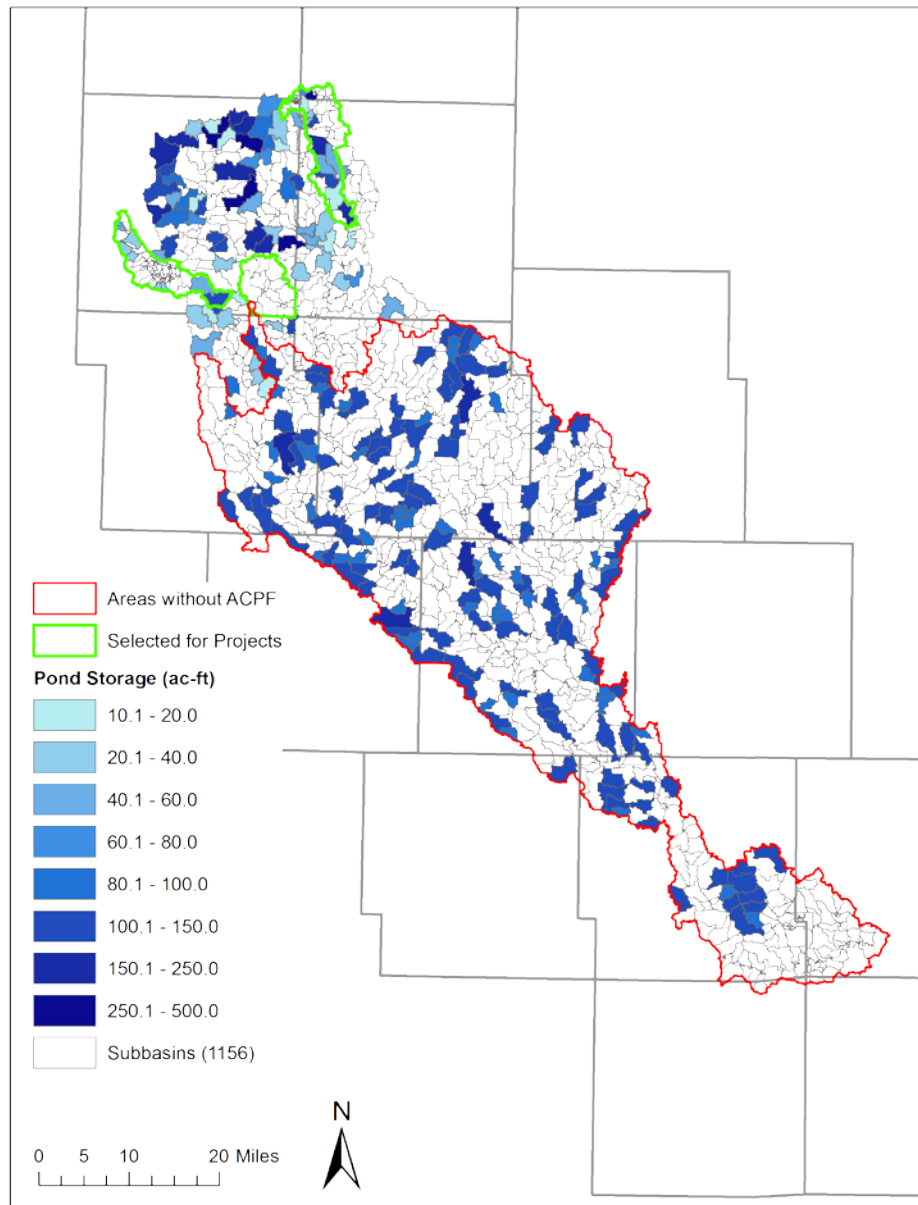


Figure 4.8. Flood storage (acre-feet) provided by ponds in each subbasin. Aggregated ACPF pond characteristics were used to develop hypothetical ponds in subbasins where ACPF data were not available.

Discrete model index points (shown in Figure 4.9) were selected throughout the watershed to compare upstream drainage area and pond characteristics. Index points were selected at head water locations and along the main stem of the North Raccoon River. Table 4.2 details the drainage area, number of upstream ACPF ponds, number of upstream aggregated ponds, and the upstream drainage area intercepted by ponds for each model index point. The available upstream pond storage depth is similar along the main stem of the North Raccoon River as drainage area increases. However, percentages of drainage are intercepted by upstream ponds decreases as total drainage area increases. The percentage of drainage area intercepted and storage provided by ponds relates directly to reductions in peak discharge.

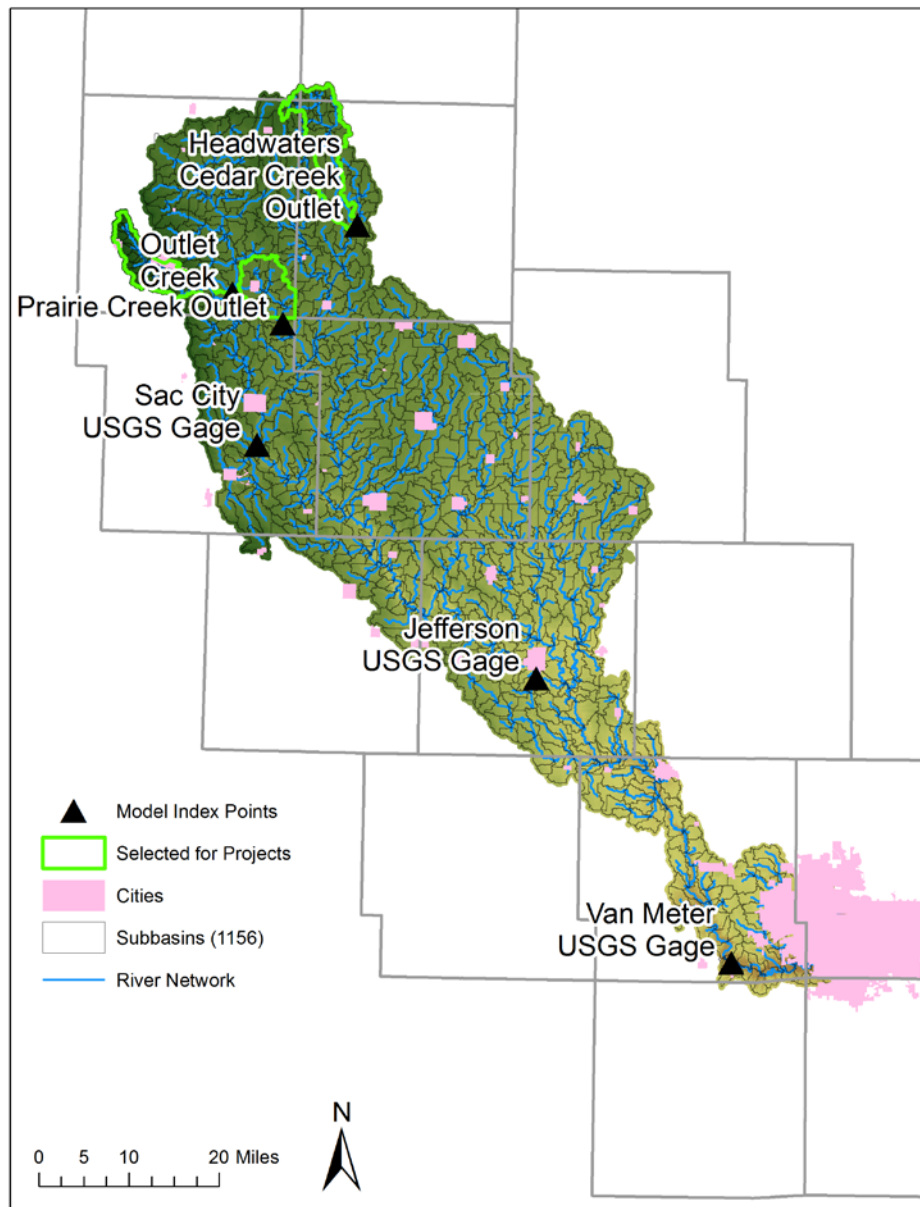


Figure 4.9. Model index locations selected for comparisons of hypothetical flood mitigation scenarios to current conditions.

Table 4.2. The flood storage available upstream of the model index locations. In general, the smaller the upland drainage area, the larger the percentage of drainage area is controlled by ponds, and the more flood storage is available.

<i>Location</i>	<i>Drainage Area (mi<sup>2</sup>)</i>	<i>ACPF Ponds Upstream</i>	<i>Aggregated Ponds Upstream</i>	<i>Drainage Area Intercepted by Ponds (mi<sup>2</sup>)</i>	<i>Upstream Pond Flood Storage (ac-ft)</i>	<i>Upstream Pond Flood Storage Equivalent Depth (in)</i>
Headwaters Cedar Creek	50.9	21	13	15.1 (29.7%)	1182.6	0.44
Outlet Creek at Storm Lake	27.8	7	7	2.4 (8.8%)	239.4	0.16
Prairie Creek	36.3	3	1	10.7 (29.5%)	511	0.26
North Raccoon River at Sac City	700	132*	93** [7]	109.1** (15.6%) [5.3 mi <sup>2</sup> ]	9005.2** [694.5]	0.24**
North Raccoon River at Jefferson	1619	133*	173** [86]	170.8** (10.5%) [66.0 mi <sup>2</sup> ]	17758.2** [9403.8]	0.21**
North Raccoon River at Van Meter (includes S. Raccoon Drainage Area)	3441	133*	232** [145]	217.2** (6.3%) [112.4 mi <sup>2</sup> ]	24378.3** [16023.9]	0.13**
*Does not include hypothetical ponds in areas where ACPF data were not available						
**Includes hypothetical ponds, hypothetical pond contributions shown in brackets[]						

### Six-Inch, 24-Hour SCS Design Storm

The HMS model with ponds to was run to simulate the effects of flood storage on peak discharges. Each simulation started with all pond water levels at the primary spillway elevation; this assumes that the permanent storage is full as the storm begins. This simulation result was compared to the simulated discharges without ponds in place (the existing baseline condition).

Figure 4.10 shows the percent reduction in peak discharge at model junction locations for the 6-inch, 24-hour SCS Design Storm. Application of this design storm assumes that a 6-inch rainfall occurs everywhere within the watershed simultaneously and produces unrealistic peak discharges at junction locations with relatively large drainage area, therefore, results are not shown at junctions with drainage area greater than 100 mi<sup>2</sup>. In general, upland sites with more drainage area intercepted by ponds had the greatest reductions in peak discharge. This coincides with the

intercepted drainage area percentages shown in Table 4.2. The northernmost portion of the watershed had the largest peak discharge reductions, approximately 15% or greater.

Ponds can effectively reduce flood peaks immediately downstream of their headwater sites. This is evident in Figure 4.10. At junctions farther downstream, floodwaters originating from locations throughout the watershed arrive at vastly different times; some areas have ponds, others do not. The result is that the storage effect from ponded areas is spread out over time, instead of being concentrated at the time of highest flows. Hence, for larger drainage areas downstream in the watershed, the flood peak reduction of storage ponds diminishes.

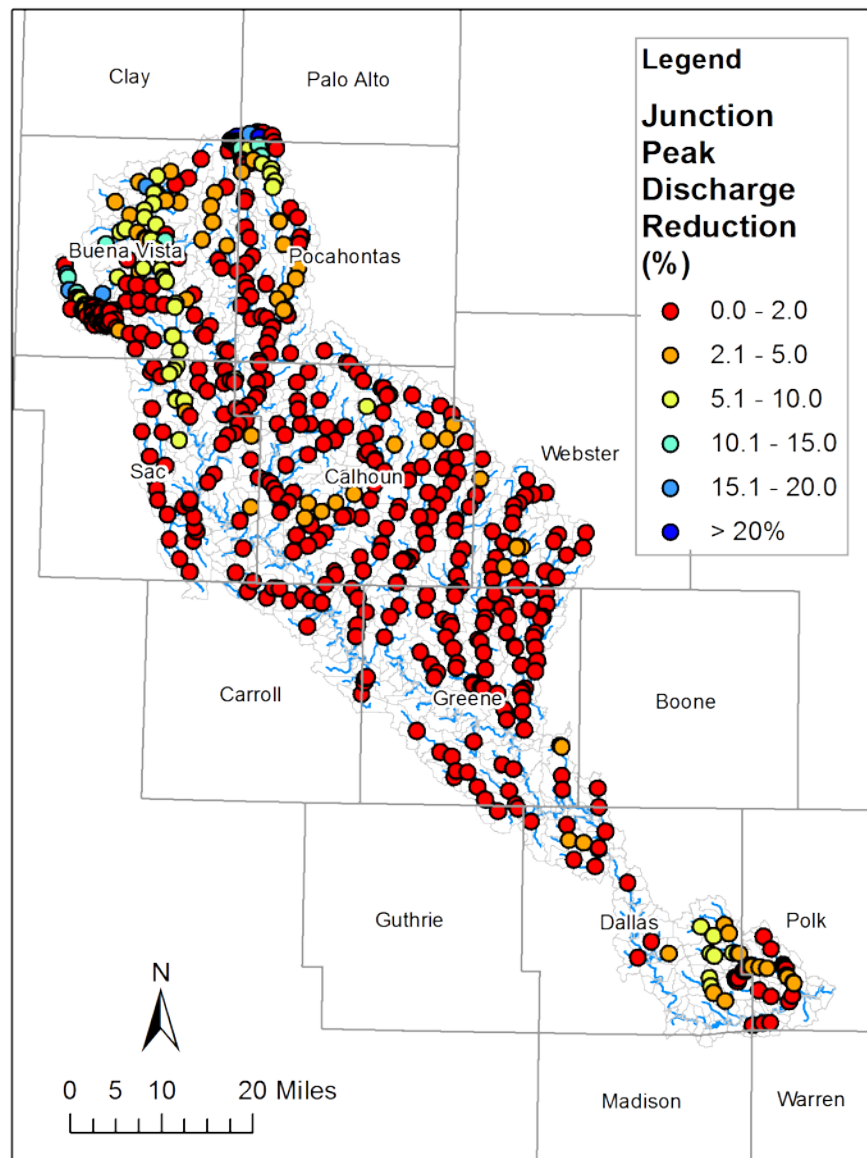


Figure 4.10. Junction peak discharge reductions with ACPF ponds in place for a 6-inch, 24-hour SCS Design Storm. . Simulation results at junctions with large drainage area are not realistic for this

design storm event, therefore, results are not shown at junctions with drainage area greater than 100 mi<sup>2</sup>.

#### d. Mitigating the Effects of High Runoff with Distributed Storage and Increased Infiltration

Implementation of actual flood reduction practices in the watershed will likely rely on a mixture of enhanced infiltration and distributed flood storage projects. The use of cover crops enhanced infiltration in this scenario, but to a lesser extent than the previous cover crop scenario. An average implementation of cover crops was assumed on 50% of the agricultural land, rather than 100%. This is a more realistic expectation for broad implementation of this practice, but it is still extremely ambitious. As with the previous cover crop scenario, this agricultural management practice would involve planting cover crops during the dormant season in an effort to improve soil quality and infiltration during the growing season. Changes in soil infiltration properties would take many years to be fully realized.

Implementation of cover crops in the HMS model was achieved by modifying the CN using values provided in Table 4.1. To represent cover crops on 50% of the agricultural land, each subbasin was assigned a CN corresponding to the average of the CNs from the baseline simulation (existing agricultural landscape) and the cover crop simulation of section 4b (all agricultural area improved because of cover crops).

Implementation of distributed flood storage projects remained the same as in section 4c, with all aggregated potential ACPF NRW sites included in the model.

#### **Six-Inch, 24-Hour SCS Design Storm**

The HMS model with ponds and implementation of cover crops on 50% of agricultural areas was run to simulate the effects of enhanced filtration and flood storage on peak discharges. Each simulation started with all pond water levels at the primary spillway elevation; this assumes that the permanent storage is full as the storm begins. Comparisons were then made for the simulated discharges without improvements in place (the existing baseline condition).

Figure 4.11 shows the percent reduction in peak discharge at subbasin outlets and junction locations with cover crops and ponds in place for the 6-inch, 24-hour SCS Design Storm. On average for the basin, planting cover crops on 50% of the agricultural land increases infiltration by 0.08 inches for the 6-inch, 24-hour SCS Design. Like the simulation of the ponds-only scenario, the largest reductions in peak discharge occur in the northernmost portion of the watershed. This is consistent with the largest concentrations of flood storage available and upstream drainage area intercepted by ponds.

Like the ponds-only simulation, upland locations with more drainage area intercepted by ponds had the greatest reductions in peak discharge. This coincides with the intercepted drainage area percentages shown in Table 4.2. Application of this design storm assumes that a 6-inch rainfall occurs everywhere within the watershed simultaneously and produces unrealistic peak discharges

at junction locations with relatively large drainage area, therefore, results are not shown at junctions with drainage area greater than 100 mi<sup>2</sup>

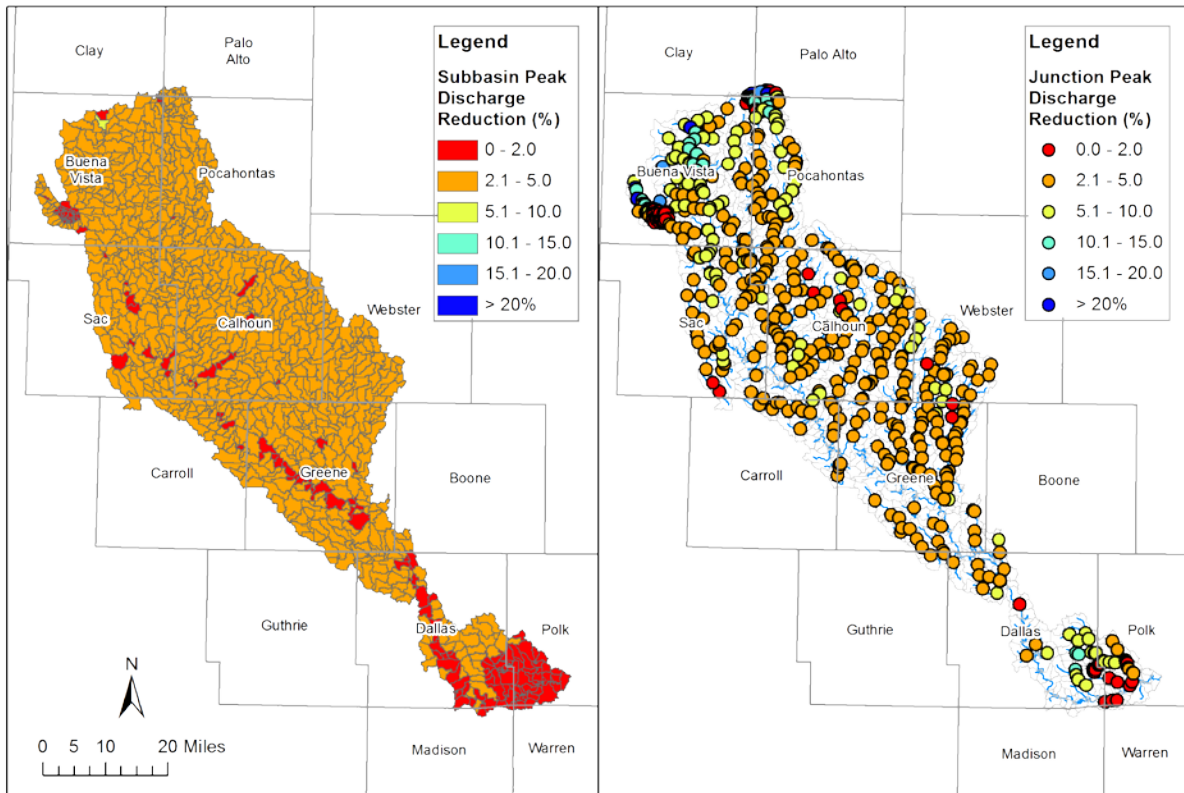


Figure 4.11. Peak discharge reductions for subbasins (left) and junctions (right) with ACPF ponds in place and improved soil infiltration following many years of 50% utilization of cover crops for a 6-inch, 24-hour SCS Design Storm. Simulation results at junctions with large drainage area are not realistic for this design storm event, therefore, results are not shown at junctions with drainage area greater than 100 mi<sup>2</sup>.

## e. Comparison of Watershed Scenarios for Historic Storm Events

In addition to the design storm event, watershed scenarios were compared through simulation of several historic storm events. Simulations of these historic events are more relevant to people than a design storm, and many likely remember the consequences of some of these events. In this section, the differences in simulation results at the model index locations are shown in Figure 4.9.

### **June 24–July 5, 2005, Storm Event**

Figure 4.12 shows the cumulative rainfall from June 24 to July 5, 2005. The largest cumulative rainfall, totaling more than 6 inches, occurred primarily along a band across the northern portion of the watershed. Figure 4.13 shows peak discharge reductions at model junction points with predevelopment prairie conditions on all agricultural lands. Figure 4.14 shows peak discharge reductions at model junction points with improved soil infiltration after many years of 100% utilization of cover crops during the dormant season for all row crop agriculture. As expected, extreme changes in land cover result in large, broad-scale reductions in peak discharge. An additional basin-averaged 0.10 inches of rainfall infiltrated as a result of cover crop use. The largest discharge reductions occurred in the northeastern part of the watershed. Peak discharge reductions along the main stem of the North Raccoon River were approximately 5-10%.

Figure 4.15 shows peak discharge reductions at model junctions with distributed storage ponds in place. Like the design storm, the largest peak discharge reductions of 5-10% just downstream of pond locations. Reductions decrease as the drainage area ratio controlled by storage ponds decreases. This is evident along the main stem of the North Raccoon River where reductions were less than 2%.

Figure 4.16 shows peak discharge reductions at model junctions with 50% utilization of cover crops and all distributed storage ponds in place. As expected, improving soil infiltration on 50% of agricultural land through use of cover crops provides broad benefits. An additional basin-averaged 0.4 inches of rainfall infiltrated as a result of cover crop utilization. Peak discharge reductions ranged from 2–10% throughout the entire watershed.

Figure 4.17 shows a time series of simulated discharge at each of the model index locations. Percent reductions in peak discharge at model index locations are shown in Figure 4.18. Reductions in peak discharge were converted to stage reductions using rating curves provided by USGS and Iowa's Statewide Floodplain Mapping Project. Stage reductions at each location are shown in Figure 4.19. Some locations may have a large reduction in peak discharge but negligible stage reduction due to simulated low flow conditions or the particular relationship between depth and flow at the location.

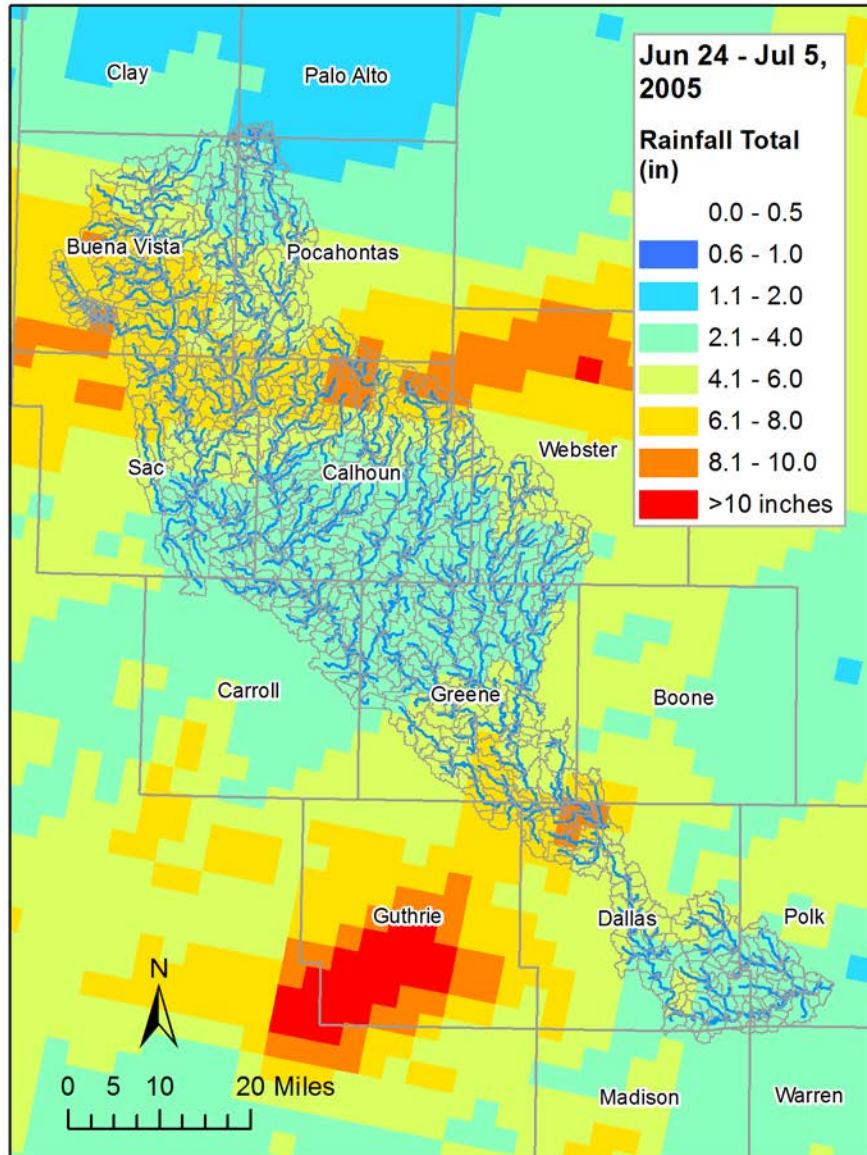


Figure 4.12. Rainfall totals for the period June 24 – July 5, 2005.

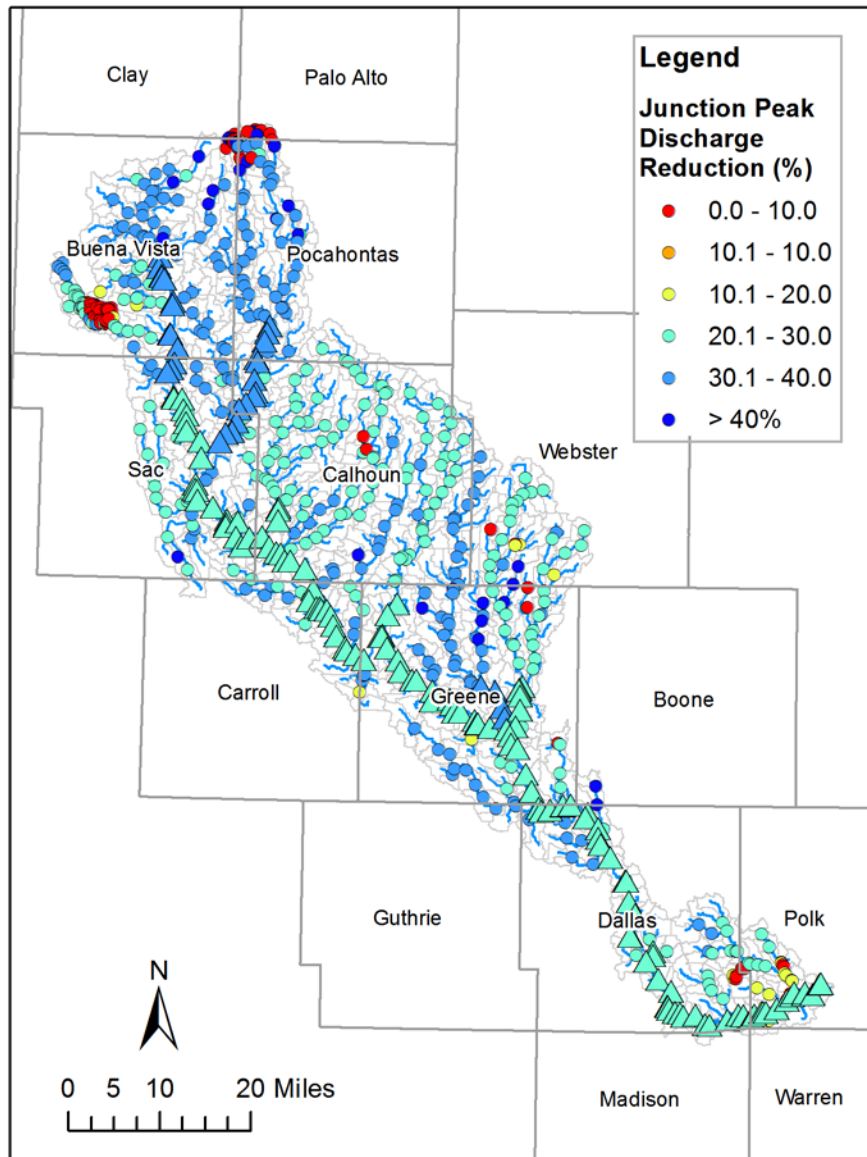


Figure 4.13 Junction peak discharge reductions with 100% conversion of agricultural lands to prairie for the June 2005 event. Junction points along the main stream are denoted by triangles.

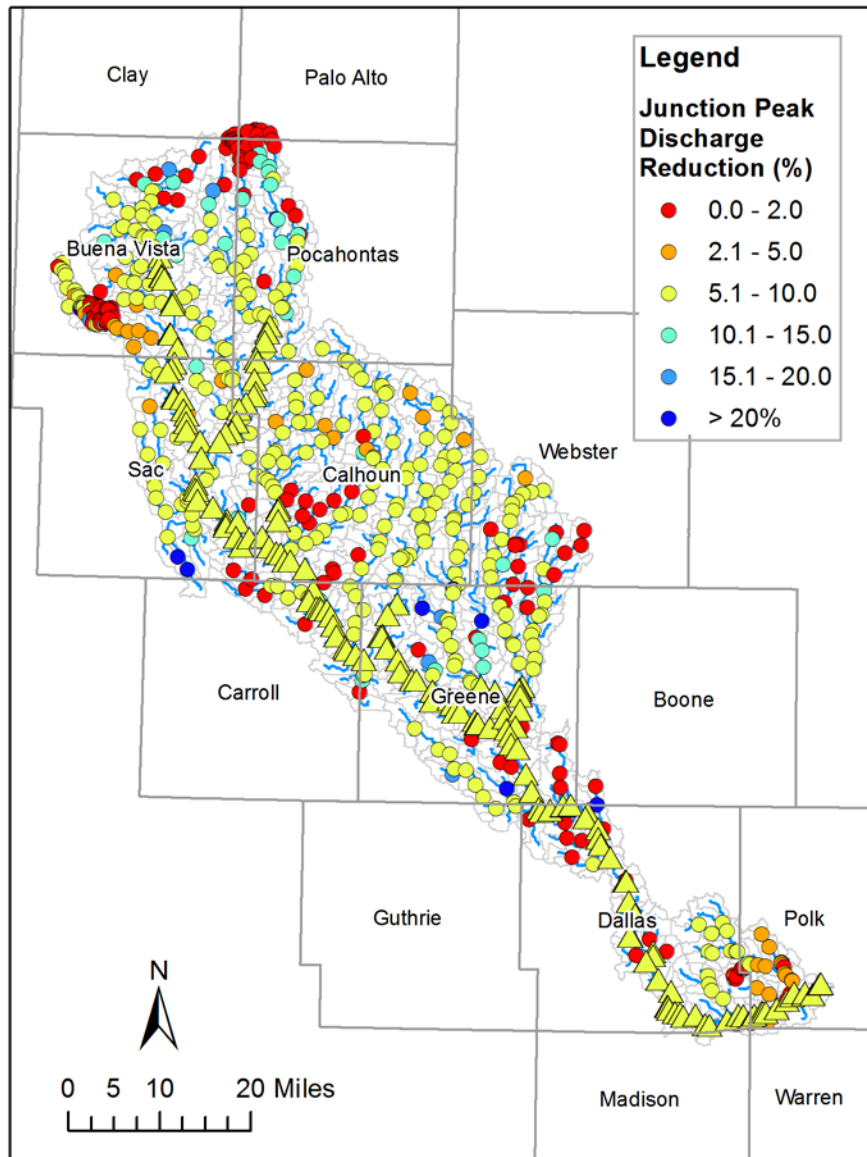


Figure 4.14. Junction peak discharge reductions with 100% utilization of cover crops on agricultural lands for the June 2005 event. Junction points along the main stream are denoted by triangles.

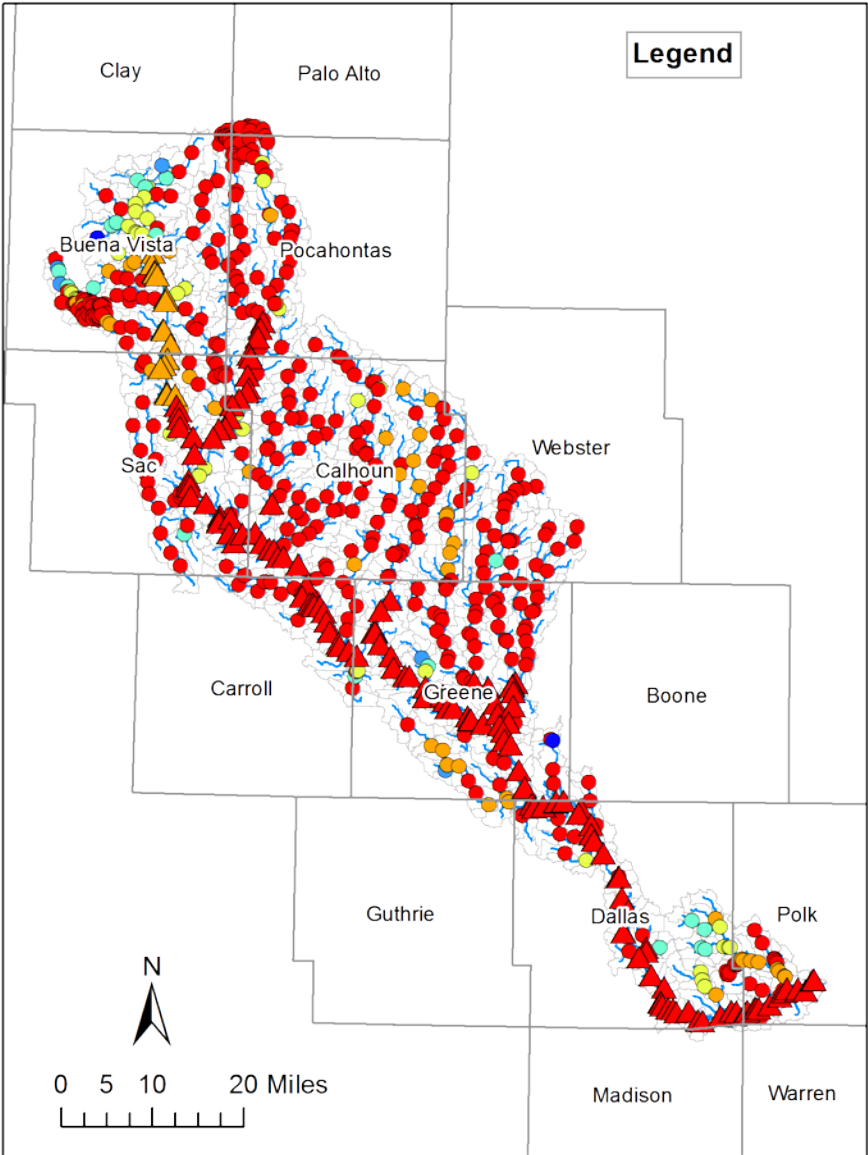


Figure 4.15. Junction peak discharge reductions with all ponds in place for the June 2005 event. Junction points along the main stream are denoted by triangles.

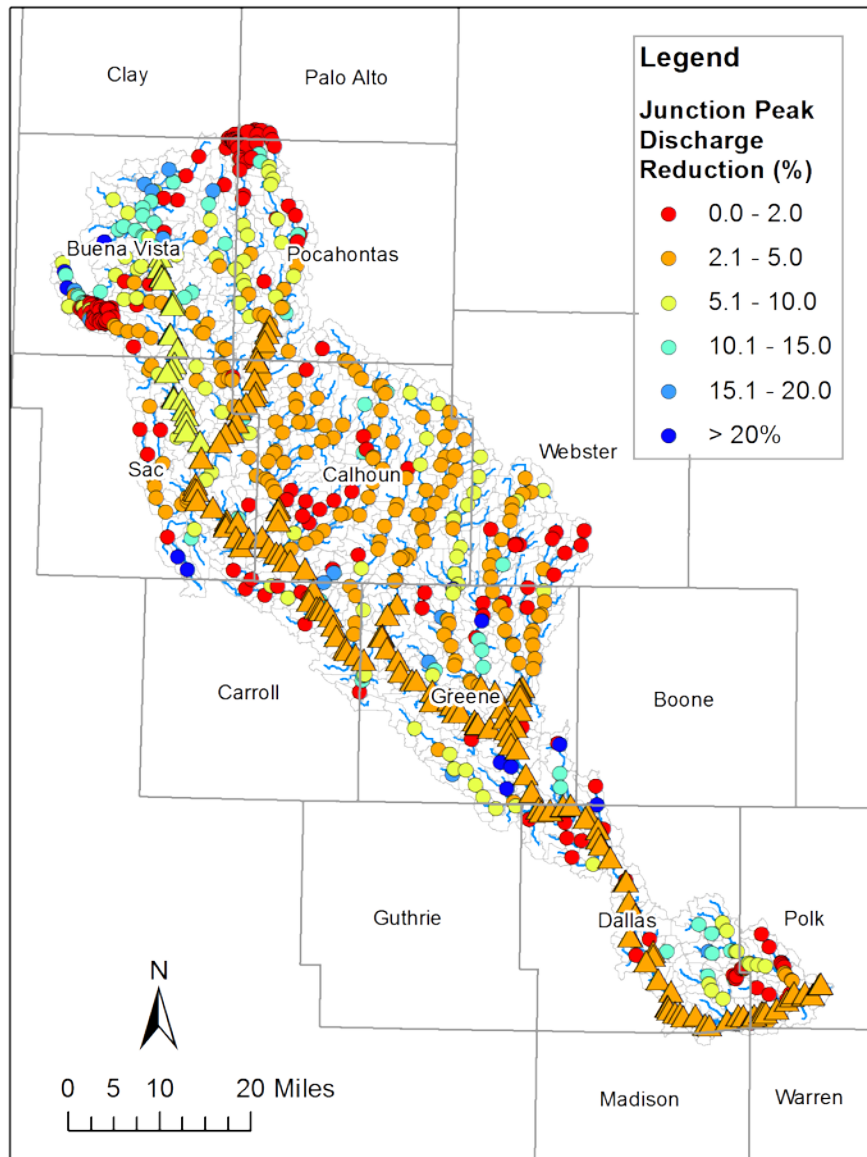


Figure 4.16. Junction peak discharge reductions with 50% utilization of cover crops on agricultural lands and all ponds in place for the June 2005 event. Junction points along the main stream are denoted by triangles.

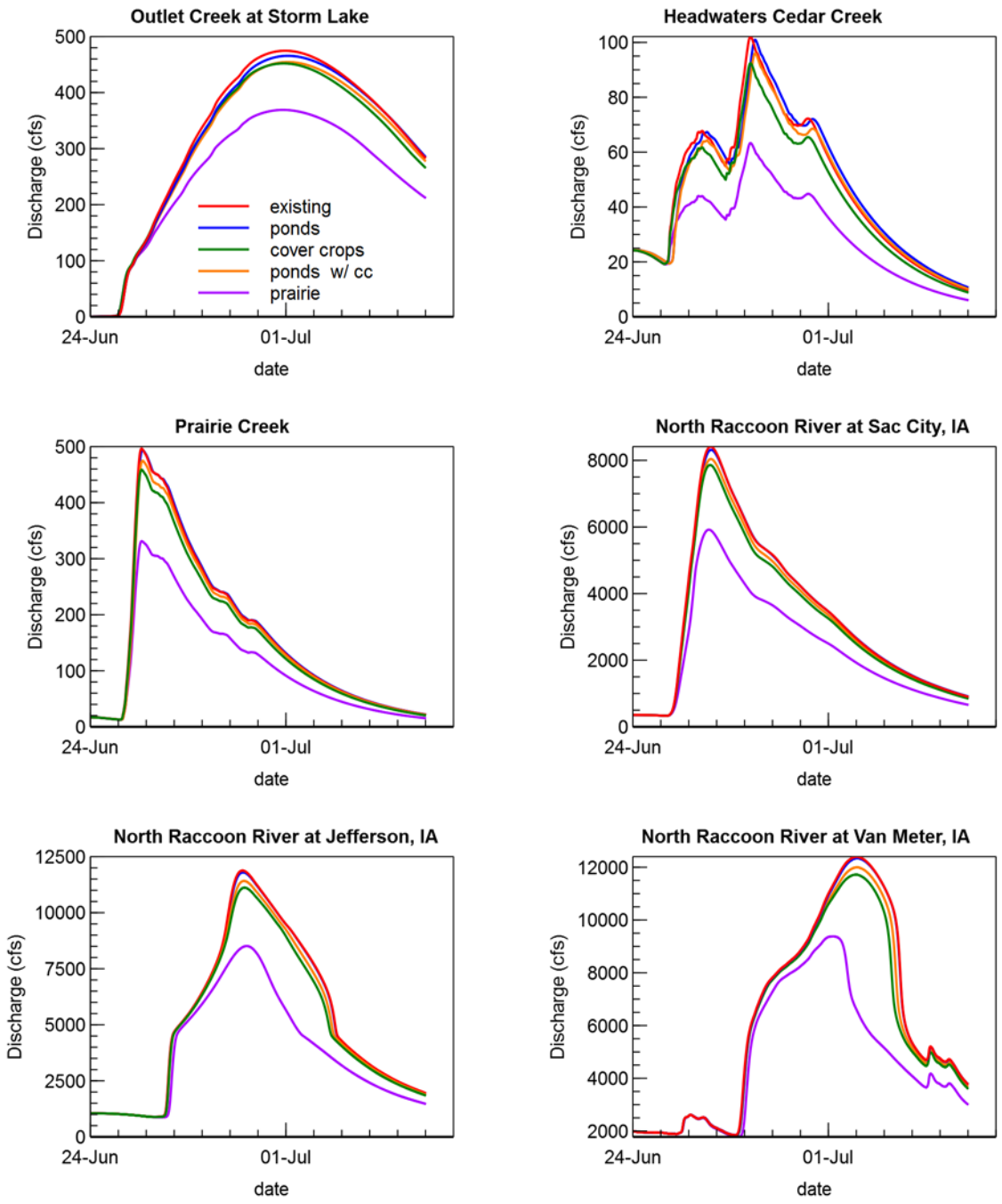


Figure 4.17. Hydrograph comparisons – with all agricultural lands converted to prairie, ACPF ponds, with 100% utilization of cover crops, and a combination of ACPF ponds and 50% utilization of cover crops for the June 2005 event.

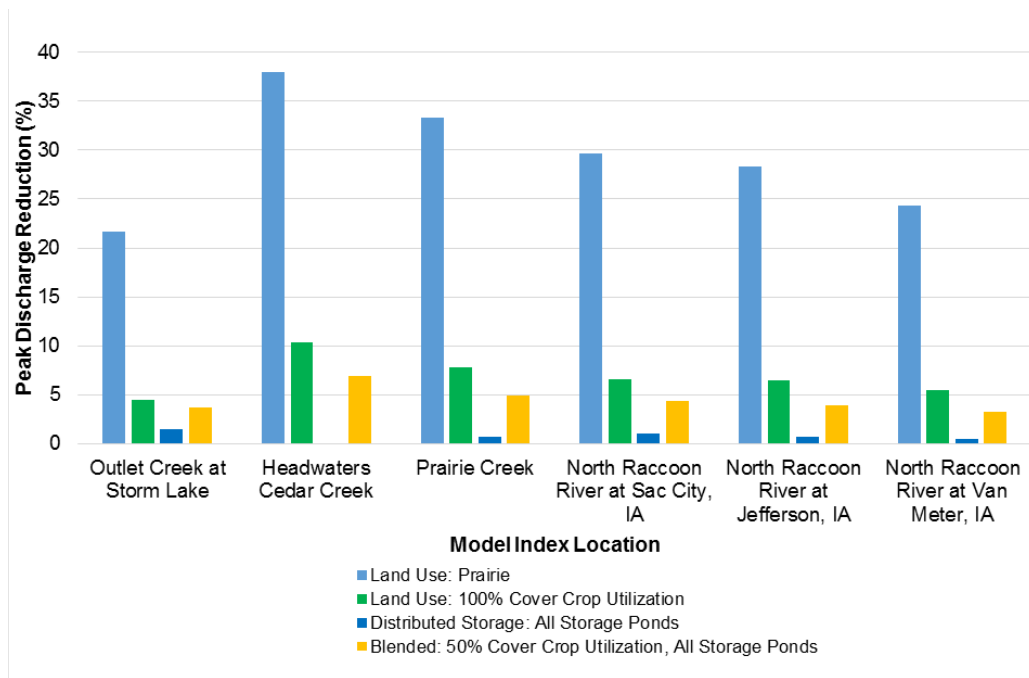


Figure 4.18. Percent reduction in peak discharge at model index locations with implementation of each watershed scenario for the June 2005 event.

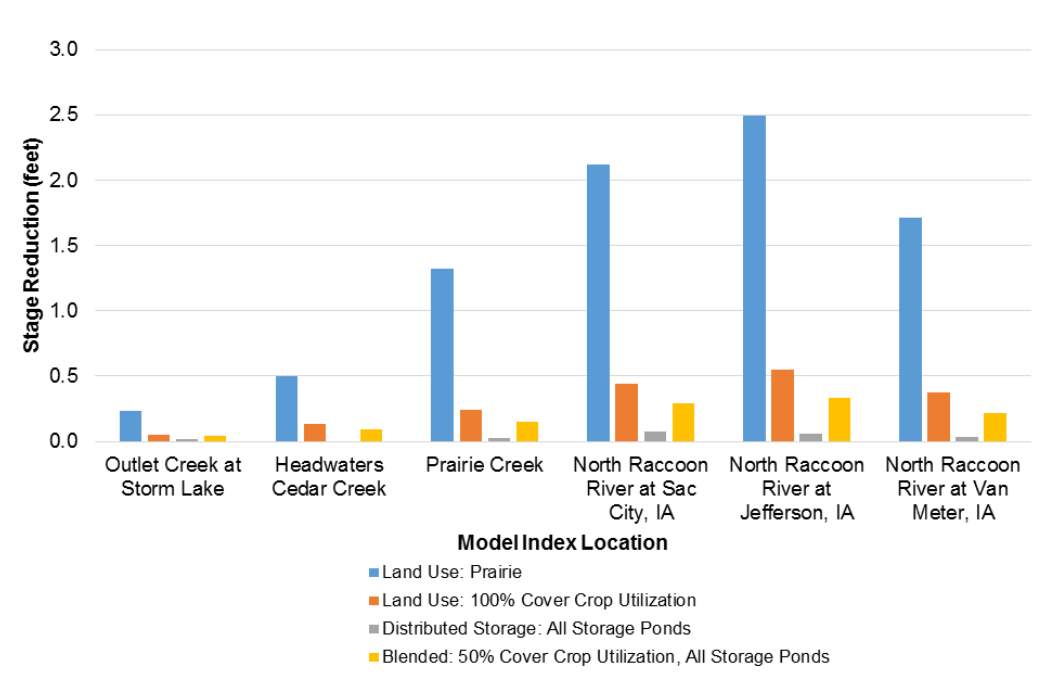


Figure 4.19. Reduction in stage at model index locations with implementation of each watershed scenario for the June 2005 event.

### **April 22-May 3, 2007, Storm Event**

Figure 4.20 shows the cumulative rainfall from April 22 to May 3, 2007. The largest cumulative rainfall, totaling more than 6 inches, occurred primarily along a band across the northern portion of the watershed. Figure 4.21 shows peak discharge reductions at model junction points with predevelopment prairie conditions on all agricultural lands. Figure 4.22 shows peak discharge reductions at model junction points with improved soil infiltration after many years of 100% utilization of cover crops during the dormant season for all row crop agriculture. As expected, extreme changes in land cover result in large, broad-scale reductions in peak discharge. An additional basin-averaged 0.12 inches of rainfall infiltrated as a result of cover crop use. The largest discharge reductions occurred in the northeastern part of the watershed. Peak discharge reductions along the main stem of the North Raccoon River were approximately 5-10%.

Figure 4.23 shows peak discharge reductions at model junctions with distributed storage ponds in place. Like the design storm, the largest peak discharge reductions of 5-10% just downstream of pond locations. Reductions decrease as the drainage area ratio controlled by storage ponds decreases. This is evident along the main stem of the North Raccoon River where reductions were less than 2%.

Figure 4.24 shows peak discharge reductions at model junctions with 50% utilization of cover crops and all distributed storage ponds in place. As expected, improving soil infiltration on 50% of agricultural land through use of cover crops provides broad benefits. An additional basin-averaged 0.1 inches of rainfall infiltrated as a result of cover crop utilization. Peak discharge reductions ranged from 2–10% throughout the entire watershed.

Figure 4.25 shows a time series of simulated discharge at each of the model index locations. Percent reductions in peak discharge at model index locations are shown in Figure 4.26. Stage reductions at each location are shown in Figure 4.27.

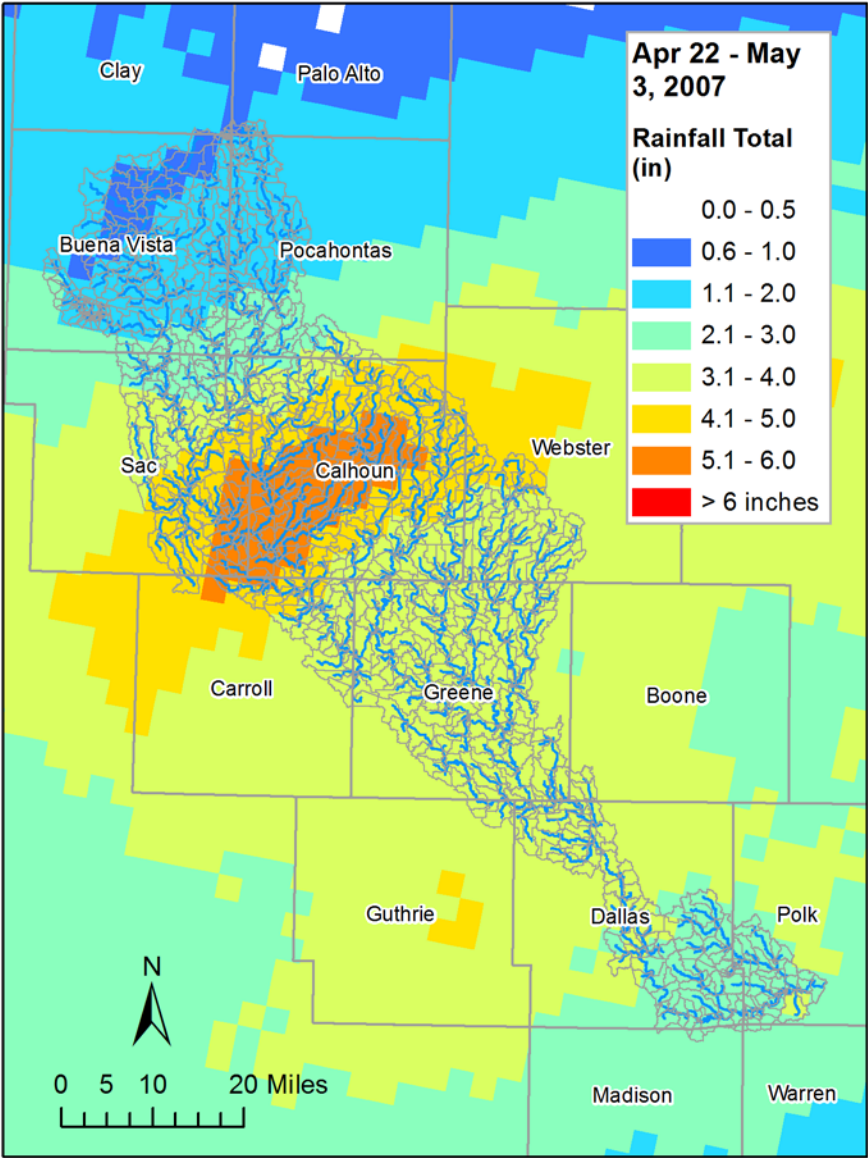


Figure 4.20. Rainfall totals for the period April 22 – May 3, 2007.

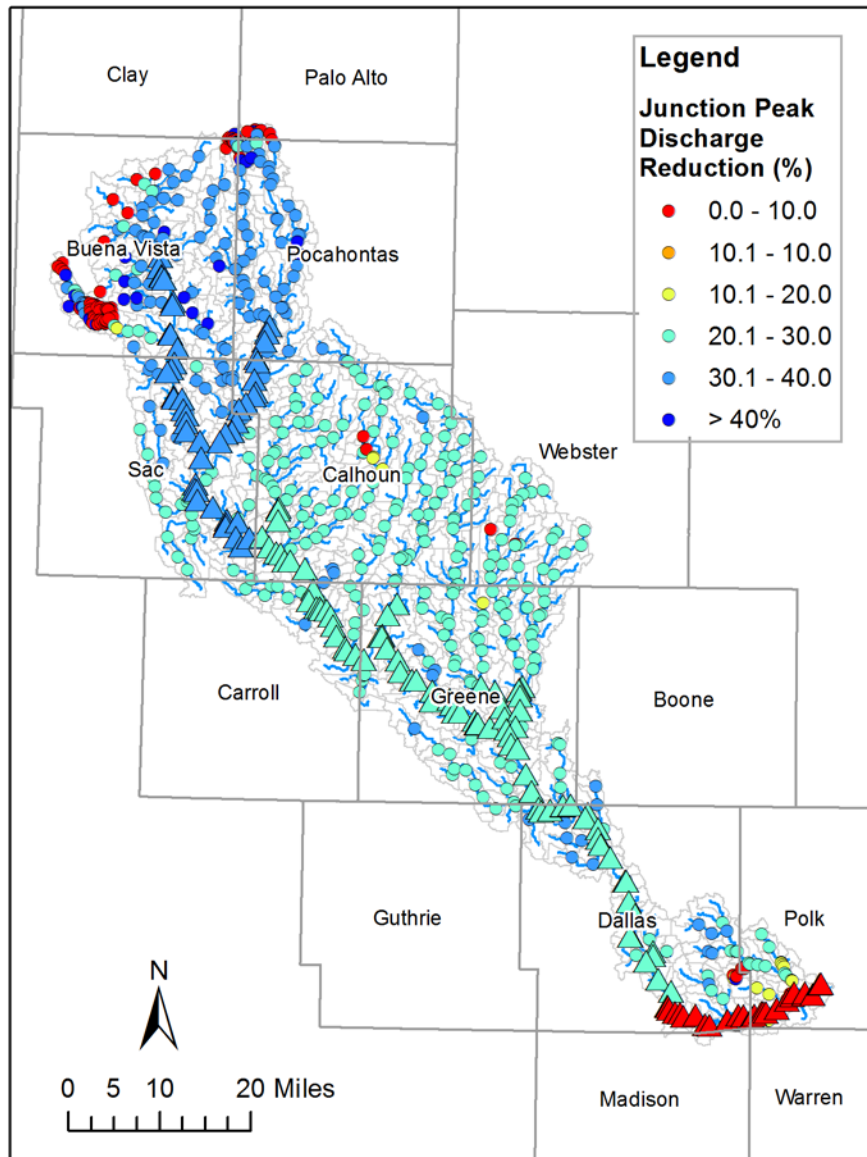


Figure 4.21. Junction peak discharge reductions with 100% conversion of agricultural lands to prairie for the April 2007 event. Junction points along the main stream are denoted by triangles.

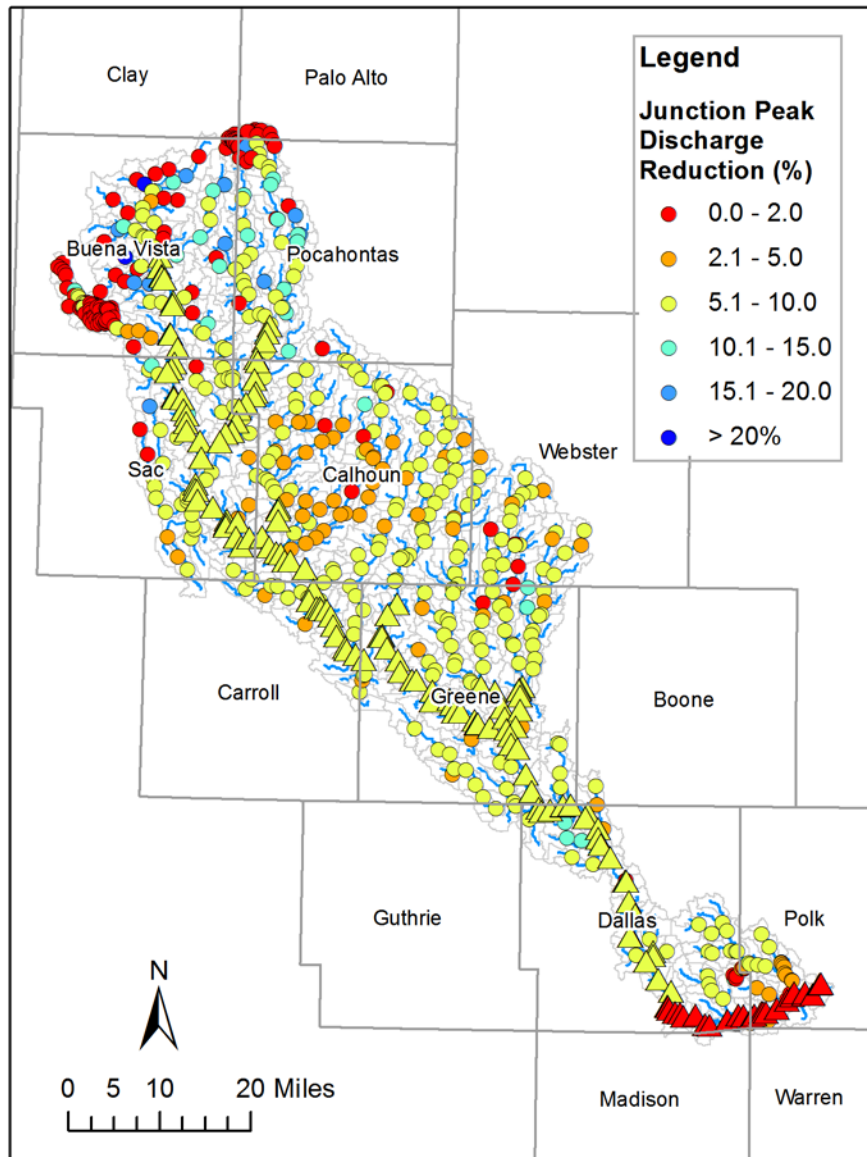


Figure 4.22. Junction peak discharge reductions with 100% utilization of cover crops on agricultural lands for the April 2007 event. Junction points along the main stream are denoted by triangles.

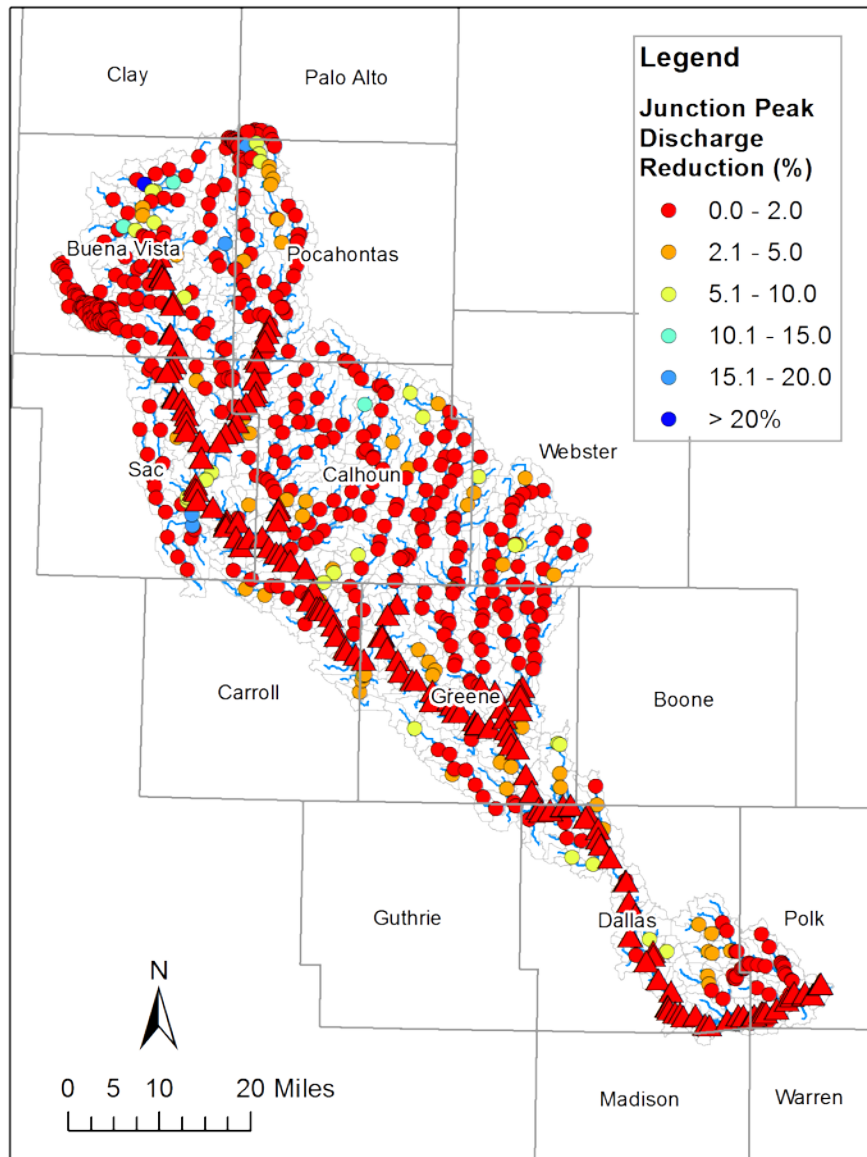


Figure 4.23. Junction peak discharge reductions with all ponds in place for the April 2007 event. Junction points along the main stream are denoted by triangles.

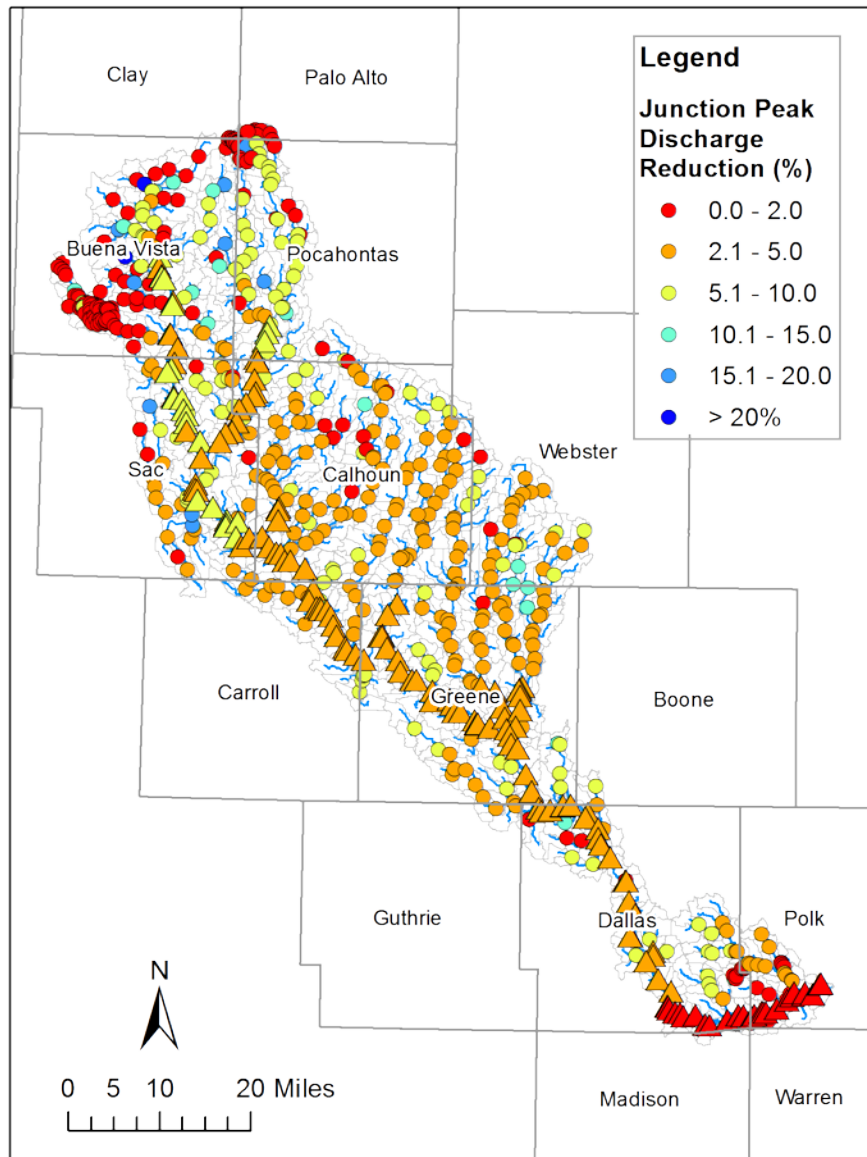


Figure 4.24. Junction peak discharge reductions with 50% utilization of cover crops on agricultural lands and all ponds in place for the April 2007 event. Junction points along the main stream are denoted by triangles.

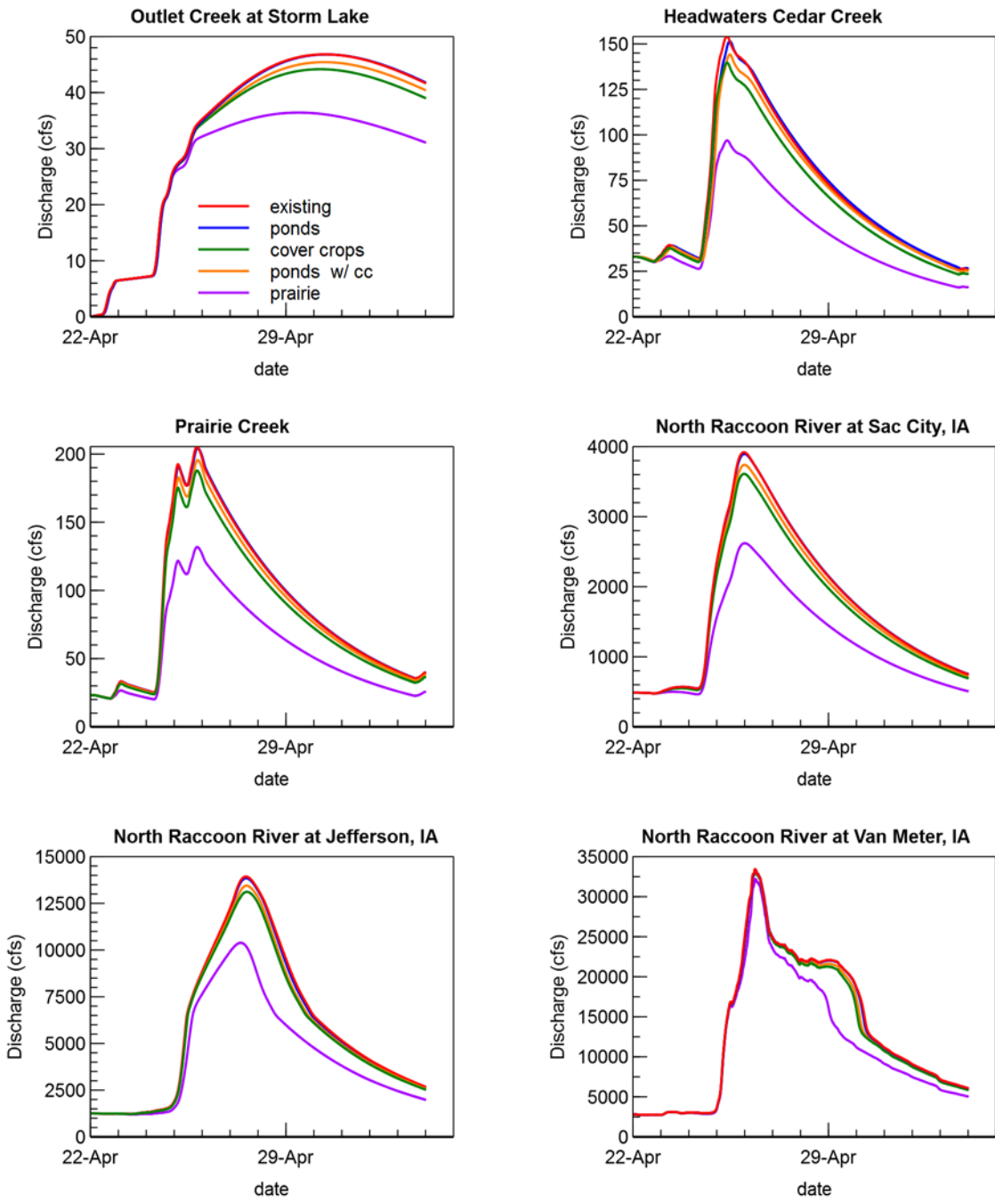


Figure 4.25. Hydrograph comparisons – with all agricultural lands converted to prairie, ACPF ponds, with 100% utilization of cover crops, and a combination of ACPF ponds and 50% utilization of cover crops for the April 2007 event.

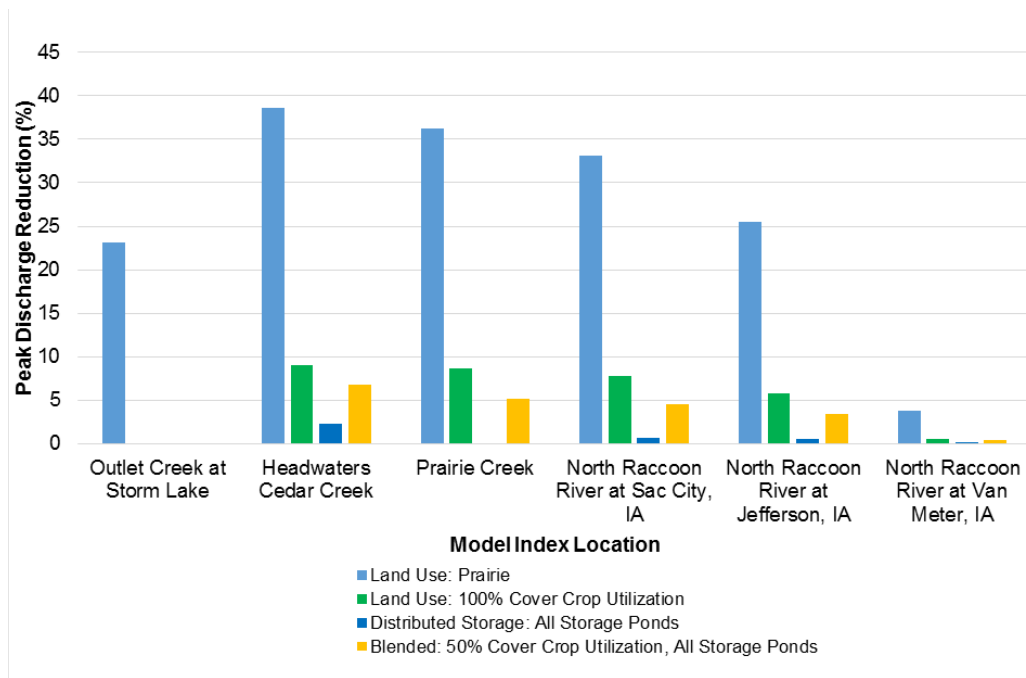


Figure 4.26. Percent reduction in peak discharge at model index locations with implementation of each watershed scenario for the April 2007 event.

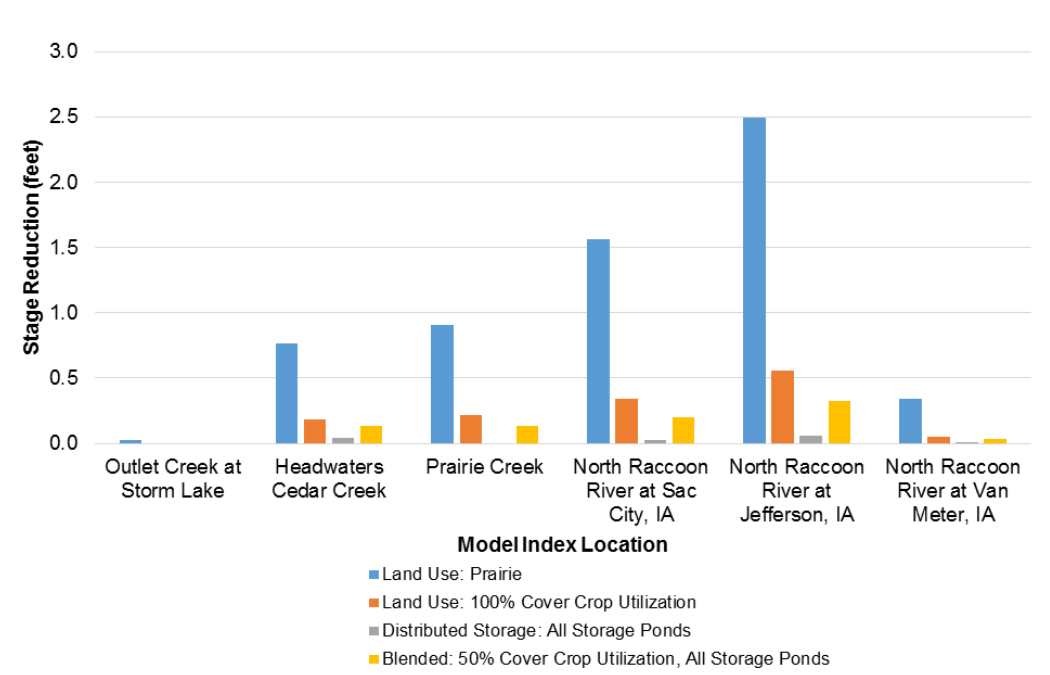


Figure 4.27. Reduction in stage at model index locations with implementation of each watershed scenario for the April 2007 event.

### **May 25 – June 4, 2013, Storm Event**

Figure 4.28 shows the cumulative rainfall from May 25 to June 4, 2013. The largest cumulative rainfall, totaling more than 6 inches, occurred primarily along a band across the northern portion of the watershed. Figure 4.29 shows peak discharge reductions at model junction points with predevelopment prairie conditions on all agricultural lands. Figure 4.30 shows peak discharge reductions at model junction points with improved soil infiltration after many years of 100% utilization of cover crops during the dormant season for all row crop agriculture. As expected, extreme changes in land cover result in large, broad-scale reductions in peak discharge. An additional basin-averaged 0.17 inches of rainfall infiltrated as a result of cover crop use. The largest discharge reductions occurred in the northeastern part of the watershed. Peak discharge reductions along the main stem of the North Raccoon River were approximately 5-10%.

Figure 4.31 shows peak discharge reductions at model junctions with distributed storage ponds in place. Like the design storm, the largest peak discharge reductions of 5-10% just downstream of pond locations. Reductions decrease as the drainage area ratio controlled by storage ponds decreases. This is evident along the main stem of the North Raccoon River where reductions were less than 2%.

Figure 4.32 shows peak discharge reductions at model junctions with 50% utilization of cover crops and all distributed storage ponds in place. As expected, improving soil infiltration on 50% of agricultural land through use of cover crops provides broad benefits. An additional basin-averaged 0.1 inches of rainfall infiltrated as a result of cover crop utilization. Peak discharge reductions ranged from 2–10% throughout the entire watershed.

Figure 4.33 shows a time series of simulated discharge at each of the model index locations. Percent reductions in peak discharge at model index locations are shown in Figure 4.34. Stage reductions at each location are shown in Figure 4.35.

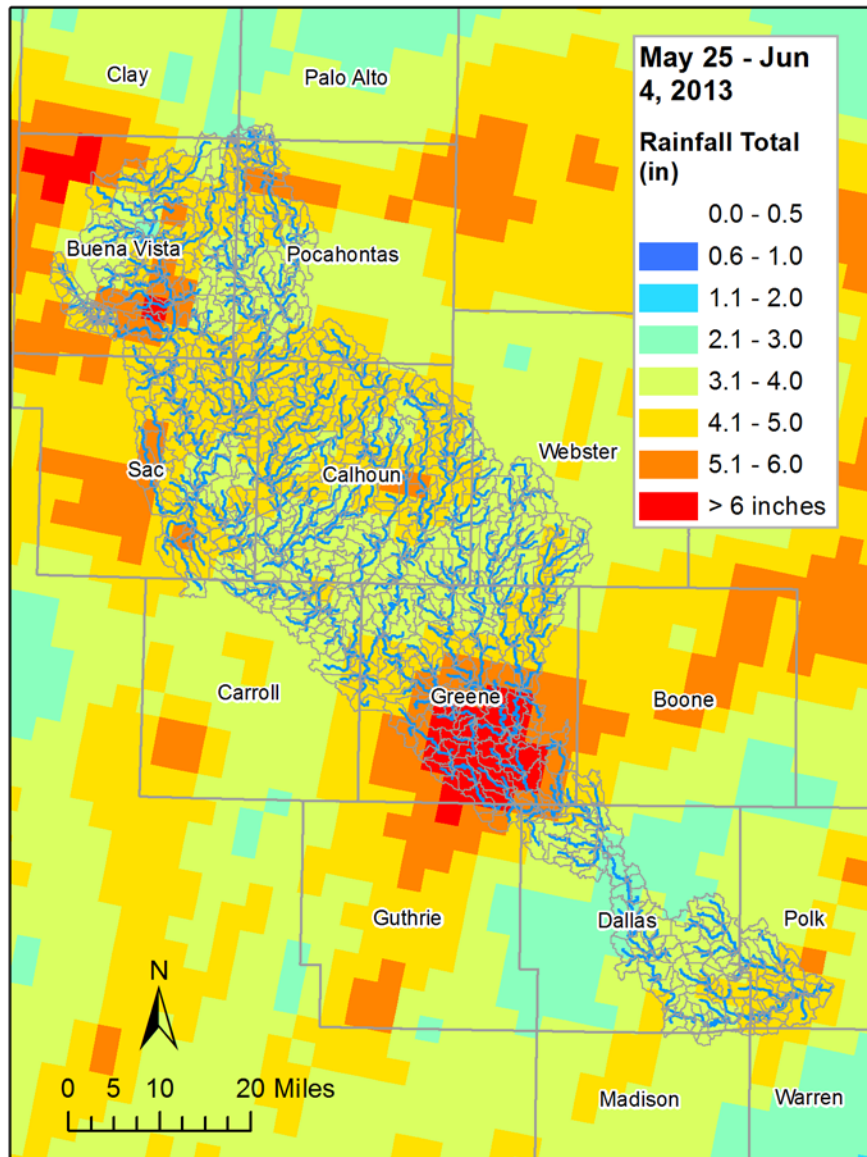


Figure 4.28. Rainfall totals for the period May 25 – June 4, 2013.

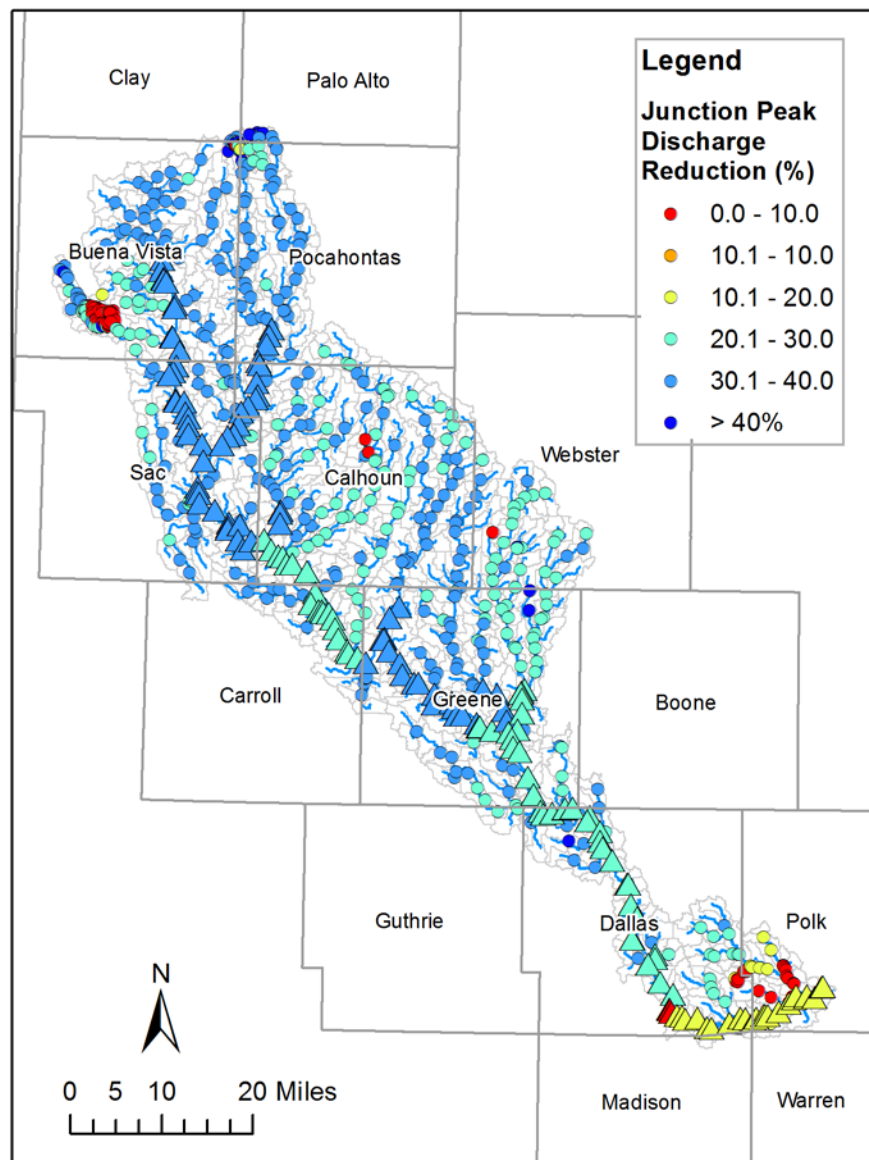


Figure 4.29. Junction peak discharge reductions with 100% conversion of agricultural lands to prairie for the May 2013 event. Junction points along the main stream are denoted by triangles.

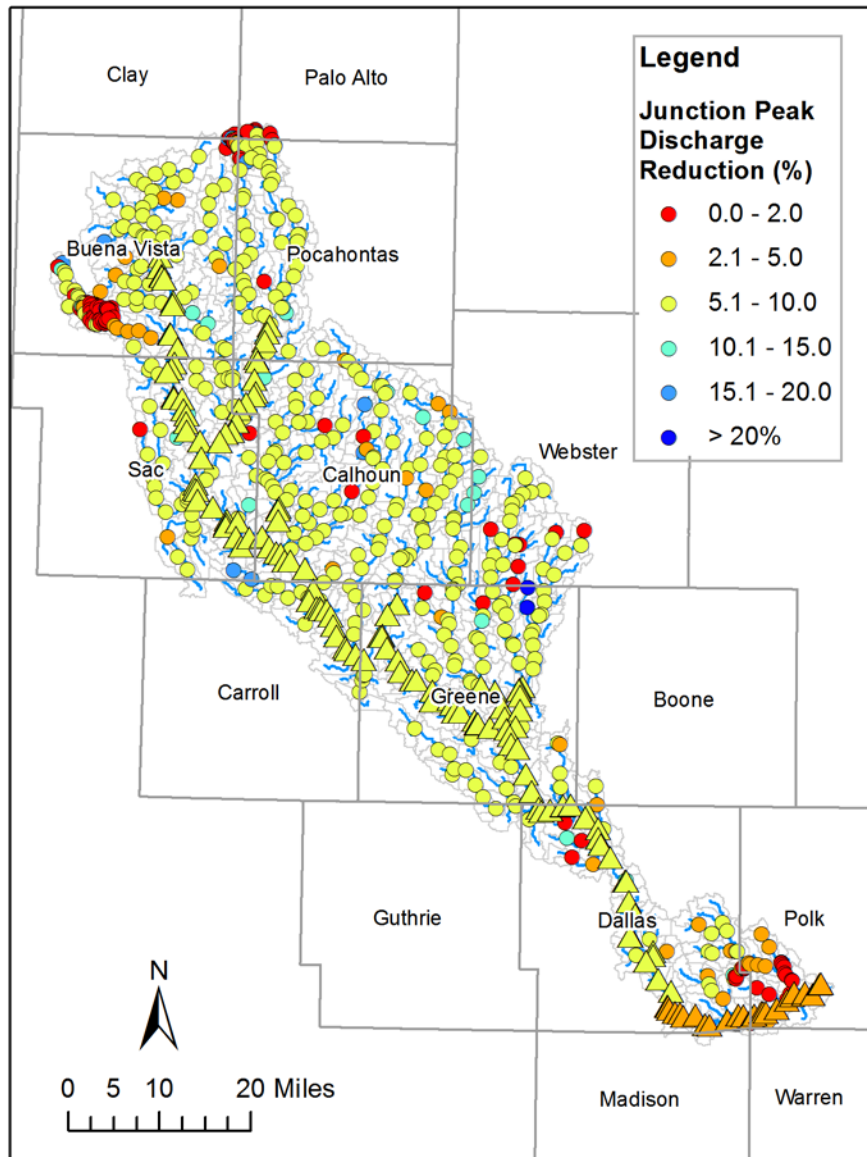


Figure 4.30. Junction peak discharge reductions with 100% utilization of cover crops on agricultural lands for the May 2013 event. Junction points along the main stream are denoted by triangles.

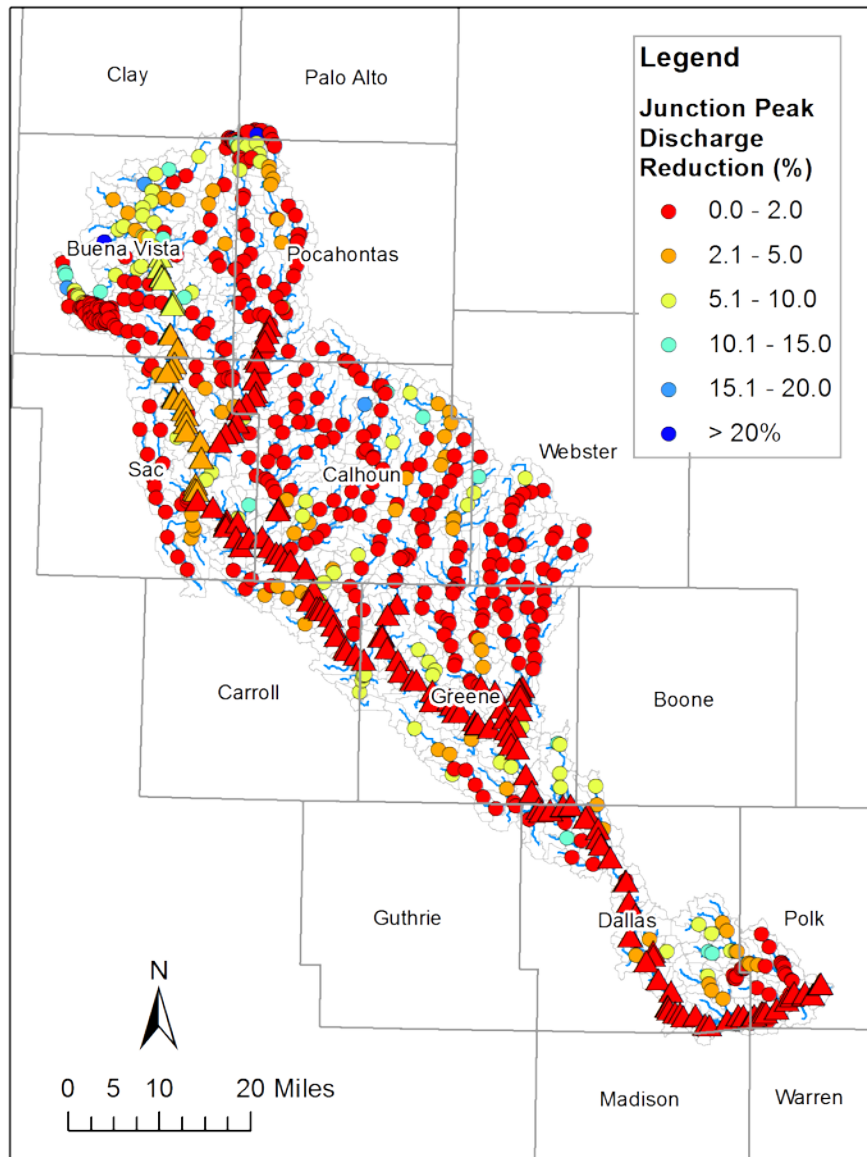


Figure 4.31. Junction peak discharge reductions with all ponds in place for the May 2013 event. Junction points along the main stream are denoted by triangles.

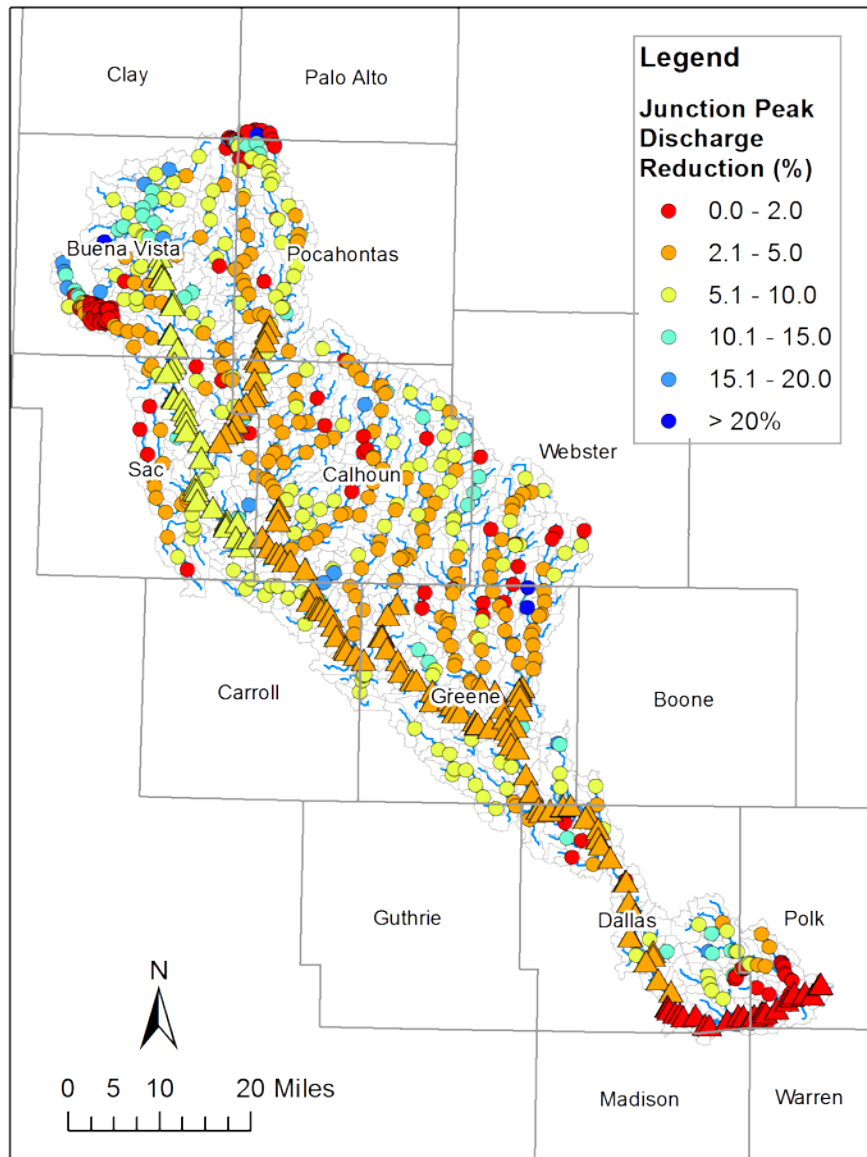


Figure 4.32. Junction peak discharge reductions with 50% utilization of cover crops on agricultural lands and all ponds in place for the May 2013 event. Junction points along the main stream are denoted by triangles.

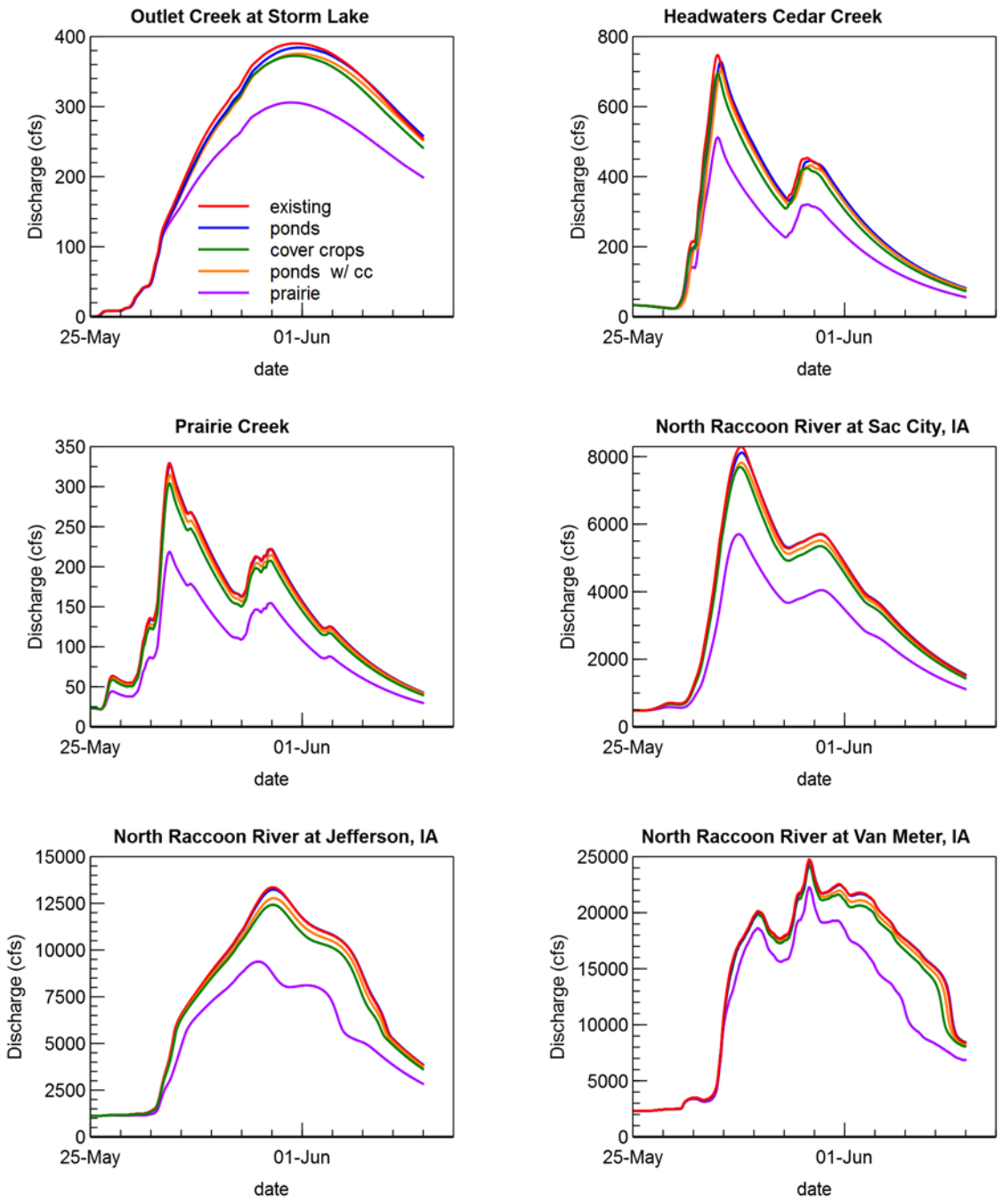


Figure 4.33. Hydrograph comparisons – with all agricultural lands converted to prairie, ACPF ponds, with 100% utilization of cover crops, and a combination of ACPF ponds and 50% utilization of cover crops for the May 2013 event.

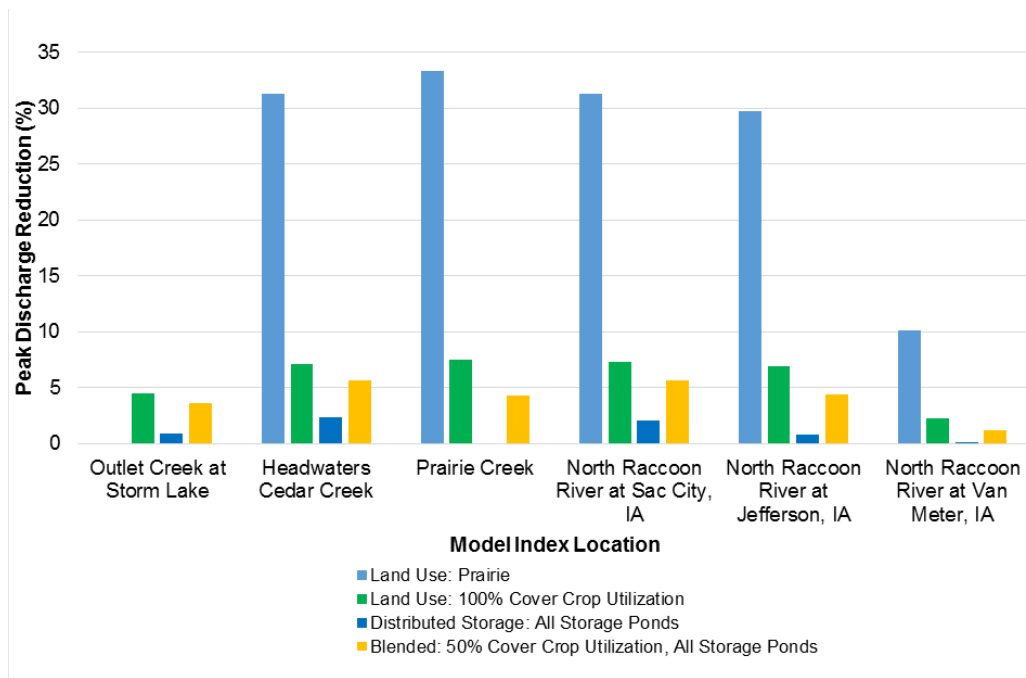


Figure 4.34. Percent reduction in peak discharge at model index locations with implementation of each watershed scenario for the May 2013 event.

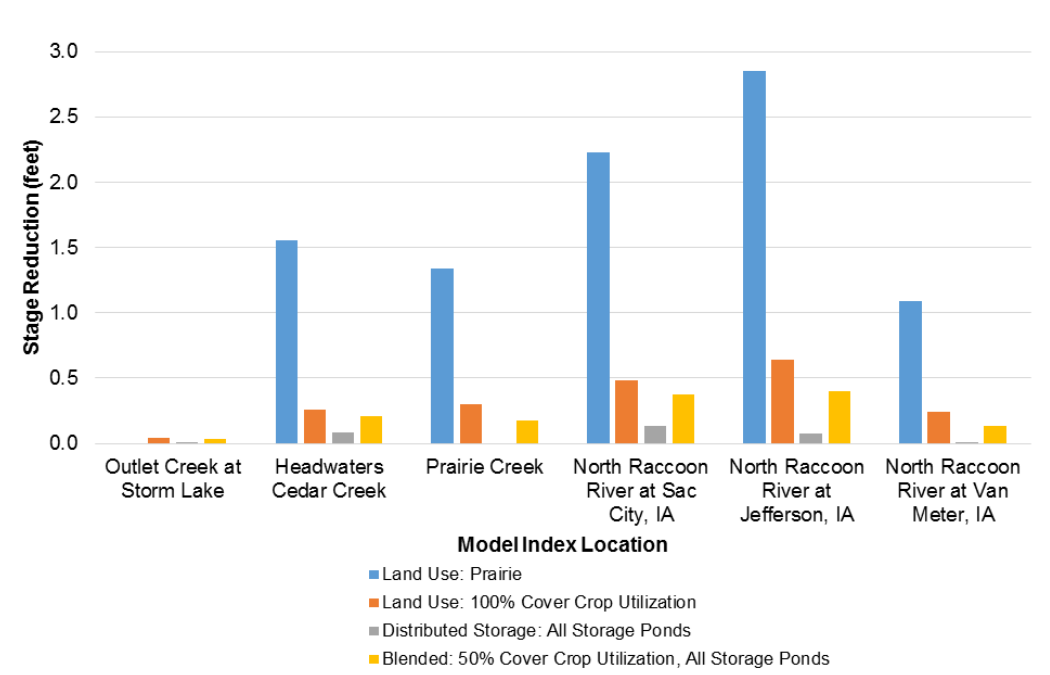


Figure 4.35. Reduction in stage at model index locations with implementation of each watershed scenario for the May 2013 event.

### **July 22, 2010, Northwest Iowa Storm Event**

A storm event that occurred July 22, 2010, in northwest Iowa was identified as an equivalent 50-year rainfall event for the North Raccoon River Watershed using the RainyDay Stochastic Storm Transposition (SST) tool. This web-based tool was developed by the Hydroclimate Extremes Research Group at the University of Wisconsin – Madison. The Stage IV radar rainfall data for this particular storm event were transposed to the approximate center of the North Raccoon River Watershed for simulation of the watershed scenarios.

Figure 4.36 shows the cumulative rainfall that occurred from July 21 - 22, 2010, transposed to the North Raccoon Watershed. Figure 4.37 shows peak discharge reductions at model junction points with predevelopment prairie conditions on all agricultural lands. Figure 4.38 shows the peak discharge reductions at model junction points with improved soil infiltration after many years of 100% use of cover crops during the dormant season for all row crop agriculture. An additional basin-averaged 0.1 inches of rainfall infiltrated as a result of cover crop use. Once again, cover crops result in large, broad-scale reductions in peak discharge. Peak discharge reductions along the main stem of the North Raccoon River were approximately 5–10%.

Figure 4.39 shows peak discharge reductions at model junctions with distributed storage ponds in place. The largest peak discharge reductions of 5–10% occur just downstream of pond locations. On average, the largest reductions occur where pond density is highest and more storage is available to intercept drainage area and store excess runoff. Like previous simulations, reductions decrease as the drainage area ratio controlled by storage ponds decreases. This is evident along the main stem of the North Raccoon River where reductions were less than 2%

Figure 4.40 shows peak discharge reductions at model junctions with 50% utilization of cover crops and all distributed storage ponds in place. An additional basin-averaged 0.05 inches of rainfall infiltrated as a result of cover crop use. As expected, improving soil infiltration on 50% of agricultural land through use of cover crops provides broad benefits. An additional basin-averaged 0.1 inches of rainfall infiltrated as a result of cover crop utilization. Peak discharge reductions ranged from 2–10% throughout the entire watershed.

Figure 4.41 shows a time series of simulated discharge at each of the model index locations. Percent reductions in peak discharge at model index locations are shown in Figure 4.42. Stage reductions at each location are shown in Figure 4.43.

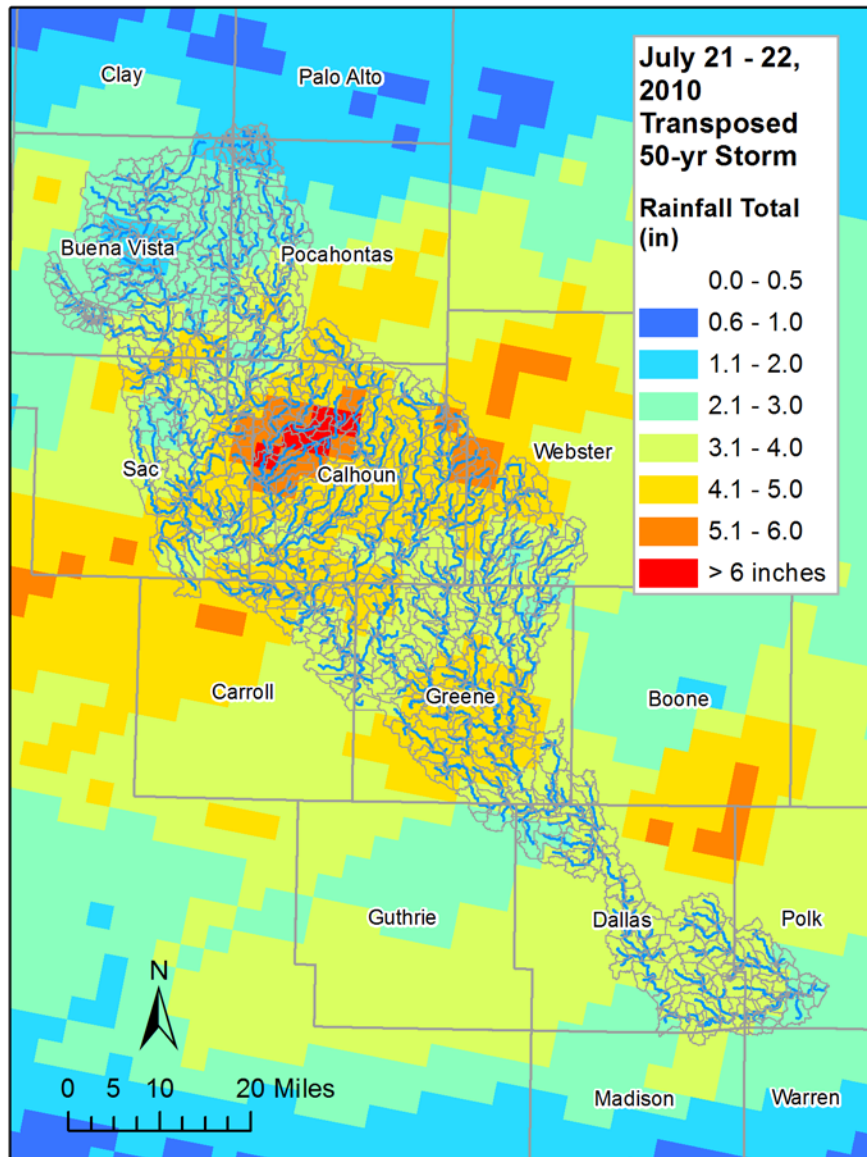


Figure 4.36. Rainfall totals for the period July 21 – 22, 2010, transposed from a location in northwest Iowa to the center of the North Raccoon River Watershed.

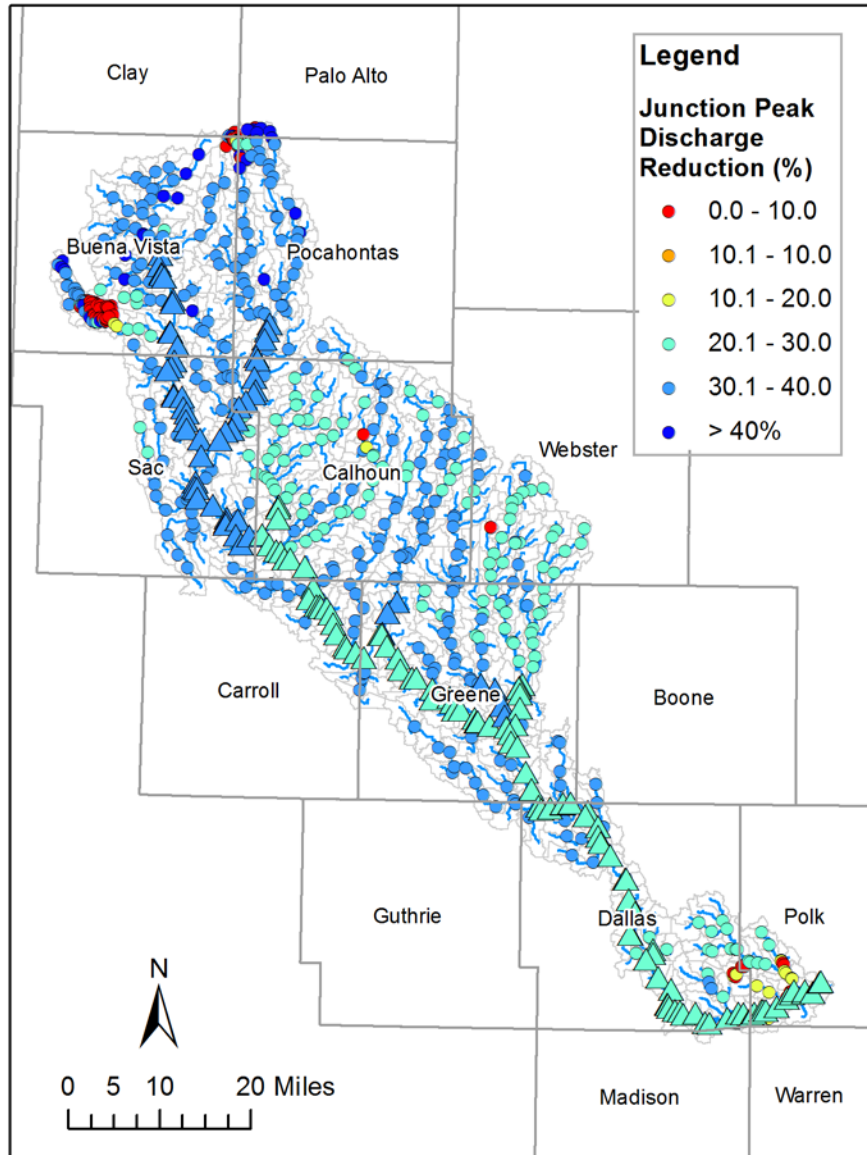


Figure 4.37. Junction peak discharge reductions with 100% conversion of agricultural lands to prairie for the July 2010 transposed event. Junction points along the main stream are denoted by triangles.

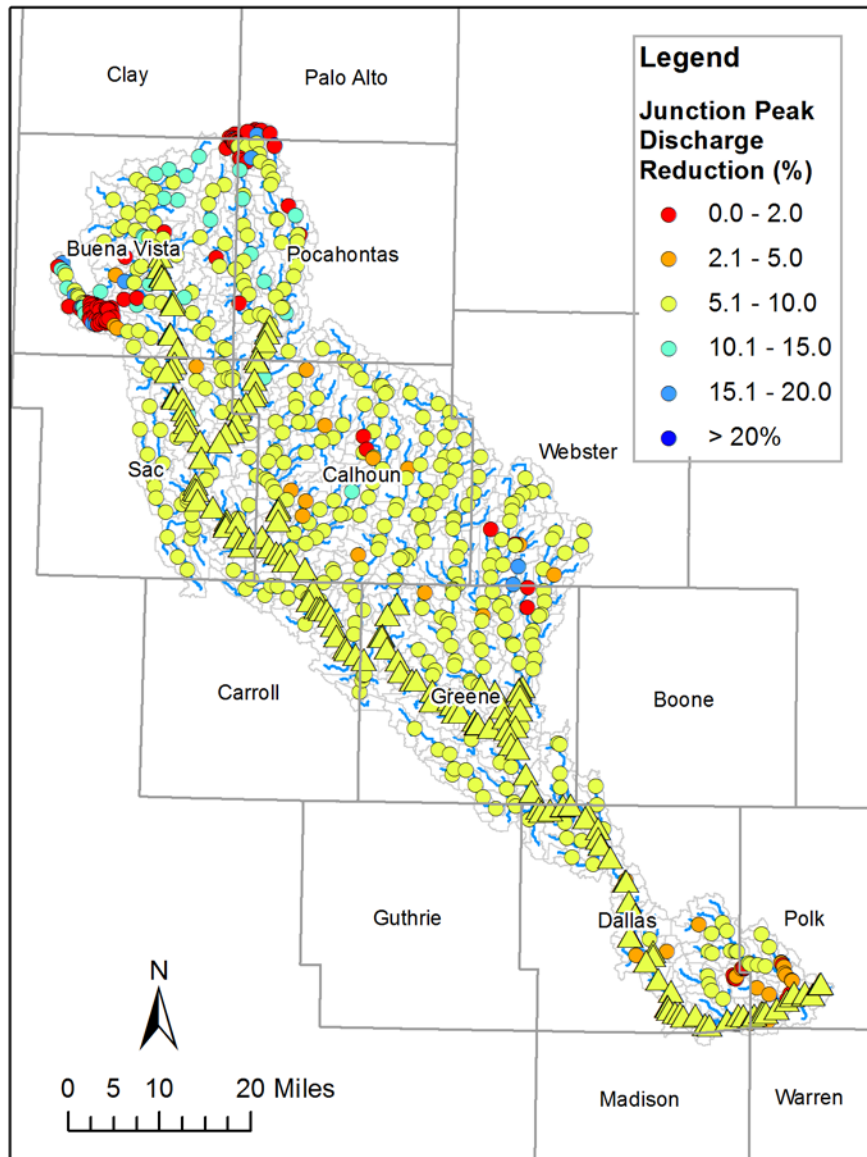


Figure 4.38. Junction peak discharge reductions with 100% utilization of cover crops on agricultural lands for the July 2010 transposed event. Junction points along the main stream are denoted by triangles.

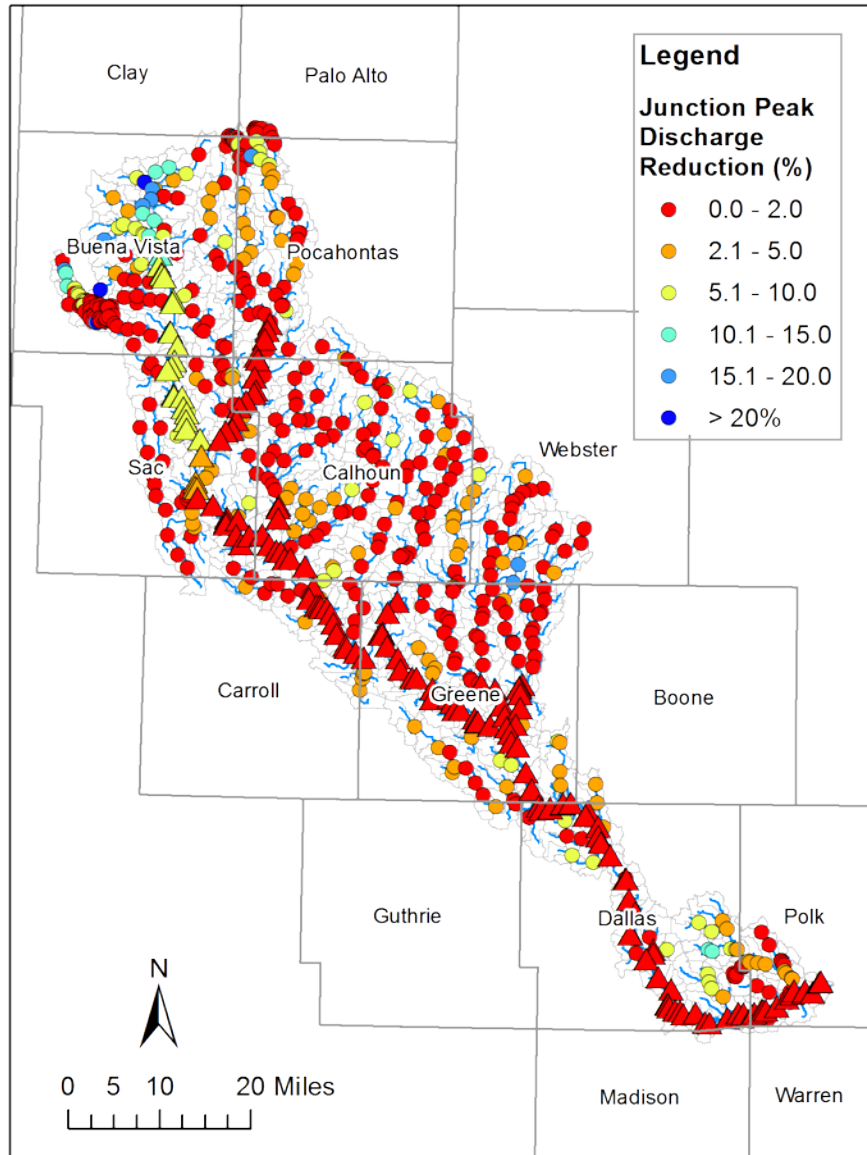


Figure 4.39. Junction peak discharge reductions with all ponds in place for the July 2010 transposed event. Junction points along the main stream are denoted by triangles.

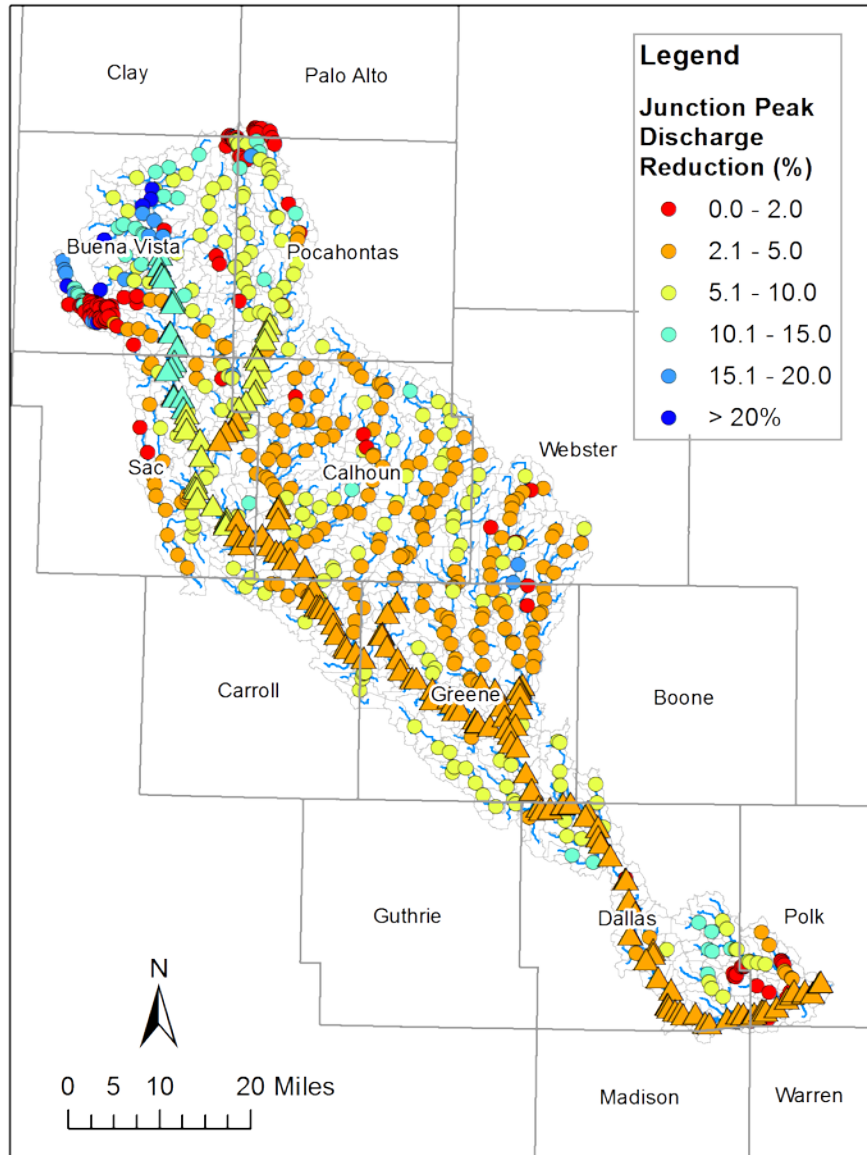


Figure 4.40. Junction peak discharge reductions with 50% utilization of cover crops on agricultural lands and all ponds in place for the July 2010 transposed event. Junction points along the main stream are denoted by triangles.

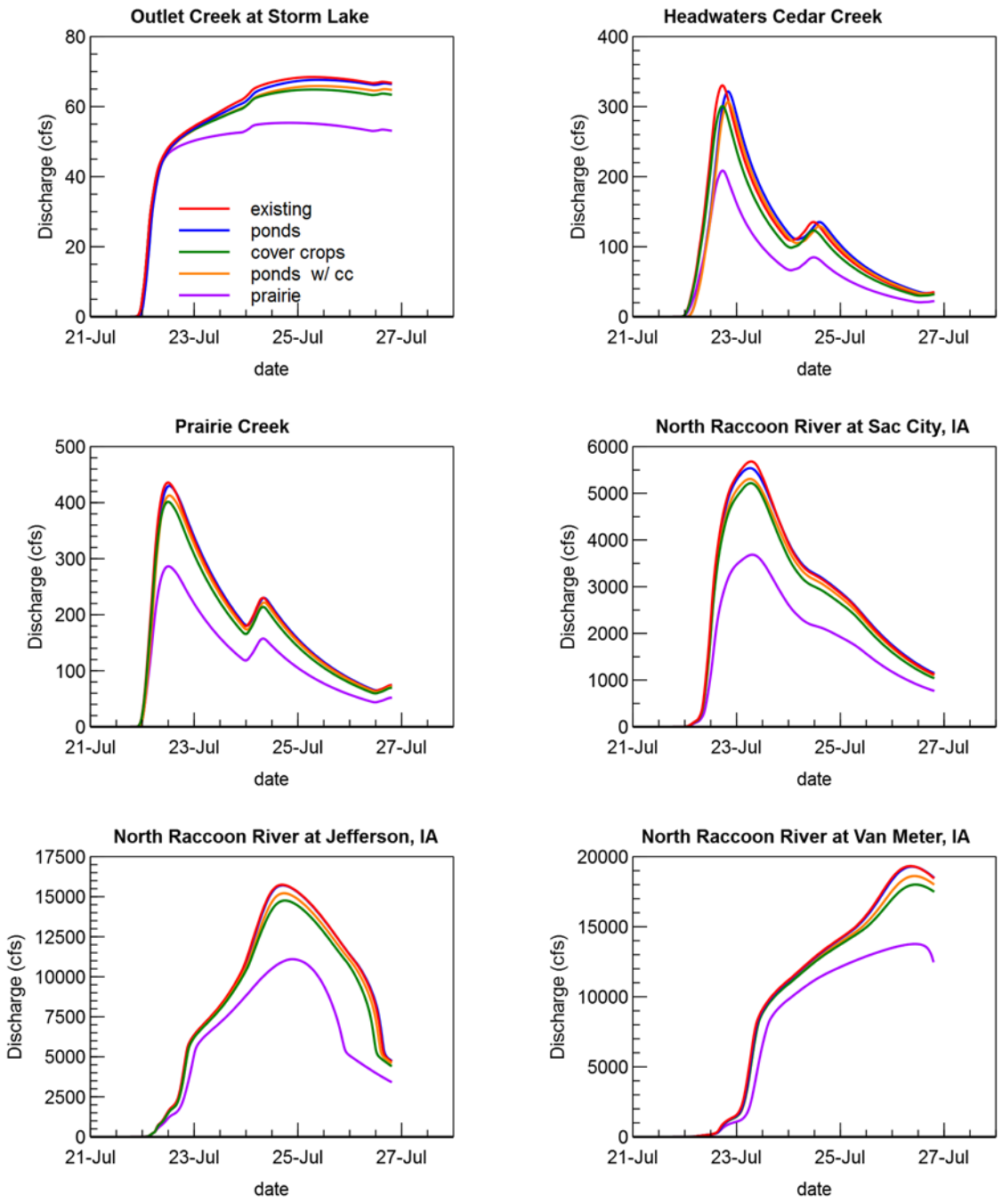


Figure 4.41. Hydrograph comparisons – with all agricultural lands converted to prairie, ACPF ponds, with 100% utilization of cover crops, and a combination of ACPF ponds and 50% utilization of cover crops, and distributed Saylorville Reservoir ponds for the July 2010 transposed event.

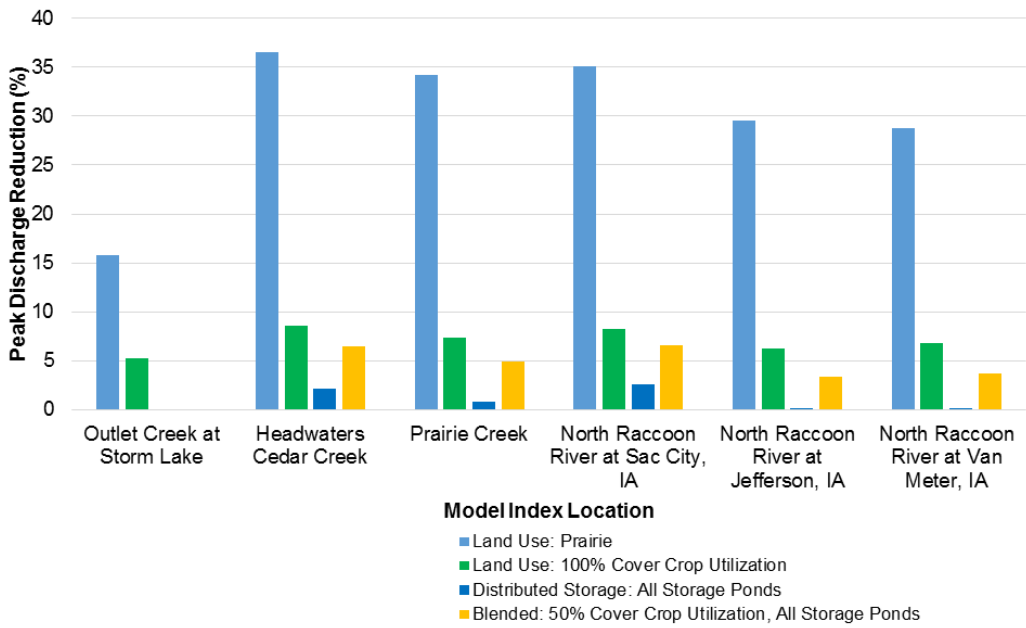


Figure 4.42. Percent reduction in peak discharge at model index locations with implementation of each watershed scenario for the July 2010 transposed event.

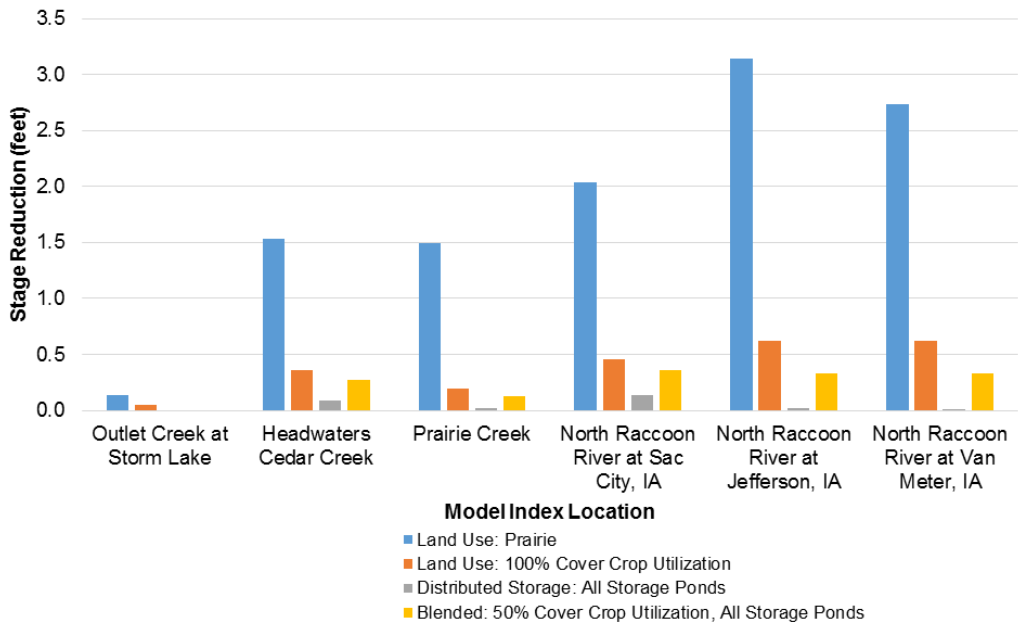


Figure 4.43. Reduction in stage at model index locations with implementation of each watershed scenario for the July 2010 transposed event.

### July 21, 2017, Northeast Iowa Storm Event

A storm event that occurred July 21, 2017, in northeast Iowa was identified as an equivalent 100-year rainfall event for the North Raccoon River Watershed using the RainyDay Stochastic Storm Transposition (SST) tool. This web-based tool was developed by the Hydroclimate Extremes Research Group at the University of Wisconsin – Madison. The Stage IV radar rainfall data for this particular storm event were transposed to the approximate center of the North Raccoon River Watershed for simulation of the watershed scenarios.

Watershed scenarios were unique for this storm event simulation. The simulation scenarios were formulated to estimate the quantity of distributed storage required for adequate reductions in peak flows along the main stem of the North Raccoon River.

A “typical pond” for runoff storage was developed assuming an 18-inch diameter pipe outlet as the principal spillway with a 20-foot wide emergency spillway set at an elevation 5 feet above the principal spillway invert. The total storage of this typical pond was approximately 49 acre-feet at the emergency spillway elevation. The stage-storage relationship of this typical pond was developed based on the average of the stage-storage relationships of ACPF ponds. These typical ponds were placed in all headwater model subbasins, totaling more than 513 locations.

The total ACPF pond storage (25,000 ac-ft) was used to distribute across all of the 513 headwater subbasins for several model scenarios. These scenarios featured multiplied storage by factors of 2, 4, 10, 20, and 27, and are summarized in Table 4.3. The scenario that utilizes 27 times the ACPF storage is equivalent to the total flood storage of Saylorville Reservoir, 675,000 ac-ft, distributed across the 513 locations. Each subbasin has an aggregated pond that mimics the storage effect of the multiple typical ponds, e.g., “Storage x27” assumes there are 27 typical 49 ac-ft ponds within the subbasin.

Table 4.3. Pond scenarios multiplying the total pond storage distributed across headwater subbasins.

Scenario	Total Storage (ac-ft)	Typical Pond Storage (ac-ft)
ACPF Ponds (25,000 ac-ft)	25,000	49
Storage x1	25,000	49
Storage x2	50,000	97
Storage x4	100,000	195
Storage x10	250,000	487
Storage x20	500,000	975
Storage x27 (Saylorville Reservoir)	675,000	1316

As the pond storage within each subbasin is increased, it is expected that a larger percentage of the subbasin drainage area would be intercepted by ponds. Based on the ACPF data, it appeared an equivalent headwater subbasin drainage area interception factor would be 15% for the “Storage x1” scenario. The “Storage x27” scenario was assumed to be at least the theoretical maximum number of ponds, and 2/3 of the subbasin area would be intercepted. Based on these assumptions,

a logarithmic relationship was developed, shown in Figure 4.44, to estimate the area intercepted by ponds for the other scenarios.

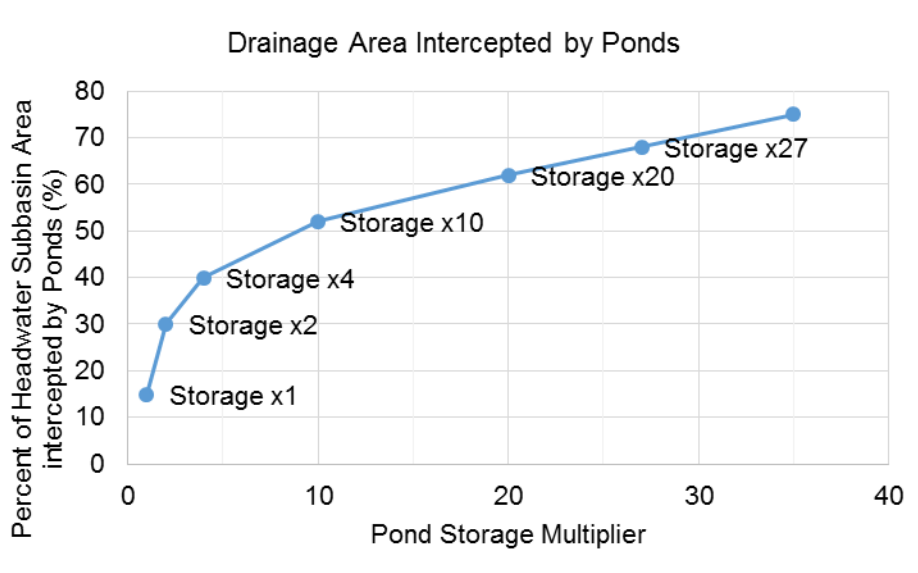


Figure 4.44. Relationship developed relating storage multiplier and percent of headwater drainage area intercepted by ponds.

Figure 4.45 shows the cumulative rainfall that occurred from July 21 - 22, 2017, transposed to the North Raccoon Watershed. Figure 4.46 shows peak discharge reductions at model junctions with distributed storage ponds in place. The largest peak discharge reductions of 5–10% occur just downstream of pond locations. On average, the largest reductions occur where pond density is highest and more storage is available to intercept drainage area and store excess runoff. Like previous simulations, reductions decrease as the drainage area ratio controlled by storage ponds decreases. This is evident along the main stem of the North Raccoon River where reductions were less than 2%.

Figure 4.47 shows junction peak discharge reductions at model junctions for multiples of pond storage. Similar to the ACPF ponds, the peak discharge reductions along the main stem was 0–2% for the 1x Storage scenario, with the largest reductions of 2-5% occurring in the farthest upstream reach. To attain a 10% or greater reduction in peak discharge at Jefferson requires between 250,000 and 500,000 ac-ft of distributed pond storage. The largest total pond storage scenario, 27x Storage, attained at least a 10% reduction along the main stem of the North Raccoon River.

Figure 4.48 shows a time series of simulated discharge at each of the model index locations. Percent reductions in peak discharge at model index locations are shown in Figure 4.49. Stage reductions at each location are shown in Figure 4.50.

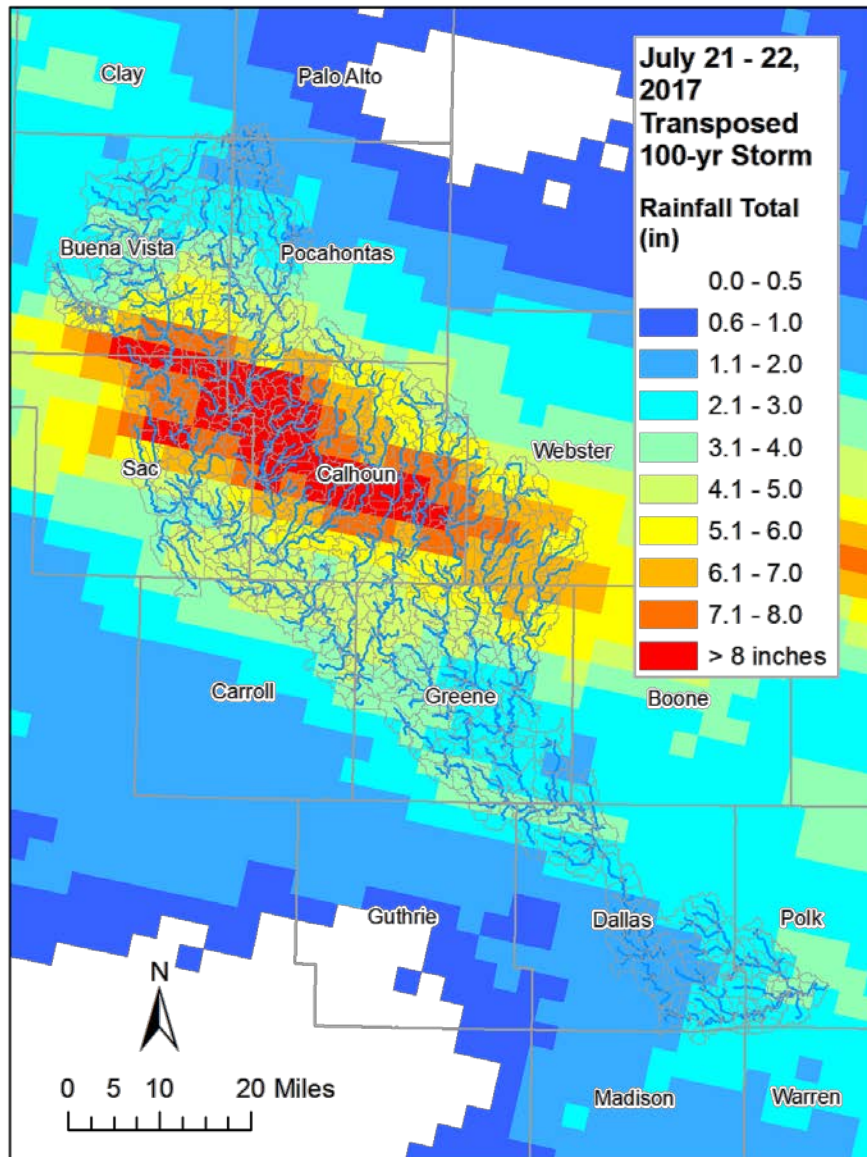


Figure 4.45. Rainfall totals for the period July 21 – 22, 2017, transposed from a location in northeast Iowa to the center of the North Raccoon River Watershed.

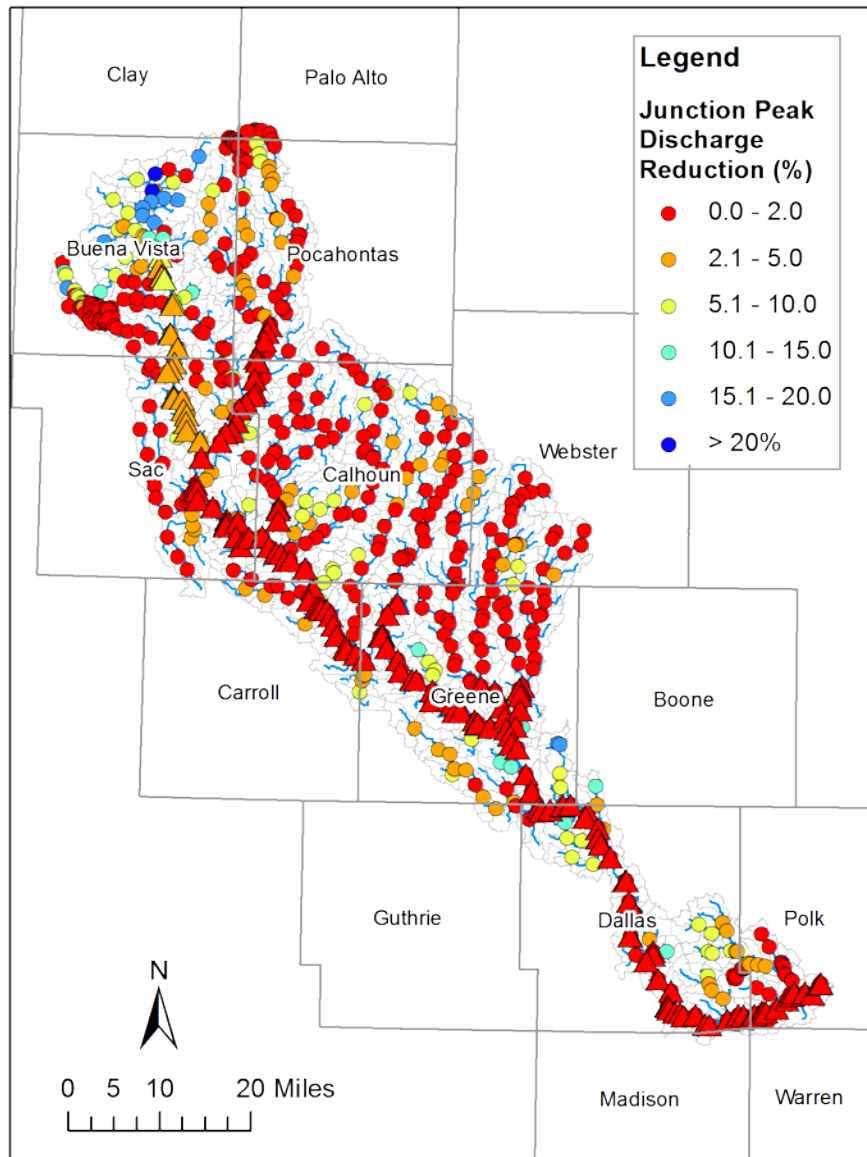


Figure 4.46. Junction peak discharge reductions with all ACPF ponds in place for the July 2017 transposed event. Junction points along the main stream are denoted by triangles.

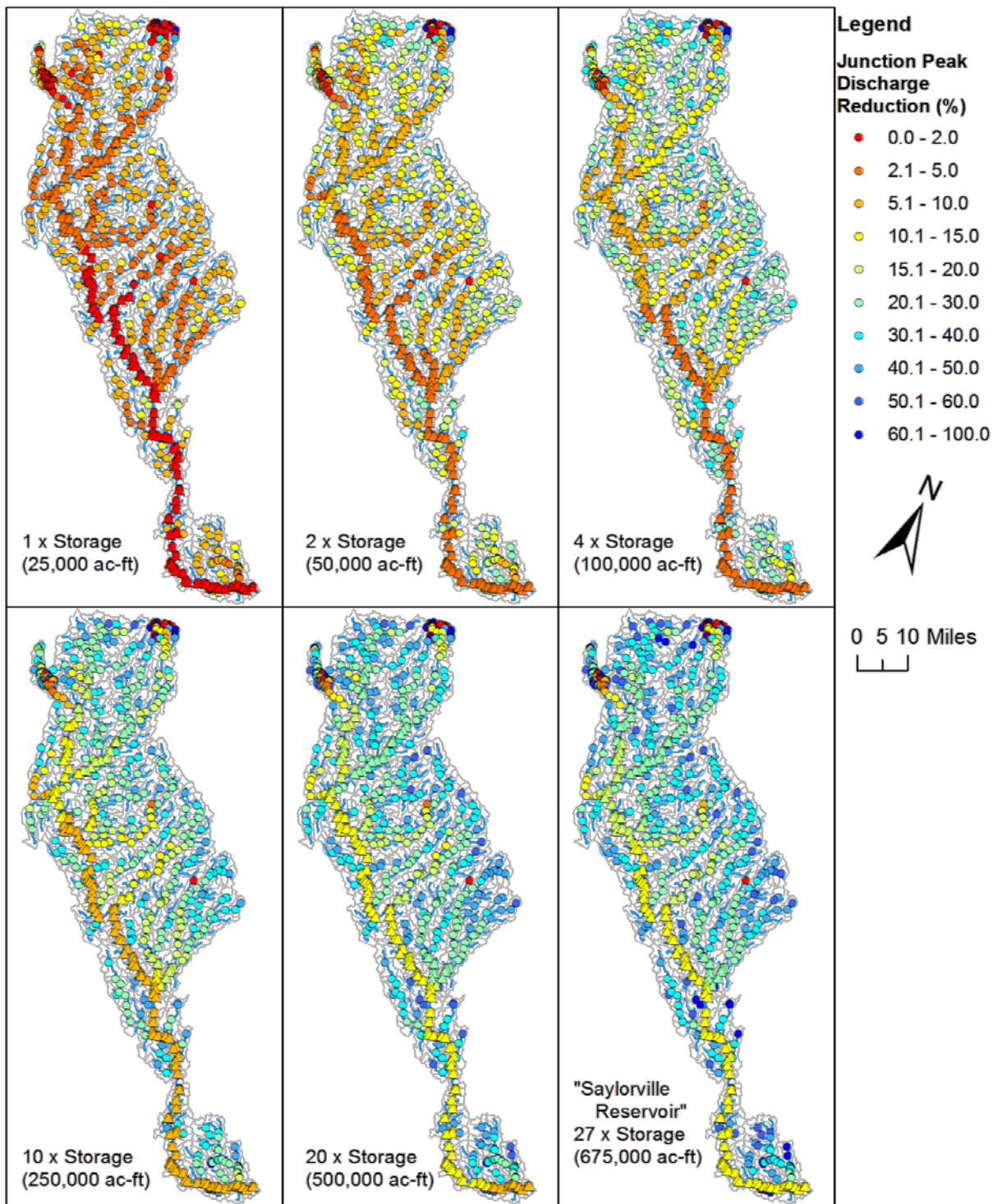


Figure 4.47. Junction peak discharge reductions with different pond storage scenarios for the July 2017 transposed event. Junction points along the main stream are denoted by triangles.

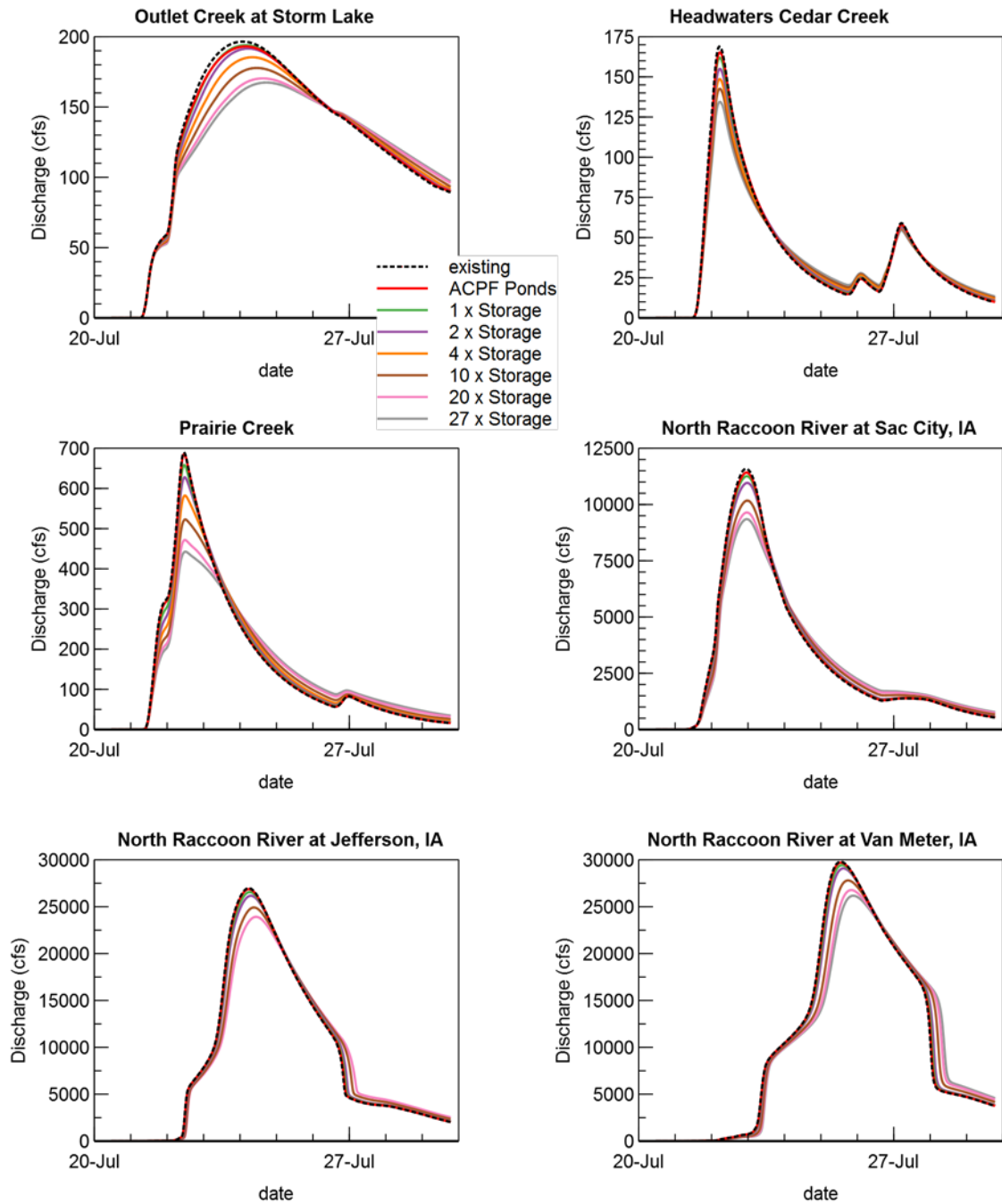


Figure 4.48. Hydrograph comparisons –with ACPF ponds, and multiples of typical pond storage for the July 2017 transposed event.

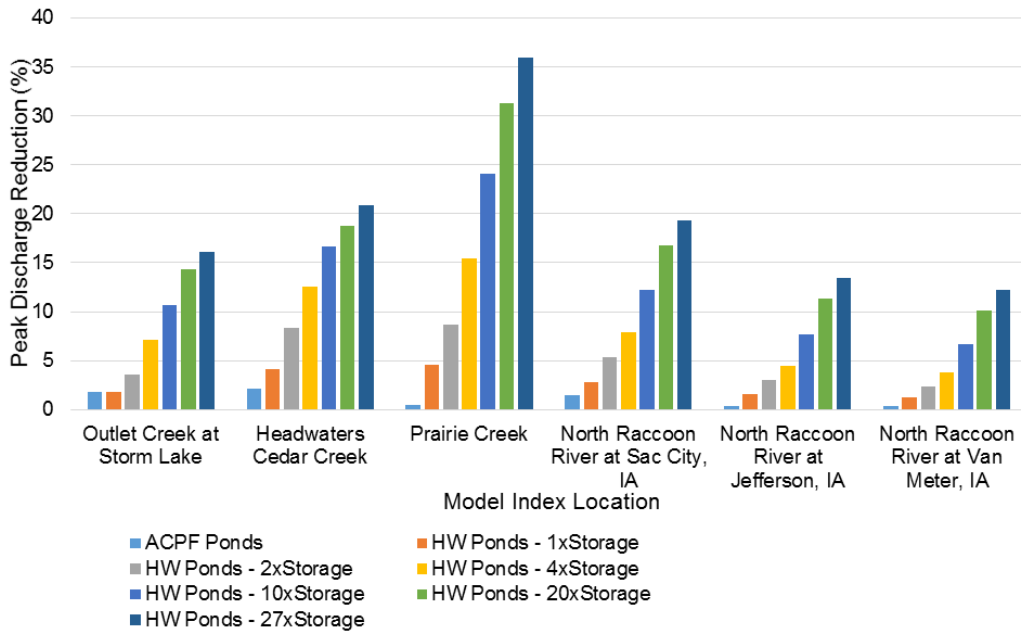


Figure 4.49. Percent reduction in peak discharge at model index locations with implementation of each pond storage scenario for the July 2017 transposed event.

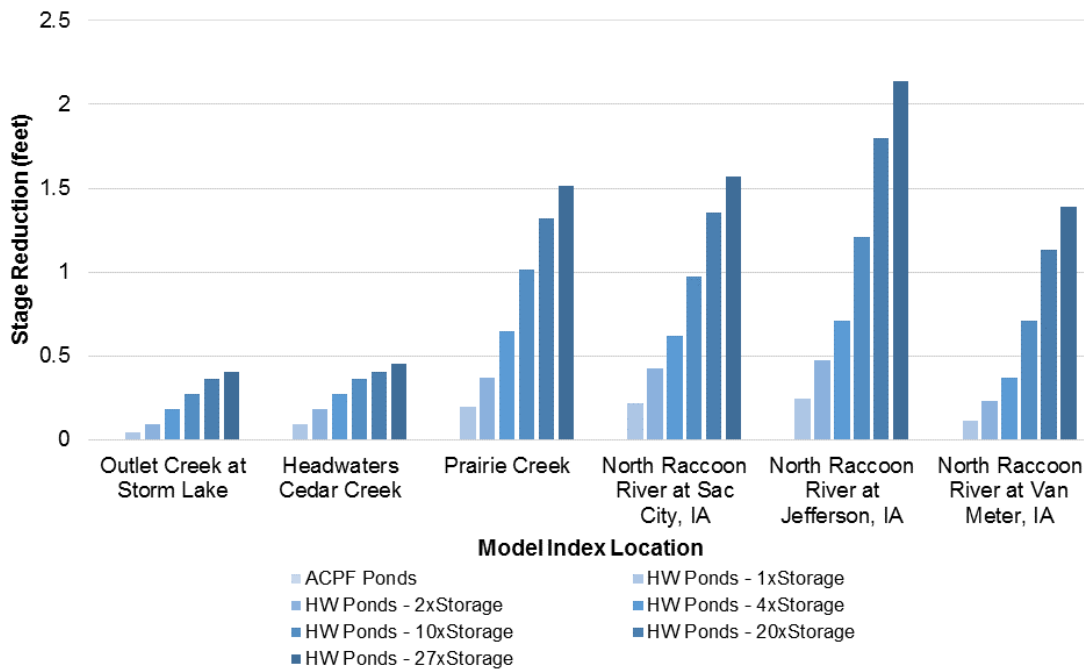


Figure 4.50. Reduction in stage at model index locations with implementation of each pond storage scenario for the July 2017 transposed event.

## 5. Summary and Conclusions

The North Raccoon River Watershed is one of nine distinct Iowa watersheds participating in the IWA program. The program will accomplish six specific goals in each watershed: (1) reduce flood risk; (2) improve water quality; (3) increase flood resilience; (4) engage stakeholders through collaboration and outreach/education; (5) improve quality of life and health, especially for susceptible populations; and (6) develop a program that is scalable and replicable throughout the Midwest and the United States. The purpose of this hydrologic assessment is to provide an understanding of the watershed hydrology in the North Raccoon basin and the potential of various hypothetical flood mitigation strategies that can be leveraged to accomplish goals of the IWA.

### a. North Raccoon River Water Cycle and Watershed Conditions

The water cycle of the North Raccoon River Watershed was examined using historical precipitation and streamflow records. The average annual precipitation for the North Raccoon River Watershed is 33.8 inches. Of this precipitation amount, 78% (26.4 inches) evaporates back into the atmosphere and the remaining 22% (7.4 inches) runs off the landscape into the streams and rivers. Most of the runoff amount is baseflow (68%, or 5.0 inches), and the rest is surface flow (32%, or 2.4 inches). Average monthly streamflow peaks in June, and decreases through the summer growing season. In most years, the largest discharge observed during the year occurs in May or June, associated with heavy spring/summer rains.

The water cycle has changed because of land use and climate changes. The largest change occurred in the late 1800s when the landscape was transformed from low-runoff prairie and forest to higher-runoff farmland. Since the 1970s, Iowa precipitation has increased in quantity, while intense rain events have changed in timing and frequency. Streamflow records in Iowa (including those for the North Raccoon River) suggest that average flows, low flows, and perhaps high flows have all increased and become more variable since the late 1960s or 1970s; however, the relative contributions of land use and climate changes are difficult to sort out.

The majority of the North Raccoon River Watershed lies in the Des Moines Lobe landform region and features poorly drained landscapes resulting from the most recent glaciation. The terrain was shaped by the slowly decaying ice sheet, around 12,000 years ago. Much of the watershed has soils with moderate runoff potential, but most of the areas have a shallow groundwater table that would typically inhibit infiltration, and must be drained. The terrain is characterized by numerous isolated topographic depressions and poorly developed natural drainage ways. Typical land slopes are between 0.3 and 1.4% (25th and 75th percentiles), with the steepest areas occurring along the major river and stream valleys. The land use is predominantly row crop agriculture, accounting for 77.7% of the area.

### b. North Raccoon River Hydrologic Model

The U.S. Army Corps of Engineers' (USACE) Hydrologic Engineering Center's Hydrologic Modeling System (HEC-HMS) was used to develop a flood prediction model for the North Raccoon River Watershed. First, the watershed was divided into 1156 smaller units, called subbasins, with an average area of 2.1 square miles. For model calibration and validation with

actual (historical) rainfall events, radar rainfall estimates were used as the precipitation input for each simulation. For the analysis of watershed scenarios, a 24-hour duration SCS Design Storm with rainfall accumulations approximately equal to the 25-year return period was used to drive the watershed response. Several historical storm events and two transposed historic events were used to evaluate the relative difference between watershed scenario simulations.

The NRCS Curve Number (CN) methodology was used to determine rainfall-runoff partitioning in the North Raccoon River Watershed HMS model. The CN methodology accounts for precipitation losses due to initial abstractions and infiltration during the rainstorm. CN value estimates are based on land use and the underlying soil type, and the area-weighted average CN was assigned to each subbasin as an initial parameter estimate. The Clark and ModClark Unit Hydrograph methods was used to convert excess precipitation to a direct runoff hydrograph for each subbasin. Baseflow was simulated for model calibration and validation with actual (historical) rainfall events but was not simulated during the design storm. Conveyance of runoff through the river network, or flood wave routing, was accomplished using Muskingum-Cunge routing methods for major streams and Muskingum routing methods for smaller tributaries. Reservoir routing through Little Storm Lake, the Storm Lake Bridge Inlet, Storm Lake, Black Hawk Lake, and Twin Lakes were incorporated into the HMS model.

Model calibration adjusts the initial set of model parameters, so the simulated results more closely match observed discharges at gauging stations more closely for historical events. The North Raccoon River Watershed HEC-HMS model was calibrated with two storm events that occurred late April 2007 and May 2013 (significant events for which radar rainfall estimates were available). After calibration of model parameters, model validation assesses the predictive capability of the model to simulate discharge for another storm event that occurred June 2005 (not used in calibration). The model generated runoff volume, hydrograph shape, and peak flow timing very similar to the observed streamflow hydrographs the validation event.

### c. Watershed Scenarios for the North Raccoon River

The HEC-HMS model was used to better understand the flood hydrology of the North Raccoon River watershed and to evaluate potential flood mitigation strategies. The runoff potential throughout the watershed was first assessed using the HMS model's representation of storm runoff generated from a design storm. Areas with the lowest runoff potential are located on the Des Moines Lobe landform region, an area with numerous isolated depressions that are not hydraulically connected to a natural water course. These areas appear to generate less runoff, but it is likely some of the precipitation that is ponded eventually infiltrates and enters the drainage system through field drainage tile. Areas with relatively higher runoff potential occur along the main stem of the North Raccoon River, or the southern edge of the watershed. From a hydrologic perspective, flood mitigation projects that can reduce runoff from these higher runoff areas should be a higher priority. It is worth noting that other land uses – particularly urban development – likely have the highest runoff potential. However, the footprint of these areas is small compared to the agricultural areas that dominate the watershed. In urban areas, local drainage issues could be improved by more effectively capturing and storing storm water (e.g., storm water detention and low-impact development practices).

The HEC-HMS model was used to quantify potential effects of flood mitigation strategies applied throughout the North Raccoon River Watershed. Several flood mitigation strategies were considered — enhancing local infiltration through changes in land use (from agricultural to native tall-grass prairie), enhancing local infiltration through improvements in soil quality through the use of cover crops, and storing floodwaters temporarily in ponds throughout the watershed to reduce downstream discharges. A blended scenario using cover crops and storage ponds was considered. The effects of these strategies were simulated for a 6-inch, 24-hour SCS Design Storm, occurring simultaneously over the entire watershed, and also for several historical rainfall events. The results of these strategies were compared to simulations of flows for the existing watershed condition. Although each scenario simulated is hypothetical and simplified, the results provide valuable insights on the relative performance of each strategy for flood mitigation planning.

There are many BMP practices not investigated in this report that could potentially increase infiltration or runoff storage at the watershed scale. However, the analysis was limited by the resolution and capability of the HEC-HMS model to simulate effects of BMP practices aggregated across subbasin areas of several square miles. Therefore, investigations were limited to distributed storage provided by ponds, which are relatively large BMP structures, and broad-scale land cover changes. Simulation of other much smaller BMP structures like terracing or WASCOBS, while demonstrably effective in this watershed, would require considering many more individual structures to make any impact at the watershed scale, and a much higher degree of model resolution to reliably quantify impacts.

### **i. Increased Infiltration in the Watershed**

Simulation results indicate that enhancements to local infiltration through changes in land use have the most significant impact on runoff. Converting current agricultural areas from row crop to native tall-grass prairie would increase rainfall infiltration by 0.7 inches during large rainfall events. This hypothetical scenario illustrates the dramatic reductions in stream flow as a result of land use change. However, converting the entire agricultural landscape back to pre-settlement tall-grass prairie is not a practical or economically desirable strategy. This scenario provides support for targeted land use changes that could be an effective part of a watershed's flood mitigation efforts.

Agricultural management practices could increase the infiltration of rain water without significantly decreasing agricultural production through the use of cover crops. Cover crop plantings during the dormant season can produce long-lasting improvements in soil quality. However, improvements in soil infiltration properties would take many years to be fully realized, and cover crops would need to be continuously implemented. From the simulation results, it is apparent that enhancement of local infiltration through soil quality improvement resulting from cover crops has a small but significant effect. The model predicts that adopting cover crop management practices would increase infiltration during large storms by 0.15 inches (for the 6-inch, 24-hour design storm), which is much less infiltration than a tall-grass prairie landscape, but significant nonetheless. Reductions in peak discharge throughout the watershed ranged from 5–10%, depending on the storm event. Given the widespread agricultural land use in the North

Raccoon Watershed and the growing interest in the use of cover crops as a part of Iowa's nutrient management strategy, cover crops could play an important role as a watershed-wide flood mitigation strategy.

## **ii. Increased Storage on the Landscape**

In some ways, using ponds to temporarily store floodwaters is an attempt to replace the loss of water that was once stored in soils (in the pre-agricultural landscape). In the hypothetical scenarios involving ACPF pond storage, approximately 25,000 acre-feet of storage was added to the North Raccoon River Watershed utilizing 133 potential ACPF nutrient reduction wetland locations and 151 similar hypothetical ponds. For the upstream areas draining to ponds, this is equivalent to an added storage depth of 2.1 inches for runoff downstream of Van Meter. However, for the North Raccoon River Watershed downstream of Van Meter, as a whole (not just the area with ponds), the added storage depth is approximately 0.13 inches. Compared to the extra water that was stored by infiltration in the previous simulated scenarios, the amount of storage replaced by ponds is quite small. As a result, the overall flood peak reduction with storage ponds is less than predicted for the other scenarios. Since there is no additional infiltration, the overall volume of runoff in the watershed is higher than the enhanced filtration scenarios. Still, compared to the other scenarios, the flood storage scenario is realistically more achievable. Ponds can effectively reduce flood peaks immediately downstream of their headwater sites. Reductions in peak discharge throughout the watershed ranged from 0–15%, depending on the storm event. Reductions in peak discharge along the main stem of the North Raccoon River were approximately 0-2%. At junctions farther downstream, floodwaters originating from locations throughout the watershed arrive at vastly different times; some areas have ponds, others do not. The result is that the storage effect from ponded areas is spread out over time, instead of being concentrated at the time of highest flows. Hence, at larger drainage areas downstream in the watershed, the flood peak reduction of storage ponds diminishes.

Siting of these ponds ACPF ponds was driven by nutrient reduction criteria, rather than flood control. If flood control was the siting criteria, additional suitable locations could be identified, particularly in the portion of the watershed without ACPF data.

## **iii. Increased Infiltration and Increased Storage: A Blend of Cover Crops and Flood Storage Ponds**

Future projects in the North Raccoon Watershed will likely use both enhanced infiltration practices and flood storage. A blended scenario was developed using agricultural management with cover crops and flood storage ponds to evaluate the flood mitigation benefits of multiple mitigation strategies. The watershed scenario assumes 50% of agricultural lands would use cover crops to improve soil infiltration. All the flood storage ponds considered in the previous scenario were incorporated. Utilizing cover crops on 50% of agricultural lands would increase rainfall infiltration by 0.08 inches during large rainfall events. Reductions in peak discharge throughout the watershed ranged from 2–15%, depending on the storm event. Reductions in peak discharge along the main stem of the North Raccoon River were approximately 2-10%. Simulation results of the design storm and historical events indicate the use of cover crops would provide much broader benefits than ponds alone and further enhance the ability of ponds to store excess runoff.

Improvements in soil infiltration properties would take many years to be fully realized, and cover crops would need to be continuously implemented.

#### **d. Concluding Remarks**

It is important to recognize that these modeling scenarios evaluate the hydrologic effectiveness of the flood mitigation strategies and not their effectiveness in other ways. For instance, while certain strategies are more effective in terms of hydrology, they may not be as effective economically. As part of the flood mitigation planning process, other factors should be considered in addition to the hydrology, such as the cost and benefits of alternatives, landowner willingness to participate, and more.



## **Appendix A – Maps**

- A-1 Existing BMP Mapping: Pond Dams
- A-2 Existing BMP Mapping: Terraces
- A-3 Existing BMP Mapping: Water and Sediment Control Basins (WASCOBs)
- A-4 Existing BMP Mapping: Grassed Waterways
- A-5 ACPF Potential BMPs: Nutrient Reduction Wetlands
- A-6 ACPF Potential BMPs: Nutrient Reduction Wetland Drainage Areas
- A-7 ACPF Potential BMPs: Contour Buffer Strips
- A-8 ACPF Potential BMPs: Water and Sediment Control Basins (WASCOBs)
- A-9 ACPF Potential BMPs: WASCOB Drainage Areas
- A-10 ACPF Potential BMPs: Grassed Waterways



## **Appendix B – Calibration and Validation**

### **Calibration**

This appendix details calibration and validation efforts for the North Raccoon River Watershed model. It includes the major calibration measures taken, a summary of the final calibrated model parameters, and results for the calibration and validation historical storms. Modeling was performed using the U.S. Army Corps of Engineers' (USACE) Hydrologic Engineering Center's Hydrologic Modeling System (HEC-HMS), Version 4.0.

#### **i. Calibration Measures**

The North Raccoon River Watershed HMS model was calibrated to two storm events that occurred in late April 2007 and May 2013. Researchers selected the storms based on their range of antecedent conditions, magnitude, the time of year, and the availability of Stage IV radar rainfall estimates and United States Geological Survey (USGS) discharge estimates. Large, high-runoff storms occurring between late April and September were selected to minimize the impacts of snow, rain on frozen grounds, and freeze-thaw effects that can happen during late fall to early spring. Global adjustments to the model parameters described in Chapter 3 were completed to best match simulated hydrographs to observed discharge time series at each USGS stage/discharge gauge location. Model performance was evaluated based on how well several variables resembled the observed hydrograph at a particular USGS gauge location: simulated hydrograph peak discharge, time of peak discharge, total runoff volume, and general shape.

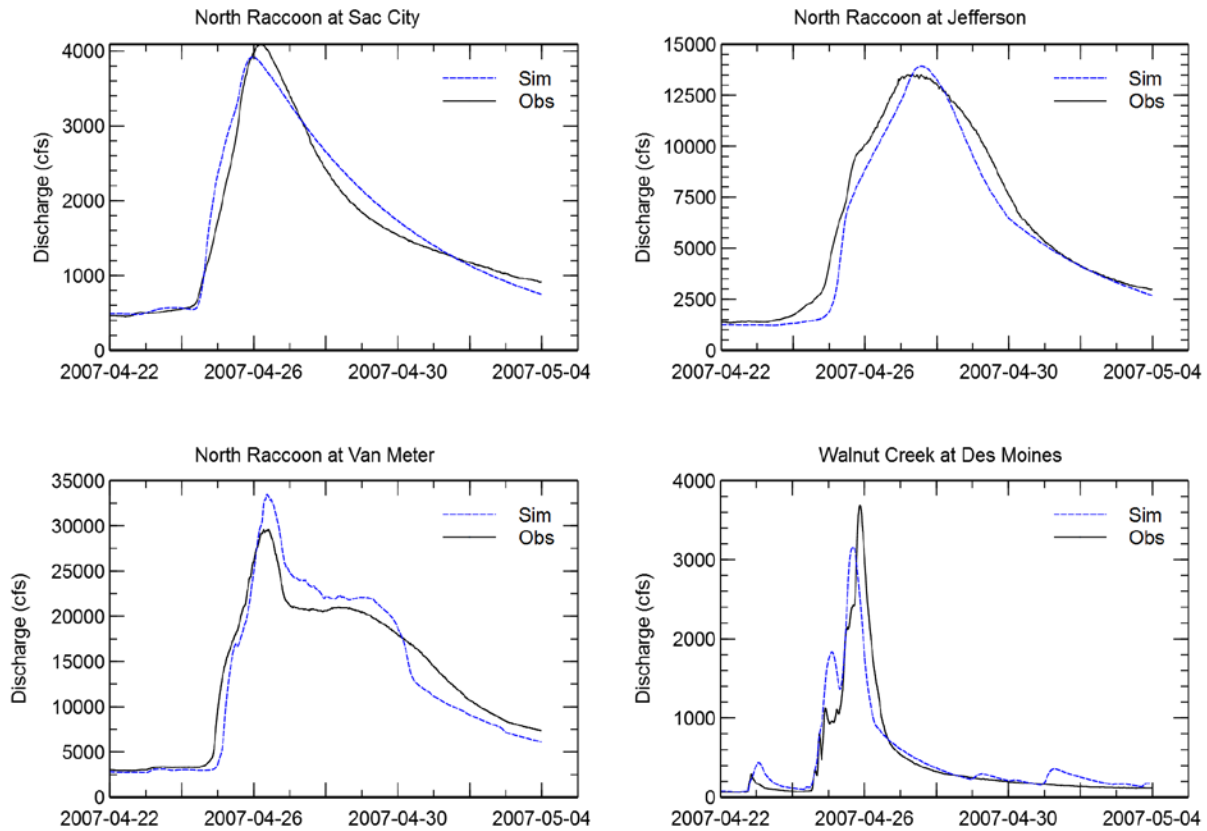
Figure B1 shows observed flow hydrographs at the Sac City, Jefferson, Van Meter and Walnut Creek USGS gauging stations, with simulated flow hydrographs for the April 2007 event. Comparisons of simulated and observed peak discharge, time to peak discharge, and total streamflow volume are also shown in tabular format. Figure B2 shows similar comparisons for the May 2013 event.

## ii. Summary of Calibrated HMS Model Parameters

Table B.1 summarizes the final set of HMS model parameters determined through calibration for the North Raccoon River Watershed.

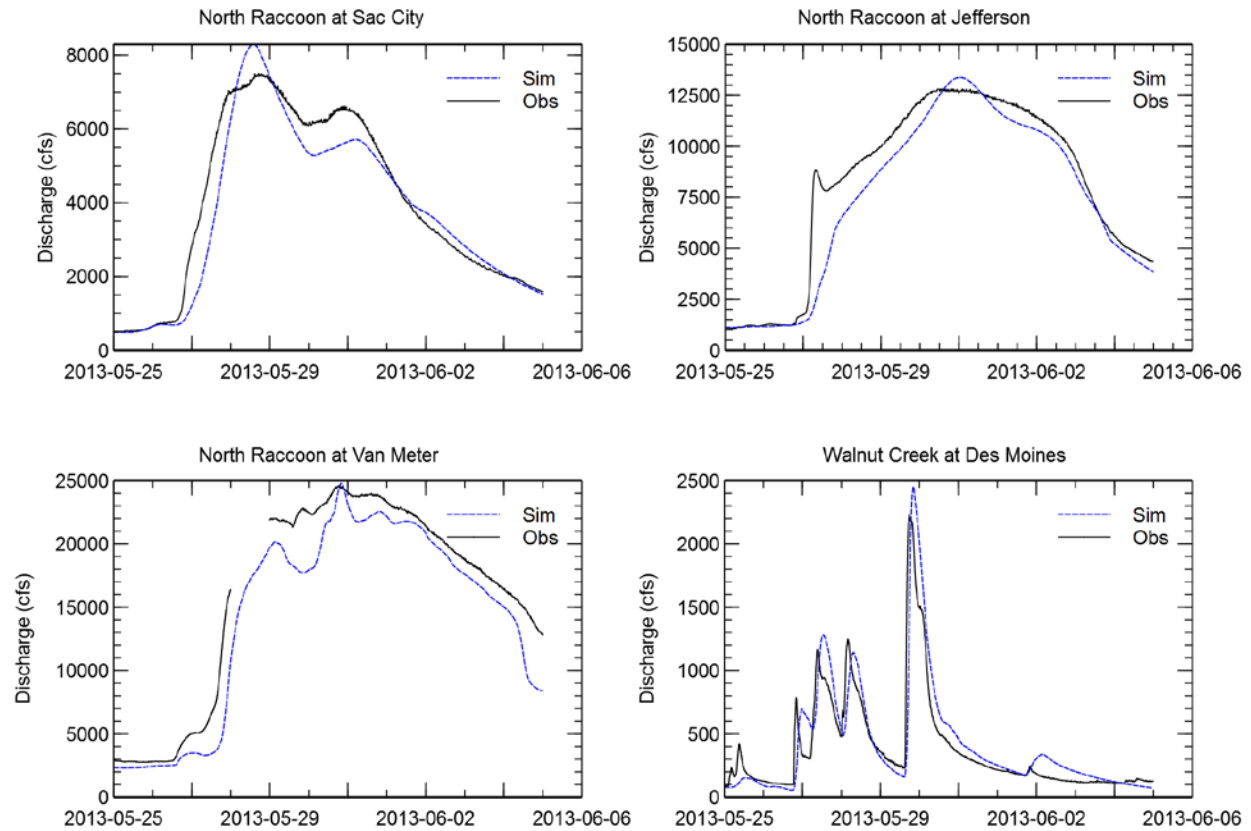
<i>Parameter</i>	<i>Initial Value</i>	<i>Calibrated Value</i>	<i>Comments</i>
<b>Runoff Estimation</b>			
Curve Number (CN)	Based on initial moisture state; subbasin CNs determined from Table 3.1	Reduced significantly in tiled regions	varied with each storm event
Initial Abstraction ( $I_a$ )	20% of potential maximum retention (S)	Increased significantly in tiled regions	varied with each storm event
<b>Subbasin Hydrograph Development</b>			
Time of Concentration ( $T_c$ )	5/3 of subbasin lag time	5/3 of subbasin lag time	Lag time calculated using original uncalibrated CNs
Basin Storage Coefficient (R)	$2T_c$	Ranged from 7 to 15 times $T_c$ , ranged from 2 to 5 times $T_c$ for Walnut Creek Area	Varied spatially, compensating for field tile
<b>River Routing</b>			
Muskingum Flood Wave Travel Time (K)	Based on a velocity of 1.2 m/s (3.9 ft/s)	Velocities ranged from 0.3 m/s (1 ft/s) to 1.6 m/s (5.2 ft/s)	Average value, varied with each storm event
Muskingum Attenuation Factor (X)	0.2	0.2	
Muskingum-Cunge Routing Manning's Roughness - Channel	0.03	0.025 – 0.03	
Muskingum-Cunge Routing Manning's Roughness - Overbanks	0.06	0.045 – 0.06	
<b>Baseflow</b>			
Decay Constant (k)	0.75	0.6 – 0.8	Average value, varied with each storm event
Baseflow Reset on Receding Limb	0.075	0.1 – 0.9	Average value, varied with each storm event

Figure B.1. Calibration Storm Events – April 22 – May 4, 2007



	<i>Peak Discharge (cfs)</i>	<i>Time of Peak</i>	<i>Total Volume (in)</i>
<b>North Raccoon River at Sac City, USGS 05482300</b>			
<b>Simulated</b>	3919.9	4/25/2007 23:20	1.52
<b>Observed</b>	4089.4	4/26/2007 4:00	1.45
<b>North Raccoon River at Jefferson, USGS 05482500</b>			
<b>Simulated</b>	13935.2	4/27/2007 13:40	2.01
<b>Observed</b>	13500.8	4/27/2007 4:00	2.21
<b>North Raccoon River at Van Meter, USGS 05484500</b>			
<b>Simulated</b>	33492.4	4/26/2007 9:00	1.96
<b>Observed</b>	29604.3	4/26/2007 6:30	2.00
<b>Walnut Creek at Des Moines, USGS 05484800</b>			
<b>Simulated</b>	3160.7	4/25/2007 16:25	2.76
<b>Observed</b>	3690.4	4/25/2007 21:00	2.52

Figure B.2. Calibration Storm Events – May 25 – June 6, 2013

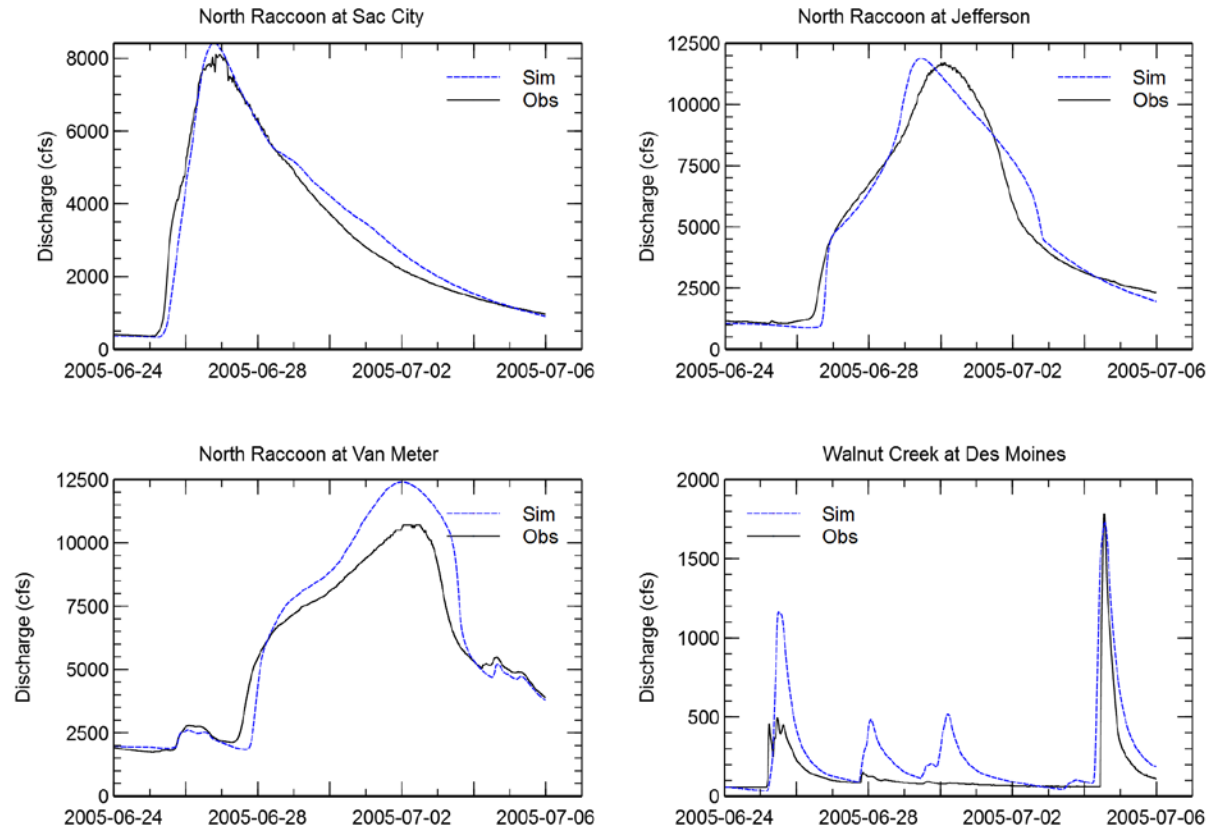


	<i>Peak Discharge (cfs)</i>	<i>Time of Peak</i>	<i>Total Volume (in)</i>
<b>North Raccoon River at Sac City, USGS 05482300</b>			
<b>Simulated</b>	8295.4	5/28/2013 13:50	2.99
<b>Observed</b>	7511.4	5/28/2013 17:00	3.19
<b>North Raccoon River at Jefferson, USGS 05482500</b>			
<b>Simulated</b>	13366.6	5/31/2013 0:40	2.33
<b>Observed</b>	12801.6	5/30/2013 10:45	2.56
<b>North Raccoon River at Van Meter, USGS 05484500</b>			
<b>Simulated</b>	24769.7	5/30/2013 19:45	1.94
<b>Observed</b>	24603.7	5/30/2013 18:30	1.96
<b>Walnut Creek at Des Moines, USGS 05484800</b>			
<b>Simulated</b>	2450.8	5/29/2013 20:15	2.18
<b>Observed</b>	2231.9	5/29/2013 17:45	1.98

### iii. Validation Storm Events

The North Raccoon River Watershed HMS model was validated using a storm event from June 2005. Comparisons of simulated and observed peak discharges, time to peak discharge, and total streamflow volume for the June 2005 event is shown in Figure B3.

Figure B.3. Calibration Storm Events – June 24 – July 6, 2005



	<i>Peak Discharge (cfs)</i>	<i>Time of Peak</i>	<i>Total Volume (in)</i>
<b>North Raccoon River at Sac City, USGS 05482300</b>			
Simulated	8412.0	6/26/2005 18:55	2.89
Observed	8111.8	6/26/2005 20:00	2.79
<b>North Raccoon River at Jefferson, USGS 05482500</b>			
Simulated	11883.4	6/29/2005 10:50	1.79
Observed	11703.3	6/30/2005 0:00	1.77
<b>North Raccoon River at Van Meter, USGS 05484500</b>			
Simulated	12402.5	7/2/2005 0:15	0.93
Observed	10700.3	7/2/2005 1:00	0.85
<b>Walnut Creek at Des Moines, USGS 05484800</b>			
Simulated	1726.9	7/4/2005 13:35	1.51
Observed	1779.9	7/4/2005 13:00	0.85

#### **iv. Calibration/Validation Summary**

The North Raccoon River Watershed HMS model has several strengths, weaknesses, and assumptions that should be reiterated. First, the HMS model is a surface water–only model, so subsurface and groundwater flow components are not accounted for explicitly. The HMS model represents baseflow with a first order exponential decay relationship, which represents the aggregated effects of all subsurface flow contributions (interflow and groundwater flow). Because this model is intended for event-based simulations, it does not account for evapotranspiration, which typically dwarfs infiltration and runoff volumes at longer time scales. Additionally, the HMS model is only applicable to estimate the watershed response to storm events occurring between late April and September. While flooding is also common at other times of the year, particularly in March and early April, this period was not considered during calibration for several reasons. These reasons include project goals (constructed projects are likely to perform better during the late spring to summer months), flood seasonality (the largest floods have occurred sporadically in the summer months), and model limitations (snowmelt was not considered in the model). Finally, the HMS model performs best when surface runoff is expected to dominate the partitioning of rainfall. This typically occurs for larger storm events when a greater overall amount of precipitation is converted to runoff or for near-saturated initial conditions.

Figure B4 compares the simulated and observed peak discharges at USGS stage/discharge gauge locations in the watershed for calibration and validation events. A line representing perfect agreement between simulated and observed peak discharges is also shown. Most of the validation data points lie on or near the line, indicating that the model is capable of reproducing observed peak discharges for a variety of storm events.

Figure B5 compares the simulated and observed runoff volumes at USGS stage/discharge gauge locations in the watershed for calibration and validation events. Once again, most of validation data points lie on or near the perfect agreement line, indicating that the model can reproduce observed runoff volumes for a variety of storm events.

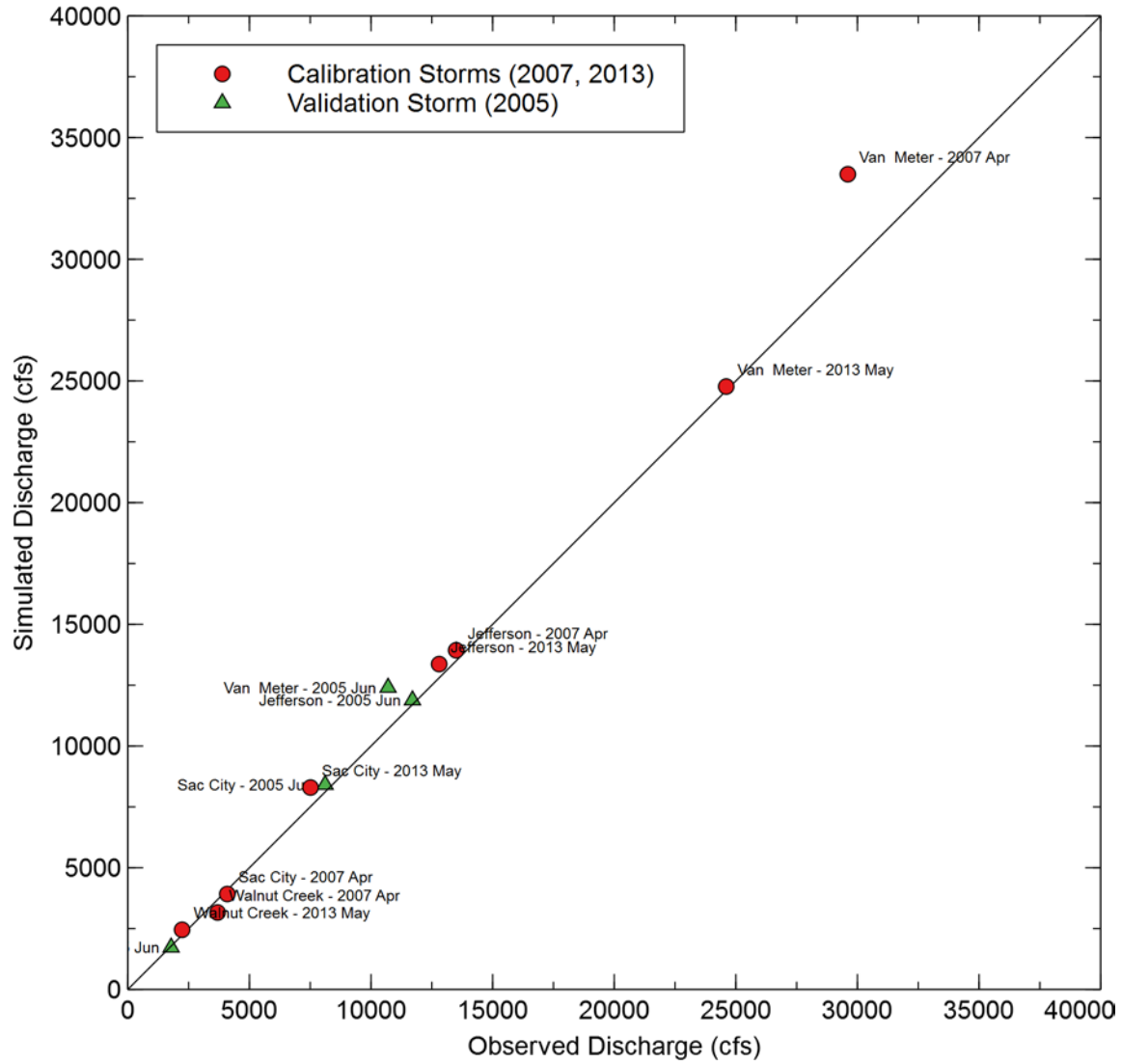


Figure B4. Comparison of simulated and observed peak discharges at USGS stage/discharge gauge locations in the North Raccoon River Watershed for calibration and validation events.

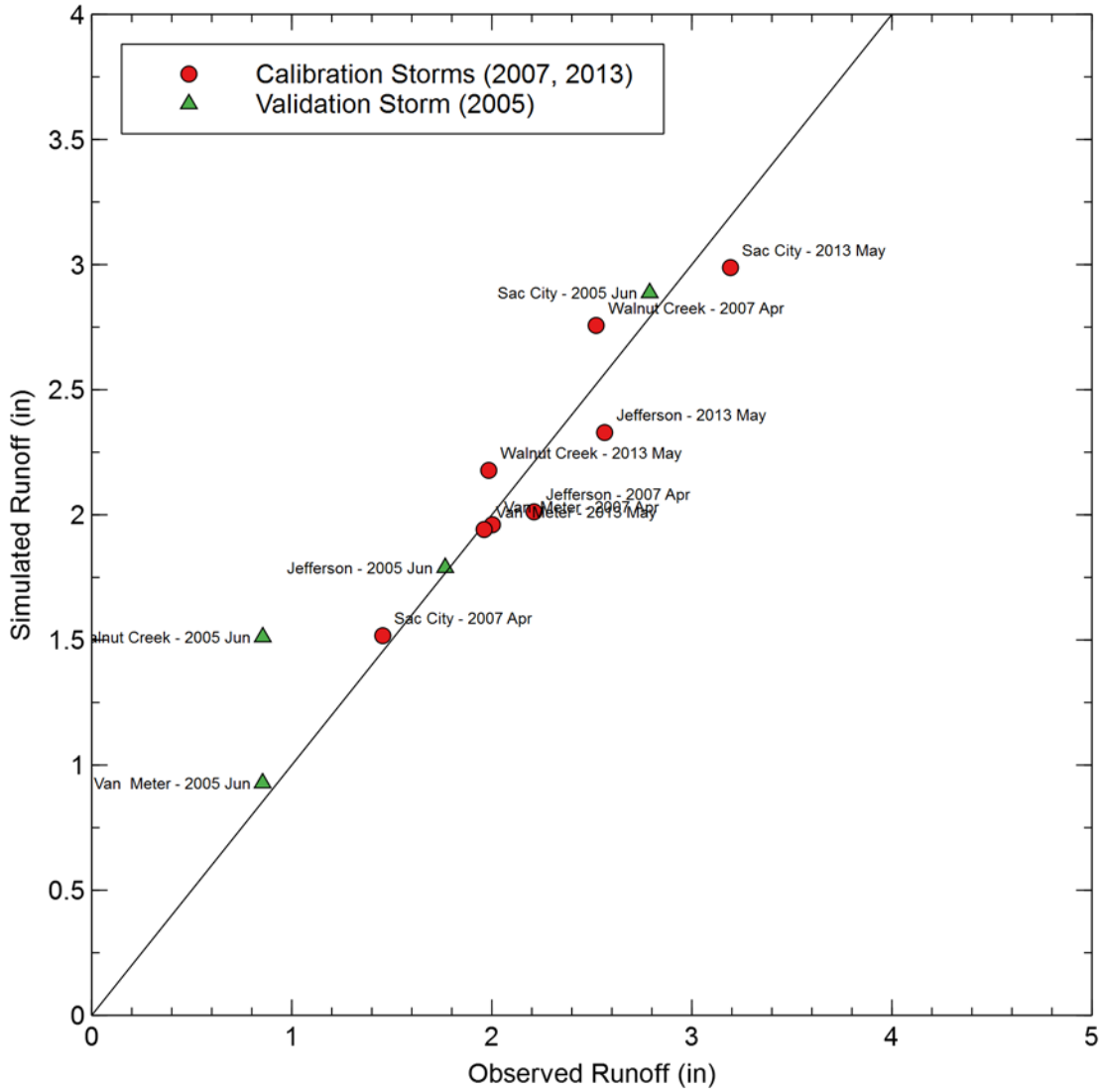


Figure B5. Comparison of simulated and observed runoff volumes at USGS stage/discharge gauge locations in North Raccoon River Watershed for calibration and validation events.

## Appendix C – Incorporated Structures

Table C.1. Storm Lake Stage-Storage-Discharge Table

<i>Elevation (ft)</i>	<i>Storage (ac-ft)</i>	<i>Discharge (cfs)</i>	<i>Notes</i>
1399.00	26619.556	0.0	Principal Spillway
1399.51	28053.489	93.8	
1399.71	28645.572	156.2	
1399.88	29149.986	216.4	
1400.07	29713.667	290.3	
1400.26	30256.739	367.3	
1400.41	30706.807	434.9	
1401.00	32518.605	700.7	
1402.00	35617.105	1151.2	
1405.00	44920.105	2502.8	
1408.00	54373.105	3854.4	

Table C.2. Little Storm Lake Stage-Storage-Discharge Table

<i>Elevation (ft)</i>	<i>Storage (ac-ft)</i>	<i>Discharge (cfs)</i>	<i>Notes</i>
1399.00	276.051	0.0	Downstream control from Storm Lake
1399.89	373.947	17.1	
1401.33	538.824	59.8	
1402.03	621.069	129.4	
1402.70	700.281	170.4	
1403.32	774.630	195.8	
1403.83	836.016	208.5	
1410.00	1593.451	362.5	
1412.00	1838.973	800.0	
1412.50	1900.353	1200.0	

Table C.3. Storm Lake Bridge Inlet Stage-Storage-Discharge Table

<i>Elevation (ft)</i>	<i>Storage (ac-ft)</i>	<i>Discharge (cfs)</i>	<i>Notes</i>
1399.00	44.566	0.0	Downstream control from Storm Lake
1401.05	206.432	639.2	
1401.66	315.725	765.6	
1402.03	393.037	843.3	
1402.70	553.760	989.3	
1403.32	726.697	1130.6	
1403.83	880.948	1250.0	
1410.00	3550.661	2694.8	

Table C.4. Black Hawk Lake Stage-Storage-Discharge Table

<i>Elevation (ft)</i>	<i>Storage (ac-ft)</i>	<i>Discharge (cfs)</i>	<i>Notes</i>
1214.5	0	0	
1214.8	0	276	
1215.1	0	552	
1215.4	0	828	
1215.7	0	1104	
1216.0	0	1380	
1216.3	0	1656	
1216.6	0	1932	
1216.9	0	2208	
1217.2	0	2484	
1217.5	0	2760	
1217.8	0	3036	
1218.1	0	3312	
1218.4	0	3588	
1218.7	0	3864	
1219.0	0	4140	
1219.3	0	4416	
1219.6	0	4692	
1219.9	0	4968	
1220.2	0	5244	
1220.5	0	5520	
1220.8	20.26	5852	Principal Spillway
1221.1	57.29	6184	
1221.4	105.25	6516	
1221.7	162.05	6848	
1222.0	226.47	7180	
1222.3	297.71	7512	
1222.6	375.15	7844	
1222.9	458.35	8176	
1223.2	519.74	8508	
1223.5	545.25	8840	
1223.8	571.15	9172	
1224.1	597.45	9504	
1224.4	624.13	9836	
1224.7	651.19	10168	
1225.0	678.62	10500	Top of Embankment

Table C.5. South Twin Lake Stage-Storage-Discharge Table

<i>Elevation (ft)</i>	<i>Storage (ac-ft)</i>	<i>Discharge (cfs)</i>	<i>Notes</i>
1399.00	276.051	0.0	Principal Spillway
1399.89	373.947	17.1	
1401.33	538.824	59.8	
1402.03	621.069	129.4	
1402.70	700.281	170.4	
1403.32	774.630	195.8	
1403.83	836.016	208.5	
1410.00	1593.451	362.5	
1412.00	1838.973	800.0	
1412.50	1900.353	1200.0	



## Appendix D – References

- Archuleta, Ray. “Cedar River Watershed Coalition Meeting – Cover Crops and Other Conservation Practices,” Personal interview, April 2014.
- Ayalew, T., Krajewski, W., Mantilla, R., (2015). “Insights into Expected Changes in Regulated Flood Frequencies due to the Spatial Configuration of Flood Retention Ponds”. *Journal of Hydrologic Engineering*. doi:10.1061/(ASCE)HE.1943-5584.000117.
- Technical Papers
- Insights into Expected Changes in Regulated Flood Frequencies due to the Spatial Configuration of Flood Retention Ponds
- Bharati, L., Lee, K.H., Isenhardt, T.M., Schultz, R.C., (2002). “Soil-water infiltration under crops, pasture, and established riparian buffer in Midwestern USA,” *Agroforest. Syst.* 56 (3), 249–257.
- Bradley, A.A. (2010). “What Causes Floods in Iowa?” *A Watershed Year: Anatomy of the Iowa Floods of 2008*, C. Mutel (editor), University of Iowa Press, Iowa City, Iowa. 7 - 17.
- Brye, K.R., Norman, J.M., Bundy, L.G., Gower, S.T., (2000). “Water-budget evaluation of prairie and maize ecosystems,” *Soil Sci. Soc. Am. J.* 64 (2), 715–724
- Burkart, M. (2010). “The Hydrologic Footprint of Annual Crops,” *A Watershed Year: Anatomy of the Iowa Floods of 2008*, C. Mutel (editor), University of Iowa Press, Iowa City, Iowa. 77 – 85.
- Chow, V.T., Maidment, D., and Mays, L. (1988). *Applied Hydrology*. McGraw-Hill, Inc.
- Cohen, D. (1993). *Iowa Prairies*. Iowa Association of Naturalists. Biological Communities (IAN). Iowa State University Extension Service. Ames, Iowa.
- Eash, D. A., Barnes, K. K., & Veilleux, A. G. (2013). Methods for estimating annual exceedance-probability discharges for streams in Iowa, based on data through water year 2010. <http://pubs.usgs.gov/sir/2013/5086/>: U.S. Geological Survey Scientific Investigations Report 2013-5086, 63 p. with appendix.
- Easterling, D.R., K.E. Kunkel, J.R. Arnold, T. Knutson, A.N. LeGrande, L.R. Leung, R.S. Vose, D.E. Waliser, and M.F. Wehner, (2017). Precipitation change in the United States. In: *Climate Science Special Report: Fourth National Climate Assessment, Volume I* [Wuebbles, D.J., D.W. Fahey, K.A. Hibbard, D.J. Dokken, B.C. Stewart, and T.K. Maycock (eds.)]. U.S. Global Change Research Program, Washington, DC, USA, pp. 207-230, doi: 10.7930/J0H993CC.
- Frans, C., Istanbuluoglu, E., Mishra, V., Munoz-Arriola, F., Lettenmaier, D.P. (2013). Are climatic or land cover changes the dominant cause of runoff trends in the Upper Mississippi River Basin? *Geophysical Research Letters*, Vol. 40 (17).
- Galloway, G.E., (2010). “The Great Flood of 1993,” *A Watershed Year: Anatomy of the Iowa Floods of 2008*, C. Mutel (editor), University of Iowa Press, Iowa City, Iowa. 227 – 233.

- Hernandez-Santana, V., Zhou, X., Helmers, M., Kolka, R., & Tomer, M. (2013). Native prairie filter strips reduce runoff from hillslopes under annual row-crop systems in Iowa, USA. *Journal of Hydrology*, 94-103.
- Iowa Department of Natural Resources (2018, January 16). 2016 305(b) Assessment Summary-2016 Impaired Waters List. <https://programs.iowadnr.gov/adbnnet/Assessments/Summary/2016>. Accessed July 01, 2018.
- Iowa Geological & Water Survey, Iowa Department of Natural Resources (2013). Landform Regions of Iowa. <http://www.igsb.uiowa.edu/browse/landform.htm>. Accessed January 2017.
- Jackson, R.B., Canadell, J., Ehleringer, J.R., Mooney, H.A., Sala, O.E., Schulze, E.D. (1996). "A global analysis of root distributions for terrestrial biomes," *Oecologia*, 389-411.
- Jones, C.S. and Schilling, K.E. (2011). "From Agricultural Intensification to Conservation: Sediment Transport in the Raccoon River, Iowa, 1916-2009," *Journal of Environmental Quality*, 40.
- Knox, J.C. (2001). "Agricultural Influence on Landscape Sensitivity in the Upper Mississippi River Valley," *Catena* 42, 193-224.
- Linhart, S.M., and Eash, D.A. (2010). Floods of May 30 to June 15, 2008, in the Iowa and Cedar River basins, eastern Iowa, Open-File Report 2010-1190, 99. U.S. Geological Survey.
- Meierdiercks, K.L., Smith, J.A., Baeck, M.L., and Miller, A.J. (2010). "Analyses of Urban Drainage Network Structure and its Impacts on Hydrologic Response," *Journal of American Water Resources Research*, 14(4), 416-424.
- Mejia, A.I., Moglen, G.E. (2010). "Impact of the Spatial Distribution of Imperviousness on the Hydrologic Response of an Urbanizing Basin," *Hydrologic Processes*, 24, 3353-3373.
- Mora, C., Abby G. Frazier, A.G., Longman, R.J., Dacks, R.S., Walton, M.M., Tong, E.J., Sanchez, J.J., Kaiser, L.R., Stender, Y.O., Anderson, J.M., Ambrosino, C.M., Fernandez-Silva, I., Giuseffi, L.M. and Giambelluca, T.M. (2013). The projected timing of climate departure from recent variability, *Nature*, 502(7470).
- Mutel, C.M. (2010). *A Watershed Year: Anatomy of the Iowa Floods of 2008*, C. Mutel (editor), University of Iowa Press, Iowa City, Iowa. 74.
- National Oceanic and Atmospheric Administration (2013). NOAA Atlas 14 Point Precipitation Frequency Estimates. [http://hdsc.nws.noaa.gov/hdsc/pdfs/pdfs\\_map\\_cont.html?bkmrk=ia](http://hdsc.nws.noaa.gov/hdsc/pdfs/pdfs_map_cont.html?bkmrk=ia).
- National Oceanic and Atmospheric Administration (2017). National Centers for Environmental Information Map Application – Version 1.8.4 Monthly Summaries Map. <https://gis.ncdc.noaa.gov/maps/ncei/summaries/monthly>. Accessed April 2017.
- North Central Region Water Network (2018). About the Agricultural Conservation Planning Framework (ACPF). <https://northcentralwater.org/acpf/>. Accessed July 01, 2018.

- Papanicolaou, A.N., Wacha, K.M., Abban, B.K., Wilson, C.G., Hatfield, J.L., Stanier, C.O., Filley, T.R. (2015). "From soils to landscapes: A landscape oriented approach to simulate soil organic carbon dynamics in intensively managed landscapes," *Journal of Geophysical Research: Biogeosciences*, 120, 2375-2401, doi:10.1002/2015JG003078.
- Petersen W. (2010). "The Hydrology of Urban Landscape," *A Watershed Year: Anatomy of the Iowa Floods of 2008*, C. Mutel (editor), University of Iowa Press, Iowa City, Iowa. 87 – 95.
- PRISM Climate Group. (2018). Oregon State University, <http://prism.oregonstate.edu>, created March 2018.
- Sabol, G.V. (1988). "Clark Unit Hydrograph and R-Parameter Estimation." *Journal of Hydraulic Engineering*. American Society of Civil Engineers (ASCE). 114. 10.1061/(ASCE)0733-9429(1988)114:1(103).
- Sayre, R. (2010). "The Dam and the Flood: Cause of Cure," *A Watershed Year: Anatomy of the Iowa Floods of 2008*, C. Mutel (editor), University of Iowa Press, Iowa City, Iowa. 103 – 109.
- Scharffenberg, W. (2013). HEC-HMS User's Manual 4.0. U.S. Army Corps of Engineers Hydrologic Engineering Center.
- Schilling, K. (2000). "Patterns of Discharge and Suspended Sediment Transport in the Walnut and Squaw Creek Watersheds, Jasper County, Iowa: Water Years 1996-1998," Iowa Department of Natural Resources, Geological Survey Bureau, Iowa City, Iowa.
- Schilling, K.E., Chan, K-S., Jha, M.K., Zhang, Y-K., and Gassman, P.W. (2008). "Impact of Land Use and Land Cover Change on the Water Balance of a Large Agricultural Watershed: Historical Effects and Future Directions," *Water Resources Research*, 44, doi: 10.1029/2007WE006644.
- Schilling, K.E., Chan, K-S., Liu, K-S., and Zhang, Y-K., Gassman, P.W. (2008). "Quantifying the Effect of Land Use Land Cover Change on Increasing Discharge in the Upper Mississippi River," *Journal of Hydrology* 387, pp. 343-345.
- Schottler, S.P., Ulrich, J., Belmont P., Moore, R., Lauer, J.W., Engstrom, D.R., Almendinger, J.E. (2013). "Twentieth Century Agricultural Drainage Creates More Erosive Rivers," *Hydrological Processes*, doi:10.1002/hyp.9738.
- Smith, J. A., Baeck, M.L., Villarini, G., Wright, D.B., Krajewski, W.F. (2013). "Extreme flood response: The June 2008 flooding in Iowa." *Journal of Hydrometeorology*. 14(6). 1810-1825., doi: 10.1175/JHM-D-12-0191.1.
- Sprague, L.A., Hirsch, R.M., Aulenbach, B.T. (2011). "Nitrate in the Mississippi River and its tributaries, 1980 to 2008: Are we making progress?" *Environmental Science & Technology*. 2011. August 9;45(17):7209–16.
- Stolze, J.H. (2018). A Tale of Soap and Water: Soap Creek Leads the State in Flood Mitigation. Retrieved from <http://www.iowawatershedapproach.org/2018/02/a-tale-of-soap-and-water-soap-creek-leads-the-state-in-flood-mitigation/>

- Take, E.S. (2010). "Was Climate Change Involved?" *A Watershed Year: Anatomy of the Iowa Floods of 2008*, C. Mutel (editor), University of Iowa Press, Iowa City, Iowa. 111 – 116.
- Thompson, J. (2003). "Wetlands Drainage, River Modification, and Sectoral Conflict in the Lower Illinois Valley," Southern Illinois University, Carbondale, IL.
- Tomer, M.D., Porter, S.A., James, D.E., Boomer, K.M.B., Kostel, J.A., and McLellan, E. (2013). "Combining precision conservation technologies into a flexible framework to facilitate agricultural watershed planning" *Journal of Soil & Water Conservation*. 68:113A-120A.
- United States Department of Agriculture-Iowa State University (2011). USDA-NIFA Award No. 2011-68002-30190. <http://sustainablecorn.org/Weather&Agriculture/Pubs/IA-Northeast.pdf>.
- United States Department of Agriculture-National Resource Conservation Service (2007). *National Engineering Handbook*. Part 630. Chapter 7. <http://directives.sc.egov.usda.gov/OpenNonWebContent.aspx?content=17757.wba>
- Urban, M.A. and Rhoads, B.L. (2003). "Catastrophic Human-Induced Change in Stream-Channel Planform and Geometry in an Agricultural Watershed, Illinois, USA", *Annals of the Association of American Geographers*, 93(4), 783-796.
- Wang, C., Chan, K., Schilling, K.E. (2016). "Total Phosphorus Concentration Trends in 40 Iowa Rivers, 1999 to 2013." *Journal of Environmental Quality*. Madison, WI. doi: 10.2134/jeq2015.07.0365.
- Weber, L.J., Muste, M., Bradley A.A., Amado Arenas, A., Demir, I., Drake, C.W., Krajewski, W.F., Loeser, T.J., Politano, M.S., Shea, B.R., Thomas, N.W. (2018). "The Iowa Watershed Project: Iowa's prototype for engaging communities and professionals in watershed hazard mitigation." *International Journal of River Basin Management*, 16:3, 315-328, doi: 10.1080/15715127.2017.1387127.
- Wehmeyer, L.L., Weirich, F.H., and Cuffney, T.F. (2011). "Effect of Land Cover Change on Runoff Curve Number Estimation in Iowa, 1832–2001," *Ecohydrol.* 4, 315–321.
- Winsor, R. (1975). "Artificial Drainage of East Central Illinois 1820-1920," PhD Thesis, Department of Geography, University of Illinois, Urbana-Champaign, Illinois .
- Wuebbles, D.J., D.W. Fahey, K.A. Hibbard, B. DeAngelo, S. Doherty, K. Hayhoe, R. Horton, J.P. Kossin, P.C. Taylor, A.M. Waple, and C.P. Weaver, (2017). Executive summary. In: *Climate Science Special Report: Fourth National Climate Assessment, Volume I* [Wuebbles, D.J., D.W. Fahey, K.A. Hibbard, D.J. Dokken, B.C. Stewart, and T.K. Maycock (eds.)]. U.S. Global Change Research Program, Washington, DC, USA, pp. 12-34, doi: 10.7930/J0DJ5CTG
- Yiping Wu, Y., Liu, S., Sohl, T.L., Young, C.J. (2013). Projecting the land cover change and its environmental impacts in the Cedar River Basin in the Midwestern United States, *Environmental Research Letters*, 8(2).
- Zhang, Y. K. and Schilling, K.E. (2006). "Effects of Land Cover on Water Table, Soil Moisture, Evapotranspiration, and Groundwater Recharge: a Field Observation and Analysis," *Journal of Hydrology*, 319(1-4), 328-338.

Zhang, Y-K. and Schilling, K.E. (2006). "Increasing Streamflow and Baseflow in the Mississippi River since the 1940s: Effects of Land-use Change," *Journal of Hydrology* 325, doi:10.1016/j.jhydrol.200509.033, 412-42.